Investigating the role of Klhl31 in striated muscle

Thesis submitted by

Constanze Ochmann

for the degree of

Doctor of Philosophy

University of East Anglia

School of Biological Sciences

October 2013

Acknowledgement

First I want to thank Professor Andrea Münsterberg for giving me the opportunity to study Klhl31 in her lab. It has been a challenging journey and I could not have done it without her advice and support.

I would also like to thank my secondary supervisors, Dr. Grant Wheeler and Professor Vince Ellis for their help, suggestions and discussions during my time at UEA.

Furthermore I would like to thank Professor Ulrike Mayer, Dr. Katarzyna Goljanek-Whysall, Dr. Timothy Grocott, Dr. Ester Camp and Dr. Surrinder Soond for giving me advice on methods, techniques and data analysis. I have learned a lot from you.

Also a big thank you to Dr. Alaa Abou-Elhamd, who started the Klhl31 project and who helped me to do my first steps in Andrea's lab.

Also to all the wonderful people in the lab, past and present, it was amazing to work with you! You made good times so much better and hard times a lot easier! I will miss you- Ruth, Nikki, Dom, Vicky, Adam, Kim, Ayisha, Camille, Abdul, Andy, Marlene and Chris! This one is for you.

I am also very grateful to Paul Thomas for his advice and help on microscopy and image acquisition, as well as to Paul Wright for helping out with any IT issue.

Also, Phil. Thanks for making my UEA experience very special and for putting my balance right by just being there and caring.

Thanks to Anke, Carly, Luke, Christina and all the guys at BIO floor 0 for happy lunch breaks, nice days out and so much more.

Also a big Thank you to my family and friends in Germany. You have been amazing!

Finally, I would like to thank the British Heart foundation for funding Andrea's lab and this project!

Abstract

Members of the Kelch-like family display various functions at the cellular level, such as being involved in signalling pathways, as mediators of cytoskeletal changes and most prominently by targeting specific substrates for proteasomal degradation.

Previous studies suggested a role for Kelch-like 31 (Klhl31) during myogenesis, as its expression is dependent on signals responsible for the induction of myogenesis in the somites and is slightly delayed compared to the expression of early myogenic regulatory factors.

With this study we wanted to analyse the function of Klhl31 during myogenesis in more detail. Using C2C12 mouse myotubes as our model cell line to study myogenic differentiation and myofibrillogenesis, we found that Klhl31 is closely associated with Actin fibres in differentiated, multi-nucleated myotubes and that observed co-localisation can be linked to C2C12 differentiation. Furthermore, we used a Yeast-2-Hybrid screen approach and GST-pull downs to find interaction partners for Klhl31. Putative interacting proteins for Klhl31 were analysed and found to be structural components of the sarcomere with many of them also being involved in myofibrillogenesis, such as Nebulin, Actin, CapZ and tropomyosin.

We also analysed a possible role of Klhl31 in proteasomal degradation, as Klhl31 was shown to negatively regulate canonical Wnt-signalling. We gathered evidence that Klhl31 might interact with components of E3-Ubiquitin ligase complexes and might target specific substrates including itself for degradation by the 26S proteasome.

Furthermore, we analysed the expression of Klhl31 during heart development in chick embryos, where it was restricted to the myocardium.

We concluded that Klhl31 might be important during myofibrillogenesis in striated muscles. A role for Klhl31 in mature muscle might involve providing structural stabilisation in sarcomeres and during muscle contraction.

Table of contents

List of figures

List of tables

Abbreviations

APS	Ammonium persulfate
BBR	Boehringer Blocking Reagent
BCIP	5-bromo-4-chloro-3'-indolyphosphate p-toluidine salt
CCD	charge-coupled device
CHAPS	3-[(3-Cholamidopropyl) dimethylammonio]-1-propanesulfonate
DAPI	4',6-diamidino-2-phenylindole
DEPC	Diethylpyrocarbonate
DIG	Digioxigenin
DMF	Dimethylformamide
DNA	Deoxyribonucleic acid
DTT	Dithiothreitol
E.coli	Escherichia coli
ECL	Enhanced chemiluminescence
EDTA	Ethylenediaminetetraacetic acid
FBS	Foetal Bovine Serum
FGF	Fibroblast growth factor
FKBP	FK506 binding protein 15
GST	Glutathione *S*-transferase
HRP	Horseradish peroxidase
H/S	Horse Serum

IPTG	Isopropyl β-D-1-thiogalactopyranoside
Klhl	Kelch-like
LB	Luria-Bertani
MLCK	Myosin light chain kinase
Mo Mu LV	Moloney Murine Leukaemia Virus
MRF	Myogenic regulatory factor
NEDD	Neural precursor cell expressed, developmentally down-regulated
NBT	Nitro-blue tetrazolium chloride
NTP	Nucleoside triphosphate
PAA	Polyacrylamide
PAGE	Polyacrylamide gel electrophoresis
PBS	Phosphate buffered Saline
PCR	Polymerase chain reaction
Pen/Strep	Penicillin/ Streptomycin
PFA	Paraformaldehyde
PMS	Presomitic mesoderm
PMSF	Phenylmethylsulfonyl-Fluoride
PVDF	Polyvinylidene fluoride
RLC	Regulatory light chain
RNA	Ribonucleic acid
ROCK	Rho-associated kinase
SDS	Sodium Dodecyl Sulfate

SOC	Super Optimal Growth with Catabolic repression
TBS	Tris Buffered Saline
TEMED	N, N, N', N'-tetramethylethylenediamine
TESPA	3-aminopropyl triethoxysilane
Tris	2-Amino-2-hydroxymethyl-propane-1, 3-diol
UTP	Uridine triphosphate
X-Gal	5-bromo-4-chloro-indolyl-β-D-galactopyranoside
Y-2-H	Yeast-2-Hybrid

1. Introduction

1.1 Somitogenesis

All vertebrates share the same body plan defined by a segmented body axis. Segmentation takes place during early development and can first be observed as the formation of somites (see figure 1.1), which are paired epithelial segments on either side of the neural tube (Christ and Ordahl, 1995; Dequeant and Pourquie, 2008). The somites originate from the posterior paraxial mesoderm, whilst the anterior paraxial mesoderm, also called the head or cephalic mesoderm, gives rise to the bones and the muscles of the head (Noden, 1991; Pourquie, 2003). Tissues generated from the presomitic mesoderm (the posterior part of the paraxial mesoderm) include skeletal muscles, smooth muscles, cartilage, bones, including the vertebrae, connective tissues and parts of the skin (Dequeant and Pourquie, 2008; Yusuf and Brand-Saberi, 2012).

Each bilateral pair of somites is segregated from the anterior tip of the PSM in regular temporal intervals until for each species a defined number of somites have formed (for a schematic overview of somitogenesis see figure 1.1; (Dequeant and Pourquie, 2008; Maroto and others, 2012; Richardson and others, 1998). Furthermore the timing of each interval of somite formation is also characteristic for each species (Dequeant and Pourquie, 2008; Maroto and others, 2012). A pair of somites in chick embryos is formed every 90 minutes, while a cycle in mice somitogenesis lasts 120 minutes and for human embryos it takes between 4 and 5 hours to form a somite pair (Dequeant and Pourquie, 2008).

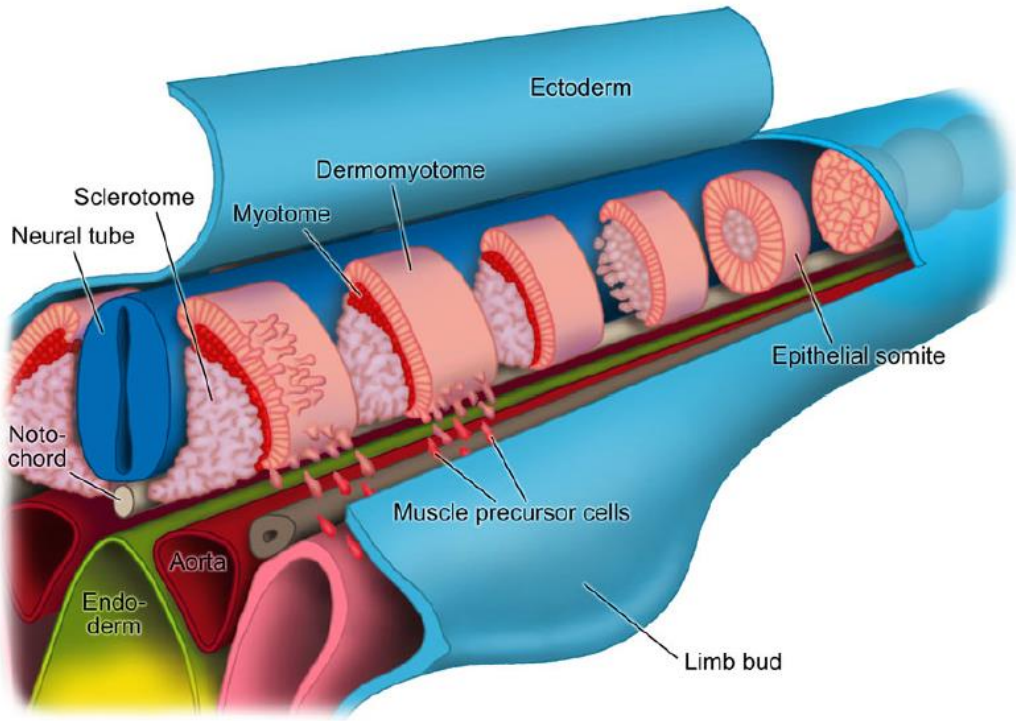

Figure 1.1: Somitogenesis

Somites are formed from the paraxial mesoderm in an anterior-posterior pattern. Once somite segregation has taken place, cells in the somite differentiate to give rise to the dermomyotome and the sclerotome.

Figure taken from Yusuf and Brand-Saberi, 2012

As soon as the new epithelial somite has separated from the pre-somitic mesoderm, it starts to differentiate and mature (Maroto and others, 2012; Yusuf and Brand-Saberi, 2012). The differentiation processes are initiated by signalling molecules from the surrounding tissues, such as the notochord, the neural tube and the surface ectoderm (Aoyama and Asamoto, 1988; Christ and others, 1992; Munsterberg and Lassar, 1995). Specification of dermal and myogenic progenitor cells is induced in the dorsal part of the somites, whilst the cells in the ventral part of the somite will undergo epithelial–mesenchymal transition (EMT) and eventually give rise to the sclerotome (Christ and others, 2007; Maroto and others, 2012; Yusuf and Brand-Saberi, 2012).

Tissues generated from the sclerotome comprise the bones of the skeleton, the vertebrae and the syndetome, which contain the progenitor cells for axial tendons (Brent and others, 2003; Christ and others, 2004; Christ and others, 2000; Dubrulle and Pourquie, 2003; Monsoro-Burq, 2005). Sclerotome differentiation in the ventral somite is

activated by Sonic Hedgehog (Shh) and Noggin / gremlin 1 signals from the notochord (Borycki and others, 1998; Brand-Saberi and others, 1993; Brunet and others, 1998; Christ and others, 2004; Christ and others, 2000; Marcelle and others, 1999; Stafford and others, 2011; Streit and Stern, 1999) resulting in the expression of *paired box 1* (*Pax1*) and *Nkx3.1* (Monsoro-Burq, 2005). In fact *Pax1* expression is activated by Noggin and Shh. It was shown that in Noggin mutants Pax1 expression is delayed (McMahon and others, 1998), whilst overexpression of Shh in cultured, unsegmented paraxial mesoderm enhanced *Pax1* expression (Fan and others, 1995; Fan and Tessier-Lavigne, 1994; Johnson and others, 1994; Munsterberg and others, 1995).

Myogenesis is induced by dorsalizing signals secreted from the dorsal neural tube and the surface ectoderm (Buckingham, 2001).

1.2 Myogenesis

Induction of the dermomyotome is first observed by the expression of myogenic determination genes, such as Pax3, Myf 5 and MyoD (Tajbakhsh and others, 1998; Tajbakhsh and Buckingham, 2000). Myogenesis is activated by Wnt-ligands Wnt-1, -3a and -4 derived from the dorsal neural tube and surface ectoderm, as well as Shh signalling from the notochord and floor plate (Tajbakhsh and Buckingham, 2000).

It was shown that ectopic expression of Wnt ligands can induce dorsal markers like Pax3 and MyoD in chick somites (Munsterberg and others, 1995; Wagner and others, 2000) and further studies revealed that myogenic induction is mediated by β-catenin/ TCF signalling (Schmidt and others, 2000); for an overview of canonical Wnt-signalling see figure 1.2).

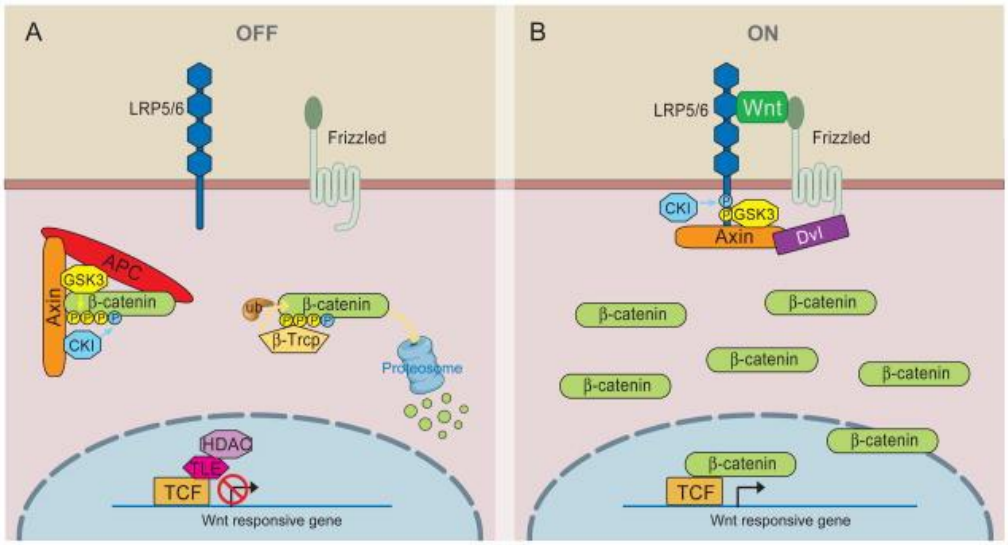

Figure 1.2: Schematic overview of canonical Wnt-signalling

(A) In the absence of Wnt-ligands, cytoplasmic β-catenin is bound to a destruction complex containing Axin, APC, GSK3β and CK1 leading to the phosphorylation of β-catenin by CK1 and subsequently by GSK3β. Following phosphorylation, β-catenin is recognised by β-Trcp, an E3-ubiquitin ligase, targeting β-catenin for proteasomal degradation.

(B) In the presence of Wnt ligands, the Wnt receptor Frizzled (Fz) forms a complex with its co-receptors LRP5/6. Furthermore, Dishevelled (Dvl) is then recruited to Fz leading to the phosphorylation of LRP5/6 and subsequent binding of Axin to the co-receptors. Subsequently the destruction complex dissociates and phosphorylation and proteasomal degradation of β-catenin is inhibited leading to β-catenin accumulation in the nucleus, where it activates Wnt-responsive genes together with TCF.

Figure taken from MacDonald and others, 2009

Wnt signalling in the ventral part of the somites, the future sclerotome is inhibited by secreted forms of Wnt-receptors, such as Frzb and secreted Frizzled-related proteins (Sfrps) (Bovolenta and others, 2008; Leyns and others, 1997). Frzb is a homologue of Frizzled, which is lacking the transmembrane domain and therefore has been described to function as a soluble antagonist of Wnt-signalling by binding and sequestering of Wnt-ligands (Leyns and others, 1997). Sfrp2, as an example for Sfrps inhibits specifically Wnt-1 and Wnt-4 signalling in the myotome, where its expression is regulated by Shh derived from the floor plate and the notochord (Lee and others, 2000).

As mentioned previously, Shh signalling is needed for myogenic induction in the somites (Buckingham, 2001; Buckingham and others, 2003). It was reported that Shh signalling in the dorsal somite is regulated by Wnt-signalling (Borycki and others, 2000). These authors reported that Wnt-1 and Wnt-4 by signalling via β-catenin together with signals from the surface ectoderm can restrict Gli2 and Gli3 expression, but not Gli1 expression, to the myotome in the developing somite. The Gli proteins are transcriptional effectors of the Shh transduction cascade (for a summary of Shh/ Gli signalling see (Hui and Angers, 2011). As ectopic expression of Shh in somites of chick embryos was shown to increase the sclerotome and to inhibit dermomyotome formation, it was thought that the function of Shh-signalling in the induction of either the myotome or the sclerotome depend on the dose of Shh (Dietrich and others, 1997; Johnson and others, 1994). Furthermore, a dose dependency was also highlighted for dorsalizing signals and it was shown that the myotome was only induced when the levels of Wnt/Shh were present in appropriate levels in a specific region of the somite (Dietrich and others, 1997). Interestingly though studies using a *Shh* null mouse still revealed the presence of the myotome, although compromised in the epaxial somite leading to the suggestion that Shh might not be directly involved in myogenic induction (Borycki and others, 1999; Kruger and others, 2001).

Muscle progenitor cells reside in the dermomyotome, where they respond to dorsalizing signals that induce myogenic differentiation (Buckingham, 2001). Myogenic precursor cells have been shown to migrate out of the dermomyotome to form the myotome (see figure 1.3). However, how the cells migrate is not fully understood yet.

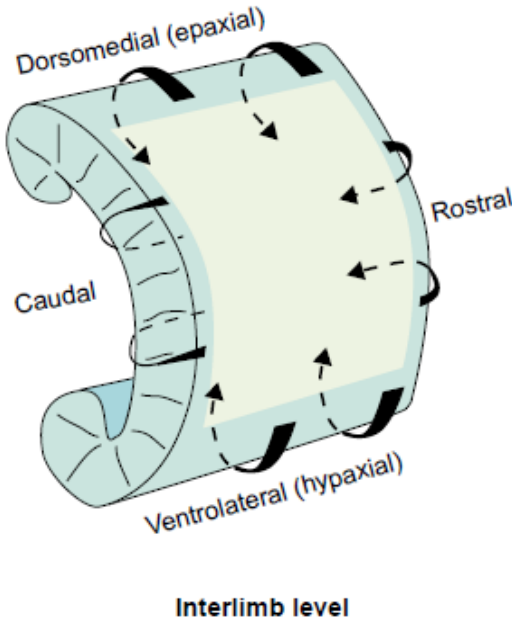

Figure 1.3: The formation of the myotome

The scheme represents the migration of muscle progenitor cells from the edges of the dermomyotome to form the myotome.

Figure taken from Buckingham, 2001

Electroporation of a GFP reporter into early somites of chick embryos followed by real-time cell lineage analysis showed that myotome formation is established in two distinct phases and requires migration of myocytes from all four borders of the dermomyotome (Gros and others, 2004). The first phase was described to mediate myotome growth, as myocytes exclusively derived from the medial border of the dermomyotome migrate into the myotome. In the following second phase myocytes from all four borders (the medial, caudal, cranial or rostral and ventrolateral dermomyotome border) contribute to the myotome.

Cells of the myotome differentiate to form myofibres. Differentiation of myoblasts involves de-novo myofibrillogenesis, the establishment of the sarcomeric structures and requires the withdrawal of the myocytes from the cell cycle, followed by expression of muscle-specific genes and fusion of myocytes to generate multi-nucleated myotubes

(Andres and Walsh, 1996; Kontrogianni-Konstantopoulos and others, 2006; Pownall and others, 2002).

Skeletal muscle development is regulated by basic helix-loop-helix (bHLH) domain containing myogenic regulatory factors (MRFs); *Myf 5* and *MyoD* as myogenic determination marker genes and *MRF4* and *myogenin* as differentiation marker genes (Pownall and others, 2002).

Myf 5 and MyoD have been shown to be expressed in proliferating myoblasts (Emerson, 1990). It was further reported that both genes auto regulate their expression to establish a constant Myf 5/ MyoD signal leading to the suggestion that both genes are involved in maintaining the myocyte population (Emerson, 1990; Thayer and others, 1989). Expression of myogenin and MRF4 is induced during myoblast differentiation and might mediate the expression of sarcomeric proteins (i.e. proteins of the contractile apparatus) by function together with Myf 5 and MyoD (Edmondson and Olson, 1989; Lassar and others, 1991; Miner and Wold, 1990; Rhodes and Konieczny, 1989; Wright and others, 1989)

1.3 Myofibrillogenesis

Myofibrillogenesis describes the assembly of sarcomeric proteins and their maturation (Sanger and others, 2002).

The first evidence for primitive myofibrils was already reported in 1913 when non-striated fibres were observed close to the cell membrane during trout muscle development (Heidenhain, 1913) as cited by (Sanger and others, 2010). Similar non-striated filamentous structures have also been seen in newly formed chick musculature (Fischman, 1967; Hibbs, 1956). Furthermore it was observed that the thick filament elongated daily during muscle development in *drosophila melanogaster* leading to the suggestion that muscle structures are assembled over a distinct period of time (Auber, 1969) as cited by (Sanger and others, 2010). Advanced techniques in microscopy and the generation of muscle cell cultures made it possible to study myofibrillogenesis in more detail. Gene expression studies revealed that during myofibrillogenesis Desmin is the first of the sarcomeric proteins to be expressed, followed by titin, muscle-specific

Actin, myosin heavy chains and Nebulin (Furst and others, 1989). Furst et al (1989) reported that during mouse development around gestation day 11-12, before fusion of myoblast to form multinucleated myotubes at gestation day 13-14, first immature myofibrils were established displaying periodic striation for myosin and Nebulin, whilst titin was seen localised to the Z-disc. It was therefore suggested that the structures of the Z-disc and the thick filament, i.e. the myosin, form separately from each other and only align during later part of muscle development (Furst and others, 1989).

As myofibrillogenesis was studied in more detail in cultured muscle cells and during embryonic muscle development, it became clear that myofibril assembly followed similar patterns. It was described that myosin was one of the earliest proteins seen to display a striated pattern during muscle differentiation (Dlugosz and others, 1984; Kulikowski and Manasek, 1979; Moncman and Wang, 1996). Furthermore it was found that a non-muscular isoform of myosin is present in early premyofibrils (the precursor for myofibrils as described by (Rhee and others, 1994), which is replaced by muscle specific myosin during muscle differentiation and maturation (see figure 1.3; (Dabiri and others, 1997; Dlugosz and others, 1984; Fallon and Nachmias, 1980; Mittal and others, 1987; Rhee and others, 1994; Sanger and others, 2002).

A further structure seen to be formed during myofibrillogenesis and also already present in premyofibrils are primitive Z-discs (Rhee and others, 1994). α-Actinin associated to early thin filament was shown to display puncta, also described as beaded Z-bands in cultured myocytes, which eventually aligned laterally and fused into linear structures during muscle maturation (Dabiri and others, 1997; Rhee and others, 1994; Sanger and others, 1986; Sanger and others, 1984a; Sanger and others, 1984b). Furthermore it was shown in cell culture and early chick hearts that non-muscular myosin aligned with the Z-bodies in an alternating fashion (Du and others, 2008; Rhee and others, 1994). These structures were termed minisarcomeres. As the minisarcomeres mature, the Z-bands connect laterally and the Actin and non-muscle myosin start to co-localise and eventually display an organised overlapping pattern (Mittal and others, 1987). Cells, which revealed overlapping Actin/ non-muscular myosin structures were termed nascent myofibrils (see figure 1.4; (Sanger and others, 2010). Furthermore, nascent myofibrils already express muscle-specific myosin II, although at this point it does not align to the present striated filaments (Rhee and others, 1994; Wang and others, 2005a).

Mature myofibrils have established sarcomeric structures containing partially overlapping, defined thick and thin filaments (see figure 1.4 and chapter 1.4;(Sanger and others, 2010; Wang and others, 2005a)). Non-muscle myosin has now completely been removed and replaced by muscle-specific myosin II (Dabiri and others, 1997; Rhee and others, 1994).

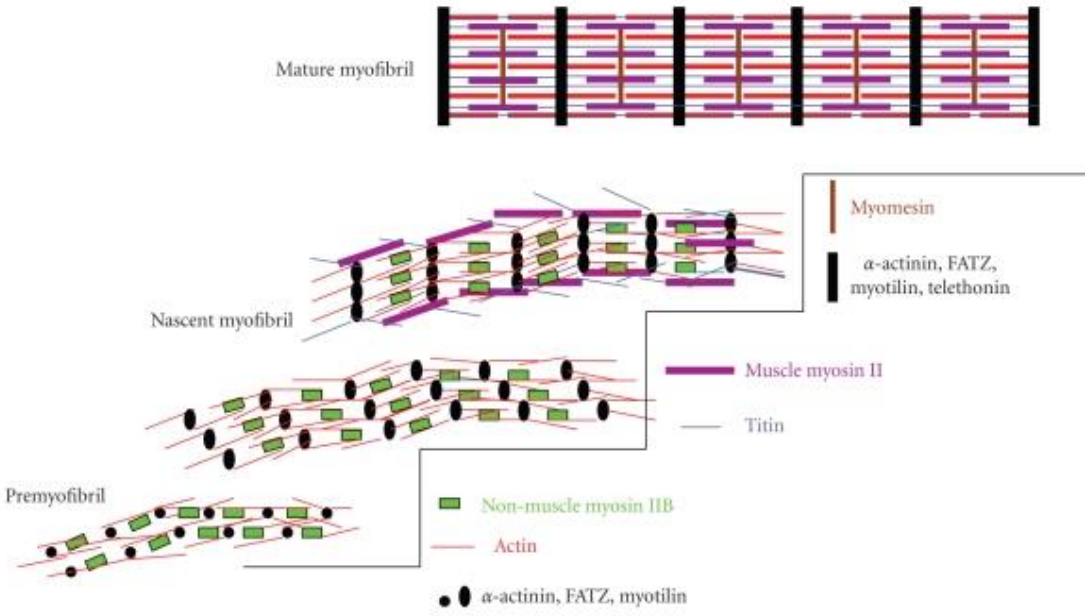

Figure 1.4: De-novo myofibrillogenesis

Schematic outline of myofibrillogenesis: Premyofibrils are formed when Z-bodies begin to form at the edges of muscle cells, comprising α-Actinin structures linked with Actin, Actin binding proteins and non-muscular myosin II. During further maturation muscular myosin and titin are added to the minisarcomeres and Z-bodies align in register to create nascent myofibrils. Mature myofibrils are defined by linear Z-discs. In mature myofibrils non-muscular myosin is absent and myosin-binding proteins are incorporated into the thick filament.

Figure taken from Sanger and others, 2010

However, there are still processes during myofibrillogenesis, which are controversially discussed. Based on their observation, Dlugosz et al. (1984) described that non-muscular myosin II fibres would act as scaffolds for myofibrils assembly, whilst Rhee et al. (1994) suggested that structures comprising α-Actinin, non-muscle myosin and

Actin would be the initiation point of myofibrillogenesis. A further hypothesis for myofibrillogenesis was proposed reporting that the Z-band proteins and the myosin thick filament (termed I-Z-I brush) would assemble separately from each other (Holtzer and others, 1997; Schultheiss and others, 1990). A similar observation was made for cardiac myofibrillogenesis (Ehler and others, 1999; Rudy and others, 2001). Furthermore it was reported that both structures, the thick and the thin filament, would eventually associate with each other mediated by interactions with the titin filament and Nebulin (Holtzer and others, 1997). However, Sanger et al. (2010) contradict the I-Z-I brush hypothesis based on the described evidence for premyofibrils, which contains Z-disc proteins associated with myosin in minisarcomeres (Rhee and others, 1994; Sanger and others, 2010). However, it was shown that titin might play a key part during myofibrillogenesis as it was suggested that titin might mediate thick filament assembly and its alignment to the Z-disc, thereby stabilising the sarcomeric protein organisation (Turnacioglu and others, 1997a; Turnacioglu and others, 1997b). Also, the involvement of non-muscular myosin for thick filament alignment during myofibrillogenesis was confirmed by using phosphorylation inhibition studies (Du and others, 2003).

On the other hand the presence of premyofibrils is also open for discussion, as premyofibrils could not be confirmed in heart muscles in some publications (Ehler and others, 1999; Rudy and others, 2001; Tullio and others, 1997). Recent studies however showed that cardiac myofibrillogenesis also requires premyofibrils (Du and others, 2003; Du and others, 2008), leading to the suggestion that myofibrillogenesis both in heart and skeletal muscles follow similar temporal patterns (Sanger and others, 2010).

Mature myofibrils display a defined complex of proteins, which will eventually mediate muscle contraction: the sarcomere.

1.4 The sarcomere

The basic unit of the contractile apparatus is called a sarcomere. Sarcomeres are linked in an end-to-end fashion forming long tubes called myofibrils. One muscle fibre is made up of a variable number of parallel aligned myofibrils, which also align parallel to each other to generate one striated muscle (see figure 1.5; (Craig and Padron, 2004).

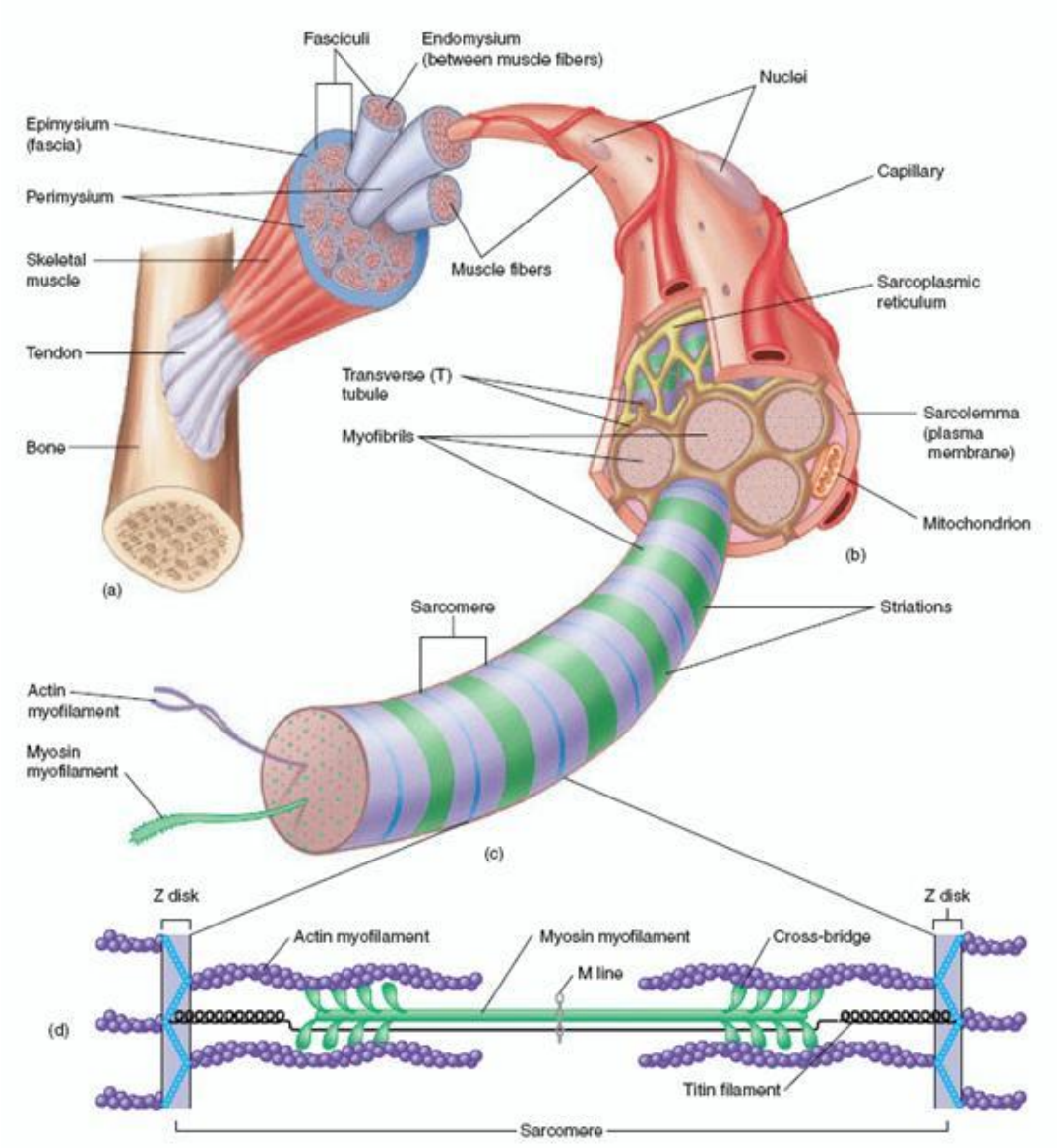

Figure 1.5: The striated muscle

The sarcomere (d) is the basic unit of striated muscles. Hundreds of sarcomeres make up myofibrils (c) and parallel aligned myofibrils are the subunits of one muscle fibre (b). The striated muscle also consists of a bundle of hundreds to thousands of muscle fibres (a).

Figure taken from SPORTS'N SCIENCE (http://sportsnscience.utah.edu/95-miles-per-hour-performance-physiology-of-pitchers/).

Skeletal and cardiac muscles are both striated muscles. These muscles have been termed striated after the striped pattern observed in images of skeletal and heart muscle fibres originating from alternating striations of the Actin and myosin filaments in the sarcomere. The Actin filament is also known as the thin filament, whilst the myosin filament was termed the thick filament (see figure 1.6).

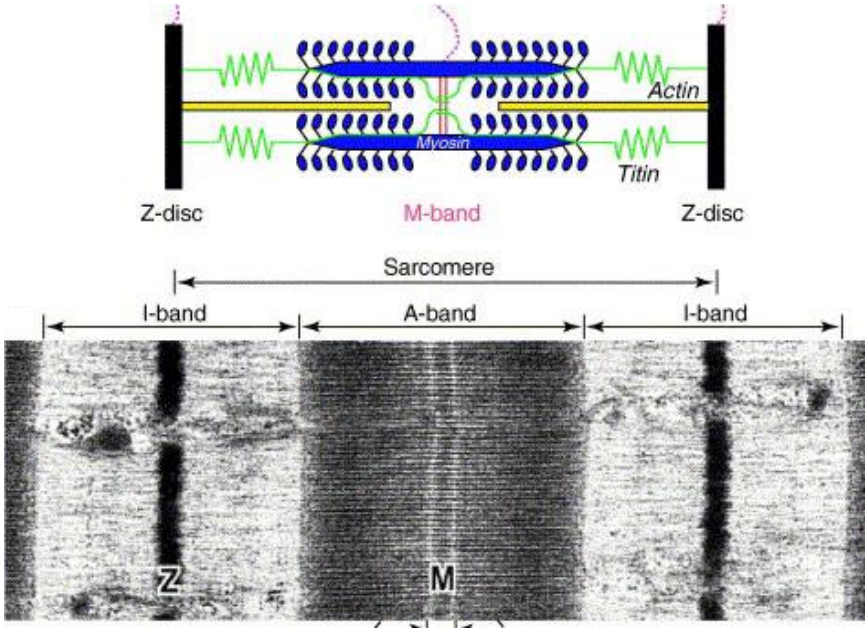

Figure 1.6: An electron microscopy image of a sarcomere

The striations of the Actin filament (light grey within the I-band) and the myosin filament (dark within in the A-band) can be observed in thin sections of a muscle fibre.

Figure modified from Agarkova and Perriard, 2005

Based on optical and electron microscope images of muscle fibres (see figure 1.6), parts of the sarcomeres have been identified and analyzed. One sarcomere stretches from one Z-disc to another Z-disc, whilst the area of the dark myosin filament is termed the A-band (anisotropic in polarised light). In the middle of the sarcomere a further dark area has been termed the M-band, derived from the German word Mittelscheibe, which means the disc in the middle, or central disc. At the M-band myosin is associated to other sarcomeric proteins, for example the elastic titin filament (Houmeida and others, 1995). The area, which contains only the Actin thin filament, is called the I-band (isotrophic in polarised light).

When sarcomeres were analysed, it was reported that Actin and myosin were the most abundant proteins in the sarcomere, making up around 70% of the myofibril (Hanson and Huxley, 1957; Huxley and Hanson, 1957).

The thin filament consists not only of Actin; it also interacts with Nebulin, tropomyosin and troponin, whilst the thick filament consists of myosin and other associated proteins, such as MyBP-C and MyBP-H (Craig and Padron, 2004; Offer and others, 1973; Squire, 1997; Starr and Offer, 1983). Titin has been reported to associate with both, the thin and the thick filament (Sanger and Sanger, 2001).

A sarcomere in the myocardium displays similar structure as a sarcomere in skeletal muscle fibres (see figure 1.7).

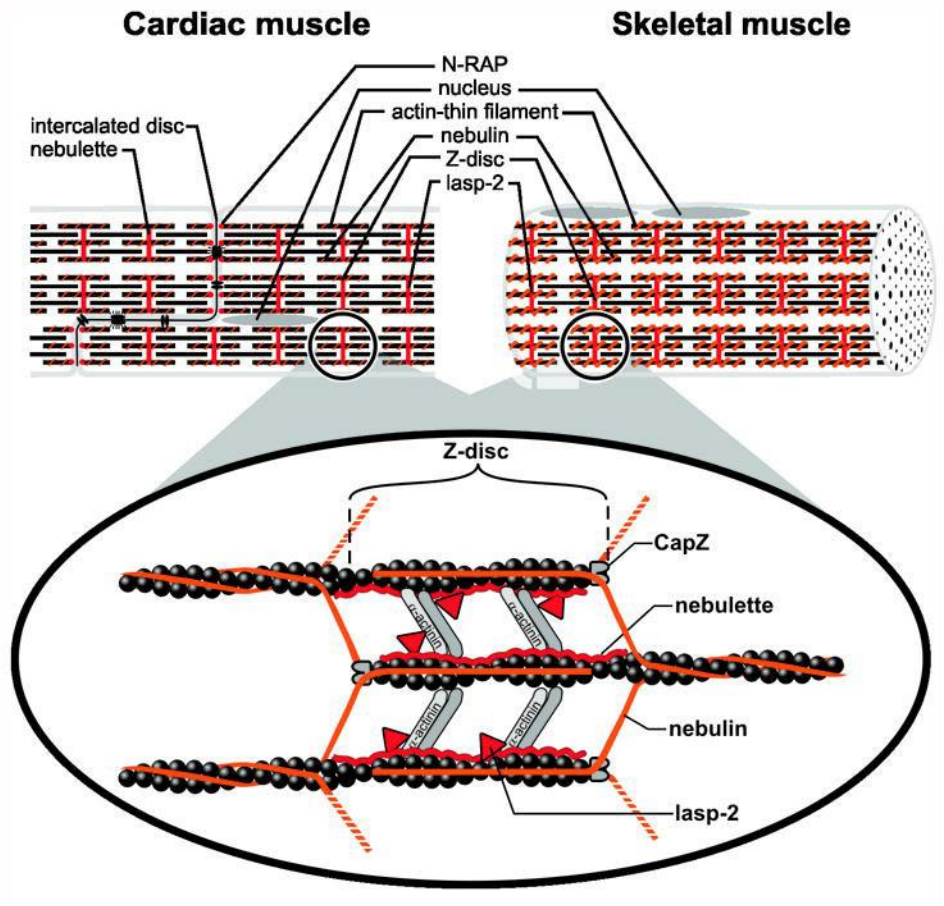

Figure 1.7: Sarcomeric structure in cardiac and skeletal muscle

Both, cardiac muscle and skeletal muscle sarcomeres, display a similar sarcomeric structure. The Actin thin filament is linked to the Z-disc via α-Actinin and overlaps partially with the thick filament. Also in both sarcomeres, Nebulin is associated with the whole length of the Actin filament. Cardiac muscle exclusively expresses Nebulette, which binds to Actin, but only close to the Z-disc.

Figure taken from Pappas and others, 2011

However, assembly of sarcomeres in the heart has been described to be much quicker compared to skeletal muscle myofibrillogenesis (Ehler and others, 1999). During heart development in chick embryos the first proteins described to associate were titin and α-Actinin during the formation of early Z-discs, followed by myosin and later Actin (Tokuyasu and Maher, 1987a; Tokuyasu and Maher, 1987b). It was furthermore reported that the cardiomyocytes aligned with other neighbouring cells very early during cardiogenesis potentially to establish a scaffold for the assembly of myofibrils (Shiraishi and others, 1993; Shiraishi and others, 1995; Tokuyasu, 1989). Further data analysing the assembly of chick heart myofibrils was obtained from triple-immuno-

stained developing hearts. It was reported that myofibrils in chick hearts assembled without the intermediate stage of premyofibrils (Ehler and others, 1999); as described previously). However, the presence of premyofibrils during heart development has been recently confirmed as well, as non-muscular myosin was detected during myofibrillogenesis in precardiac mesoderm explants and during avian heart development in situ (Du and others, 2003; Du and others, 2008).

Each sarcomeric protein has a specific localisation and function as described in the following sections.

1.5 The thin filament

1.5.1 Actin

Together with myosin, the Actin filament is the most abundant protein in the sarcomere and it is the main component of the thin filament (Pollard, 1990; Pollard and Cooper, 2009). The thin filament is assembled as globular (G) Actin monomers self-associate to form filamentous Actin, or F-Actin (Pollard, 1990). Furthermore, two Actin polymer-strands twist around each other forming a double helix (O'Brien and Dickens, 1983).
Within the structure of the Actin monomer lie binding sites for the thick filament. One Actin monomer was described to consist of two major domains each comprising 2 subdomains. The smaller of the two major domains comprises subdomains 1 and 2 and is located at the periphery of the thin filament, whilst subunits 3 and 4 built the core of the filament. Between both major domains is the central cleft, which contains a tightly bound nucleotide, in vivo Mg^{2+}, and either an ATP or an ADP molecule (Cooke, 1997). The cation is potentially involved in stabilising the structural organisation of the two major domains, whilst hydrolysis of ATP is needed for polymerization of the Actin filament (Kabsch and others, 1990; Kabsch and Vandekerckhove, 1992; Pollard, 1990). Only subdomain 1 in the Actin monomer was shown to associate with the myosin head during muscle contraction (Miller and others, 1995; Sutoh and others, 1991).
The Actin fibres within the thin filament associate to various other sarcomeric proteins, such as Nebulin, tropomyosin, troponin and capping proteins (Craig and Padron, 2004).

1.5.2 Proteins of the Z-disc

α-Actinin is the main part and the backbone of the Z-disc. However, various other proteins, such as Z-protein, Znin, FATZ, amorphin, myotilin, ZASP and myopalladin, as well as overlapping ends of Nebulin, titin and CapZ can be identified in the Z-disc. The intermediate filaments can also be associated to the Z-disc (Craig and Padron, 2004).

The major protein of the Z-disc as mentioned previously is α-Actinin. Its function is the connection and stabilisation of the Actin and the titin filament in adjacent sarcomeres (Vigoreaux, 1994). It was suggested that α-Actinin can itself form bridge-like structure cross-linking the thin filament of neighbouring sarcomeres, whilst for the binding of the titin filament a complex of α-Actinin together with Actin is needed (Luther, 1991; Young and others, 1998).

Further compounds of the Z-disc amongst others are myopalladin, myopodin and myozenin. Myopalladin has been reported to connect Nebulin to α-Actinin and thereby associating it to the Z-disc (Bang and others, 2001), whilst myopodin is an actin-bundling protein potentially involved in stabilising the Z-disc (Weins and others, 2001). Myozenin or FATZ has been shown to bind to α-Actinin, γ-filamin and telethonin and might cross-link these proteins with each other (Takada and others, 2001). It was also suggested that myozenin might be involved in mediating dimerization of Z-disc proteins.

Most other proteins of the Z-disc are less well described, but a brief overview of various other Z-disc related proteins can be found in Craig and Padron (2004).

1.5.3 Nebulin

Nebulin has been described to be a potential ruler for the thin filament (Labeit and others, 1991). It was reported that Nebulin interacts with Actin monomers along the whole length of the Actin filament and that the size of Nebulin correlates with the length of the Actin fibre in different muscle types (Kruger and others, 1991; Labeit and others, 1991; Labeit and Kolmerer, 1995a). Furthermore it was shown that Nebulin interacts with the thin filament capping proteins consistent with a potential role for Nebulin as a length specifier (McElhinny and others, 2001; Pappas and others, 2008). Nebulin has also been shown to be involved in muscle contraction (Bang and others, 2009; Chandra and others, 2009)

1.5.4 Tropomyosin/Troponin

The thin filament is interacting with the troponin/tropomyosin complex as mentioned previously. This complex contains tropomyosin associated to one molecule of troponin C, troponin I and troponin T (Craig and Padron, 2004; Farah and Reinach, 1995; Squire, 1997). Only troponin C can bind free Calcium ions, whilst troponin T connects troponin C and troponin I with tropomyosin. Troponin I associate with tropomyosin along the Actin thin filament in non-active muscle, partially covering myosin binding sites and thereby preventing Actin-myosin interactions (Bailey, 1948; Farah and Reinach, 1995; Gomes and others, 2002). In active muscle troponin I stays associated to tropomyosin along the Actin filament, although its localisation is slightly shifted as compared to in non-active muscles (Farah and Reinach, 1995).

The troponin/tropomyosin complex regulates muscle contraction by responding to changes of cellular Ca^{2+} concentrations (see chapter 1.9;(Farah and Reinach, 1995).

1.5.5 Thin filament capping proteins

A constant, stable Actin filament is necessary for the sarcomere, as muscle contraction is dictated by the ratio of overlapping thin filament to thick filament (Huxley, 1957; Huxley and Simmons, 1971). Capping proteins are preventing depolymerization and also additional polymerization above specific length in the thin filament (Cooper and Schafer, 2000; Fowler, 1996; Littlefield and Fowler, 1998). Cap Z, also known as β-Actinin, interacts with Actin at its barbed end (at the Z-disc) (Casella and others, 1986; Fowler, 1996; Maruyama and others, 1990). Therefore, Cap Z prevents disassociation and re-association of the Actin filament. Furthermore it was shown that CapZ also interacts with the Z-disc protein α-Actinin thereby anchoring the thin filament to the Z-disc (Papa and others, 1999). This link is established during myofibrillogenesis and also involves the specification of the polarity of the Actin filament (Schafer and others, 1995).

At the pointed ends the thin filament is capped by tropomodulins (Fowler and others, 1993; Gregorio and others, 1995; Weber and others, 1994). Capping of the thin filament by tropomodulins has been described as being tight in striated muscle to prevent further polymerization and elongation of the thin filament (Fowler and others, 1993; Gregorio and Fowler, 1995; Mudry and others, 2003). Tropomodulin in association with tropomyosin prevents shortening of Actin fibres (Kostyukova and others, 2006; Kostyukova and others, 2005; Mudry and others, 2003). It was furthermore suggested that Nebulin might place tropomodulin at the end of growing pointed ends of the thin filament (McElhinny and others, 2001). Recently it was shown that both capping proteins display a highly dynamic nature in cultured myocytes (Gregorio and others, 1995; Littlefield and others, 2001). Although the capping proteins still restrict the length of the thin filament, a constant de-and repolymerisation of Actin monomers at both ends has been observed.

1.6 The thick filament

1.6.1 Myosin

Myosins belong to the family of ATP-dependent motor proteins and are usually associated with Actin (Sellers, 2000). Myosins in smooth and skeletal muscle have been described extensively and have been shown to play a key role in muscle contraction and force transmission (Cooke, 1997; Sellers, 2000), but myosins have also been described in eukaryotes, mammals and plants (Sellers, 2000). Based on differences and/ or similarities mainly in the motor domain, myosins have been organised into 15 classes (for a phylogenic tree and description of each class, see (Sellers, 2000).

All known myosins so far have been described to interact with Actin, hydrolyze ATP and produce different types of movement including previously mentioned muscle contraction, but also trafficking along fibres and cell migration (Cooke, 1997; Lecuona and others, 2009; Rayment and others, 1993; Vicente-Manzanares and others, 2009). Myosins typically contain three functional subdomains: the motor domain, which comprises Actin-binding properties and a catalytic centre for ATP hydrolysis, a neck domain, which is associated with either myosin light chains or Calmodulin and the distal tail domain, which is involved in anchoring and positioning the myosin head or motor domain in the right orientation for its interaction with Actin (Sellers, 2000). Whilst the motor domain across different types of myosin have been reported to be relatively conserved, the neck and the tail domain can vary across species and even across myosin classes themselves (Sellers, 2000). The neck domain can contain a diverse number of Calmodulin/ light chain binding sites, whilst the tail domain can contain distinct additional functional domains (Cheney and Mooseker, 1992; Sellers, 2000). Furthermore, many myosins can dimerize and therefore form two-headed molecules (Sellers, 2000). Dimerization takes place along the myosin tail comprising specific coiled-coil forming sequences.

In striated muscles, myosin is a hexamer comprising two identical myosin heavy chains and two pairs of myosin light chains (Lowey and others, 1979; Lowey and others, 1969; Lowey and others, 1991). The C-terminus of the myosin heavy chains form a dimer along the tail region (Lowey and others, 1969), whilst the N-terminus of each heavy

chain separately forms a globular head (Rayment and others, 1993). The globular head contains the distinct ATP- and Actin-binding sites and structural changes in the myosin head mediated by ATP hydrolysis are a requirement for muscle contraction (Cooke, 1997; Rayment and others, 1993). The role for myosin during muscle contraction is described in chapter 1.9.

1.6.2 The proteins of the M-band

Creatine kinase, M-protein and Myomesin make up the M-band. However, parts of the myosin filament, as well as the C-terminus of titin and a splicing isoform of myomesin, Skelemin can also be found in the M-band (Agarkova and others, 2000; Furst and others, 1999; Wallimann and Eppenberger, 1985).

As proteins of the M-band are not a main focus of this project, I will not describe the M-band any further. However, further information about Creatine kinase, Myomesin, M-protein and Skelemin be found in (Agarkova and others, 2000; Furst and others, 1999; Grove and others, 1984; Kushmerick, 1998; Morimoto and Harrington, 1972; Obermann and others, 1996; Obermann and others, 1995; Price and Gomer, 1993; Steiner and others, 1999; Turner and others, 1973; Van Der Ven and others, 1996; Wallimann and others, 1977; Woodhead and Lowey, 1983).

Based on obtained data for the proteins found in the M-band, it was reported that the main functions of the M-band involve stabilizing the thick filament between neighbouring sarcomeres, as well as restoring and buffering the ATP-levels within the myofibril (Agarkova and Perriard, 2005; Elliott and others, 1963; Kushmerick, 1998; Obermann and others, 1996; Wallimann and Eppenberger, 1985).

1.7 The intermediate filament

The intermediate filaments can be observed in the periphery of the sarcomere and its main function is the establishment and maintenance of the structure of muscle fibres by transverse cross-linking of neighbouring myofibrils (Craig and Padron, 2004; Goldman and others, 2012). Intermediate filaments also connect myofibrils to the sarcolemma and surrounding nuclei (Herrmann and Aebi, 2000; Stromer, 1990; Wang and Ramirez-Mitchell, 1983).

Intermediate filaments have been reported to surround the myofibril around the Z-disc and also along the M-band by forming filamentous rings (Stromer, 1990; Wang and Ramirez-Mitchell, 1983). These rings have been shown to connect adjacent Z-disc- and M-band- rings of neighbouring myofibrils with each other (Stromer, 1990).

Desmin is the main protein of the intermediate filament in both developing and adult muscles (Edstrom and others, 1980; Herrmann and Aebi, 2000; Paulin and Li, 2004). It has been shown to be linked to the Z-disc as well as to associate with Nebulin along the Actin filament (Bang and others, 2002). Furthermore Desmin forms cross-links between a sarcomere and the sarcolemma, mitochondria and nuclei in skeletal muscle fibres (Lazarides, 1982). It was therefore suggested that Desmin might play a crucial role in sarcomere alignment, sarcomere stabilisation, muscle contraction and force transmission (Balogh and others, 2005; Boriek and others, 2001; Paulin and Li, 2004). The generation of Desmin KO mice have further highlighted the function of Desmin in myofibril stabilisation, maintenance of myofibril integrity and myofibril regeneration (Li and others, 1996; Milner and others, 1996).

Further proteins of the intermediate filaments are Vimentin, Synemin, Nestin and Paranemin. These proteins are not described any further in this section, as they are not relevant for this project. However, their functions are described in following publications: (Bellin and others, 1999; Bilak and others, 1998; Granger and others, 1982; Hemken and others, 1997; Herrmann and Aebi, 2000; Lendahl and others, 1990; Ngai and others, 1985; Sax and others, 1989; Schweitzer and others, 2001).

1.8 The titin filament

Titin is a huge muscle-specific protein, which can be between 3-4 MDa large. It is associated to the Z-disc, where it interacts with α-Actinin and elongates into the M-band, where it binds to the M-band protein myomesin (Gautel, 1996; Gautel and others, 1996; Labeit and Kolmerer, 1995b; Maruyama, 1976; Maruyama and others, 1976; Obermann and others, 1996; Obermann and others, 1995; Vinkemeier and others, 1993; Wang and others, 1979). After myosin and Actin, titin is the third most abundant protein is striated muscle (Fukuda and others, 2008). Analysing the structure and properties of titin in more detail, it was shown that titin can act as a molecular spring thereby sustaining elasticity in the sarcomere (Labeit and Kolmerer, 1995b; Linke and Granzier, 1998). However, only the region of titin localised to the I-band is elastic (Labeit and Kolmerer, 1995b). This region consists of two segments of tandemly arranged immunoglobulin-like (Ig) domains, one close to the Z-disc the second one further distal, which are spatially separated by a PEVK amino acid sequence, rich in proline (P), glutamate (E), valine (V) and lysine (K) residues and a N2B element (Labeit and Kolmerer, 1995b), see figure 1.8). All of the mentioned domains display spring-like functions and allow the protein to extend (Helmes and others, 1999; Labeit and Kolmerer, 1995b).

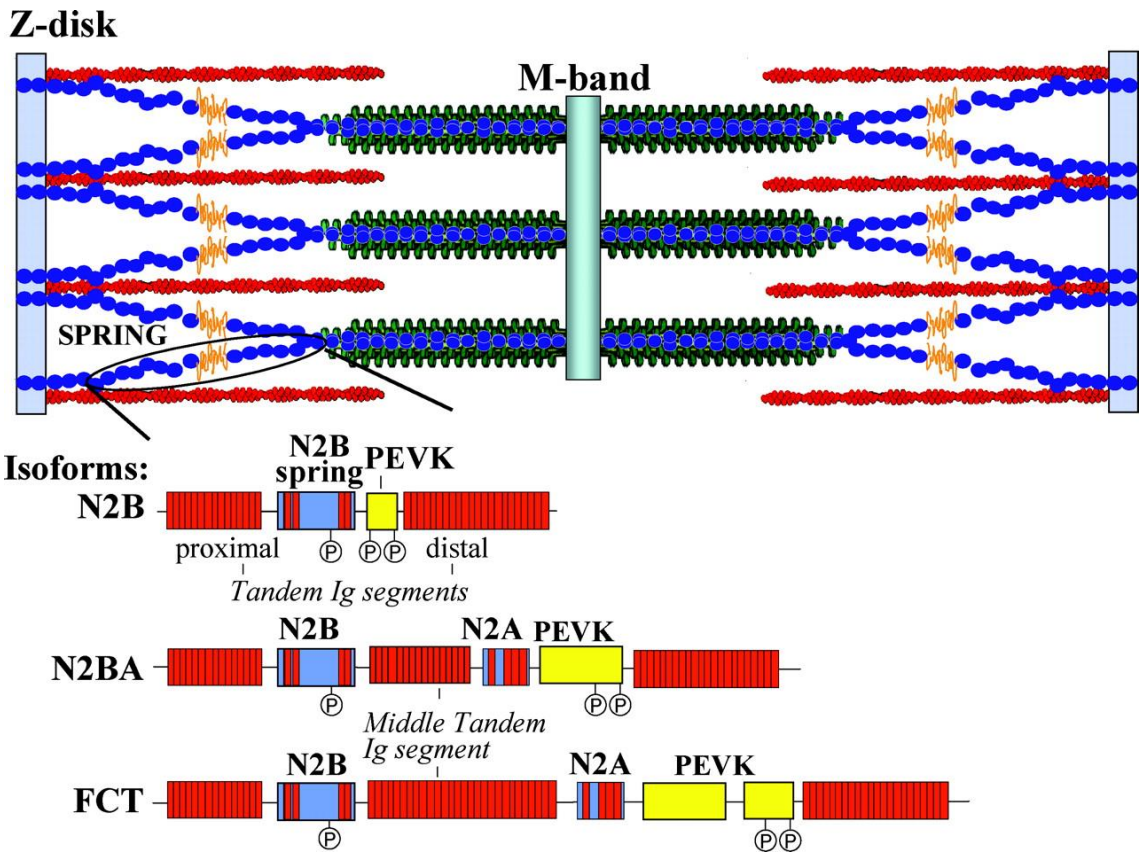

Figure 1.8: The titin spring in the sarcomere

Titin functions as a spring localised in the I-band of the sarcomere. In heart muscle three splicing isoforms for titin have been reported. However, all titin isoforms share conserved structural domains in the extensible region, such as Ig segments and the PEVK domain.

Figure taken from LeWinter and Granzier, 2010

Functions of the titin filament have been studied extensively in cardiomyocytes and also in skeletal myocytes. For cardiac titin three isoforms have been described, whilst skeletal titin exists in at least two isoforms (Fry and others, 1997; Granzier and Labeit, 2002; LeWinter and Granzier, 2010) During relaxation the muscle is stretched and a passive force independent of actomyosin interaction is generated leading to the extension of the sarcomere (Fukuda and others, 2008). The titin Ig domain has been shown to respond first to the passive force by changing their alignment. If the muscle is stretched further, the PEVK domain can extend and furthermore the Ig domain is also able to unfold allowing further extension of the titin spring (Fukuda and others, 2005; Helmes and others, 1999).

Furthermore, the titin filament is also responsible for generating a restoring force pushing the Actin fibres away from the Z-disc, increasing the myosin/Actin overlapping area and re-establishing the original structure and length of the sarcomere (Helmes and others, 1996)

More recently, a role for titin in myofibrillogenesis was also reported (Gregorio and others, 1999; Holtzer and others, 1997; Turnacioglu and others, 1997a; Turnacioglu and others, 1997b).

1.9 Muscle contraction

Muscle contraction is needed to generate force to mediate various processes inside the organism's body. For example, muscle contraction in skeletal muscles mediates movement, while contraction of cardiac muscle is needed to provide a constant circulation of blood.

Muscle contraction was first described as the sliding of the Actin and myosin filaments due to cross-bridges formed between the myosin from the A-band with specific binding sites in the actin filaments (Huxley, 1957). Since then the two-filament model has been reviewed and refined (Herzog and others, 2012). With the revelation of the structure of the myosin head bound to its attachment site in the Actin filament, a more detailed model for the formation of cross-bridges was described (Rayment and others, 1993). Not only did this model describe how the sliding of the two filaments was regulated, it also explained how ATP hydrolysis was involved in generating the energy for muscle contraction.

Actomyosin complex formation and muscle contraction has been described to involve as 3-step process, which starts with the formation a collision complex between Actin and myosin, followed by a direct interaction of both (attached state), which then in turn is coupled to ATP hydrolysis, as myosin bound to ATP is inhibited from binding to Actin (Geeves and Conibear, 1995; McKillop and Geeves, 1993). Following the formation of the attached state, muscle contraction takes place and subsequently both the Actin and myosin filament dissociate (rotated state) (Geeves, 1991; Geeves and Conibear, 1995)

Geeves and Conibear (1995) further reported that potentially two myosin heads are associated to one Actin binding site. However only one of these myosin heads is directly attached to the Actin filament, whilst the other stays detached.

Based and summarised on published data, muscle contraction can be described as follows (Alberts and others, 1994):

Muscle contraction is initiated by an action potential, which triggers the release of Calcium-ions from the sarcoplasmic reticulum. Free Ca^{2+} is subsequently bound to troponin C, which leads to a rearrangement of the tropomyosin/troponin complex along the Actin filaments and opens up binding sites for myosin in the Actin filament (Farah and Reinach, 1995; Gordon and others, 2000; Perry, 2001; Squire, 1997). The myosin head can now bind to Actin and formation of the actomyosin complex leads to the activation of the ATPase. ATP is subsequently hydrolyzed within the catalytic site of the myosin head and a weak association of the myosin head and the Actin filament is initiated. Release of the inorganic phosphate (Pi), which was also reported to interact with the Actin polymer, leads to strengthening of the interaction between myosin and Actin. Furthermore, the ADP is released changing the conformation of the myosin head triggering a pulling action along the Actin fibres, called the power-stroke. The myosin head will stay interlocked with the Actin filament until a new ATP molecule is bound. Upon binding of ATP, the myosin head undergoes structural changes releasing it from its Actin binding site and allowing it to travel along the Actin fibres towards a new Actin binding site. Once the myosin head is close to a further Actin binding site, the ATP cycle starts again and ATP hydrolysis will eventually trigger a further power stroke (see figure 1.9).

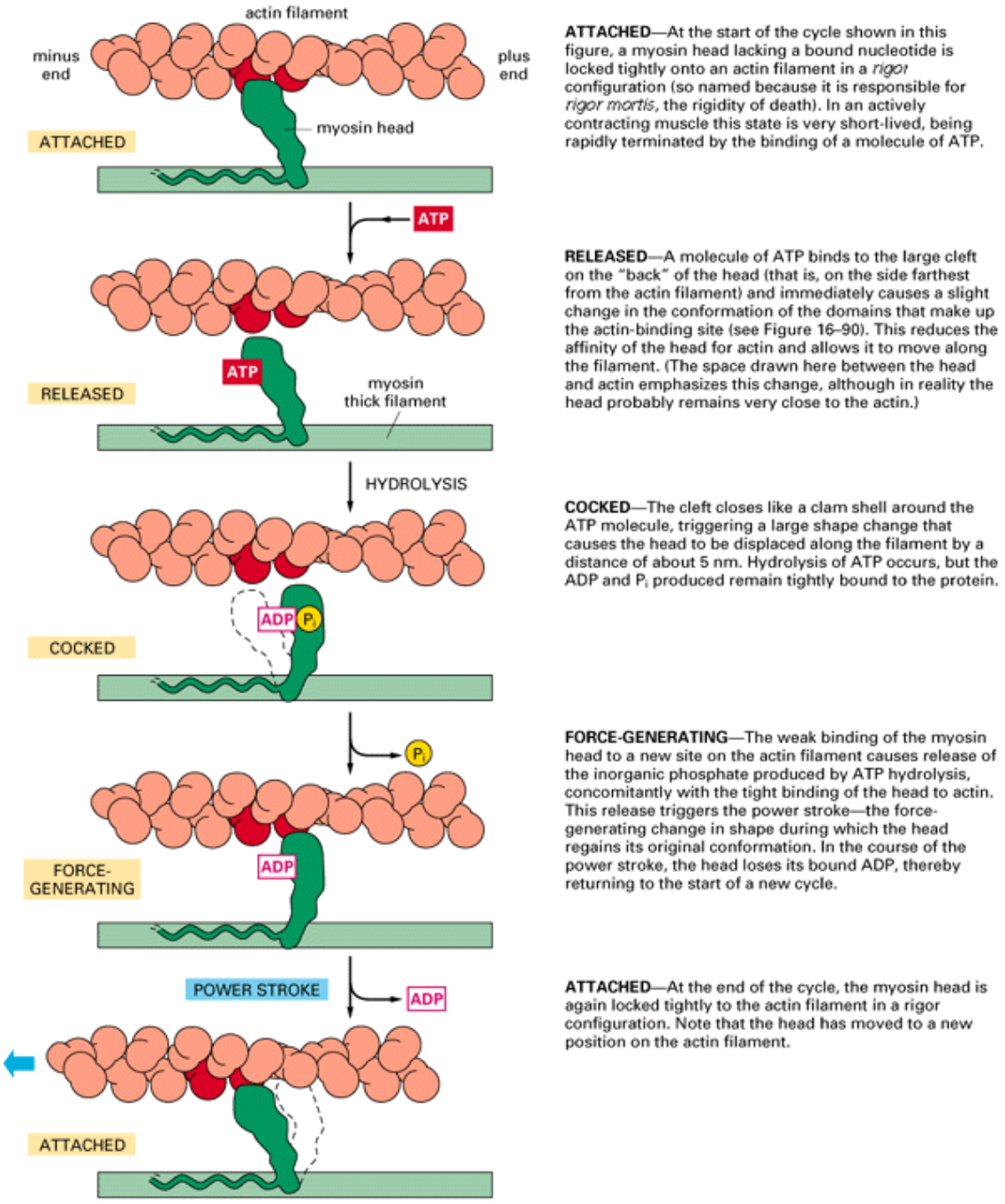

Figure 1.9: The Actomyosin complex during muscle contraction

A myosin head binds to the Actin filament. Upon release of Pi, structural changes in the myosin head occurs leading to the establishment of a strong Actin/myosin interaction and force generation. The obtained force is used upon ADP release to mediate a power stroke initiating muscle contraction.

Figure taken from Alberts and others, 1994 and based on Rayment and others, 1993

1.10 Kelch

Kelch was first identified in *Drosophila melanogaster* and based on its specific kelch-repeats domain further Kelch-like and Kelch-related proteins have been found (Adams and others, 2000; Xue and Cooley, 1993)

1.10.1 Kelch

As mentioned previously, Kelch was first identified in *Drosophila melanogaster* (Schupbach and Wieschaus, 1991; Xue and Cooley, 1993). It was reported that drosophila females bearing a mutation in the kelch gene are sterile due to insufficient cytoplasm transport throughout oogenesis (Schupbach and Wieschaus, 1991; Xue and Cooley, 1993). Cytoplasm transport from nurse cells to the oocyte in drosophila takes place along intercellular bridges, also known as ring canals, and transport of cytoplasm is important for the oocyte as with the cytoplasm the oocyte receives mRNAs, proteins and organelles needed for its development (Mahajan-Miklos and Cooley, 1994). It was shown that ring canals in egg chambers of *Kelch*-mutant drosophila contained all necessary cytoskeletal protein except Kelch, but the proteins of specifically the inner rim of the ring canal, such as Actin and HTS, were disorganized (Robinson and others, 1994; Tilney and others, 1996). It was reported that the Actin cytoskeleton was affected the most, as Actin-filament bundles were shown to grow into the lumen of the ring canal thereby partially blocking the lumen and preventing the influx of cytoplasm into the oocyte (Robinson and others, 1994; Tilney and others, 1996). Kelch was named based on the shape of sterile eggs affected by Kelch-mutation as sterile oocytes displayed a cup-like egg shell structure (Kelch is a German word for a goblet or cup) (Xue and Cooley, 1993). The structure of Kelch was analysed further revealing an N-terminal BTB-domain and six C-terminal Kelch repeats (Robinson and Cooley, 1997). Furthermore it was suggested that Kelch based on its structure and its mutation phenotype could organize the Actin filament of the ring canals by cross-linking Actin bundles. It was additionally reported that both the BTB domain and the Kelch-repeats were involved in binding to the Actin filament and that Kelch might function as a dimer being linked via its BTB-domains (Robinson and Cooley, 1997). Recently Robinson

and Cooley's hypotheses were tested and confirmed by (Kelso and others, 2002). However, Kelso et al. (2002) also found a temporal correlation between the Arp2/3 complex function in potentially de novo actin polymerization and Actin cross-linking properties by Kelch. But it is not clear yet, how this correlation is mediated.

More recently a role for Kelch as part of a Cullin3-RING ubiquitin ligase complex was reported suggesting that Kelch might target ring canal proteins other than Actin for ubiquitinylation and subsequent protein degradation (Hudson and Cooley, 2010).

1.11 The structural domains of Kelch

Drosophila Kelch protein was shown to contain an N-terminal BTB domain and C-terminal Kelch repeats (Robinson and Cooley, 1997). Since the discovery of Kelch, 41 Kelch-like proteins have been identified in human beings displaying the same structural properties (http://www.genenames.org/genefamilies/KLHL).

1.11.1 Structure and function of the BTB domain

The BTB/POZ domain has first been identified in *Drosophila melanogaster* and was later described to be a conserved motif, which has also been found in bric-à-brac, tramtrack and broad complex transcription (BTB) regulators and various pox virus and Zinc-finger (POZ) proteins (Bardwell and Treisman, 1994; Robinson and Cooley, 1997; Xue and Cooley, 1993; Zollman and others, 1994).

The core part of the BTB domain was termed the BTB fold and was shown to contain a 95 amino acid cluster of 5 α-helix structures, which is capped by a short three-stranded β-sheet. Both clusters are linked by an additional hairpin-like motif and an extended region (Stogios and others, 2005).

Interestingly though, although the tertiary structure of the BTB fold is very similar between all members of the BTB family, the amino acid sequences display little

similarity (Stogios and others, 2005). It was reported that the flexibility in the primary sequence of the fold allows the BTB domain to exhibit a huge array of functions.

BTB-domain containing proteins have been shown to be involved in transcriptional repression, cytoskeleton regulation, ion channel gating and most prominently in protein ubiquitinylation and degradation by binding associated proteins or substrates via the BTB-domain (Ahmad and others, 2003; Furukawa and others, 2003; Geyer and others, 2003; Kang and others, 2004; Kobayashi and others, 2004; Krek, 2003; Minor and others, 2000; Pintard and others, 2004; Xu and others, 2003).

However it was also suggested and proven for some BTB-proteins that, via its BTB-domain, Kelch and other related proteins can form homodimers (Chen and others, 2002; Robinson and Cooley, 1997; Stogios and others, 2005; Zhang and others, 2005).

1.11.2 Structure and function of the Kelch-repeats

Kelch contains six Kelch repeats and it was shown that other proteins containing kelch-repeats can have between 4 and 7 of these motifs (Bork and Doolittle, 1994; Robinson and Cooley, 1997).

The Kelch motif contains between 44-46 amino acids and the sequence identity between individual kelch-repeats is again rather low (Bork and Doolittle, 1994). However, the primary structure has some highly conserved features. It was shown that the centre of a kelch-repeat domain comprises eight conserved residues; four hydrophobic amino acids followed by two glycine residues and two aromatic amino acids. Structural analysis of crystals of kelch motifs revealed that seven of described kelch-repeats collectively form a β-propeller, wherein each single kelch motif folded as a four-stranded β-sheet makes up on blade of the propeller (Ito and others, 1994; Li and others, 2004). The propeller structure is assembled around a central axis and is closed by an interaction between the first and the last blade of the propeller (Adams and others, 2000) (see figure 1.10).

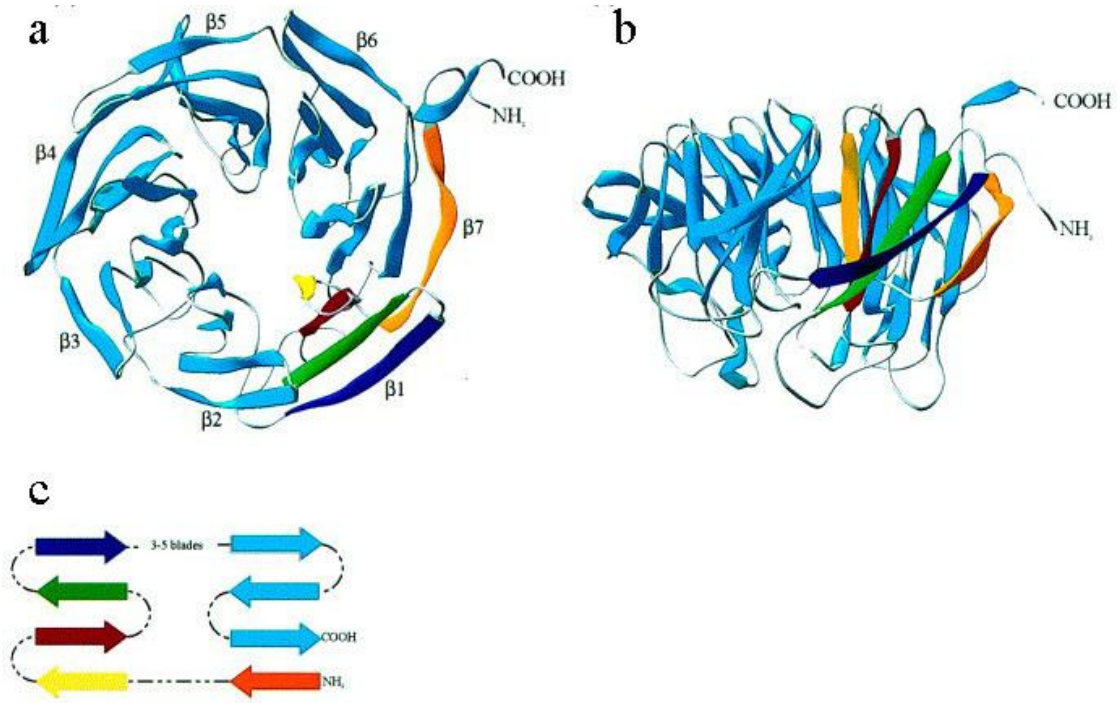

Figure 1.10: The β-propeller of the kelch-repeats

B-propellers consist of 7 kelch-repeats (β1-β7).

(a) View from the top inside a β-propeller based on the crystal structure for the galactose oxidase from hypomyces rosellus. The β-propeller contains 7 kelch-repeat blades

(b) Side view of the galactose oxidase β-propeller as seen in (a)

(c) The ring of the galactose oxidase β-propeller is closed by an N-terminal β4 strand (orange)

Figure modified from Adams and others, 2000

Many Kelch motif containing proteins have been characterised and their function varies just as their sequence similarities vary, including being part of a virus, transcriptional repression, for example Leucine-zipper-like transcriptional regulator 1 or muscle specific function, e.g. like sarcosin, which is involved in myofibrillogenesis (Adams and others, 2000; Goebel and others, 1990; Kurahashi and others, 1995; Paxton and others, 2011; Taylor and others, 1998). A number of Kelch motif containing proteins have been shown to associate with the Actin cytoskeleton (Chen and others, 2002; Kim and others, 1999; Robinson and Cooley, 1997; Sasagawa and others, 2002; Schmid and others,

1994; Soltysik-Espanola and others, 1999; Way and others, 1995), whilst others influence the cytoskeleton indirectly without associating to Actin (Adams and others, 1998; von Bulow and others, 1995).

1.12 The Kelch-like protein family

Kelch-like (Klhl) proteins contain both described structural domains, i.e. the BTB/POZ domain and the Kelch-repeats. As more Kelch-like proteins were analysed it was shown that Klhl proteins are conserved in nearly all eukaryotes (Adams and others, 2000; Robinson and Cooley, 1997).

1.12.1 The structure of Kelch-like proteins

Like BTB-containing proteins, Kelch-like proteins have been shown to be involved in targeting various substrates for ubiquitinylation and subsequent proteasomal degradation as part of an E3 ubiquitin ligase complex (Angers and others, 2006; Furukawa and Xiong, 2005; Maerki and others, 2009; Salinas and others, 2006; Sambuughin and others, 2012; Zhang and others, 2004). Furthermore, several Klhl proteins bind to Actin via their Kelch-repeats (Aromolaran and others, 2012; Chen and others, 2002; Hara and others, 2004; Kim and others, 1999; Soltysik-Espanola and others, 1999).

Based on structural analysis of both, the Kelch-repeats and BTB domain a model for dimerization and formation of a Cullin based E3- ubiquitin ligase complex was described (Stogios and others, 2005). Dimerization was reported to occur at the BTB domain, whilst the Kelch-repeats are thought to be involved in binding of the ligands, such as Cullin-3 (Stogios and others, 2007; Stogios and others, 2005). Between the N-terminal BTB domain and the Kelchlike repeats at the C-term, a linker domain, the BACK-domain, can be found. The model described above suggests a role of the BACK domain in positioning bound substrate in the vicinity of the Cul3-ligase complex, but

the function of the BACK domain has so far not been proven due to the lack of a crystal structure of this domain (Stogios and others, 2005). Recently, Klhl proteins as part of an E3 ubiquitin ligase complex have been described in more detail and data obtained from functional and structural studies helped describing a better picture of the role of Kelch-like proteins as part of proteasomal degradation processes (Canning and others, 2013)

1.12.2 Ubiquitinylation as a code for protein degradation

Ubiquitinylation is a process used in cells to encode information about the fate of proteins. In general, ubiquitinylation is a process involving three types of enzymes; the ubiquitin-activating enzymes (E1), the ubiquitin-conjugating enzymes (E2) and the ubiquitin ligase enzymes (E3) (Komander and Rape, 2012). Ubiquitin is first activated by the E1 enzyme in an ATP-dependent manner, which involves the transfer of ubiquitin to an active site cysteine of an E2 enzyme. The E3 enzyme subsequently catalyzes the transfer of the activated ubiquitin from the E2 to a substrate lysine residue (Hershko and Ciechanover, 1998; Schulman and Harper, 2009).

Initially the target protein will be mono-ubiquitinylated. Later lysine-residues in the attached ubiquitin-molecule will subsequently by ubiquitinylated as well (Komander and Rape, 2012). The generated ubiquitin-chains can vary in length and can be linear or branched. Within these ubiquitin chains, it was suggested, lies a code that determines the future of the ubiquitinylated protein, for example Lys11- linked ubiquitin-chains mediate proteasomal degradation, while Lys63 ubiquitinylation is linked with kinase activation and Met1-linked chains are involved in regulating NF-κB signalling (Deng and others, 2000; Jin and others, 2008; Rahighi and others, 2009).

As mentioned before ubiquitin will eventually be ubiquitinylated itself in distinct pattern, e.g. in a linear or branched pattern. This is possible as ubiquitin contains 7 lysine residues along it N-terminus, which all point into a different directions (Komander and Rape, 2012). Which type of ubiquitinylation is used on specific substrates is coordinated by the co-operation of E2 and E3 enzymes.

The ubiquitin-code for proteasomal degradation has been studied in yeast and was shown to start with the mono-ubiquitinylation of Lys48 (Chau and others, 1989). This

was later shown to be the case in other eukaryotes as well (Li and others, 2007; Petroski and Deshaies, 2005b). It was later reported that mono-ubiquitinylation at Lys11 residues could also trigger a proteasomal response (Jin and others, 2008; Matsumoto and others, 2010). Some E3 Ubiquitin ligase enzymes not only mediate ubiquitinylation, they also bind to the proteasome to link ubiquitinylation and proteasomal degradation of targeted proteins (Seeger and others, 2003; Verma and others, 2000).

Members of the Kelch-like family belong to a group of proteins that are subunits of Cullin-really interesting new gene (RING) E3 ubiquitin ligase (CRL) complexes (Angers and others, 2006; Canning and others, 2013; Kigoshi and others, 2011; Lee and others, 2010; Maerki and others, 2009; Moghe and others, 2011; Nam and others, 2009; Ohta and others, 2013; Sumara and others, 2007). CRLs, depending on present subunits and their spatial arrangements, can modify various distinct proteins (Canning and others, 2013). CRLs furthermore contain a Cullin-subunit (Cul 1-5 or Cul7). Cullins have been reported to form a scaffold, which is involved in placing the substrate binding site and other catalytic centres in the right orientation for ubiquitinylation of the target protein (Petroski and Deshaies, 2005a; Zimmerman and others, 2010). Also the Cullin subunit has been reported to be able to bind to both the target protein and the RING protein, which itself can then associate with an E2 enzyme (Canning and others, 2013; Zimmerman and others, 2010). Furthermore Neddylation (NEDD8 in CRLs) of the carboxy terminus of the Cullin subunit is a requirement for ubiquitinylation as it mediates structural changes in the CRL complex allowing the E2 enzyme and the substrate to locate in close vicinity to each other (Duda and others, 2008; Saha and Deshaies, 2008).

Kelch-like proteins and in general proteins containing a BTB-domain bind to Cullin3 as their CRL subunit (Pintard and others, 2004). Cullin3 based E3 ubiquitin ligase complex containing BTB-proteins differ distinctively from other known E3 enzymes as they can form dimers, which allows them to bind to two Cullin subunits and as they also usually contain a second substrate binding domain. Therefore the Klhl/ BTB-domain containing protein in the CRL can act both as a substrate recognition element and a substrate adaptor for E3 ubiquitin ligase complexes (Canning and others, 2013; Pintard and others, 2004).

1.12.3 Functions of Kelch-like proteins

As mentioned previously, various functions for Kelch-like proteins have been described in vertebrates. A muscle-specific protein of the Kelch related protein family is Kelch-related protein 1 (Krp1) or Sarcosin. Although not named a member of the Klhl protein family, Sarcosin too has the defined protein domains that characterise Kelch-like proteins, an N-terminal BTB domain and five C-terminal Kelch-repeats (Spence and others, 2000; Taylor and others, 1998). Sarcosin was reported to be expressed in skeletal muscle and at much lower levels in the cardiac muscles (Taylor and others, 1998) and it was suggested that it might play a role in myofibrils as it was shown to interact with Nebulin and Nebulin-related anchoring protein (N-RAP) (Lu and others, 2003; Spence and others, 2006). Expression studies in mouse muscles, which were carried out in embryonic and adult muscles revealed that Sarcosin is highly expressed between laterally fusing nascent myofibrils (du Puy and others, 2012). Furthermore studies in C2C12 cell culture showed that *Sarcosin* was expressed in low levels in myoblasts and was upregulated during later stages of muscle differentiation (du Puy and others, 2012). At around day 3 of C2C12 differentiation Sarcosin was shown to align to α-Actinin along primitive Z-discs. However although Sarcosin expression seemed to be linked to myofibrillogenesis, a silencing approach of Sarcosin during C2C12 differentiation did not disturb C2C12 fusion and myofibrillogenesis (du Puy and others, 2012). It was therefore thought that Sarcosin might be involved in mediating the correct function of sarcomeres, rather than its assembly.

Kelch-like ECH associating protein 1 (Keap1) has been shown to control the expression of antioxidant genes by targeting the transcriptional factor Nrf2 for ubiquitinylation and subsequent degradation (Furukawa and Xiong, 2005). Further E3-Ubiquitin-ligase associated Klhl proteins include among others Klhl20, Klhl21 and Klhl9 and Klhl13. It has been described that Klhl20 binds to Death-associated protein kinase (DAPk), locating it close to a Cul3-E3-Ligation complex, which subsequently leads to the proteasome-dependent degradation of the DAPk (Lee and others, 2010). Functions for Kelch-like proteins have also been described in the regulation of cell division. Klhl21/Klhl22 could be shown to be involved in the completion of cytokinesis by mediating ubiquitinylation of Aurora B (Maerki and others, 2009). A similar role was described for Klhl9 and Klhl13 in the ubiquitinylation of Aurora A (Sumara and others,

2007). It has been observed that the Cul3-Klhl9/Klhl13-E3 and the Cul3-Klhl21/Klhl22-Ubiquitin ligase complex are involved in aligning the chromosomes to the midline during anaphase (Maerki and others, 2009; Sumara and others, 2007). Recently Klhl12 has been shown to be involved in the regulation of Wnt-β-catenin signalling by targeting dishevelled for ubiquitinylation (Angers and others, 2006).

Table 1.1: Members of the Kelch-like protein family

Various Klhl proteins have different functions and few have been described to associate to the Actin cytoskeleton. The following list gives an overview of function and localisation of published Kelch-like proteins.

Legend: 'x' confirms an existing interaction with Actin or a reported function as an E3- Ubiquitin Ligase, KR-Kelch-repeats

Gene	alternative name	Actin-binding	Actin binding domain	E3-Ubiquitin-Ligase function	Function	Literature
Kelch-like 1	MRP2	x	KR	not reported	Klhl1 is an actin-binding protein in neuronal tissues. Klhl1 modulates calcium channel activity/calcium influx. Klhl1 may also be involved in mediating neurite outgrowth of oligodendrocytes in a GSK3β-dependent manner.	Aromolaran and others, 2010; Aromolaran and others, 2012
Kelch-like 2	Mayven	x	KR	x	Klhl2 is an actin-binding protein involved in regulating outgrowth in oligodendrocytes. It also has been shown to target neuronal pentraxin for ubiquitinylation.	Tseng and Bixby, 2011; Williams and others, 2005
Kelch-like 3		not reported		x	Klhl3 in a Cul3-Klhl3 E3 ligase complex has been shown to regulate blood pressure by interacting with / and ubiquitinylating of WNK isoforms.	Louis-Dit-Picard and others, 2012; Ohta and others, 2013
Kelch-like 4		not reported		not reported	Klhl4 mutation can cause X-linked cleft palate (CPX), a rare non-syndromic form of orofacial clefting.	Braybrook and others, 2001; Cheroki and others, 2008
Kelch-like 5		x	not reported	not reported	Klhl5 might participate in cytoskeletal reorganization as a part of platelet activation. Klhl5 expression is regulated by miR-495.	Nagalla and others, 2011
Kelch-like 6		not reported		not reported	A mutation in Klhl6 causes defects in B-lineage cells and might therefore play a role in the immune system by mediating BCR signal transduction.	Kroll and others, 2005
Kelch-like 7		not reported		x	Mutations Klhl7 cause autosomal-dominant retinitis pigmentosa.	Friedman and others, 2009; Kigoshi and others, 2011

Kelch-like 8		not reported		x	Klhl8 is involved in ubiquitinylation of rapsyn and GLR-1 receptors.	Nam and others, 2009; Schaefer and Rongo, 2006
Kelch-like 9		not reported		x	Klhl9 mutation leads to slow progressing distal myopathies. Furthermore it was reported that Klhl9 is important for completion of cytokinesis by regulating Aurora B dynamics.	Cirak and others, 2010; Sumara and others, 2007
Kelch-like 10		not reported		not reported	Mutations in Klhl10 are linked to male infertility (process not completely understood).	Kaplan and others, 2010; Qiu and others, 2009
Kelch-like 11		not reported		not reported	Klhl11 is downregulated in human colorectal cancer.	Cekanova and others, 2008
Kelch-like 12		not reported		x	Klhl12 targets dishevelled for ubiquitinylation (thereby negatively regulating Wnt-signalling) and has also been shown to interact with/ target the dopamine D4 receptor and SEC31 for ubiquitinylation.	Angers and others, 2006; Jin and others, 2012; Rondou and others, 2011
Kelch-like 13		not reported		x	Klhl9 and Klhl13 are both part of a Cul3-Ubiquitin ligase complex which is required for the chromosome alignment during metaphase and completion of cytokinesis. The Cul3-Ubiquitin ligase complex removes components of the chromosomal passenger complex, such as Aurora B from mitotic chromosomes thereby allowing their accumulation on the central spindle during anaphase. Furthermore Aurora B is bound directly by Klhl9/Klhk13.	Sumara and others, 2007
Kelch-like 14	Printor	not reported		not reported	Klhl14 interacts with torsinA in the brain.	Giles and others, 2009

Kelch-like 15		not reported		x	Klhl15 targets B'β, a subunit of the Protein phosphatase 2A, for ubiquitinylation and proteasomal degradation.	Oberg and others, 2012
Kelch-like 16	Gigaxonin	not reported		x	Mutations in Klhl16 lead to neurodegenerative disorders with alterations in the neurofilament network. It was furthermore shown that Klhl16 targets Tubulin Folding Cofactor B for ubiquitinylation and degradation.	Bomont and others, 2000; Ganay and others, 2011 ; Wang and others, 2005b
Kelch-like 17	Actinfilin	x	KR	x	Klhl17 targets GluR6 kainate receptor subunits for ubiquitinylation and degradation. It was further suggested that Klhl16 regulates the stability of the actin cytoskeleton in neurons.	Chen and Li, 2005; Salinas and others, 2006
Kelch-like 18		not reported		x	Klhl18 is required for the timely entry into mitosis by potentially ubiquitylating and activating Aurora-A.	Moghe and others, 2011
Kelch-like 19	KEAP 1, Inhibitor of Nrf2 (INrf2)	not reported		x	Klhl19 represses Nrf2 activation Nrf2 regulates expression of genes of the antioxidant-response element (ARE), such as phase II detoxifying and oxidative stress enzymes.	Tkachev and others, 2011; Villeneuve and others, 2010
Kelch-like 20	KLEIP	x	KR	x	Klhl20 negatively regulates Death-associated protein kinase (DAPK).	Hara and others, 2004; Lee and others, 2010
Kelch-like 21		not reported		x	The Cul3-Klhl21 E3-ubiquitin ligase targets aurora B for ubiquitinylation and is required for cytokinesis by regulating the localisation of the chromosomal passenger complex to the microtubular midzone during anaphase.	Maerki and others, 2009
Kelch-like 22		not reported		x	The Cul3- Klhl22 E3-ubiquitin ligase targets aurora B for ubiquitinylation and is required for cytokinesis by regulating the localisation of the chromosomal passenger complex to the microtubular midzone during anaphase.	Maerki and others, 2009

Kelch-like 23		not reported		not reported	Klhl23 might be involved in autosomal dominant cone-rod dystrophy.	Manes and others, 2011
Kelch-like 24	DRE1, KRIP6	not reported		not reported	Klhl24 regulates kainate receptors by directly binding to its subunit GluR6 and by inhibiting modulation of the kainate receptor by PICK1.	Laezza and others, 2007; Laezza and others, 2008
Kelch-like 25	Ectoderm-neural cortex protein 2					
Kelch-like 26		not reported		not reported	Klhl26 might be regulated by P53.	Simeonova and others, 2012
Kelch-like 27	IPP, intracisternal A particle-promoted polypeptide	x	KR	not reported	Klhl27 is activated by calphoglin, a mediator of Ca^{2+} mammalian cell activation.	Kim and others, 1999
Kelch-like 28	btbd5					
Kelch-like 29						
Kelch-like 30						
Kelch-like 31					Klhl31 might play vital roles during muscle and heart development. It might also be an inhibitor of canonical Wnt –signalling.	Abou-Elhamd; Abou-Elhamd and others, 2009; Yu and others, 2008
Kelch-like 32						
Kelch-like 33						
Kelch-like 34						
Kelch-like 35		not reported		not reported	Klhl35 is methylated in hepatocellular carcinoma and in renal cell carcinoma.	Morris and others, 2011; Shitani and others, 2012
Kelch-like 36						
Kelch-like 37	ENC1, Klhl35					

Kelch-like 38						
Kelch-like 39	influenza virus NS1A binding protein, IVNS1ABP, NS1-BP			not reported	Klhl39 interacts with alpha-enolase/MBP-1 and might be involved in c-Myc gene transcriptional control. Klhl39 also binds to the NS1 protein of the influenza A virus.	Perconti and others, 2007; Wolff and others, 1998
Kelch-like 40	sarcosynapsin, kbtbd5					
Kelch-like 41						

In summary, recent findings suggested that Kelch-like proteins can be involved in mediating cell signalling, as well as various cellular processes and cytoskeletal changes. In some of these functions, Kelch-like proteins have been shown to regulate associated protein levels, especially by targeting specific substrates for ubiquitin-dependent degradation.

1.13 Klhl31

Klhl 31 was first described in zebrafish showing high expression in cardiac and skeletal tissues (Wu and Gong, 2004). It was also observed that *Klhl31* is also expressed in human skeletal muscles and the heart. Further studies on human Klhl31 revealed that *Klhl31* encodes for a 70 kDa protein containing 634 amino acids (Yu and others, 2008). Klhl31 was shown to contain an N-terminal BTB-domain and six kelch-like repeats at the carboxy-terminus (see figure 1.11).

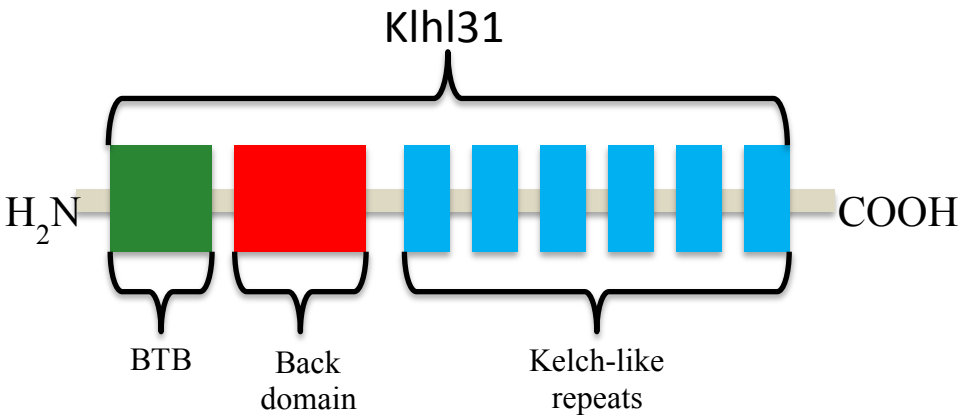

Figure 1.11: Schematic representation of the human Klhl31 protein

Klhl31 contains two conserved structural domains, the BTB domain at the N-terminus and six kelch-like repeats at the C-terminus, linked by the BACK domain.

Expression studies showed that Klhl31 was highly expressed in human cardiac and skeletal muscle tissues. Localisation studies in Cos-7 cells and mouse cardiomyocytes revealed a cytoplasmic and nuclear localisation for Klhl31 (Yu

and others, 2008). Furthermore it was reported that Klhl31 could act as transcriptional repressors for TRE and SRE-mediated transcriptional activation with the BTB-domain being the main domain involved. In addition, Klhl31 was also able to decrease MAPK/JNK-signalling (Yu and others, 2008).

Data obtained in our lab further analysed a role for *Klhl31* during muscle development (Abou-Elhamd and others, 2009). Expression studies in chick embryos showed that *Klhl31* is first detected at Hamburger-Hamilton (HH) stage 8 (Hamburger and Hamilton, 1992) in the mesoderm of the anterior intestinal portal (figure 6.3; a). Cardiac progenitors express *Klhl31* from HH stage 9 onwards and the gene is expressed throughout heart development. *Klhl31* was also shown to be expressed in the myotome and later in development in all skeletal muscles tissues, including muscles of limbs (see figure 1.12).

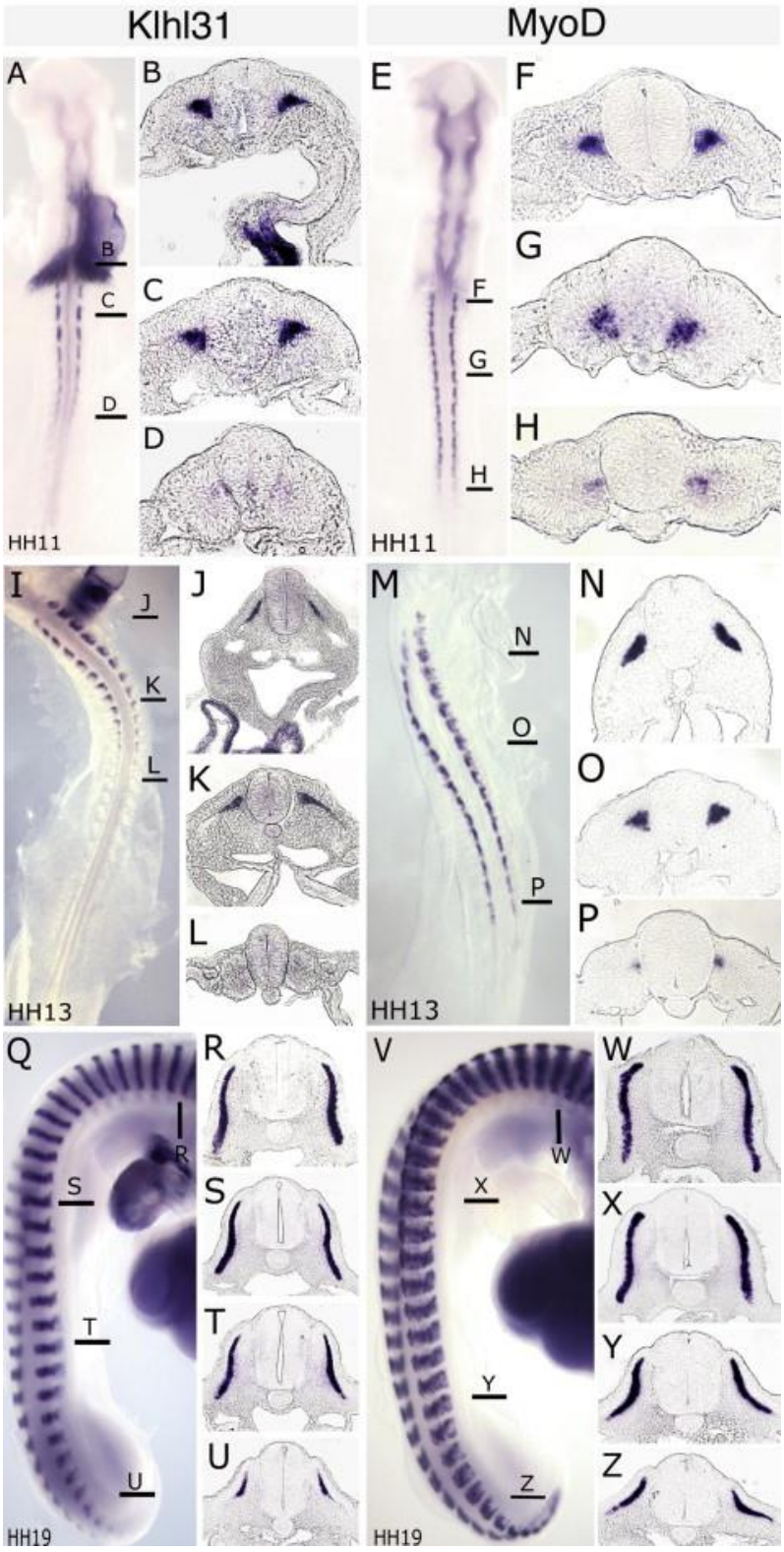

Figure 1.12: expression pattern of Klhl31in chick embryos compared to the expression of MyoD

Whole mount in-situ hybridisation of chick embryos for Klhl31 and MyoD and related cryosections revealing the expression pattern of Klhl31 during myogenesis.

(C, D; E-H) Klhl31 was observed first in the dorsomedial somite at around HH 11, temporally delayed compared to the expression of MyoD.

(I-K; M-P) At HH 13 Klhl31 was still seen to be expressed in the somites, still lacking behind MyoD expression.

(Q-U; V-Z) During later stages of Klhl31 expression (HH 19+), Klhl31 expression overlapped with MyoD expression.

Figure taken from Abou-Elhamd and others, 2009

Tissue ablation and rescue experiments showed that in the myotome *Klhl31* is activated by combined signalling of sonic hedgehog together with either Wnt-1 or Wnt-6 (Abou-Elhamd and others, 2009). Furthermore, ectopic expression of Myf 5, but not of myogenin, was able to induce Klhl31 expression in the neural tube (Abou-Elhamd). Comparing the temporal expression of Klhl31 with known myogenic markers, such as MyoD, it was shown that Klhl31 expression was detected 6 hours after MyoD expression (see figure 1.12). This data, together with the suggestion that Klhl31 expression might be activated by early MRFs, lead to the hypothesis that Klhl31 expression might be important for myogenesis and myogenic differentiation in skeletal muscles of the somites.

Further data obtained in our lab indicated a role of *Klhl31* in the negative regulation of Wnt signalling. Klhl31 was able to rescue an ectopic axis induced by injection of Wnt3a or β-catenin RNA into the ventral side of a *Xenopus laevis* embryo (Abou-Elhamd and Garcia-Morales). Furthermore, by using a luciferase assay, it was shown that Klhl31 can inhibit the expression of a reporter plasmid (TOPFLASH) responsive to Wnt3a and β-catenin (see figure 1.13; (Abou-Elhamd)

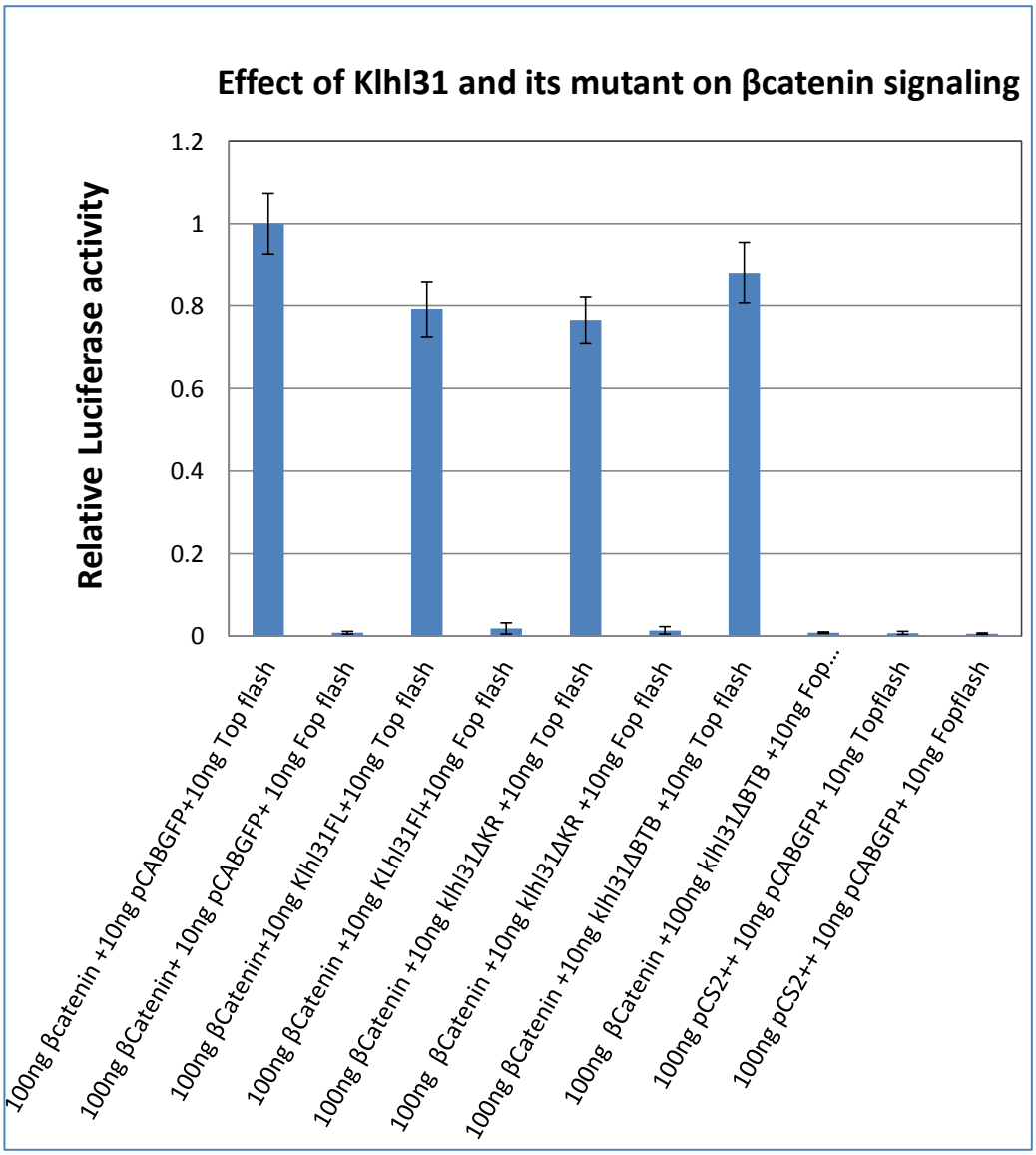

Figure 1.13: Klhl31 can inhibit β-Catenin induced luciferase activity

Klhl31 full length protein and Klhl31 lacking the C-terminal kelch-repeats were able to inhibit β-catenin stimulated luciferase expression by around 20 %, whilst a BTB deletion mutant of Klhl31 could only inhibit luciferase activity by around 10%.

Figure kindly provided by Dr. Alaa Abou-Elhamd

Both, the luciferase assay and the axis-duplication assay highlighted the functions of the distinct structural domains of Klhl31 (see figure 1.13; (Abou-Elhamd). Only the deletion of the BTB domain reduced the ability of Klhl31 to antagonize canonical Wnt-signalling, revealing that interaction between a target substrate and Klhl31 is potentially mediated by the BTB domain. However, it is still not clear if Klhl31 targets β-catenin directly or a potential substrate downstream of β-catenin in the Wnt-signalling pathway.

1.14 Aims of this project: Investigating the role of Klhl31 during myogenesis

Klhl31 expression during development is highly restricted in heart and skeletal muscles. In developing somites it has been shown to be activated by signalling factors, including Wnt signals, which also activate early MRFs and regulate cardiac fate (Abou-Elhamd and others, 2009; Tzahor, 2007). However, a specific function for Klhl31 during muscle development has not been described so far.

We were interested in analysing the function of Klhl31 during skeletal muscle development on a cellular level.

Firstly, we wanted to analyse Klhl31 expression and localisation during differentiation of myogenic cells. We chose C2C12 cells, which have the potential to form multi-nucleated myotubes and which are a good tool to study myofibrillogenesis.

A further aim was to investigate potential interaction partners for Klhl31 during myogenesis and also in adult musculature. To achieve this, we used a Yeast-2-Hybrid screen and GST-pull down assays.

Selected hits from the screens were analysed further with the aim to verify interactions with Klhl31.

As myogenesis and myofibrillogenesis also take place in cardiac muscle, we analysed Klhl31 expression in more detail during chick cardiogenesis.

Overall the work contributes novel insights into the possible role of Klhl31 during striated muscle development.

2. Material and Methods

2.1 Materials

2.1.1 Chemicals, Biochemicals and Services

Chemicals used in the laboratory were purchased from Sigma-Aldrich (Sigma-Aldrich Company Ltd, Dorset, UK), Fisher Scientific (Fisher Scientific UK Ltd, Loughborough, UK), Roche (Roche Diagnostics Ltd, Burgess Hill, UK), BDH (VWR International Ltd., Lutterworth, UK) and Melford (Melford Laboratories Ltd., Ipswich, UK).

Kits for Mini- , Midi-, or Hi-speed purification of DNA were obtained from Qiagen (Qiagen Ltd, Crawley, UK).

Restriction enzymes and buffers were purchased from either Roche (Roche Diagnostics Ltd, Burgess Hill, UK) or NEB (New England Biolabs (UK) Ltd, Wilbury Way Hitchin, UK).

Fertilized eggs were ordered from Henry Stewart & Co. Ltd (Louth, Lincolnshire, UK).

Designed primers were obtained from Operon (Eurofins MWG Operon, Ebersberg, Germany).

Sepharose beads for GST-pull down were purchased from GE Healthcare Life Sciences Amersham (GE Healthcare Life Sciences Amersham, Place little Chalfont, Buckinghamshire, UK).

Sequencing was carried out by DNA Sequencing & Services (Dundee, Scotland, UK) and the Yeast-2-Hybrid Screen was carried out by Hybrigenics (Hybrigenics Services, Paris, France).

2.1.2 Frequently used Solutions

APS (Ammonium persulfate)

10% w/v APS

BCIP (5-bromo-4-chloro-3'-indolyphosphate p-toluidine salt)

50 mg/ ml BCIP in DMF

Coomassie Blue Staining Solution

10% v/v glacial acetic acid, 50% v/v Methanol, 0.25% w/v Coomassie brilliant Blue R-250

DAPI (4', 6-diamidino-2-phenylindole)

5 mg/ml in PBS

Destain Solution for SDS-PAGE Gels (Coomassie-Blue staining)

7.5% v/v glacial acetic acid, 25 % v/v Methanol

DIG (Digioxigenin) labelled NTP mixture

10 mM ATP, 10 mM GTP, 10 mM CTP, 6.5 mM UTP, 3.5 mM DIG-11-UTP

DNA Loading Buffer 6x

50% v/v Glycerol, 0.1% w/v Bromophenol-Blue, 0.1% w/v Xylene Cyanol

dNTP mix 10 mM in sigma water

10 mM ATP, 10 mM TTP, 10 mM GTP, 10 mM CTP

Fixing solution for SDS-PAGE Gels (prior to Coomassie-Blue staining)

10% v/v glacial acetic acid, 50 % v/v Methanol

Gelatine

0.3% w/v Gelatine (autoclaved)

Hybridisation Mix

50% v/v Formamide, 1.3 x SSC, 5mM EDTA pH8, 50µg/ml Yeast RNA, 0.2% v/v Tween-20, 0.5% w/v CHAPS, 100µg/ml Heparin

IPTG (Isopropyl β-D-1-thiogalactopyranoside)

200 mg/ml

LB (Luria-Bertani) -Agar

1.5% w/v bacto-agar in LB-Medium (autoclaved)

LB (Luria-Bertani) Medium

1% w/v bacto-tryptone, 1.5% w/v bacto-yeast extract, 1% w/v NaCl, pH 7.5 (autoclaved)

MABT

100mM maleic acid, 150mM NaCl, 0.1% v/v Tween-20, pH 7.5 (autoclaved)

MABT-BBR

MABT, 2% w/v Boehringer Blocking Reagent (BBR)

$MgCl_2$ (Magnesium Chloride)

2 M $MgCl_2$

Mild Lysis Buffer (for GST Pull-down assays)

50mM Tris pH 7.5, 150mM NaCl, 5mM EDTA pH7.5, 1% v/v NP-40, 10% v/v Glycerol, 1mM Na_3VO_4, 1mM PMSF, add 1 Complete Mini, EDTA-free Protease inhibitor cocktail tablet (Roche Diagnostics Ltd, Burgess Hill, UK) per 10ml of buffer

Mild stripping buffer pH 2.2

0.2M Glycine, 0.1% w/v SDS, 1% v/v Tween-20

Mild washing buffer (for GST Pull-down assays)

50mM Tris pH 7.5, 150mM NaCl, 5mM EDTA pH7.5, 0.1% v/v NP-40, 10% v/v Glycerol, 1mM Na_3VO_4, 1mM PMSF

NaF (Sodium Fluoride)

100 mM NaF

NaCl (Sodium Chloride)

5M NaCl (autoclaved)

NaOAc (Sodium Acetate)

3M CH_3COONa pH 5.2

Na_3VO_4 (Sodium Vanadate)

100 mM Na_3VO_4

NBT (nitro-blue tetrazolium chloride)

75 mg/ ml in 70% v/v DMF

NTMT

100mM NaCl, 100mM Tris pH 9.5, 50mM $MgCl_2$, 1% v/v Tween-20

PBS (Phosphate Buffered Saline)

0.14M NaCl, 2.5mM KCl, 8mM Na_2HPO_4, 1.5mM KH_2PO_4 pH 7.3 (autoclaved)

PFA (Paraformaldehyde)

4% w/v PFA in PBS

PMSF (Phenylmethylsulfonyl-fluoride)

200 mM in Ethanol

Ponceau-Red

0.1% w/v Ponceau S, 5% v/v acetic acid

Proteinase K

10 µg/ ml in PTW

Protein Loading Buffer 5x

25% v/v Glycerol, 200mM Tris, 5% w/v SDS, 0.1% w/v Bromophenol-Blue

Protein Lysis (RIPA) Buffer

50mM Tris pH 7.5, 150mM NaCl, 25mM EDTA, 1% v/v NP-40, 0.2% w/v SDS, 1mM DTT, add 1 Complete Mini EDTA-free Protease inhibitor cocktail tablet (Roche Diagnostics Ltd, Burgess Hill, UK) per 10ml of buffer

Protein Lysis Buffer for Klhl31

50 mM Tris pH 7.5, 150 mM NaCl, 5 mM EDTA pH 8, 1% v/v NP-40, 0.2% w/v SDS, 1 mM Na_3VO_4 (sodium vanadate), 1 mM NaF (sodium fluoride), add 1 Complete Mini EDTA-free Protease inhibitor cocktail tablet (Roche Diagnostics Ltd, Burgess Hill, UK) per 10ml of buffer and store at – 20 °C for up to 12 weeks. On the time of usage, defrost buffer, remove an aliquot with the volume needed and add PMSF to 1mM final concentration. Use Buffer immediately.

PTW

PBS, 0.1 % v/v Tween-20

SOC (Super Optimal Growth with Catabolic repression) Medium

2% w/v bacto-tryptone, 0.5% w/v bacto-yeast extract, 10mM NaCl, 2.5mM KCl, 10mM $MgCl_2$, 20mM Glucose (autoclaved)

SSC-Buffer 20x pH 5.0

3M NaCl, 0.3M Na Citrate ($Na_3C_6H_5O_7$ x $2H_2O$), adjust pH to 5.0 with citric acid (autoclaved)

STE Buffer

0.1M NaCl, 10mM Tris pH 8.0, 1mM EDTA pH 8.0

TAE Buffer

20 mM Tris pH 8.0, 1mM EDTA, 1 % v/v acetic acid

TBS (Tris buffered Saline) 10x

1.4 M NaCl, 0.2M Tris pH 7.5, 0.02M KCl (autoclaved)

TBST

1x TBS, 0.1% v/v Tween-20

TG (Tris –Glycine) 10x

0.25M Tris, 2M Glycine (autoclaved)

Wash Buffer (for GST-pull down)

50 mM Tris pH 7.5, 150 mM NaCl, 5 mM EDTA pH 8, 0.1% v/v NP-40, 0.2% w/v SDS, 1 mM Na_3VO_4 (sodium vanadate), 1 mM NaF (sodium fluoride), add 1 Complete Mini EDTA-free Protease inhibitor cocktail tablet (Roche Diagnostics Ltd, Burgess Hill, UK) per 10ml of buffer and store at – 20 °C for up to 12 weeks. On the time of usage, defrost buffer, remove an aliquot with the volume needed and add PMSF to 1mM final concentration. Use Buffer immediately.

Washing solution (for in situ hybridisation)

50% v/v Formamide, 1x SSC, 0.1% v/v Tween-20

Western blot colour development solution 1

0.1M Tris pH 8.8, 2.5mM Luminol, 0.4mM *p*-Coumaric acid

Western blot colour development solution 2

0.1M Tris pH 8.5, 0.02% v/v H_2O_2

Western blot lower gel buffer

1.5M Tris pH8.8

Western blot Running Buffer

1x TG, 0.1% w/v SDS

Western Blot Transfer Buffer

1xTG, 20% v/v Methanol

Western blot upper gel buffer

0.6M Tris pH6.8

X-Gal (5-bromo-4-chloro-indolyl-β-D-galactopyranoside)

20 mg/ml in DMF

2.2 Methods

2.2.1 Transformation of competent DH5α- cells

100 µl of chemically competent *E.coli* DH5α cells (Sambrook, 1989) were aliquoted into a 1.5 ml eppendorf tube and kept on ice. Up to 0.5µg of plasmid DNA were added to the cells and the mixture was incubated on ice for further 30 minutes. The heat shock treatment was carried out for 5 minutes at 37 °C followed by five minutes of further incubation on ice. After addition of 200µl of SOC-medium, the mixture was shaken at approx. 200 rpm at 37 °C for 40 minutes. 100µl of the cell suspension were plated out on LB-Agar plates containing the selected antibiotic, to which the plasmid confers resistance. For blue-white selections, if the plasmid contained a β-galactosidase gene, the cell suspension was plated out on LB-agar plates coated with 40 µl Xgal and 4 µl IPTG. Plates were incubated overnight at 37 °C and later stored at 4 °C.

2.2.2 Mini- Midi- and Hispeed DNA purification protocols

DNA-preparations using either Mini- , Midi- or Hispeed purification kits were carried out as described in the manufacturer's manual delivered with each kit by Qiagen (Qiagen Ltd, Crawley, UK). After purification of the DNA, the DNA was diluted in water (Sigma-Aldrich Company Ltd, Dorset, UK) and stored at -20 °C. The concentration of the DNA was measured based on the absorption of the solution at 260 nm using a Nanodrop spectrophotometer (Thermo Scientific, Wilmington, USA). Purity was determined by calculating the 260/280 and the 260/230 ratios.

2.2.3 Restriction digests of DNA

Restriction enzymes were selected based on the restriction sites of the DNA plasmid. The reaction was either carried out for 3 hours at 37 °C or overnight at room temperature, depending on the efficiency of the restriction enzyme.

For digest reactions using two different restriction enzymes, the plasmid was cut with both restriction enzymes simultaneously when compatibility of both enzymes in the same restriction buffer was expected. If the enzymes were not guaranteed to work in the same buffer, the enzymes would be used separately in a two-step process. After the first enzymatic digest, the DNA was purified using the QIAquick PCR purification kit (Qiagen Ltd, Crawley, UK) or by Ethanol precipitation (see section 2.2.4). Following the purification the linearised DNA was then digested with the second restriction enzyme.

Digested DNA was analysed on a 1% Agarose gel (as described in section 2.2.7).

2.2.4 Ethanol precipitation

DNA or RNA, which are kept in aqueous solutions, can be purified or concentrated by using the process of Ethanol precipitation. Up to 50µl DNA solution in an eppendorf tube was mixed with 50µl of sodium acetate solution, pH 5.2. RNA was mixed with 50 µl of 5M sodium chloride solution. 500µl of 100 % ethanol was added and the liquids were briefly mixed by inverting the eppendorf tube. Precipitation was allowed to occur for one hour or overnight at -20 °C. The obtained DNA or RNA pellet was recovered by spinning down at 13000 rpm for 10 – 15 minutes at 4 °C and subsequently washed with 70 % ethanol. The pellet was again recovered by centrifugation as described before, the ethanol supernatant completely removed and the pellet dried at room temperature until it became clear. The DNA or RNA pellet were then re-dissolved in water (Sigma-Aldrich Company Ltd, Dorset, UK) and stored at -20 °C.

2.2.5 Preparation of an antisense RNA probe for in-situ hybridisation

A probe is a RNA molecule, which is labelled with a fluorophore, a radioactive element or an organic group that can be detected with an antibody. An antisense probe contains a nucleotide sequence, which is complimentary to the mRNA of a specific gene. Therefore an antisense RNA probe can be used to visualize the transcripts of a gene in cells or embryonic tissue. For the preparation of a RNA probe the plasmid (for a full list of RNA probes, see table 2.1), which contains the DNA fragment on which the probe was based, was linearised first by restriction digest as described in section 2.2.3. The linearised DNA was subsequently purified by using a Phenol/Chloroform extraction (see section 2.2.6). The purified and linearised DNA was then used for the synthesis of the RNA probe. The antisense probe was made by using an NTP mixture containing digioxigenin (DIG) -labelled UTP.

The reaction mixture for the synthesis of the probe was prepared as described below:

5 µl	sigma water
2 µl	(DIG-labelled UTP) NTP mix (100 mM)
4 µl	Transcription buffer (5x)
2 µl	DTT (100 mM)
1 µl	RNAse inhibitors
4 µl	DNA construct/ template
2 µl	transcription enzyme
20µl	total volume

The reaction was incubated for two hours at 37 °C. Success of probe synthesis was analysed on a 1% Agarose gel (as explained in section 2.2.7).

After the synthesis, the RNA probe needed to be cleansed from residual NTPs and enzymes. Therefore 30µl of Diethylpyrocarbonate (DEPC) treated H_2O was added to the RNA probe synthesis sample and the mixture was placed into a freshly prepared illustra ProbeQuant G-50 Micro Column (GE Healthcare, Little Chalfont, UK). The transcribed RNA probe was recovered and purified by centrifugation at 3000 rpm for two minutes at room temperature. The obtained 50µl of solution were mixed with 50µl of formamide to prevent degradation of the RNA probe. The diluted probe was then stored at -20 °C or mixed with hybridisation mix (5µl of probe in 1 ml of hybridisation buffer), when used for an in-situ hybridisation.

Table 2.1: List of RNA-probes

The table gives details about the plasmid backbone, the restriction site and the transcription enzyme of various RNA antisense probes

antisense RNA probe	vector	Restriction enzyme for linearization	Transcriptional promoter	source
Klhl31	pGEM-T	NcoI	Sp6	Abou-Elhamd and others, 2009
Nkx2.5	Bluescript II SK-	HindIII	T3	Schultheiss and others, 1995
Pitx2	no information available	BamHI	T7	Campione and others, 1999
vMHC	pGEM 4Z	NdE7	T7	Bisaha and Bader, 1991
Islet1	no information available	XbaI	T7	gift from Frank Schubert
cHex1	no information available	EcoRI	Sp6	gift from Frank Schubert

2.2.6 Phenol/Chloroform Extraction

To purify an aqueous DNA or RNA solution the process of Phenol/Chloroform extraction can be used, as it achieves high purity for short nucleotide sequences. A specified volume of DNA solution is mixed with the same volume of phenol. Both solutions were mixed by vortexing and separated by centrifugation at 13000 rpm at 4 °C for 5 minutes. The DNA or RNA should now be in the top layer, the aqueous phase, which is removed from the phenol mixture and placed into a fresh eppendorf tube. After adding the same volume of Chloroform: Isoamylalcohol mixture (24:1) and mixing of both phases, the layers were again separated by centrifugation as described before. Again, the top aqueous phase was removed and DNA purified from the phase by using the ethanol precipitation as described in section 2.2.4.

2.2.7 Agarose gel electrophoresis

To prepare a 0.8 – 1% Agarose gel, 0.4 – 0.5 g of Agarose powder was dissolved in 50 ml of TAE-buffer. To achieve complete solubilisation, the mixture was heated until boiling using a microwave. The dissolved agarose solution was cooled down and Ethidium bromide (Sigma-Aldrich Company Ltd, Dorset, UK) was added before pouring the solution into the gel tank. Once the gel was settled, 100 ml of TAE-buffer were poured on top of the gel into the gel tank. DNA samples were prepared by mixing a specified volume of DNA with 1/6 of the total volume of DNA loading buffer. 6 µl of the sample were applied to the gel and the gel was run at 65 V for approximately 45 minutes. Obtained DNA bands were analysed using a trans-illuminator of the ChemiDoc™ XRS+ System (Life Science, Bio-Rad Laboratories Ltd., Hemel Hempstead, UK)

2.2.8 Culturing and harvesting of chick embryos

Fertilized eggs were stored after arrival at 16 °C. The eggs were then slowly warmed up to room temperature and subsequently incubated at 37 °C using a humidified incubator to grow to desired stages as described by Hamburger and Hamilton (Hamburger and Hamilton, 1992). Embryos were harvested by opening the egg shell with blunt forceps or scissors, cutting the embryo out of the vitelline membrane and washing in DEPC treated PBS. Subsequently the embryos were fixed in 4 % PFA for five to ten minutes. Following the fixation, the extra-embryonic membranes were dissected using a fine needle and fine forceps. Harvesting and dissecting the embryos was carried out on a Zeiss SV 11 dissecting microscope (Carl Zeiss Microscopy Ltd, Cambridge, UK). Embryos were subsequently dehydrated by passing through a methanol series (25%, 50%, 75% and 100% methanol in PBS). Harvested embryos were stored at -20 °C in 100% methanol.

2.2.9 Whole mount In Situ Hybridisation (WISH)

- Rehydration of chick embryos

Chick embryos which were stored in 100% methanol were rehydrated by using a methanol series (100%, 75%, 50% and 25% and 0% methanol in PBS). Embryos were then placed into 6-well dishes and washed twice in PTW.

- Treatment with Proteinase K

Subsequently the embryos were treated with 10 µg/ ml proteinase K according to their HH stages (Hamburger and Hamilton, 1992) as described in table 2.2.

Table 2.2: Proteinase K treatment of chick embryos

Proteinase K treatment is dependent of the age of the chick embryos.

Chick embryos HH stages	Time of treatment
6-12	10 minutes
12-20	15 minutes
21-25	20 minutes

- Post-fixing and pre-treatment for Hybridisation

Following the proteinase K treatment, the embryos were carefully rinsed with PTW and post-fixed with PFA containing additional glutaraldehyde to 0.1% for 20 minutes at room temperature. The PFA was removed and embryos washed twice in PTW, before incubated in 1:1 (v/v) PTW/hybridisation mix for about 10-15 minutes or until embryos have settled down in the bottom of the well. The same process was repeated once more, but now the embryos were incubated in hybridisation buffer only. Once the embryos settled down in the bottom of the well, the hybridisation mix was replaced with a fresh aliquot of hybridisation solution which had previously been preheated to 65 °C. The chick embryos were then incubated in hybridisation mix at for a minimum of one hour at 65 °C.

- Preparation of the RNA probe and Hybridisation

In the meantime the antisense RNA probe diluted in hybridisation solution was also preheated to 65 °C. Once the chick embryos had been incubated in the warm hybridisation mixture, the hybridisation buffer was removed and the embryos were incubated in the pre-warmed hybridisation / RNA probe solution overnight at 65 °C. The following morning the RNA probe in hybridisation buffer was recovered from the embryos and stored at -20 °C. The embryos were rinsed twice in to 65 °C pre-heated hybridisation mixture and washed with a fresh aliquot of pre-warmed hybridisation buffer for 10 minutes, before being washed twice with pre-heated washing solution for 30 minutes at 65 °C. Following the described washing steps, the chick embryos are incubated for 10 minutes at 65 °C in pre-heated washing solution/MABT (1:1 v/v).

- Blocking and antibody incubation

All following steps were carried out at room temperature. Firstly, the chick embryos were rinsed three times in MABT, followed by two washes at each 30 minutes in MABT. The embryos were subsequently blocked in MABT-BBR for a minimum of one hour, before being incubated with MABT-BBR containing 10% heat-treated goat serum for between one or two hours. After removing the blocking solution, the chick embryos are incubated overnight at 4 °C with an anti-DIG antibody (Roche Diagnostics Ltd, Burgess Hill, UK) diluted 1:2000 in MABT-BBR-goat serum buffer. The anti-DIG antibody is conjugated to an alkaline phosphatase. The next morning the antibody was removed and the embryos rinsed three times with MABT at room temperature. After six washes in MABT at room temperature, each wash lasting approximately one hour, the embryos were incubated overnight in fresh MABT.

- Colour reaction, post-fixing and storage

The MABT was removed the following morning and the embryos washed twice for 10 minutes in NTMT at room temperature. For the colour reaction the chick embryos were incubated in the dark with NTMT containing additional 9 µl NBT and 7 µl BCIP per 1 ml of NTMT at room temperature. NBT and BCIP are substrates for the alkaline phosphatase and when reacted with are displaying a blue precipitate. Therefore, if a gene is transcribed into mRNA and the RNA probe can bind to the mRNA, expression can be seen as a dark blue staining in specific embryonic tissues. The time of colour development or also known as the time of incubation in the substrates is depending on the strength of a specific probe and can vary from 10 minutes to several days. If the colour was developed to desired strength the colour reaction was stopped by removing the substrates and washing in 5X TBST. Should the colour has not been developing to the desired extent, the embryos were washed overnight at 4 °C in TBST. The next day the colour reaction was then repeated as described before. Once the blue staining was strong enough and the colour reaction had been stopped, the embryos were post-fixed overnight at room temperature in PFA containing 0.1% Glutaraldehyde, washed three times with PTW and stored in PTW at 4 °C until processed further.

2.2.10 Processing chick embryos for imaging

Chick embryos harvested from eggs or obtained from in-situ hybridisation can reveal staining either from contamination with egg yolk or in older embryos from blood residues. Blood stains could be removed from the embryos by washing the chick embryos at room temperature in PTW containing 0.2 % v/v H_2O_2. Further staining and clearance of the embryos could be achieved by incubating the embryos in a gradient of glycerol (25%, 50%, 75% and 100% glycerol in PTW). Embryos can be stored in 100% glycerol at 4 °C. Images of whole embryos were taken on a Zeiss SV11 dissecting microscope with a micropublisher 3.5 camera using the associated acquisition software. Images were exported into Adobe Photoshop (Adobe Systems Europe Ltd, Maidenhead, UK) for labelling and formatting.

2.2.11 Sectioning of chick embryos

To prepare embryos for cryosectioning the embryos that were stored in glycerol after WISH were firstly passed through a gradient of Glycerol (75%, 50%, 25% and 0% Glycerol in PTW) until diluted in PTW. To remove all residual Glycerol embryos were then washed with fresh PTW three times for 5 minutes at room temperature. Subsequently the embryos were mounted in OCT (a frozen section embedding medium, Agar Scientific, Stansted, UK) and placed into plastic mounting capsules (VWR International Ltd, Lutterworth, UK). The embryos were incubated in OCT overnight at 4 °C. The following day, the OCT saturated embryos were adjusted in the capsules to lie with their anterior side towards the bottom of the capsules. The embryos were immediately frozen in a dry ice/ isopropanol mixture to prevent further movement. Frozen specimens were stored at -20 °C until further usage. Cryosectioning was carried out using a Leica CM 1850 Cryostat (Leica Microsystems (UK) Ltd, Milton Keynes, UK). Embryos were sectioned at 20 µm and the obtained sections were collected on TESPA or Poly-L-Lysine coated slides (prepared in our laboratory). Slides were dried overnight at 37 °C and subsequently washed twice in pre-warmed PBS. Pre-

warmed Hydromount (AGTC Bioproducts t/a National Diagnostics UK, Hessle, UK) was gently pipetted on top of the sections and a coverslip was placed unto the slide to cover the sections on the slide. Mounted sections can be stored at room temperatures. Images of the sections were taken at a widefield upright microscope (Carl Zeiss Microscopy Ltd, Cambridge, UK) equipped with a monochrome CCD camera using AxioVision software (Carl Zeiss Microscopy Ltd, Cambridge, UK). Images were exported into Adobe Photoshop (Adobe Systems Europe Ltd, Maidenhead, UK) for labelling and formatting purposes.

2.2.12 Extracting RNA from cell tissue and chick embryos

Mammalian cells were grown to about 80% confluency, washed with PBS and then trypsinised. Detached Cells were resuspended in 500 µl PBS and pipetted into a 1.5 ml Eppendorf-tube. The cell suspension was kept on ice. Cells were spun down at 4°C and 20000 rpm, the supernatant removed and the cell pellet further processed for RNA extraction. RNA was either extracted using the RNeasy® Mini Kit (Qiagen Ltd, Crawley, UK) or by following the TRIZOL® Reagent manufacturer's instructions (Invitrogen, Life Technologies Ltd, Paisley, UK).

For RNA extraction from chick embryos, the embryos were harvested as described in section 2.2.8. Embryos were placed into a 1.5 ml eppendorf tube and manually homogenized in RTL-buffer containing 143 mM β- Mercaptoethanol. RNA was obtained by using the RNeasy® Mini Kit as described in the manufacturer's instructions (Qiagen Ltd, Crawley, UK). Obtained RNA was diluted in sigma water (Sigma-Aldrich Company Ltd, Dorset, UK) and stored at -20 °C.

The quality and concentration of the purified RNA was measured by using the RNA Nanodrop device (Thermo Scientific, Wilmington, USA).

2.2.13 Transcription of RNA into complementary DNA (cDNA)

RNA was transcribed into cDNA using the Moloney Murine Leukaemia Virus (MoMuLV) reverse transcriptase and MMLV-RT Buffer (Thermo Fisher Scientific UK Ltd, Loughborough, UK). Firstly, extracted RNA was denatured at 70°C for 15 minutes and the M-MLV-RT Buffer was warmed up to 37 °C to dissolve any occurring precipitation.

For the transcription reaction between 1 – 2 µg of total RNA has been used.

A standard mixture for one sample contained:

9.9 µl Sigma H_2O

6 µl M-MLV-RT Buffer (5x)

1 µl dNTP mixture (10 mM)

1 µl MoMuLV reverse transcriptase

1 µl DTT (100 mM)

1 µl random Hexamer mixture (200 ng/ µl)

0.1 µl RNAsin

10 µl RNA extract (1-2 µg)

30 µl total volume

Transcription into cDNA was carried out at 42 °C for 1 hour. Synthesised cDNA was stored at – 20 °C.

The quality of obtained cDNA was analysed by PCR as described in the following section (2.2.14).

2.2.14 Polymerase chain reaction (PCR) for controlling the quality of cDNA

To control the quality of cDNA, a PCR against housekeeping genes (see list in table 2.3) was performed using the Bioline Bio-Mix Red (Bioline, London, UK). The PCR was carried out by using a DNA Engine Dyad Peltier Thermal Cycler (Bio-Rad Laboratories Ltd, Hempstead, UK).

Table 2.3: List of primers designed for PCR

Following list contains the sequence information of primers used in PCR processes, either for cloning, expression analysis or quality control.

Primer	Sequence	product size	restriction site	Source
chick GAPDH	Forward 5’ AGTCATCCCTGAGCTGAATG 3’	330 bp	/	Munsterberg and Lassar, 1995
	Reverse 3’ ACCATCAAGTCCACAACACG 5’		/	
Mouse β-Actin	Forward 5’ GAAATCGTGCGTGACATTAAGGAG 3’	500 bp	/	Given by Dr. Niels Haan
	Reverse 3’ ATACTCCTGCTTGCTGATCCACAT 5’		/	obtained from MWG Biotech AG
Chick β-Actin	Forward 5’ CCAGCTGGGAGGAGCCGGT 3’	300 bp	/	Dr. Katarzyna Goljanek-Whysall
	Reverse 3’ CTGGGGAACACAGCCCGCTT 5’		/	
mouse Klhl31 FL for expression analysis	Forward 5' AAGGCAACAGCCCAGAAAT 3'	1177 bp	/	Constanze Ochmann
	Reverse 3' ACTTCTTCTCGCCCTCGTTC 5'		/	

human Klhl31 for expression analysis	Forward 5' AAAGCAGCAGCCCAGAAAT 3'	1177 bp	/	Constanze Ochmann
	Reverse 3' ACTTCTTCTCGCCCTCGTTC 5'		/	
human Klhl31 FL for GST-pull down (pGEX-5X-1)	Forward 5' GAATTCATGGCACCCAAAAAGAAGATT 3'	1900 bp	EcoRI	Constanze Ochmann
	Reverse 3' CTCGAGTCAGATACTGACTGGCACAGAAG 5'		XhoI	and Dr. Timothy Grocott
internal for sequencing	Reverse 3' AAATACTCACTGCATGAAGCCAT 5'	/	/	
chick Klhl31 for pEGFP-C1 constructs FL / ΔBTB	Forward 5' TCCGGAATGGCACCTAAGAAGAAGAAC 3'	1900 bp / 1400 bp	BspEI	Constanze Ochmann
	Reverse 3' GAATTCTCAAGCGTAATCTGGAACATCGTATGGGTAAATACTGACTGGTACAGAAG 5'		EcoRI	
ΔKR	Reverse 3' GAATTCTCAAGCGTAATCTGGAACATCGTATGGGTATCTGAATCCTCCACGAATCC 5'	900 bp	EcoRI	

chick Klhl31 for pEGFP-N1/ DsRed-N1 constructs FL / ΔBTB	Forward 5' CTCGAGATGGCACCTAAGAAGAAGAAC 3'	1900 bp / 1400 bp	XhoI	Constanze Ochmann
	Reverse 3' GAATTCCAATACTGACTGGTACAGAAGA 5'		EcoRI	
ΔKR	Reverse 3' GAATTCCTCTGAATCCTCCACGAATCCT 5'	900 bp	EcoRI	
Nebulin Variation 2 (HA tag)	Forward 5' ATGCGGCCGCATGGACACAGTCAGTGATGTAAA 3'	500 bp	Not1	Constanze Ochmann
	Reverse 3' ATGAATTCTCAAGCGTAATCTGGAACATCGTATGGGTATTTATAAAGGATATCG 5'		EcoRI	
Nebulin Variation 3 (HA tag)	Forward 5' ATGCGGCCGCATGGATGCCCTAGACATTGTCTA 3'	600 bp	Not1	Constanze Ochmann
	Reverse 3' ATGAATTCTCAAGCGTAATCTGGAACATCGTATGGGTATTTATAAAGGATATCG 5'		EcoRI	

The reaction mixture for the PCR was prepared as described below:

10 µl Bio-Mix Red 2x (Bioline, London, UK)

0.5 µl forward primer

0.5 µl reverse primer

3 µl template DNA (diluted 1:1000)

6 µl sigma water

20 µl total volume

The PCR reaction was carried out using the PCR program "PCR housekeeping gene" with following settings:

1. 5 minutes 94 °C
2. 1 minute 94 °C
3. 1 minute 50 °C
4. 1 minute 72 °C

} Repeated for 30 circles

5. 5 minutes 72 °C

Following the Polymerase Chain reaction the samples were run on a 0.8 – 1% Agarose gel to analyse the obtained PCR products as described in section 2.2.7.

2.2.15 Polymerase chain reaction (PCR) for analysing the expression of Klhl31

The expression of Klhl31 was detected by PCR. The samples were prepared in Bioline Bio-Mix Red (Bioline, London, UK) as described in section 2.2.14 and the PCR was carried out by using a DNA Engine Dyad Peltier Thermal Cycler (Bio-Rad Laboratories Ltd, Hempstead, UK).

The settings for the polymerase chain reaction were saved as the program “Kelch PCR” and contained following steps:

1. 60 seconds 95 °C
2. 30 seconds 95 °C
3. 30 seconds 61 °C
4. 40 seconds 72 °C
5. 5 minutes 72 °C

} Repeated for 30 circles

The samples were analysed as described before on a 1% Agarose Gel (section 2.2.7).

2.2.16 Polymerase chain reaction (PCR) to amplify DNA for Cloning

Polymerase chain reactions to amplify the sequences for Klhl31- full length, Klhl31-ΔBTB and Klhl31-ΔKR were carried out by using a DNA Engine Dyad Peltier Thermal Cycler (Bio-Rad Laboratories Ltd, Hempstead, UK). The Klhl31 Full length sequence as well as the Klhl31-ΔKR sequence have been amplified from chick complementary DNA (cDNA) HH stage 10 (Hamburger and Hamilton, 1992). The Klhl31-ΔBTB sequence was amplified from the pCaβ-IRES-GFP-Klhl31- ΔBTB plasmid (created by Oliver Cooper and Alaa Abou-Elhamd).

For the cloning of GST-Klhl31 construct, a human Klhl31 clone (IMAGE clone 9021264) was obtained from Source BioScience Life Sciences (Source BioScience UK Limited, Nottingham, UK). The fragments of Nebulin Variation 2 and Nebulin Variation 3 have been amplified from the plasmids sent from Hybrigenics (Hybrigenics Services, Paris, France). Sequence and plasmid information for Nebulin Isoform 1 and Isoform 2 can be found in the appendix.

For a complete list of primers see table 2.3 in sub-chapter 2.2.14.

The PCR was carried out by using the high fidelity polymerase Phusion (New England Biolabs, Herts, UK).

The reaction mixture for one sample was prepared as described below:

5 µl	5x Phusion buffer (New England Biolabs, Herts, UK)
0.5 µl	dNTPs (100 mM)
1 µl	forward primer (10 nM)
1 µl	reverse primer (10 nM)
1.3 µl	DNA template (diluted 1:1000)
0.75 µl	DMSO
14.5 µl	sigma water
0.25 µl	Phusion (New England Biolabs, Herts, UK) enzyme
0.5 µl	Taq-Polymerase
25 µl	total volume

The polymerase chain reaction was carried out using the PCR program "Gradient Phusion" designed with the following settings:

1.	60 seconds	95 °C	
2.	30 seconds	95 °C	} Repeated for 30 circles
3.	30 seconds	gradient of 50 - 65 °C	
4.	40 seconds	72 °C	
5.	5 minutes	72 °C	

To elongate the PCR product with a Poly-Adenine-Tag, 1µl of taq-polymerase was added to each sample. The mixture was then incubated for further 15 minutes at 72 °C.

PCR products were analysed using a 1% Agarose gel as described in section 2.2.7.

2.2.17 Purification of DNA fragments out of an agarose gel

DNA bands in the agarose gel were visualised under UV light using a trans-illuminator whilst wearing suitable face protection. DNA bands displayed the desired sequence length were excised from the gel using a clean razor blade and placed in a 1.5 ml Eppendorf tube. The DNA was extracted from the agarose gel as described in the manufacturer instructions for the use of the QIAEX® II gel extraction kit (Qiagen Ltd, Crawley, UK) and stored diluted in water at -20 °C.

2.2.18 Ligation of the PCR products in pGEM-T easy

The pGEM-T easy Vector contains a single 3' thymidine-residue at both strands to ligate PCR products with overhanging adenines into the pGEM-T vector. Ligation of DNA fragments into the pGEM-T vector was carried out using below described ligation mix.

0.5 µl	pGEM-T vector (25 ng)	(Promega UK Ltd, Southampton, UK)
5 µl	2 x ligation buffer	(Promega UK Ltd, Southampton, UK)
1 µl	T4 Ligase	(Promega UK Ltd, Southampton, UK)

DNA insert was added to the vector in a ratio vector : DNA of 1 : 3, using up to 3.5µl of DNA insert, making the total volume of each ligation to 10µl. Sigma water was added to the pGEM-T ligation mixture as a negative control for the ligation.

The ligation sample was incubated at room temperature for 3 hours or at 16° C overnight. Immediately after the ligation process, the obtained pGEM-T constructs were transformed into DH5α cells as described in section 2.2.1 and plated out on carbenicillin containing LB-agar plates. The following day several clones were picked from the plate, grown up in 5 ml LB medium with additional carbenicillin and the DNA extracted from the cells using a Qiagen Mini prep approach as described in section 2.2.2. The presence of the desired insert was firstly analysed by restriction digest (as described in section 2.2.3) using the enzyme EcoRI, as the multiple cloning site of the pGEM-T easy vector is flanked on both sides with the recognition sequence for EcoRI. The digested DNA was run on a 1% Agarose Gel as

described in section 2.2.7 and positive clones were sent for sequencing to verify the exact sequence of the inserted DNA fragment.

2.2.19 Cloning of DNA inserts from pGEM-T into expression vectors

To subclone DNA inserts into the desired overexpression vector, the DNA insert were cut out of the pGEM-T vectors using the restriction enzymes as stated in table 2.4 in this section. Digested DNA was analysed on a 1% agarose gel and obtained fragments were purified from the agarose gel as described in chapter 2.2.16. Purified DNA was stored at –20 °C until further usage. The chosen vectors were linearised as described in chapter 2.2.3 using the same restriction sides as used for the DNA insert which is to be cloned into the vector backbone.

A list of all cloned overexpression constructs including information about the plasmid size, the protein size and the used restriction enzymes can be found below:

Table 2.4: List of cloned overexpression constructs

The following list gives detailed information about the cloned overexpression constructs. It contains data about the plasmids used including plasmid sizes inclusive of the DNA fragments, the protein sizes of the cloned Fusion proteins and the restriction sides, which were used to cut and paste the DNA from the pGEM-T vector into the chosen vector. All protein sizes marked with an asterisk (*) are predicted protein sizes.

Overexpression construct	use	plasmid size	protein size	restriction site
pGEX-5X-1 Klhl31 FL	prey for GST-pull down experiments	6700 bp	95 kDa	EcoRI N-term XhoI C-term
pEGFP-C1 Klhl31 FL	overexpression constructs / GFP Fusion proteins GFP at N-terminus of Klhl31	6800 bp	96 kDa	BspEI N-term
pEGFP-C1 Klhl31 dBTB		6300 bp	~ 77 kDa *	EcoRI C-term
pEGFP-C1 Klhl31 ΔKR		5800 bp	~ 59 kDa *	for all constructs
pEGFP-N1/ DsRed-N1 Klhl31 FL	overexpression constructs / GFP or DSRED Fusion proteins GFP or DSRED at C-terminus of Klhl31	6800 bp	96 kDa	XhoI N-term
pEGFP-N1 / DsRed-N1 Klhl31 ΔBTB		6300 bp	~ 77 kDa *	EcoRI C-term
pEGFP-N1/ DsRed-N1 Klhl31ΔKR		5800 bp	~ 59 kDa *	for all constructs
pCaβ Nebulin Variation 2 IRES GFP (HA tag)	bait for GST pull down	>4900 bp	~ 18 kDa *	Not1 N-term EcoRI C-term
pCaβ Nebulin Variation 3 IRES GFP (HA tag)	bait for GST pull down	> 5000 bp	~ 23 kDa *	Not1 N-term EcoRI C-term

To control the linearization of the overexpression vector and the excision of the DNA fragment, both samples were analysed using a 1% agarose gel (section 2.2.7). If successful, both the DNA insert from the pGEM-T vector, as well as the linearised overexpression vector backbone were purified from the agarose gel as explained in 2.2.17.

The ligation of the insert into the chosen overexpression vector was carried out using T4 DNA ligase. Variations of vector to insert ratios (from 1:1, up to 10:1 insert : vector) were tested to find the most successful ligation settings. These ratios were calculated based on the concentration of the vector used.

A calculation would be set up as follows:

$$\text{ng (insert)} = \frac{\text{ng (vector)} \times \text{kb (size of insert)} \times \text{ratio}}{\text{kb (size of vector)}}$$

For example; Using 200 ng vector with a size of 3.5 kb, the DNA fragment size being 0.6 kb. The ratio insert : vector would be 3:1.

$$\text{y ng} = \frac{200 \text{ ng} \times 0.6 \text{ kb} \times 3}{3.5 \text{ kb}}$$

$$= 102.9 \text{ ng DNA insert}$$

The calculated ng for insert and vector DNA would then be converted into a volume that can be used in a T4 Ligation sample preparation.

A mixture for one sample is usually made up as described below:

1	µl of 10x Ligation Buffer	(Roche Diagnostics Ltd, Burgess Hill, UK)
1	µl of T4 DNA Ligase	(Roche Diagnostics Ltd, Burgess Hill, UK)
x	µl of vector DNA	
y	µl of DNA insert	
z	µl of sigma water	
10	µl of total volume	

The ligation reaction was incubated overnight at 16 °C and the next morning transformed into competent DH5α cells, as described for the ligation into pGEM-T in 2.2.18.

The clones were checked for presence of the insert by using a colony PCR approach using the primers that were designed for the cloning process (for primer information see table 2.3, section 2.2.14).

The colony PCR was set up using the Bioline Mix, picking one bacterial colony from the LB-agar plate with a pipette tip. A fresh LB-agar plate was scratched with the pipette tip to inoculate it with the bacterium and the residues of the bacterial colony were then resuspended in the PCR mixture.

A reaction mixture for one sample was prepared as described below:

10 µl Bio-Mix Red 2x (Bioline, London, UK)

0.5 µl forward primer

0.5 µl reverse primer

9 µl sigma water

20 µl total volume

The program "Colony" was used to run the PCR reaction using the DNA Engine Dyad Peltier Thermal Cycler (Bio-Rad Laboratories Ltd, Hempstead, UK).

The PCR program contained the following settings:

1.	4 minutes	98 °C	
2.	30 seconds	98 °C	} Repeated for 30 circles
3.	30 seconds	55 °C	
4.	60 seconds	72 °C	
5.	5 minutes	72 °C	

Once the presence of the right sized insert was verified by the colony PCR, a few clones, which contained the DNA insert, were cultured in 5 ml of LB medium. The DNA was then extracted as explained in section 2.2.2 and further analysed using a restriction enzyme approach (as described in section 2.2.3). Two or three clones, which revealed the expected sized insert of the cloned DNA fragment, were sent for sequencing. Only clones with the

correct nucleotide sequences were used for further experiments. The DNA was stored at -20 °C.

2.2.20 Culture of mammalian Cells

Human Embryonic Kidney 293 cells (HEK 293) (Graham and others, 1977) and 3T3 mouse fibroblast cells (Todaro and Green, 1963) were cultured in Nunc EasYFlask 75cm^2 flasks (Thermo Scientific, Fisher Scientific UK Ltd, Loughborough, UK) using DMEM (Dulbecco's Modified Eagle's Medium) containing low glucose, GlutaMAX™ and pyruvate (Invitrogen Life Technologies Ltd, Paisley, UK) in a humidified chamber in a 5% CO_2 environment at 37 °C. The medium contained additional heat inactivated foetal bovine serum (FBS) (10% v/v) and a penicillin/ streptomycin antibiotic mixture (1% v/v) (both obtained from Invitrogen Life Technologies Ltd, Paisley, UK). Cells were cultured until they reached a confluency of about 95%, before they were passaged either in a 1:10 or 1:20 ratio.

2.2.21 Culture and Differentiation of C2C12 (mouse myoblasts)

C2C12 (Yaffe and Saxel, 1977) mouse myoblasts were cultured in growth medium made up of DMEM (high glucose, NEAA, no glutamine), 10% heat inactivated FBS and 1% Pen/Strep (all obtained from Invitrogen Life Technologies Ltd, Paisley, UK) in Nunc EasYFlask 75cm^2 flasks (Thermo Scientific, Fisher Scientific UK Ltd, Loughborough, UK). C2C12 were grown in a humidified incubator at 37 °C with 5% CO_2. As C2C12 myoblasts commence differentiation due to cell-cell contact, when becoming very confluent (> 90%), the growing C2C12 cells were splitted at a confluency of 60 – 70 % to prevent self-induced myotube formation.

C2C12 destined to differentiate were cultured up to a confluency of 90%, washed with PBS and the medium changed to differentiation medium (DMEM high glucose, NEAA, no glutamine) with added 2% of horse serum and 1% Pen/Strep (all purchased from Invitrogen Life Technologies Ltd, Paisley, UK). Myotube formation begins to occur within 2-3 days of

starvation and fully formed myotubes can be observed after 4-5 days in differentiation medium.

However, the C2C12 cells cultured and used in the here described experiments differentiated slower compared to fresher and healthier C2C12 cells. We did occasionally observe fully differentiated myotubes at day 4, but most cells were still differentiating. Also due to technical difficulties and increasing cell detachment, we were not able to culture C2C12 for more than 4-5 days in starvation medium.

During differentiation the medium was changed every day and in later stages twice a day, as metabolic products from the cell culture start to acidify the medium (information and protocol according to Katherine Fisher-Aylor and Brian Williams: http://genome.ucsc.edu/ENCODE/protocols/cell/mouse/C2C12_Wold_protocol.pdf)**.**

Occasionally C2C12 cells differentiated poorly, which could be seen in a further temporal delay of differentiation or by a very low differentiation index (number of differentiated C2C12 divided by number of present cells). Usually we would expect to see elongated myotubes by around Day 2 of differentiation and the first multi-nucleated myotubes would be observed around day 3. We usually also expected to see a differentiation index above 30 %. When we did not observe normal differentiation, e.g. when differentiation was significantly delayed or the differentiation index fell below 30%, cultured cells were checked for mycoplasma infection.

2.2.22 Screen and treatment of cells for mycoplasma

Mycoplasma are small, self-replicating organisms, which depend on host cells to perform major metabolic processes, such as synthesizing nucleic acids and amino acids. In cell culture, mycoplasma cannot be seen, neither by the naked eye nor by using a microscope and although they do not necessary change properties of the medium (for example, the pH or metabolic products), they can have major implication on the behaviour of cultured cell lines (McGarrity and others, 1992).

We used a PCR based approach to detect mycoplasma designed by Dr. Rosemary Bass.

Mycoplasma DNA can be detected in culture media. Therefore for this approach at least 1 ml of medium, in which cells have been cultured in for a minimum of two days, was removed from the cell culture and boiled at 100 °C for 5 minutes. The solution was then spun down for one minute at 13000 rpm at room temperature.

Subsequently the PCR sample was prepared as described below using the high fidelity DNA polymerase Phusion:

5 µl	5x Phusion buffer (New England Biolabs, Herts, UK)
0.5 µl	dNTPs (100 mM)
2.5 µl	forward primer (10 nM)
2.5 µl	reverse primer (10 nM)
3 µl	boiled culture supernatant
11.25 µl	sigma water
0.25 µl	Phusion (New England Biolabs, Herts, UK) enzyme
25 µl	total volume

Following the sample preparation, the polymerase chain reaction was carried out in a DNA Engine Dyad Peltier Thermal Cycler (Bio-Rad Laboratories Ltd, Hempstead, UK).

Primers used are described below:

Myco1	GGGAGCAAACAGGATTAGATACCCT
Myco2	TGCACCATCTGTCACTCTGTTAACCTC

The settings for the PCR were saved under the file name “MycoPCR” and comprised of following steps:

1.	30 seconds	98 °C	
2.	10 seconds	98 °C	} Repeated for 40 circles
3.	20 seconds	52 °C	
4.	30 seconds	72 °C	
5.	2 minutes	72 °C	

The samples were then analysed on a 1% Agarose Gel as described in 2.2.7. Presence of mycoplasma was detected as a band on the gel with a size of around 270 bp. Infected cells were treated subsequently with the antibiotic Ciprofloxacin (final concentration in cell culture 10 µg/ ml) for a time course of up to one week or until the mycoplasma could not be detected anymore. The treated cells were incubated in fresh medium for a couple of days afterwards to recover from the antibiotic stress and were subsequently used for further experiments.

2.2.23 Passaging of mammalian cells

For the preparation of the cells for splitting, the culture medium was removed from the cells and the cells washed twice in PBS. Then the cells were incubated with 0.25% Trypsin-EDTA (Invitrogen Life Technologies Ltd, Paisley, UK) until the cells detached from the flask. Following trypsination, detached cells were resuspended in fresh medium and splitted in desired ratio.

If a specified number of cells were needed, for example for a transfection experiment, the number of cells was counted using a haemocytometer. For this approach 100 µl of resuspended cells after detaching from the flask were aliquoted into an eppendorf tube. A couple of drops of described cell suspension were added between the coverslip and the gridded haemocytometer slide. As the depth and length of the grids are specified, the volume of each square is known. Therefore, by counting the number of cells in a minimum of 5 squares, the number of cells in the original suspension can be calculated based on counted

amount and theoretical volume. The specified number of cells was subsequently passaged into a fresh flask or a multiple well dish.

2.2.24 Transfection of mammalian cells

Transfection was performed by using the transfectant Lipofectamine® 2000 (Invitrogen Life Technologies Ltd, Paisley, UK) following the manufacturer's instructions.

The number of cells required for transfection of different volumes in either wells or flasks can be found in the instructions, as well as information about the amount of DNA and Lipofectamine® 2000 reagent needed for transfection.

For example, for one well of a 6-well dish 0.25–1 x 10^6 cells were plated out in 2 ml of growth medium. After 48 hours of further incubation cells were prepared for transfection by replacing the growth medium with growth medium without additional FBS (serum-free medium). Cells were transfected with 6-15µl of Lipofectamine® 2000 reagent and up to 14 µg of plasmid DNA. After 4 hours in the Transfection medium, cells were incubated in growth medium containing FBS for further 48 hours before being harvested or processed for further experiments.

2.2.25 Luciferase Assay

A luciferase assay is a tool to study the involvement of a protein with mediators of signalling pathways or transcriptional activators and repressors.

- Preparation

For the preparation of a luciferase assay, 30,000 3T3 cells were seeded into each well of a Nunc 96-well dish (Thermo Scientific, Fisher Scientific UK Ltd, Loughborough, UK) and cultured in DMEM containing low glucose, GlutaMAX™ and pyruvate (Invitrogen Life Technologies Ltd, Paisley, UK) for further 24 hours.

- Transfection

Transfection was carried out as described in the manufacturer's instruction for Lipofectamine® 2000 (Invitrogen Life Technologies Ltd, Paisley, UK) as explained in section 2.2.24. Each assay was carried out at least three times in triplicates.

The luciferase reporter vector pGL3 (Promega UK, Southampton, UK) was used as a transfection control. As the reporter vector for the luciferase assay, a Super 8X TOPFLASH vector containing 8 active LEF/TCF binding sites fused to a firefly luciferase was used. As a negative control, we used a Super 8X FOPFLASH firefly luciferase vector, in which the LEF/TCF binding sites were mutated and therefore non-active. Both vectors were gifts from Randy Moon. Activation of the reporter assay was achieved by co-transfecting the cells with pCaβ-β-Catenin-IRES-GFP. For normalisation purposes 3T3 cells were also transfected with the plasmid pRLTK (Promega UK, Southampton, UK) expressing a renilla luciferase. To analyse the influence of our cloned constructs on the reporter vector, 3T3 cells were also transfected with a plasmid expressing the fusion-protein or with a plasmid containing only the vector backbone as a negative control.

The preparation of a set of experiments with one sample for each condition would look as follows:

Table 2.5: Setting up a Luciferase assay

The following list gives details about the volume of medium, the amount of DNA and the volume of Lipofectamine® 2000 used for one sample of each setting in a luciferase reporter assay.

	pGL3	β-catenin	8x TOP-FLASH	8x FOP-FLASH	vector	over-expression construct	Renilla	Lipofect-amine® 2000	volume (transfection mixture)	volume in well
trans-fection control	100ng	/	/	/	/	/	/	0.5µl	2 x 25µl	100µl
vector only positive	/	100ng	10ng	/	10ng	/	10ng	0.5µl	2 x 25µl	100µl
vector only negative	/	100ng	/	10ng	10ng	/	10ng	0.5µl	2 x 25µl	100µl
construct positive	/	100ng	10ng	/	/	10ng	10ng	0.5µl	2 x 25µl	100µl
construct negative	/	100ng	/	10ng	/	10ng	10ng	0.5µl	2 x 25µl	100µl

After the Transfection, the cells were incubated in fresh medium containing 10% FBS for further 48 hours.

- Measurement of Luciferase activity

The Luciferase activity was measured as described for the dual-luciferase® reporter assay (DLR®) (Promega UK, Southampton, UK) according to the manufacturer's instruction. The DLR® system allows the detection of two different luciferase signals. Firefly luciferase and renilla luciferase are evolutionary distinct enzymes and require different substrates, which makes this dual reporter assay ideal for experimental purposes. In the first instance the signal obtained from the metabolic reaction for the firefly luciferase is measured indicating the success of activating or inhibiting the LEF/TCF transcription factors. The reaction is then stopped and the renilla firefly activity is measured by adding a different substrate. The renilla firefly activity is a reading for the transfection efficiency for each sample and can be used to normalise the samples against each other.

To prepare the transfected cells for luciferase activity measurement, the medium was removed from the cells and the 3T3 cells were rinsed gently once with PBS. Subsequently 20µl of 1x passive lysis buffer (Promega UK, Southampton, UK) were added to each well and cells were lysed for 20 minutes at room temperature whilst rocking slowly. The lysate was then aliquoted into a black Nunc 96-well dish (Thermo Scientific, Fisher Scientific UK Ltd, Loughborough, UK).

The Luciferase activity was measured on an EnVision Multilabel Plate Reader (PerkinElmer, Cambridge, UK).

The first step was to measure the firefly luciferase activity. 100µl of Luciferase Assay Reagent II (LARII) (Promega UK, Southampton, UK) were added to each lysate and the reading was taken. The second step comprised the immediate stop of firefly luciferase activity and the measurement of the renilla luciferase activity. The firefly activity was quenched by adding 100µl of Stop&Glo solution (Promega UK, Southampton, UK) to each sample and as the Stop&Glo solution also contained the substrate for the renilla luciferase, the activity could be measured directly after addition of the second solution. Obtained firefly luciferase readings were normalised based on the measured renilla activity. The luciferase activity obtained for the sample transfected with the reporter genes and the empty vector was set to 100% and all other measured activities were

compared to this sample. Statistics were carried out using the non-parametric Mann-Whitney-U-test using SPSS statistics software (IBM Corporation, New York, USA).

2.2.26 Immuno-Staining of C2C12 cells

- Preparation of C2C12 myoblasts

Round coverslips with a diameter of 5 mm were sterilised by autoclaving and carefully placed into each well of a Nunc 6-well dish (Thermo Scientific, Fisher Scientific UK Ltd, Loughborough, UK). The coverslips were coated with gelatine by incubation for 15-20 minutes in a 0.3% gelatine solution. C2C12 myoblasts were aliquoted onto each coated coverslip and cultured in growth medium for further 24 hours before being processed for immuno-histochemistry. For immuno-staining of differentiated mouse myotubes, C2C12 were seeded unto gelatine covered coverslips, grown to high confluency and the medium changed to differentiation medium (as described in section 2.2.21) until cells reached the desired stage of differentiation.

- Fixing and Permeabilisation of C2C12 cells

The medium was removed from the C2C12 and cells were immediately fixed with 3% PFA. Undifferentiated C2C12 cells were incubated in PFA for 15 minutes, whilst differentiated C2C12 were fixed in PFA for 30 minutes. After fixation, the coverslips were moved into a clean Nunc 6-well dish (Thermo Scientific, Fisher Scientific UK Ltd, Loughborough, UK) and the cells were washed three times with PBS for 5 minutes each at room temperature shaking on a very slow rocker. Cells were then permeabilized by using a 0.25% Triton X solution (in PBS); either 20 minutes for C2C12 myoblasts or 30 minutes for C2C12 myotubes. Again, the cells were washed subsequently three times with PBS as described before.

- Blocking and antibody treatment

Following the pre-treatment, the cells were blocked with 10% goat serum (in PBS) at room temperature for 40 minutes without shaking. In the meantime the antibodies were diluted in 0.1% goat serum. For a list of antibodies used and dilution factors see table 2.6. Two antibodies could be used at the same time when the species of the animal, in which they were raised, was different.

Table 2.6: Primary Antibodies used for Immuno-histochemistry

Following list contains information of all primary antibodies used for the Immuno-histochemistry of C2C12 cells.

name	species	detection	dilution	manufacturer
ab62181	rabbit	Klhl31	1:1000	abcam®, Cambridge,UK
YL1/2	rat	alpha tubulin	1:1000	MorphoSys UK Ltd t/a AbD Serotec, Oxford,UK
NB2	mouse	Nebulin	1:200	abcam®, Cambridge,UK

Also, whilst the cells were blocked in 0.1% goat serum, a humidified chamber was prepared. The humidified chamber comprised of a large western blot blocking tray, which was covered with wet paper tissue. On top of the wet layer squares of parafilm (Alcan Packaging, Bristol, UK) were laid out.

40 – 50 µl of each antibody solution were pipetted onto the parafilm layer and the coverslips were carefully placed on top of the drop with the cell-displaying surface facing towards the solution. The cells were incubated in the primary antibody solution for 2 hours at room temperature or overnight in the cold room at 4 °C. Following the incubation with the primary antibody, the coverslips were placed into a new Nunc 6-well dish (Thermo Scientific, Fisher Scientific UK Ltd, Loughborough, UK) and washed 7 times, each step lasting for 5 minutes, with PBS.

- Treatment with the secondary antibody

The secondary antibodies were chosen based on the species the primary antibody was raised in. For example, when using the Klhl31 antibody, the secondary antibody had to be an anti-rabbit secondary antibody to be able to bind to the primary antibody. Dyes and secondary antibodies used are conjugated to a fluorophore and can be excited by specific wavelengths of light. The emitted light from the fluorophore can then be visualised using a detector. For a list of dyes and secondary antibodies see *table 2.7* below.

Table 2.7: Secondary Antibodies and Dyes used for Immuno-histochemistry

Following list contains information of all secondary antibodies and dyes used for the Immuno-histochemistry of C2C12 cells.

name	antibody	dye	species	emitted colour	De-tection	dilution	manufacturer
Alexa Fluor® 488	x		rabbit	green	/	1:1000	Invitrogen Life Technologies Ltd, Paisley, UK
Alexa Fluor® 488	x		rat	green	/	1:1000	Invitrogen Life Technologies Ltd, Paisley, UK
Alexa Fluor® 488	x		mouse	green	/	1:1000	Invitrogen Life Technologies Ltd, Paisley, UK
Alexa Fluor® 568	x		rabbit	red	/	1:1000	Invitrogen Life Technologies Ltd, Paisley, UK
Alexa Fluor® 568	x		mouse	red	/	1:1000	Invitrogen Life Technologies Ltd, Paisley, UK
Texas-Red® X Phalloidin		x	/	red	F-Actin	1:400	Invitrogen Life Technologies Ltd, Paisley, UK
Phalloidin-488		x	/	green	F-Actin	1:1000	Invitrogen Life Technologies Ltd, Paisley, UK
DAPI		x	/	blue	DNA	1:10000	Invitrogen Life Technologies Ltd, Paisley, UK

The secondary antibodies or dyes were diluted in 0.1% goat serum and a humidified chamber was prepared as previously described. Again, 40-50 µl of dye or secondary antibody solution was pipetted onto the parafilm surface and the coverslip placed on top of it with the cells facing the liquid. The cells were incubated with the secondary antibody or dye for 35 minutes at room temperature in the dark without shaking. The coverslips were subsequently carefully placed into a clean 6-well dish and washed gently 7 times in PBS for 5 minutes each without shaking. Following the washing steps the cells were incubated in a DAPI solution (1:10000 in PBS) for 5 minutes in the dark and then washed immediately 3 times in PBS for 5 minutes each time.

- Mounting of the coverslip on microscopy slides

Whilst the cells were incubated with the secondary antibody or dye, the hydromount solution (AGTC Bioproducts t/a National Diagnostics UK, Hessle, UK) was warmed up to 37 °C. The slides were labelled and a drop of hydromount was pipetted onto the slide. The washed coverslips were gently removed from the well, briefly dried on paper and placed on the slide with the cells facing the hydromount solution. The slides were left to dry overnight at room temperature in the dark. The following day, residual hydromount was carefully removed. The coverslips were stored for 2-3 weeks at -20 °C without any significant loss in signal strength of the fluorophore.

Images of the cells were taken at a widefield upright microscope (Carl Zeiss Microscopy Ltd, Cambridge, UK) equipped with a monochrome CCD camera using AxioVision software (Carl Zeiss Microscopy Ltd, Cambridge, UK). Images were exported into Adobe Photoshop (Adobe Systems Europe Ltd, Maidenhead, UK) for labelling and formatting purposes.

- Image processing techniques

As we had experienced high, mainly red, background fluorescence in C2C12 cells, we needed to process images to exclude falsely-observed labelling. Negative samples for immuno-staining were prepared by processing fixed cells exactly as described previously. However, these cells were only incubated in incubation solution without primary antibody for the primary antibody step and later in incubation medium with the secondary antibody added. Negative samples for cells labelled with a dye were incubated in both incubation steps in incubation solution only.

For the image processing, pictures were taken for both the negative and the positive samples at the same settings (same wavelength, same (fixed) time of exposure, same saving mode .tif). Firstly the background signal was removed from the negative images by using the feature 'levels' in Adobe Photoshop (Adobe Systems Europe Ltd, Maidenhead, UK) and the setting for obtained exposure levels were saved for each channel. To remove potential background level from positive images, the determined exposure levels were imposed onto the original image. An example is given in the figure below:

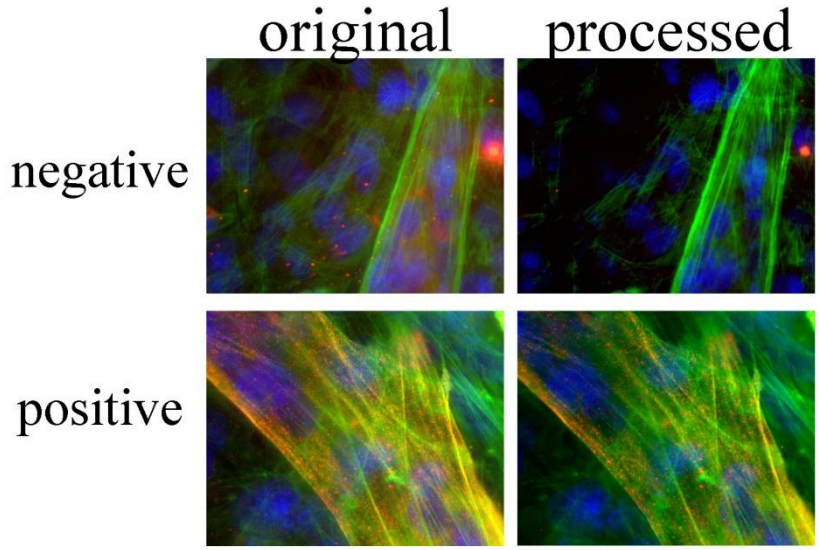

Figure 2.1: Reducing the background noise from immuno-labelled C2C12 myotubes

High autofluorescence in C2C12 myotubes overshadowed real fluorescent signalling. Removing the red background signal revealed a clearer labelling. However, the potential real signal was also weakened.

2.2.27 Latrunculin B treatment of C2C12 cells

Latrunculin B is a drug that can be used to reversibly depolymerise the actin cytoskeleton of a mammalian cell (Spector and others, 1983).

For preparation of C2C12 cells, myoblasts were cultured in a Nunc 6-well dish (Thermo Scientific, Fisher Scientific UK Ltd, Loughborough, UK) and differentiated into myotubes as described in section 2.2.21.

Once the C2C12 myoblasts reached a medium confluency of around 75% or C2C12 myotubes had differentiated to a specific degree, the cells were incubated in fresh growth or differentiation medium (see 2.2.21) containing 1 nM latrunculin B. The incubation with latrunculin B was carried for 15 minutes in the humidified incubator at 37 °C. Loss of Actin was calculated based on a) presence of rounded C2C12 cells and b) on signal strength of Actin fibres.

After the treatment with the toxin, the medium was removed quickly and immediately the afterwards the cells were fixed in 4% PFA containing additional Triton-X-100 to 0.25%. For recovery of the actin fibers, latrunculin B treated cells were incubated in fresh growth or differentiation medium for a specified amount of time. After recovery, the cells were fixed in 4% PFA with added 0.25% Triton-X-100.

Subsequently, fixed cells were processed for immuno-histochemistry as described in section 2.2.26.

2.2.28 Protein extraction from mammalian cells

Mammalian cells were cultured in Nunc EasYFlask 75cm^2 flasks (Thermo Scientific, Fisher Scientific UK Ltd, Loughborough, UK) as described in section 2.2.20 and 2.2.21.

Before lysis, the cells were washed twice in PBS and trypsinised as described in section 2.2.23. Once the cells detached from the surface of the flask, the enzymatic activity of trypsin was stopped by adding 1ml of cell culture medium to each flask. The cells were resuspended in the added medium and subsequently aliquoted into a sterilised eppendorf tube. The flasks were then rinsed with further 500 µl of cell culture medium to catch residual cells. The harvested mammalian cells were subsequently pelleted by centrifugation at 3000 rpm for 5 minutes. Obtained cell pellets were kept on ice to slow down protein degradation. The supernatant was completely removed and cells were lysed in 200 µl of RIPA protein lysis buffer on ice for 30 minutes. Samples were mixed by vortexing every 5-10 minutes. For the extraction of Klhl31 protein from mammalian cells, a mild lysis buffer was used including additional inhibitors of proteases, such as PMSF and sodium vanadate. Cells that were lysed with the mild lysis buffer were incubated on ice for 30 minutes without mixing or shaking.

To separate the cell debris from the protein solution, the lysis mixture was spun down at 4 °C for 10 minutes at 13000 rpm. The protein solution was pipetted into a clean eppendorf tube and stored at - 20°C. The concentration of the protein was measured by using the Bradford assay.

2.2.29 Measurement of protein concentration

The Bradford protein assay was developed by Marion Bradford and uses a colorimetric approach to calculate the concentration of proteins in a solution (Bradford, 1976). The Bradford solution, usually coloured red, will change to a blue colour upon binding of proteins. The strength of colour can be measured as the absorbance at 595 nm and is an indicator for the amount of protein present.

The protein concentration of the obtained samples was calculated based on a bovine serum albumin (BSA) standard. For the preparation of the BSA standard, a stock solution of 10 mg/ ml BSA in water was prepared. The stock solution was then further diluted to give a range of protein solutions with varying concentrations from 1 – 8 mg/ ml of BSA. 1µl of each BSA solution was then pipetted into a 1.5 ml disposable cuvette containing 1 ml of 1x Bradford reagent (Bio-Rad Laboratories Ltd., Hemel Hempstead, UK). The solution were gently mixed and incubated at room temperature for up to 2 minutes to allow development of the colour reaction. The absorbance of each sample was then measured at 595 nm using a bench-top spectrophotometer (Biochrom Ltd, St.Albans, UK). Based on measured absorbance values, a standard curve was drawn and the linear trendline and equation were calculated.

The protein lysate samples were prepared for the Bradford assay as described for the BSA standard and the absorbance measured at 595 nm. The approximate concentration of the protein lysates were calculated based on the values obtained for the BSA protein standard.

2.2.30 Preparation of Acrylamide Gel for SDS-PAGE

Depending on the sizes of proteins, which should be separated using a SDS-PAGE, different percentages of Acrylamide/bisacrylamide can be used when preparing the lower or protein separating polyacrylamide (PAA) gel.

For a standard 8% PAA gel the mixture was prepared as follows:

4.6 ml	dH_20
2.7 ml	Acrylamide/Bisacrylamide mixture (ProtoGel 30%, AGTC Bioproducts t/a National Diagnostics UK, Hessle, UK)
2.5 ml	1.5 M Tris pH 8.8
0.1 ml	10% SDS
0.1 ml	10% APS
10 µl	TEMED

To prepare the gel, the glass slides for a 0.75 mm thick PAA gel were assembled using fitted casting frames and casting stands as described by the manufacturer (Bio-Rad Laboratories Ltd., Hemel Hempstead, UK).

In a 50 ml beaker water, the Acrylamide mixture, Tris, SDS and APS were mixed together and TEMED was added to induce polymerisation. The solution was carefully filled into the glass plates up to a height of 2/3 of the glass plates without developing any air bubbles in the gel. The gel was then topped up with isopropanol and left to settle and polymerise.

Once the gel was set, the isopropanol was completely removed and the upper gel solution was added on top of the lower, protein separation gel. The upper gel is used to collect the samples and to make sure that protein samples enter the lower gel at the same time.

The mixture for the upper gel was prepared as described below:

3.4 ml	dH_20
0.83 ml	Acrylamide/Bisacrylamide mixture (ProtoGel 30%, AGTC Bioproducts t/a National Diagnostics UK, Hessle, UK)
0.63 ml	1 M Tris pH 6.8
0.05 ml	10% SDS
0.05 ml	10% APS
5 µl	TEMED

A 10-well comb (Bio-Rad Laboratories Ltd., Hemel Hempstead, UK) was placed into the upper gel and the gel was left to polymerise. Poured gels could be stored at 4 °C wrapped in wet paper for up to two days.

2.2.31 Protein sample preparation for SDS-PAGE

Up to 50 µg of protein was freshly prepared for SDS-PAGE. The protein solution was added in a ratio of 4 : 1 to a 5x protein loading buffer. The sample was mixed thoroughly by vortexing and incubated for 10 minutes at 70 °C. The samples were subsequently spun down at 13000 rpm for 2 minutes and immediately loaded on a PAA gel.

2.2.32 Sodium Dodecyl Sulfate Polyacrylamide Gel Electrophoresis (SDS-PAGE)

The SDS-PAGE is a well establish method to separate proteins based on their size and their charge. SDS is used in this method to introduce further negative charges to the proteins proportional to the size of protein.

The prepared gels were placed into a Mini Protean 3 Gel tank (Bio-Rad Laboratories Ltd., Hemel Hempstead, UK) and the tank was filled with SDS-PAGE running buffer

5 µl of Precision Plus Protein™ All Blue Standard (Bio-Rad Laboratories Ltd., Hemel Hempstead, UK) was loaded in one well of the PAA gel and usually 50 µg of total protein were loaded for each sample. The SDS-PAGE was usually carried out at 200 V for 45 minutes or until the blue loading dye was just about to move out of the bottom of the gel. The SDS-PAGE was stopped and the gel was either stained with Coomassie Blue or processed further for western blotting.

2.2.33 Coomassie-Blue staining

The gel used in the SDS-PAGE was carefully removed from the glass plates and rinsed once with PBS. The gel was then immediately fixed in fixing solution for 10 minutes at room temperature under constant moderate shaking. After the fixing the PAA Gel was stained with staining solution containing Coomassie brilliant blue R-250 for 15 minutes or up to several hours at room temperature. Coomassie staining of PAA gel is reversible and excess stain can eventually be removed by washing the stained gel several times in Destain solution. Once the gel was destained to the desired amount, the gel was placed on a transilluminator and a picture was taken with a standard digital camera. Images were labelled by using Adobe Photoshop (Adobe Systems Europe Ltd, Maidenhead, UK).

2.2.34 Western Blotting

The western blot is a method used to detect specific proteins in lysates or other protein mixtures. In the first part of the method, proteins are separated by an SDS-PAGE as described in 2.2.32, before they are transferred onto a membrane.

- Preparation of the membrane and the electro-blotting chamber

For the preparation of the blotting process, a piece of a Polyvinylidene fluoride (PVDF) (Bio-Rad Laboratories Ltd., Hemel Hempstead, UK) membrane with approximately the size of the lower gel was activated by incubation in 100 % methanol for 5 minutes. Once it was activated, the membrane was then incubated in western blotting transfer buffer. The lower gel from the SDS-PAGE (after being carefully removed from the

glass plates), as well as pieces of Whatman filter paper and the foam pads were also incubated in transfer buffer.

- Assembly of a wet electro-blotting chamber and western blotting

The western blot uses an electric current to move proteins out of the gel and unto the PVDF membrane. Therefore the proteins on the membrane will resemble the proteins as separated in the lower PAA gel. As proteins are negatively charged, they move towards the cathode or negative pole in a wet electro-blotting chamber.

The wet electro-blotting chamber, the Mini Trans-blot® cell (Bio-Rad Laboratories Ltd., Hemel Hempstead, UK), was prepared as described below.

Firstly, the gel holder cassettes were assembled in following fashion:

Cathode (+)

Foam pad

3 x Whatman filter paper (Whatman plc, Maidstone,UK)

Activated PVDF membrane (Bio-Rad Laboratories Ltd., Hemel Hempstead, UK

Lower PAA gel

3 x Whatman filter paper (Whatman plc, Maidstone, UK)

Foam pad

Anode (-)

The cassettes were then placed in the right orientation into the electrode-frame, which in turn was then placed into the tank. The tank was subsequently filled with transfer buffer and a cooling unit was placed into the tank.

The electroblotting was carried out at 100 V for 1 hour. The success of protein transfer was analysed by Ponceau-Red staining.

- Ponceau Red Staining

The Ponceau Red staining is a sensitive and reversible staining method for proteins on a PVDF or nitrocellulose membrane. For staining, the membrane was washed twice in

water and then incubated in the Ponceau-staining solution until bands became visible. The red staining could be completely removed by washing the membrane in water. The water was changed when saturated with the red stain.

- Blocking of the PVDF membrane and incubation with primary antibodies

After the red stain was completely removed the PVDF membrane was blocked with 10% milk (Marvel dried milk powder) diluted in TBST or 3 % BSA diluted in PBS depending on the primary antibody used. Blocking was carried out for 2 h at room temperature on a slow rocker. Subsequently the membrane was incubated in the desired primary antibodies, as listed in table 2.8.

Table 2.8: Primary Antibodies used for western blotting

Following list contains information about primary antibodies, their dilution factors and blocking solutions used for western blotting

name	species	detection	dilution	blocking solution	incubation solution	manufacturer
ab62181	rabbit	Klhl31	1:1000	10% milk (TBST)	1.25-2.5% milk (TBST)	abcam®, Cambridge,UK
ab290	rabbit	GFP	1:2000 - 1:5000	3% BSA (PBS)	3% BSA (PBS)	abcam®, Cambridge,UK
ab3280	mouse	Actin	1:5000	10% milk (TBST)	1.25-5% milk (TBST)	abcam®, Cambridge,UK
NB2	mouse	Nebulin	1:400	10% milk (TBST)	1.25-2.5% milk (TBST)	abcam®, Cambridge,UK

The membrane was incubated in the primary antibody overnight at 4 °C whilst shaking. The next morning the membrane was washed 6 times, each for 10 minutes, either in TBST or PBS depending on the primary antibody used, before being incubated in the secondary antibody.

- Treatment with the secondary antibody

For secondary antibodies, we used a horseradish peroxidise (HRP) conjugated antibody, which was able to detect the primary antibody based on the species the primary antibody was raised in. Antibodies used were either an anti-mouse

Immunoglobulins/HRP antibody or an anti-rabbit Immunoglobulins/HRP antibody (DakoCytomation Denmark A/S, Glostrup, Denmark). The secondary antibodies were diluted (1:1000 for the α-mouse HRP and 1:5000 for the α-rabbit HRP) in the same incubation solution as described for the treatment with the primary antibody. The incubation was carried out for one hour at room temperature. After treatment with the secondary antibody, the membrane was washed 6 times for 10 minutes each, either in TBST or PBS depending on the used primary antibody. After the washing steps, the membrane was prepared for the signal development.

- Signal development by ECL detection

Enhanced chemiluminescence (ECL) is a highly sensitive method to detect proteins from a western blot. The protein which has been detected with a primary antibody and which has been then further recognized by the secondary antibody can be visualised on the membrane by the oxidation of luminol by the horseradish peroxidise attached to the secondary antibody. Emitted light from the oxidation of the substrate by the HRP is then detected and visualizes a specific band on the membrane.

For the ECL reaction, the substrate solutions (western blot colour development solution 1 containing 0.1M Tris pH 8.8, 2.5mM Luminol, 0.4mM *p*-Coumaric acid and western blot colour development solution 2 made up with 0.1M Tris pH 8.5, 0.02% v/v H_2O_2) were prepared and stored in the dark. In the meantime the dark chamber of the LAS-3000 Imaging System (Fujifilm Medical Systems, Stamford, USA) was cooled down to -30 °C. Once cooled down, the membrane was taken out of the washing solution, briefly dried on paper and immediately incubated for one minute in the freshly mixed western blot colour development solution 1 and western blot colour development solution 2. Following the incubation with the oxidation substrates, the membrane was briefly dried, carefully wrapped in clingfilm and the protein marker labelled with a lumocolor pen. The membrane was immediately placed on a tray in the dark chamber and focused. Once the ECL signal was detected, a picture was taken by the LAS-3000 Imaging system (Fujifilm Medical Systems, Stamford, USA) with an inbuilt CCD camera. Images were exported into Adobe Photoshop (Adobe Systems Europe Ltd, Maidenhead, UK) for labelling purposes.

2.2.35 Stripping a membrane for reprobing

The method of stripping can be used to remove primary and secondary antibodies from the membrane, making it possible to use the same membrane to stain for a different protein. Therefore one protein was detected on a western blot as described in section 2.2.34, followed by the gentle removal of all bound antibodies from the membrane without affecting the transferred proteins. For this method, the membrane was washed 3 times in PBS after the ECL detection and subsequently incubated for 10 minutes in mild stripping buffer (0.2M Glycine, 0.1% w/v SDS, 1% v/v Tween-20, pH 2.2) at room temperature whilst gently rocking. The buffer was removed and replaced by a fresh volume of mild stripping buffer. After further incubation of 10 minutes, the membrane was twice washed for 10 minutes in PBS followed by two washes in TBST for 5 minutes each. The membrane was then ready to be blocked and incubated in a primary antibody as described in section 2.2.34.

2.2.36 Glutathione S-transferase (GST) pull downs

Interaction of proteins can be verified by using a GST-pull down. GST-proteins are in *E.coli* expressed fusion proteins which contain a GST-tag. This GST can be used to purify the GST-protein by affinity chromatography on immobilised glutathione, as it forms strong dimers with the GST-tag. Contamination can then easily be removed by washing the glutathione. Incubating the purified GST-protein with cell or other protein lysates will eventually lead to the binding of interaction partners to the GST-protein, which can then be purified and gently be removed from the glutathione phase. Obtained samples can then be analysed by mass spectrometry or western blot to identify interaction partners.

- Preparation of the GST-Klhl31 protein

The first part of the preparation was the production of a stable GST-Klhl31 Fusion protein. We have cloned a pGEX-5X-1 Klhl31 construct having the GST fused to the N-term of the Klhl31 protein (see section 2.2.18). In the pGEX- vectors the expression of the GST-Fusion protein is controlled by a *tac* promoter, which can be activated by IPTG.

Competent cells (DH5α) were transformed with either pGEX-5X-1 or with pGEX-5X-1-Klhl31 as described in section 2.2.1. A 5 ml pre-culture was grown for each construct and stored at 4 °C. The evening before the IPTG induction a 50 ml culture for each construct was started by adding 50 µl of each pre-culture. The cells were shaken overnight at 200 rpm and 37 °C. The next morning the whole 50 ml culture was added to 500 ml of fresh medium and cells were grown for 3 hours at 37 °C to achieve an optical density of 0.3-0.6. The medium was cooled down to 21 °C and the expression of the GST or GST-Fusion protein was induced by the addition of IPTG to a final concentration of 1 mM. The two *E.coli* cultures were shaken at 21 °C for further 3 hours. After the incubation, the cells were pelleted from the medium by centrifugation at 4500 rpm using 50 ml falcon tubes. Each falcon tube contained a cell pellet from at least 100 ml of cell culture. The cell pellets were stored at -20 °C until processed for purification of the fusion proteins.

- Purification of the GST-Fusion protein

The frozen cells containing the overexpressed proteins, either GST only or GST-Klhl31 FL, were thawed on ice and lysed with 9 ml STE-Buffer (0.1M NaCl, 10mM Tris pH 8.0, 1mM EDTA pH 8.0) containing 50 µg of lysozyme (50 µl of 100 mg/ml stock solution). From this point onwards, both samples, the GST and the GST-Klhl31 FL lysates were treated exactly the same. The bacterial cells were incubated in the lysis buffer for 15 minutes on ice without mixing or shaking. Following the lysis step Sarkosyl (10% in STE-Buffer) was added to the lysate to a final concentration of 2%, as well as DTT to a final concentration of 1 mM and PSMF was also added to 1 mM final concentration. The cells were then further disrupted by french pressing and the lysate was centrifuged at 15000 rpm for 5 minutes. The supernatant was subsequently placed into a clean 10 ml Falcon tube. 50 µl of supernatant were kept for analysis by SDS-PAGE, whilst Triton X-100 was added to the supernatant in the falcon tube to a final concentration of 1%. 500 µl of GST-beads slurry (Glutathione Sepharose High Performance beads, GE Healthcare Life Sciences, little Chalfont, UK) were added to each sample and incubated for up to 2 hours in the cold room at 4 °C on a slow shaker. The proteins should have now bound to the glutathione Sepharose beads. A sample of 50 µl was removed from the suspension and the beads were gently spun down at a maximum of 2000 rpm for 1 minute. The supernatant was removed and discarded. The beads were then washed 6 times for each 5 minutes in PBS. The GST and GST-Klhl31 bound beads were be kept in the fridge at 4°C for up to 3 weeks. To approximate the

amount of proteins on the beads, specified volumes between 5 – 20 µl of bead suspension were analysed on a 1% PAA gel next to a gradient of known BSA concentration of 1-5 mg/ml (as described in section 2.2.32).

- Lysis of C2C12 myoblast and C2C12 myotubes

C2C12 cells were cultured and differentiated as described in section 2.2.21. For a GST-Pull down C2C12 cells were lysed in 2 ml of mild lysis buffer (50mM Tris pH 7.5, 150mM NaCl, 5mM EDTA pH7.5, 1% v/v NP-40, 10% v/v Glycerol, 1mM Na_3VO_4, 1mM PMSF, 1 Complete Mini, EDTA-free Protease inhibitor cocktail tablet (Roche Diagnostics Ltd, Burgess Hill, UK) per 10ml of buffer) for 30 minutes on ice without shaking. The protein lysate was obtained as described in section 2.2.28 and immediately processed further for the GST-pull down.

Fresh PMSF was added to the C2C12 protein lysate and 100µl of GST or GST-Klhl31 beads were added to the lysate. The suspension was incubated for up to 1 hour on a rocker at 4 °C. The supernatant was then removed from the beads and kept as a control for further analysis, whilst the beads were washed 6 times in mild washing buffer at 4 °C. The beads were pelleted down by centrifugation between each washing step, using 3000 rpm at 4 °C. After the 6^{th} wash the buffer was removed until only 100µl of slurry was left. As the GST-beads suspension was higher concentrated compared to the GST-Klhl31 bound beads, the GST beads were further diluted in PBS to give equal amounts of GST-Klhl31 to GST. 100µl of each suspension was prepared for SDS-PAGE by adding protein loading buffer to 1x and DTT to 1mM. The protein samples were heated up to 70 °C for 10 minutes and immediately run on a large (17 x 15 cm) 10% PAA Gel, which were subsequently processed for silver staining, or on normal sized 10% PAA gels for western blotting (as described in section 2.2.33).

- Preparing a V15.17 10 % PAA gel

To give proteins from the GST-pull down enough space to separate during SDS-PAGE, we chose to use a larger (17 x 15 cm) 10% PAA gel based on the BRL Vertical Gel electrophoresis apparatus model V15.17 (Biometra, THISTLE SCIENTIFIC LTD, Glasgow, UK). The apparatus was kindly lent to us by Dr. Tracey Swingler, BMRC.

For the preparation of the gel, the glass plates were assembled and the sides of the glass plates were taped and clipped to keep them tight. The glass plates were then placed into a large, square dish and sealed in an approximately 1cm high layer of 1 % agarose. A

lower gel was prepared based on the mixture as described for the PAA gel as described in sub chapter 2.2.30. After letting the gel set, the upper gel was prepared as described previously (section 2.2.30) and poured on top of the lower gel. A 20 well comb was added and the gel left to polymerize. Gels could be stored in the fridge at 4 °C wrapped in wet tissue for one day. To run the SDS-PAGE the gel was placed into the gel chamber with the comb facing inwards resting on the orange sponges. The gel was pressed tightly against the sponges and spaces between glass plates and chamber closed with Vaseline. Running buffer was filled into the upper tray and if no leakage was observed the lower tray was filled up as well. Up to 100 µl of sample could be loaded per well. The SDS-PAGE was run as described in section 2.2.32.

- Protein visualisation in a PAA gel by Silver Stain and mass spectrometry

Silver staining is a method to detect proteins in a PAA gel. This method is up to 50 times more sensitive when compared to Coomassie Blue staining (Kerenyi and Gallyas, 1973; Switzer and others, 1979). To prevent contamination, the gel was only touched with tweezers or when wearing fresh gloves, as proteins from the skin will be detected by the silver stain. Using Pierce® Silver Stain for Mass Spectrometry (Thermo Fisher Scientific, Cramlington, UK), borrowed from Dr. Samuel Fountain, the gel was prepared and stained as described by the manufacturer's instructions. After the staining, interesting protein bands were excised from the gel and stored in a clean eppendorf tube at -80 °C. Excised bands were analysed by mass spectrometry, carried out by the FingerPrints Proteomics Facility at the College of Life Sciences (University of Dundee, UK).

3. Results

Klhl31 associates with the actin cytoskeleton in mouse myoblasts

3.1 Introduction

3.1.1 C2C12 cells are a well-characterized model for myogenesis

C2C12 cells are subclones of C2 mouse myoblasts, which have the ability to differentiate into myotubes or osteoblasts based on culturing in different conditioned media. First obtained by Yaffe and Saxel in 1977 from satellite cells generated from the thigh muscle of C3H mice (Yaffe and Saxel, 1977) C2C12 have been shown to be a good tool for studying myogenesis and osteogenesis on a cellular level.

Differentiation into osteoblasts is triggered by BMP-2 signalling, which has been shown to inhibit myotube formation whilst inducing the expression of osteoblast markers, such as various alkaline phosphatases and osteocalcin (Katagiri and others, 1994). Myotube formation is achieved by starvation of C2C12 myoblasts from various growth factors, for example TGF-β (Brennan and others, 1991; Furutani and others, 2011; Vaidya and others, 1989) and β-catenin dependent or canonical Wnt ligands, such as Wnt3a (Tanaka and others, 2011). Serum Starvation will lead to the expression of late myogenic markers in C2C12, switching myoblasts from a proliferative state towards differentiation (see figure 3.1). This process is characterised by the withdrawal from cell cycle followed by elongation of the myoblasts and fusion of these to form multinucleated myotubes (Andres and Walsh, 1996; Walsh and Perlman, 1997).

As C2C12 cells have been shown to express endogenous Klhl31 (Abou-Elhamd), we chose this cell line as a model to study Klhl31 expression during muscle development.

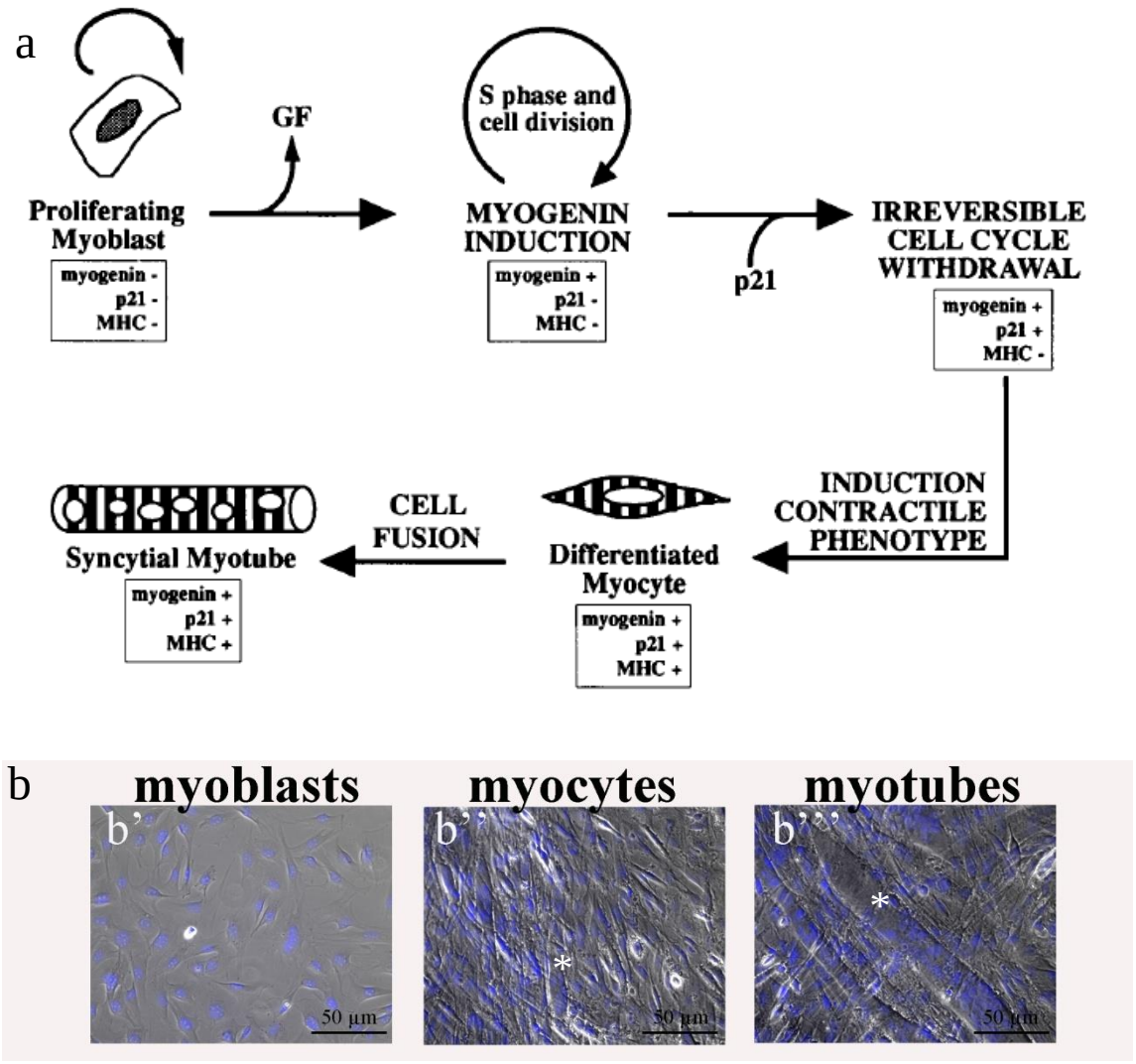

Figure 3.1: Schematic outline and time course of differentiation of C2C12

(a) Multiple steps are involved in the differentiation of C2C12 myoblasts

Upon starvation from growth factors C2C12 start to express the late myogenic marker myogenin followed by expression of p21 leading to cell cycle withdrawal. C2C12 myoblasts will then undergo major cytoskeletal changes including elongation and subsequent fusion to form multinucleated myotubes.
Scheme taken from Andres and Walsh, 1996

(b) Differentiation of C2C12 myoblasts

C2C12 were grown on coverslips and stained with DAPI to visualize DNA in the nucleus. On Day 0 C2C12 myoblasts are single cells, either polygonal (b'), which proliferate and upon growth factor removal start to elongate, indicated by * (b''). After approximately four to five days of differentiation multinucleated myotubes (indicated by *) are formed (b''').

As differentiation of C2C12 is well described, both on genetic and molecular level, we use this myogenic cell line to study the localisation and function of Klhl31 during the cellular processes of myogenesis.

3.1.2 Cytoskeletal changes during differentiation of C2C12

Cytoskeletal dynamics in C2C12 myoblasts have been intensively studied. The cytoskeleton is involved in generating, stabilising and changing the shape of cells. Microfilaments, microtubules as well as intermediate filaments and cell surface receptors all play key roles in cytoskeletal changes (Alberts, 2008; Mermelstein and others, 2003).

A major part of the cytoskeleton is composed of Actin fibres (Alberts, 2008; Pellegrin and Mellor, 2007; Tojkander and others, 2012). These fibres are formed by two-stranded helices. In fibroblasts, Actin bundles are attached to each other by alpha-actinin (Lazarides and Burridge, 1975), an Actin crosslinking protein, that is also involved in the organisation of Actin to the Z-discs of sarcomeres (Crawford and Horowits, 2011; Lazarides, 1975). Changes in Actin fibres can be mediated by signalling from integrins and other cell surface receptors, which interact with Actin at focal adhesion sites in the cell (Arora and others, 1999; Hinz, 2006; Sandbo and Dulin, 2011). As Actin fibres are polarised structures it has been shown that various myosin motor proteins use the Actin fibres to transport cargo throughout the cell (Kapitein and Hoogenraad, 2011).

Microtubules have also been studied as a vital part of the cytoskeleton being also involved in cell shape formation and stabilisation (de Forges and others, 2012; Suzuki and others, 2012). Microtubules are dynamic structures constantly assembling and de-assembling to adapt to cellular changes (Alberts, 2008). They are made of α-tubulin and β-tubulin dimers, which polymerize to form Microtubules (Alberts, 2008). Microtubules also play an important role in intracellular transport (Stehbens and others, 2009). Active transport is carried out by motor proteins, kinesin and dynein, which travel along microtubules in a polarity–driven fashion. For example kinesin moves along microtubules in an anterograde orientation, whilst dynein moves along microtubules towards their minus-end (Vale, 2003; Welte, 2004)

The cytoskeleton undergoes various changes during differentiation of C2C12 (Ohtake and others, 2006). Studies carried out by immuno-fluorescence, as well as electron microscopy, have given detailed insight into myoblast differentiation and cytoskeletal changes (Burattini and others, 2004; Kontrogianni-Konstantopoulos and others, 2006). Analysing the Actin cytoskeleton it was shown that in undifferentiated C2C12 cells, Actin seems to be diffusely distributed throughout the cytoplasm with thicker Actin bundles appearing at the periphery of the cell (Burattini and others, 2004). Using antibodies against α-sarcomeric and cardiac Actin it was shown that both Actin isoforms are expressed at high levels in C2C12 myoblasts (Burattini and others, 2004).

Around day two or day three of differentiation (labelled as intermediate differentiation stage by Burattini et al. in 2004) C2C12 cells elongate and intercellular spaces seem to narrow down. Phalloidin labelling revealed that the Actin fibres become denser and align in fibrillar orientation until Actin fibres are seen along the whole myotube (Burattini and others, 2004). Analysing the cytoplasm of myocytes in more detail, initial myofibrils can be seen by electron microscopy. Thin filament organization can be observed as well as premature Z-bodies (see figure 3.2). Premyofibrils have been described previously in C2C12 (Sanger and others, 2002). These authors also described structures termed minisarcomeres in C2C12 cells and avian primary muscle cells. They found that in differentiating primary muscle cells premature Z-bodies (termed primitive Actin anchoring structures by Sanger et al., 2002) are formed of alpha-actinin attaching Actin to itself, as well as to mini-A-bands comprising non-muscular myosin II filaments.

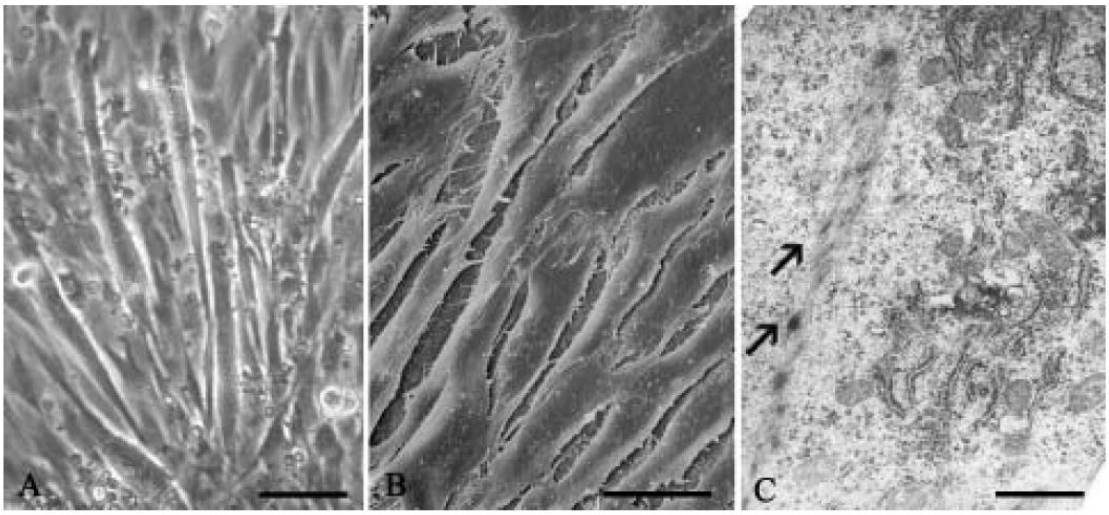

Figure 3.2: The intermediate differentiation stage of C2C12

Using reverted microscopy (A) as well as scanning electron microscopy (B), C2C12 can be seen to elongate. Analysing C2C12 myocytes by transmission electron microscopy revealed the presence of premature myofibrils and Z-bodies (indicated by arrows)

Legend: A, bar = 50 µm; B, bar = 20 µm; C, bar = 0.5 µm

Figure taken from Burattini and others, 2004

Sanger et al. further investigated the formation of mature myofibrils. Myofibrils are established by the alignment of primitive myofibrils (Rhee and others, 1994; Sanger and others, 2002). Furthermore, it was described that early Z-bodies fuse and non-muscle myosin II is removed from the minisarcomeres as titin and muscle myosin II are added to the myofibrils. Analysing fully differentiated C2C12 by transmission electron microscopy, sarcomeres and myofibrils can be observed as described by (Rhee and others, 1994; Sanger and others, 2002).

During C2C12 differentiation the foundation is laid for the formation of mature sarcomeres. In differentiated C2C12 myotubes thin and thick filament containing structures are already present, showing a similar organization to mature myofibrils (Burattini and others, 2004; Sanger and others, 2002). The differentiation process of C2C12 can therefore be used to study the tightly regulated process of early myofibrillogenesis.

3.1.3 Expression analysis of Klhl31 by RT-PCR

We used the ability of C2C12 to differentiate into myotubes to investigate the role of endogenous *Klhl31* during differentiation of C2C12 and fusion of myocytes into myotubes. After transfer of C2C12 into differentiation medium (section 2.2.21), we collected RNA from each day between day 0 (non-differentiated) and day 4 inclusive (early myotubes). Transcribing $2\mu g$ of collected RNA into cDNA (section 2.2.13) we assessed the quality and relative quantity of the obtained cDNA by analysing the presence of an abundant gene, mouse *β-Actin* (see figure 3.3).

Figure 3.3: Quality control of cDNA of C2C12 Differentiation time course

cDNA obtained from C2C12 cells undergoing differentiation were tested for relative quantity and quality. Using mouse β-Actin primers a 480 bp PCR product was amplified. As a positive control for the PCR we used a previously established sample of chick cDNA and primers against chick β-Actin amplifying a 400 bp PCR product. Water was used as a negative control. cDNA obtained from 3T3 mouse embryonic fibroblasts were used as a positive control for the mouse β-Actin primers.

Legend: M - marker, + - positive control (chick cDNA), - - negative control, D0- Day 0, D1 – Day1, D2 – Day2, D3 – Day3, D4 – Day4

Examination of generated cDNA for the presence of mouse *β-Actin* suggested that a similar amount of C2C12 cDNA had been obtained for each day of the differentiation time course (see figure 3.3; D0-D4). We then moved on to analyse the expression of *Klhl31* during myotube formation.

Klhl31 expression was only detected at Day 3 and Day 4 of differentiation of C2C12 myoblasts showing an increase in the PCR product obtained for *Klhl31* as differentiation progressed (see figure 3.4).

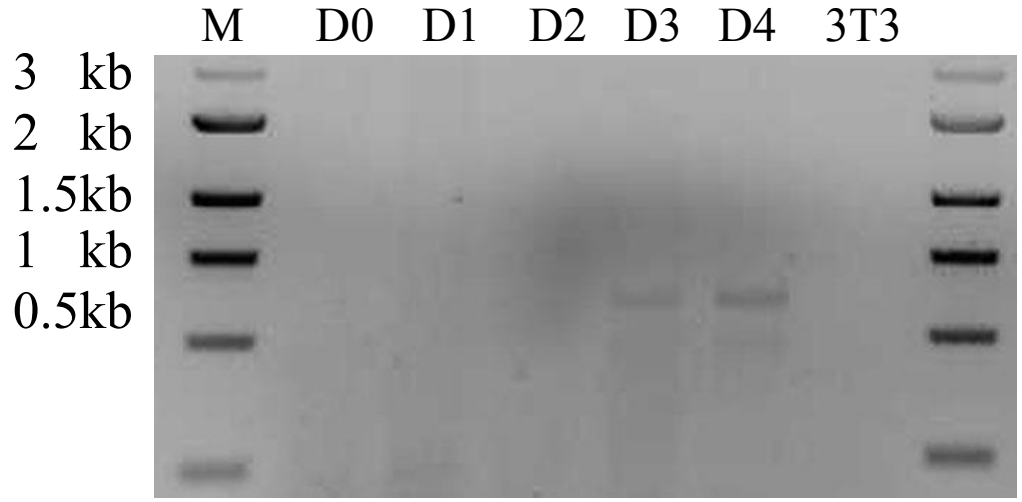

Figure 3.4: Klhl31 expression during differentiation of C2C12

We used primers designed against mouse Klhl31 to detect gene expression for Klhl31 during C2C12 differentiation. The predicted size for the DNA fragment was 1177 bp. 3T3 were used as a negative control.

Legend: M - marker, D0- Day 0, D1 – Day1, D2 – Day2, D3 – Day3, D4 – Day4

Klhl31 expression was not detected during early differentiation of C2C12 myocytes (figure 3.4; D0-D2). However, Klhl31 expression seemed to increase significantly during later stages of differentiation of C2C12 (see figure 3.4; D3-D4). In 3T3 mouse fibroblasts the Klhl31 PCR product was not detected (figure 3.4; 3T3).

As Klhl31 mRNA levels seemed to increase after day 2 of C2C12 differentiation, we wondered if protein levels of Klhl31 also increase during C2C12 elongation and fusion.

3.1.4 Klhl31 protein levels increased during differentiation of C2C12

To investigate protein levels of Klhl31 during myotube formation, we collected protein samples at different time points of C2C12 differentiation as described in section 2.2.28. 50 µg of whole protein lysate was loaded onto a 10 % PAA Gel, transferred to a PVDF membrane and subsequently blotted for Klhl31. The membrane was then stripped and re-probed with an Actin antibody as a loading control (see 2.2.35).

The western blot against Actin revealed that similar amounts of proteins were loaded onto the gel (see figure 3.5). Blotting the membrane against Klhl31 showed a low level of Klhl31 proteins in myoblasts. However, the protein amount for Klhl31 increased during myotube formation (see figure 3.5; a). Stripping and reprobing the western blot with an anti-Actin antibody revealed loading of similar protein amounts per sample (figure 3.5; b).

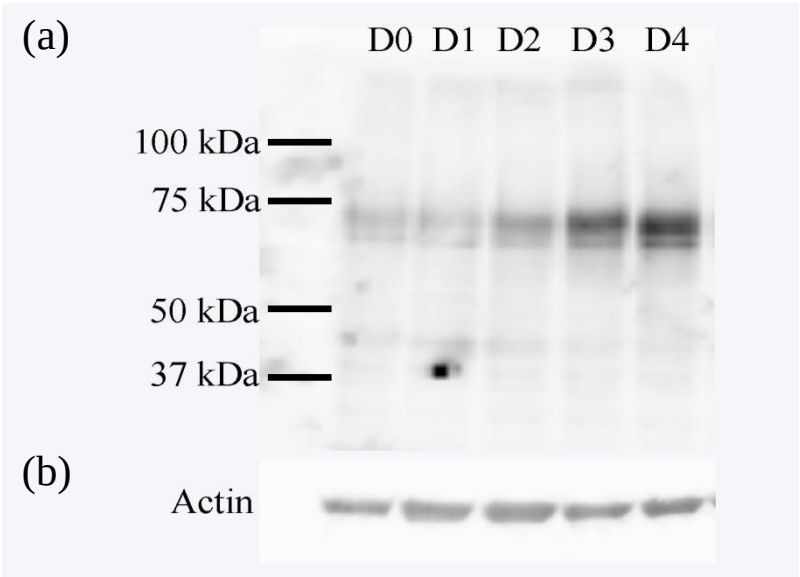

Figure 3.5: Klhl31 protein levels during Differentiation of C2C12

(a) Protein lysates obtained during a 5-day time course of C2C12 differentiation were analysed by western blot incubated with an antibody against Klhl31.

(b) Blotting against Actin was used as a protein loading control.

Legend: M - marker, D0- Day 0, D1 – Day1, D2 – Day2, D3 – Day3, D4 – Day4

Overall, data from both the RT-PCR as well as the Western Blot revealed an increase of Klhl31 expression during C2C12 differentiation.

3.2 The sub-cellular localisation of Klhl31 during differentiation of C2C12

3.2.1 Klhl31 was localised in the cytosol in undifferentiated C2C12, but changed its localisation during myotube formation

Data from a recent publication reported a localisation of Klhl31 in the cytosol and around the nucleus of COS-7 and HeLa cells based on GFP-labelled fusion-proteins (Yu and others, 2008). To determine the localization of Klhl31 protein in C2C12 cells we used an immuno-staining approach to detect endogenous Klhl31 during a five-day time course of differentiation (from undifferentiated myoblasts to differentiated myotubes) of C2C12. It could be shown, that Klhl31 was localised in the cytoplasm of myoblasts (see figure 3.7: a and a') in a punctate pattern. A potential punctate, nuclear localisation of Klhl31 could also be observed in some C2C12 myoblasts (see figure 3.6: a'). In elongating C2C12 these puncta remained visible. Furthermore, they seemed to increase in quantity and then align to generate a filamentous pattern (figure 3.6: b and b'). After myotube formation Klhl31 puncta followed straight, well-organized lines similar to fibrillar structures inside the C2C12 myotubes (figure 3.6: c and c').

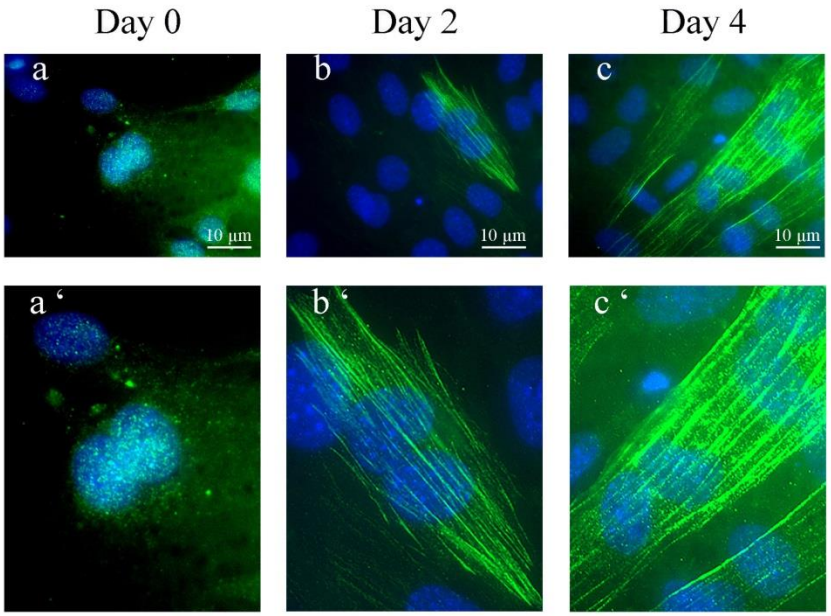

Figure 3.6: Localization of Klhl31 protein during C2C12 differentiation

Endogenous Klhl31 was detected with a polyclonal rabbit anti- human Klhl31 antibody and visualised with a secondary Alexa Fluor 488 antibody (green). Nucleic DNA was labelled with DAPI (blue).

Klhl31 levels changed during the differentiation of C2C12. An increase of Klhl31 was observed at mRNA and protein level by PCR and Western blot. Furthermore, Klhl31 localization was dynamic during C2C12 differentiation. These changes seem to correlate with major changes in the shape and structure of C2C12 cells themselves.

3.2.2 Klhl31 co-localises with Actin fibres, but not with Microtubules

We have seen that Klhl31 forms puncta that are organized in a linear pattern in differentiated C2C12 cells (figure 3.6). This organised Klhl31 localisation seems to be established around the time point in C2C12 differentiation that is defined by the changes of Actin leading to the formation of premature myofibrils. Based on the described localisation pattern, similar to motor proteins and previous data stating that members of the Kelch-like family bind to Actin (Hara and others, 2004; Robinson and

Cooley, 1997; Stogios and Prive, 2004), we were wondering if Klhl31 could associate to the cytoskeleton in C2C12 myotubes.

We analysed the possible co-localisation of Klhl31 with cytoskeletal components using immuno-histochemistry. Double immuno-staining was carried out detecting Klhl31 either together with Actin or α-tubulin in myoblasts and during the differentiation process of C2C12.

Using either Texas-Red labelled phalloidin (red) or an Alexa-Fluor 488 conjugated phalloidin (green) we were able to reproduce the cytosolic localisation described for Actin in myoblasts, as well as in differentiating C2C12 myocytes (Burattini and others, 2004). In addition, we were able to visualize the changes of the Actin cytoskeleton during differentiation of C2C12 mouse myoblasts (figure 3.7).

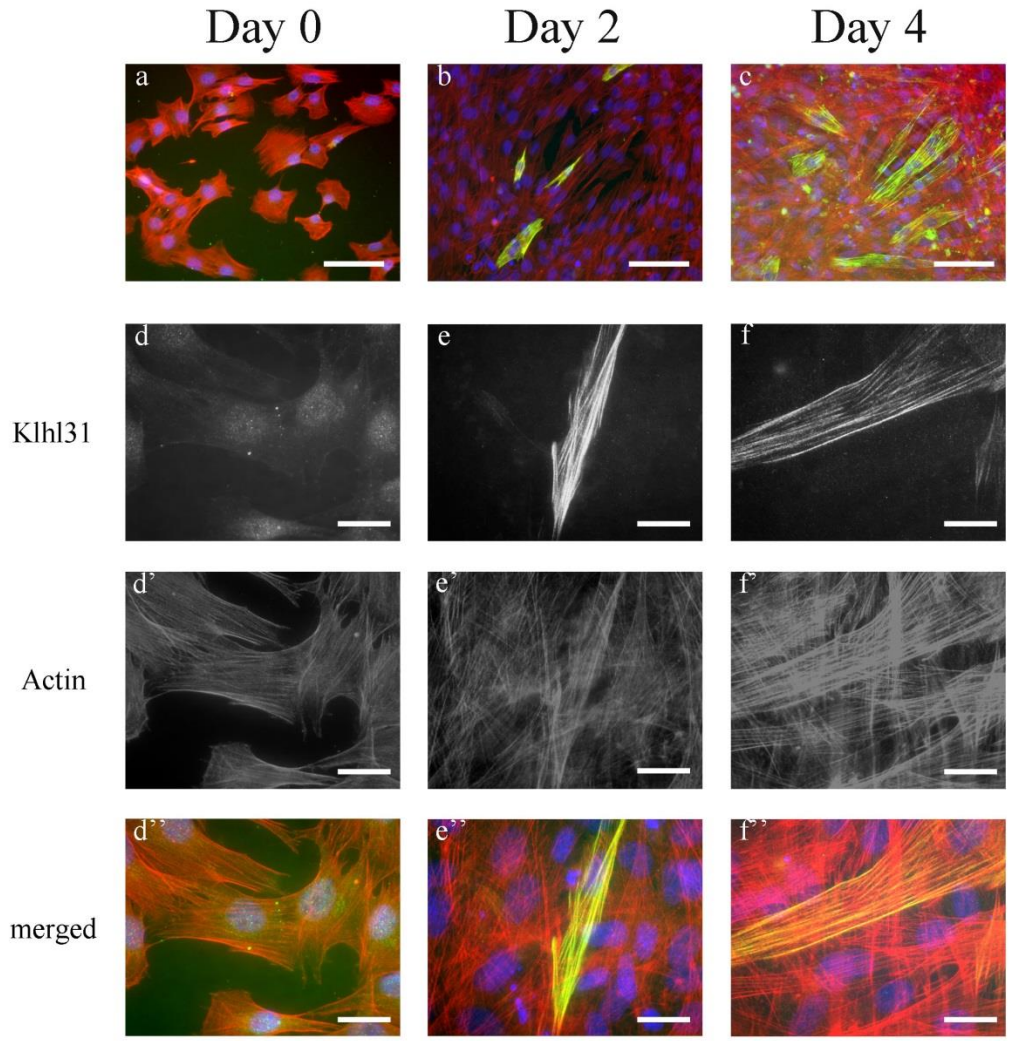

Figure 3.7: Klhl31 co-localizes with Actin, but only in differentiating myocytes

The figure shows the localisation of Klhl31 and Actin in C2C12 during differentiation. Endogenous Klhl31 was detected with a polyclonal rabbit anti-human Klhl31 antibody and visualised with a secondary Alexa Fluor 488 antibody (green). Actin was visualized using Texas-Red-Phalloidin (red). Nuclear DNA was labelled with DAPI (blue). Single channel images for either Klhl31 (d ,e, f) and for Actin (d' ,e', f') are shown in grayscale and have been merged in images d'' ,e'' and f''.

Scale bars: (a, b, c) – 50 µm, (d ,e, f, d', e', f', d'', e'', f'') – 10 µm

(a, d, d', d'') Klhl31 and Actin localisation in C2C12 myoblasts (Day0) using a 20x objective (a) and a 63x objective (d, d', d'')

(b, e, e', e'') Klhl31 and Actin localisation during the intermediate stage of C2C12 differentiation (Day2) using a 20x objective (b) and a 63x objective (e, e', e'')

(c, f, f', f'') Klhl31 and Actin localisation in more mature differentiating C2C12 (Day4) using a 20x objective (c) and a 63x objective (f, f', f'')

In C2C12 myoblasts Actin fibres can be seen in the cytoplasm spanning the polygonal cell in a non-organised fashion, but linear pattern (figure 3.7; a and d'). However around day 2 of C2C12 differentiation Actin fibres elongate in correlation with elongation of the cells and the Actin fibres now reveal a parallel pattern, as the cell itself has now changed its form to resemble a more tube-like phenotype (figure 3.7; b and e'). In further differentiated, tube-like C2C12 myocytes the Actin fibres span the whole cytoplasm in a parallel pattern (figure 3.7; c and f'). Furthermore, the Actin density seem to have increased during differentiation, as also described by (Burattini and others, 2004).

In undifferentiated C2C12 myoblasts Klhl31 did not co-localize with Actin (figure 3.7; a and d''). Again, a nuclear staining for Klhl31 could be observed (figure 3.7; d). However in more mature, differentiating C2C12 myocytes and in fully differentiated myotubes, Klhl31 was found to align to Actin fibres (see figure 3.7; c, f'', figure 3.8). The co-localisation seemed to be established during the intermediate stage of differentiation (see figure 3.7; b, e'') when the foundation for primitive myofibrils is laid down and Actin is incorporated into early Z-bodies (Rhee and others, 1994; Sanger and others, 2002). Furthermore it was again observed that the protein levels of Klhl31 increased during C2C12 differentiation (figure 3.7; a-c).

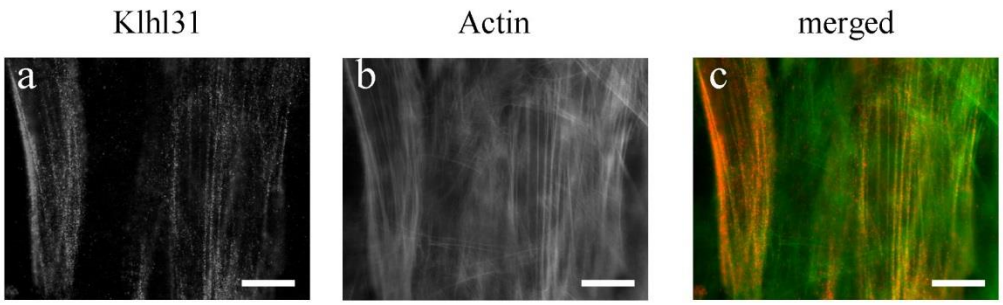

Figure 3.8: Klhl31 co-localizes to Actin fibres in myotubes

Endogenous Klhl31 was detected with a polyclonal rabbit anti-human Klhl31 antibody and visualised with a secondary Alexa Fluor 568 antibody (red). Actin was visualized using an Alexa-Fluor 488-Phalloidin (green).

The image was taken with a 100x objective of a single, fully differentiated C2C12 myotube. Images a and b, respectively show single channel frames of the same myotube for Klhl31 (a) and Actin (b). Both single channel images were merged in image c.

Scale bar (a, b, c) – 10 µm

Next, the possible association of Klhl31 with microtubules was investigated.

As before double immuno-staining was used, this time for Klhl31 and α-tubulin (see figure 3.9). We observed similar localisation patterns of microtubules in C2C12 myoblasts and myotubes as described previously by Tassin (1985). Microtubules in C2C12 myoblasts span the whole cell with an organised network of fibres around the nucleus, from where the tubulin organisation centre originates. In myotubes however the microtubules exhibit longitudinal structures parallel to the sarcolemma (Azakir and others, 2010; Tassin and others, 1985).

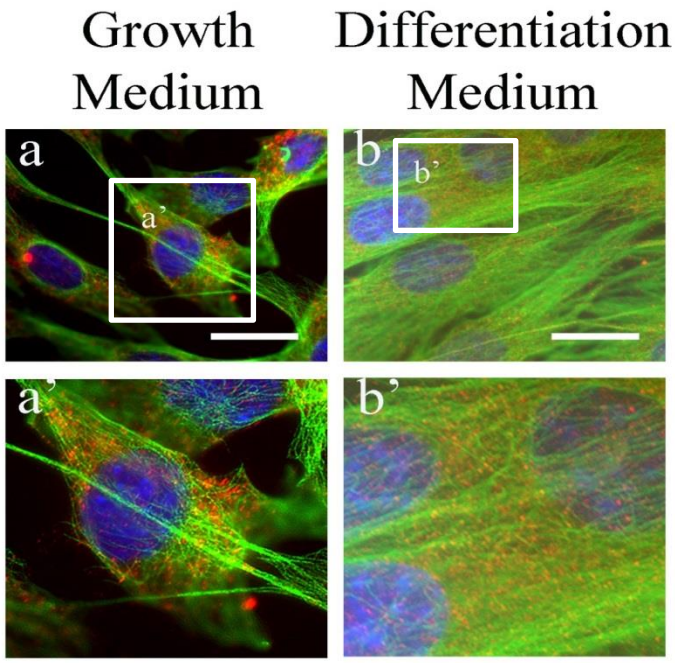

Figure 3.9: Klhl31 might co-localize with microtubules

Endogenous Klhl31 was detected with a polyclonal rabbit anti-human Klhl31 antibody and visualised with a secondary Alexa Fluor 568 antibody (red). Microtubules were detected with a rat anti-α-tubulin antibody and visualized with a secondary Alexa-Fluor 488 antibody (green). Nuclear DNA was labelled with DAPI (blue).

Scale bar (a, b) – 10 µm

Klhl31 co-localization with microtubules was not as clear as seen for Klhl31 with Actin, either in C2C12 myoblasts or in differentiating myocytes (see figure 3.9; a, b). Most of the Klhl31 did not seem to co-localise with α-tubulin. However some yellow fluorescence signal was observed indicating a close localisation of Klhl31 and microtubules. Co-localisation is difficult to analyse using an upright microscope and confocal images would help investigating the interaction of Klhl31 with microtubules during C2C12 differentiation. As we did not observe a strong close alignment of Klhl31 to α-tubulin in C2C12 cells as compared to seen co-localisation for Klhl31 and Actin, we therefore assumed that Klhl31 is mainly associated with the Actin cytoskeleton.

To further investigate the relationship between Klhl31 and Actin, we decided to analyse the effects of Latrunculin B on both the Actin cytoskeleton and Klhl31.

3.2.3 Latrunculin B treatment of C2C12 myoblasts disrupts Klhl31 localisation

Latrunculin A and latrunculin B are both toxins that are produced by red sea sponges of the latrunculia family (I. Neeman, 1975; Spector and others, 1983). One molecule of latrunculin can bind one Actin monomer and prevent it from polymerising (Coue and others, 1987; Spector and others, 1983). Not only is Actin -polymerisation disabled by latrunculin A and latrunculin B, both drugs also depolymerise the existing Actin-cytoskeleton. The process is fast and reversible after latrunculin removal (Coue and others, 1987; Morton and others, 2000; Spector and others, 1983).

Table 3.1: Optimization of Latrunculin B experiments

As we have not used Latrunculin B on C2C12 before, we first optimized treatment conditions for each cell culture type, C2C12 myoblasts (table 3.1a) and C2C12 myotubes (table 3.1b). We tested various concentration, as well as different incubation times with the drug and different recovery time after treatment to find the best settings to carry out the final experiments. The table shows how experiments were planned and the results we gathered from it. The table also contains information about the microscopy settings used for image acquisition.

Abbreviations: LaB – Latrunculin B

table 3.1a			experimental settings						microscope setting			results
Number	cells	dish	concen-tration LaB (2mM stock)	treatment time (min)	recovery time (min)	negatives	control	Fix	GFP exposure time	568 exposure time	objective	
1	titration C2C12 growth	12 well/ 1ml	1:10000 1:5000 1:2000	15/30 15/30 15	60		non treated C2C12	PFA + 0.25% Triton X-100	1.9 sec	14 sec	20x/100x	C2C12 loose actin and recover, best choice 1:2000 for 15 min
2	C2C12 growth	12 well/ 1ml	1:2000	15	60	phalloidin only	non treated C2C12	PFA + 0.25% Triton X-100	4 sec non-treated/ 12 sec treated	10 sec fixed	20x/100x	C2C12 loose actin but Klhl31 needs more recovery time
3	C2C12 growth	12 well/ 1ml	1:2000	15	30/60/120/ 180/240/300	phalloidin only	non treated C2C12	PFA + 0.25% Triton X-100	no GFP	17 sec fixed	20x/100x	fixing did not work/ phalloidin not visible
4	C2C12 Growth	12 well/ 0.5ml	1:2000	15	60/180/300	phalloidin only	non treated C2C12	PFA + 0.25% Triton X-100	8 sec	18 sec fixed	100x	Actin recovers after 1 h, Kelchlike 31 after 3 h
5	C2C12 growth	12 well/ 0.5ml	1:2000	15	60/180/300	phalloidin only	non treated C2C12	PFA + 0.25% Triton X-100	7 sec	18 sec fixed	20x/100x	Double Immuno Klhl31/ Actin QUANTIFICATION

table 3.1b			experimental settings						microscope setting			results
Number	cells	dish	concen-tration LaB (2mM stock)	treatment time (min)	recovery time (min)	negatives	control	Fix	GFP exposure time	568 exposure time	objective	
1	titration C2C12 Diff	12 well/ 1ml	1:5000 1:2000 1:1000	30 15/30 15/30	60		non treated C2C12	PFA + 0.25% Triton X-100	2 sec	11 sec	20x/100x	C2C12 loose actin and do not recover
2	C2C12 Diff	12 well/ 1ml	1:1000 1:2000	15/30	60	phalloidin only	non treated C2C12	PFA + 0.25% Triton X-100	no GFP	14 sec fixed	20x/100x	fixing did not work/ phalloidin not visible
3	C2C12 Diff	12 well/ 1ml	1:1000 1:2000	15/30	60	phalloidin only	non treated C2C12	PFA + 0.25% Triton X-100	3-5 sec	8 sec fixed	20x/100x	different PFA, 1:2000 LaB 15 min-cells recover
4	C2C12 Diff	12 well/ 0.5ml	1:2000	15	60/180/300	phalloidin only	non treated C2C12	PFA + 0.25% Triton X-100	2.5 sec	12 sec fixed	100x	Actin did not completely recover after 5h, Klhl31 seems to have been affected by LaB treatment, accumulations
5	C2C12 Diff	12 well/ 0.5ml	1:2000	15	60/180	tubulin only	non treated C2C12	PFA + 0.25% Triton X-100	4-5 sec	14 sec fixed	20x/100x	Double Immuno Klhl31/ alpha Tubulin

6	C2C12 Diff	12 well/ 0.5ml	1:2000	15	60/180/300	phalloidin only	non treated C2C12	PFA + 0.25% Triton X-100	4-5 sec	15 sec fixed	20x/100x	Double Immuno Klhl31/ Actin QUANTIFICATION

We tested the best conditions for Latrunculin B treatment in both C2C12 myoblasts and myotubes, but later only used Latrunculin B to disrupt the Actin components of the cytoskeleton in C2C12 myotubes, as we could only see co-localisation of Klhl31 to Actin in differentiated C2C12. Firstly the best conditions for usage of Latrunculin B on fully differentiated C2C12 cells were tested (see table 3.1b). We found that completely disrupting the Actin cytoskeleton (table 3.1; number 1; 1/1000 dilution of 2 mM stock: 2 µM for 30 minutes; Phalloidin-staining gave only background signal, but no Actin fibres were visualised) led to a non-recoverable collapse of cell structures followed by detachment of the C2C12 myotubes from the coverslips, potentially due to cell death (see figure 3.10: b, c). However, in cells that remained attached to the coverslips, the immuno-staining revealed a dense accumulation of Klhl31 protein in the condensed cytosol. In the periphery of the cells, Klhl31 protein could still be seen to have the previously observed punctate phenotype, although more condensed (figure 3.10: b', c')

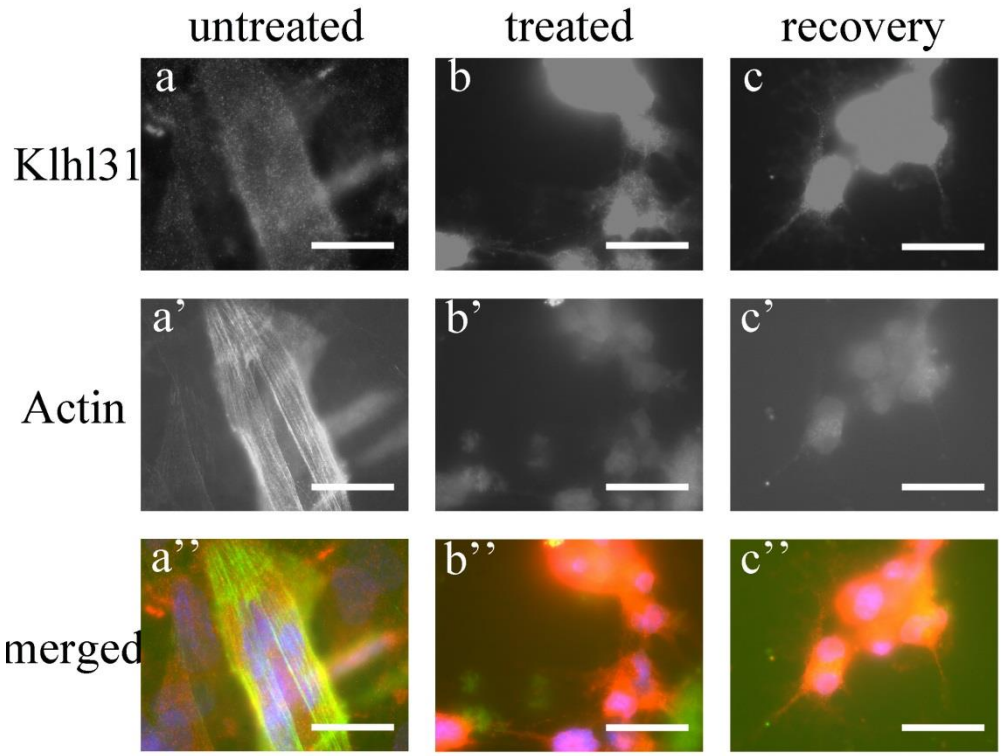

Figure 3.10: Latrunculin B treatment of C2C12 myotubes

C2C12 myotubes after 5 days of differentiation were treated with 2µM of Latrunculin B for 30 minutes and then left to recover for further 60 minutes. Cells were then processed for Immuno-histochemistry. (a, b, c) Endogenous Klhl31 was detected with a polyclonal

rabbit anti-human Klhl31 antibody and visualised with a secondary Alexa Fluor 568 antibody (red). (a', b', c') Actin was visualised using Alexa Fluor 488-conjugated Phalloidin (green). Nuclear DNA was labelled with DAPI (blue). Pictures a''-c'' are merged images for Klhl31 and Actin.

Scale bar (a-c'') – 10 µm

C2C12 myotubes treated with high concentration of Latrunculin B did not recover from the loss of the Actin cytoskeleton. However, Klhl31 could still be detected with high levels in the cytosol of the cells (figure 3.10: c, c''). The observed high levels of Klhl31 were potentially due to concentration of the cytosol due to cell structure collapse. Differentiated myotubes seemed to break down without the Actin fibres, which led to a rounded cell phenotype (see figure 3.10: b, c). Similar observations were made by other groups, when using Actin-depolymerising drugs (Nowak and others, 2009).

Previous data suggested that treatment of differentiating C2C12 with Latrunculin B led to elongation of C2C12, whilst fusion of the cells was inhibited due to loss of Actin and therefore lack of filopodia and lamellipodia formation (Nowak and others, 2009). Furthermore it was shown that cell migration was negatively affected. Nowak et al. also reported that after treating differentiated C2C12 with either Latrunculin B or cytochalasin D, they could observe large, rounded myoblast bodies. These authors claimed that this phenotype appeared because cell contact with the dish or coverslip was diminished, but these cells were not undergoing apoptosis (Nowak and others, 2009).

Complete Actin repolymerisation was never observed, when using Latrunculin B at a concentration of 2 µM for 30 minutes. Once the Actin fibres were depolymerised C2C12 cells did not re-establish their cell shape and kept the rounded appearance. Also, treated C2C12 cells seemed to lose the attachment to the coverslip and were washed off during the immuno-staining preparation steps.

Based on these findings, we therefore decided to use lower concentrations of Latrunculin B preventing complete depolymerisation of Actin fibres in differentiating myocytes and potentially allowing repolymerisation to occur. The best condition for incomplete depolymerisation of Actin fibres was determined as treatment of myocytes with 1 µM Latrunculin B (1/2000 dilution of a 2mM stock) for 15 minutes (see table 3.1b, experiment number 3). However, the effects of Latrunculin B treatment were

variable. Some C2C12 myotubes were affected more by Latrunculin B and therefore lost more Actin fibres compared to others. In general, a high percentage of C2C12 differentiated cells (>70%) were left with enough Actin fibres to be able to recover, and all treated and processed cells on coverslips were shown to rebuild their Actin cytoskeleton in a time course of up to five hours (figure 3.11, c-e).

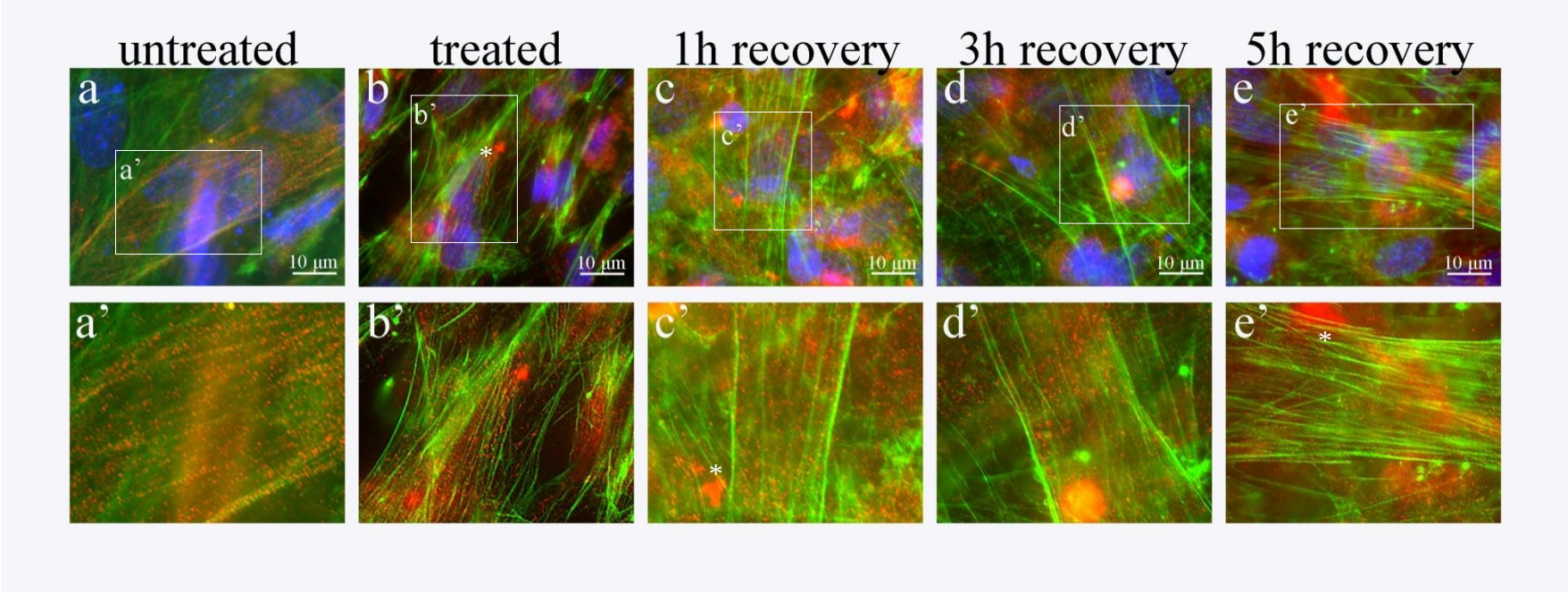

Figure 3.11: Latrunculin B treatment of C2C12 myotubes leads to the disorganisation of Klhl31 localisation

Figure 3.11: Latrunculin B treatment of C2C12 myotubes leads to the disorganisation of Klhl31 localisation

Differentiated C2C12 myotubes were treated with 1µM Latrunculin B for 15 minutes (b). Treated cells were fixed and processed for immuno-staining (b) or left to recover from 1-5 hours in fresh medium (c-e) and then fixed and stained. Untreated C2C12 were processed as controls (a). Endogenous Klhl31 was detected with a polyclonal rabbit anti- human Klhl31 antibody and visualised with a secondary Alexa Fluor 568 antibody (red). Actin was visualised using an Alexa Fluor 488-conjugated Phalloidin (green). Nucleic DNA was labelled with DAPI (blue), but the DAPI channel is not enabled in magnified images (a'-e'). Images were taken with a 63x objective.

In untreated C2C12 myotubes Klhl31 was shown to associate to Actin fibres (figure 3.11; a). Treatment with Latrunculin B lead to a slight reduction of the Actin cytoskeleton and the loss of Klhl31 localisation to Actin fibres (figure 3.11: b), as well as a general disorganized accumulation of Klhl31 in the cytosol (figure 3.11: b', *).

These Klhl31 accumulations (potentially indicating Klhl31 protein aggregates (figure 3.11: b', c', e') were observed at any stage during a recovery time course of up to 5 hours. Although C2C12 myotubes recovered and their Actin fibres repolymerized (see figure 3.11: c-e), Klhl31 did not seem to re-localise to the newly build fibres, rather Klhl31 protein remained cytosolic still displaying a disorganized distribution and cytosolic protein aggregates (figure 3.11: c-e).

Having characterised Klhl31 during C2C12 myotube formation, we then decided to investigate potential interaction partners for Klhl31. Finding interacting proteins would help us to further analyse a role for Klhl31 during C2C12 differentiation.

4. Generation of Klhl31- fusion proteins as tools to study function in C2C12

4.1 Introduction

4.1.1 Structure and function of proteins of the Kelch-like family

Kelch-like proteins all show the same structural properties (see figure 4.1). They have three main functional domains: The amino-terminal broad complex/ tram-track/ bric-a-brac (BTB) or poxvirus and zinc finger (POZ) domain, a central linking domain, called the BACK domain and the carboxy-terminal Kelch repeats (Stogios and others, 2005; Stogios and Prive, 2004). Various members of the Kelch -like protein family have been shown to bind to Actin via their Kelch β-propeller (Aromolaran and others, 2009; Aromolaran and others, 2012; Kelso and others, 2002), whilst the BTB-domain is involved in binding substrate proteins as part of E3 Ubiquitin Ligase complexes (Furukawa and others, 2003; Geyer and others, 2003; Stogios and others, 2005; Xu and others, 2003). Also, via their BTB-domain, Kelch-like proteins have been shown to form homodimers (Geyer and others, 2003).

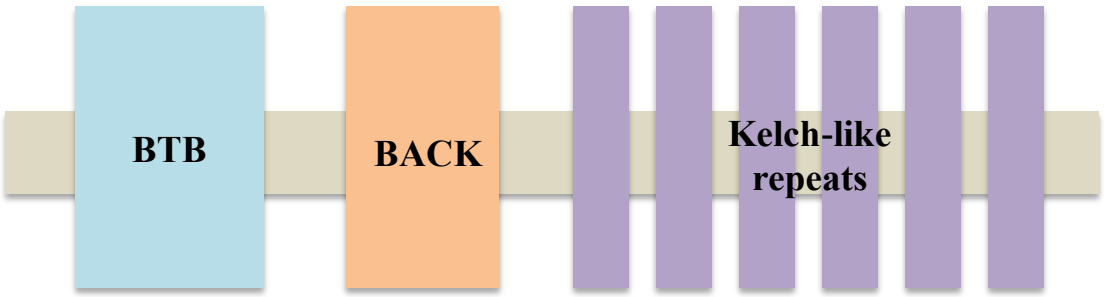

Figure 4.1: Structure of Klhl31

Human and chick Klhl31 have been reported to display an N-terminal BTB domain (light blue), a central BACK domain (beige) and 6 C-terminal Kelch repeats (light violet) (Abou-Elhamd and others, 2009; Yu and others, 2008).

Klhl31 was identified in zebrafish and a human and a chick homologue was reported recently (Abou-Elhamd and others, 2009; Wu and Gong, 2004; Yu and others, 2008). Both, human and chick Klhl31 encode a protein of 634 amino acids with a predicted size of 70 kDa (Abou-Elhamd and others, 2009; Yu and others, 2008). Furthermore, sequence analysis revealed that chick and human Klhl31are highly conserved displaying 84.4% sequence homology (Abou-Elhamd).

4.2 Results

4.2.1 Cloning and analysis of an amino-terminal GFP-Klhl31 Fusion-protein

Previous work in our laboratory described the expression of Klhl31 in developing chick embryos and also examined how the expression was regulated during myogenesis (Abou-Elhamd; Abou-Elhamd and others, 2009). By analysing the localisation of Klhl31 in C2C12, we found that Klhl31 seems to localise to the Actin cytoskeleton, but only in differentiated myotubes (figure 3.9). This co-localisation was established at a stage of differentiation (see figure 3.8), which was proposed to lead to changes in the Actin cytoskeleton in formation of primitive myofibrils (Burattini and others, 2004; Kontrogianni-Konstantopoulos and others, 2006; Sanger and others, 2002).

We decided to generate GFP-Fusion proteins of Klhl31, which would enable us to use it as a tool to study interactions in the C2C12 cell line by analysing localisation patterns, as well as studying protein dynamics using live-imaging. Another approach could also be to find direct interaction partners of Klhl31 by using the GFP as an anchor that can be pulled down with an immobilized GFP-binding protein (GBP) (Angers and others, 2006).

Kelch-like proteins have two distinct structural domains, which both have specific function in binding substrates: the BTB domain at the amino terminus and the Kelch repeats at the C-terminus (Stogios and others, 2005). Preliminary data for Klhl31 suggests that both domains are necessary for the functionality of Klhl31, although the

BTB-domain seems to be the domain that is involved in binding substrates destined for ubiquitinylation and subsequently proteasomal degradation.

We created a fusion protein, which would have an EGFP-tag attached at the Klhl31 amino-terminus to the BTB-domain of the protein (see scheme in figure 4.2). As vector backbone, we used the pEGFP-C1 vector (Clontech Laboratories Inc., Mountain View, CA, USA). A full-length version of Klhl31 (EGFP-Klhl31 FL, 1.9 kb), as well as a mutant version lacking the Kelch-repeat domains (EGFP-Klhl31 ΔKR, 0.9kb) were cloned from chick cDNA. A second mutant with deletion of the BTB domain (EGFP-Klhl31 ΔBTB, 1.4 kb) was previously generated and sub-cloned from pCaβ Klhl31 ΔBTB IRES-GFP. For the cloning protocol and primers, see section 2.2.16.

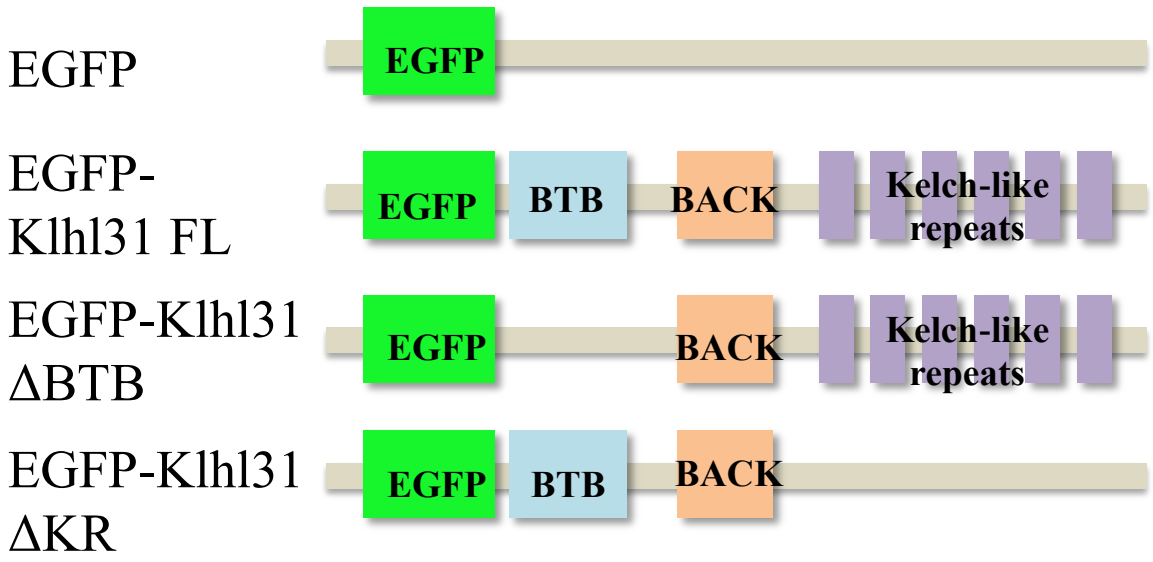

Figure 4.2: Schematic representation of EGFP-Klhl31 fusion proteins

We created Klhl31 fusion protein tagged with an N-terminal EGFP-protein. EGFP-Klhl31 FL comprising of the full length protein sequence of Klhl31 fused to the EGFP-tag, whilst the EGFP-Klhl31 ΔBTB protein lacks the N-terminal BTB binding domain. The EGFP-Klhl31 ΔKR protein does not include the Kelch-repeats.

Once the sequences were verified (see Appendix), we transfected C2C12 myoblasts with the different pEGFP-C1-Klhl31 constructs and examined GFP-expression in C2C12 myoblasts and myotubes.

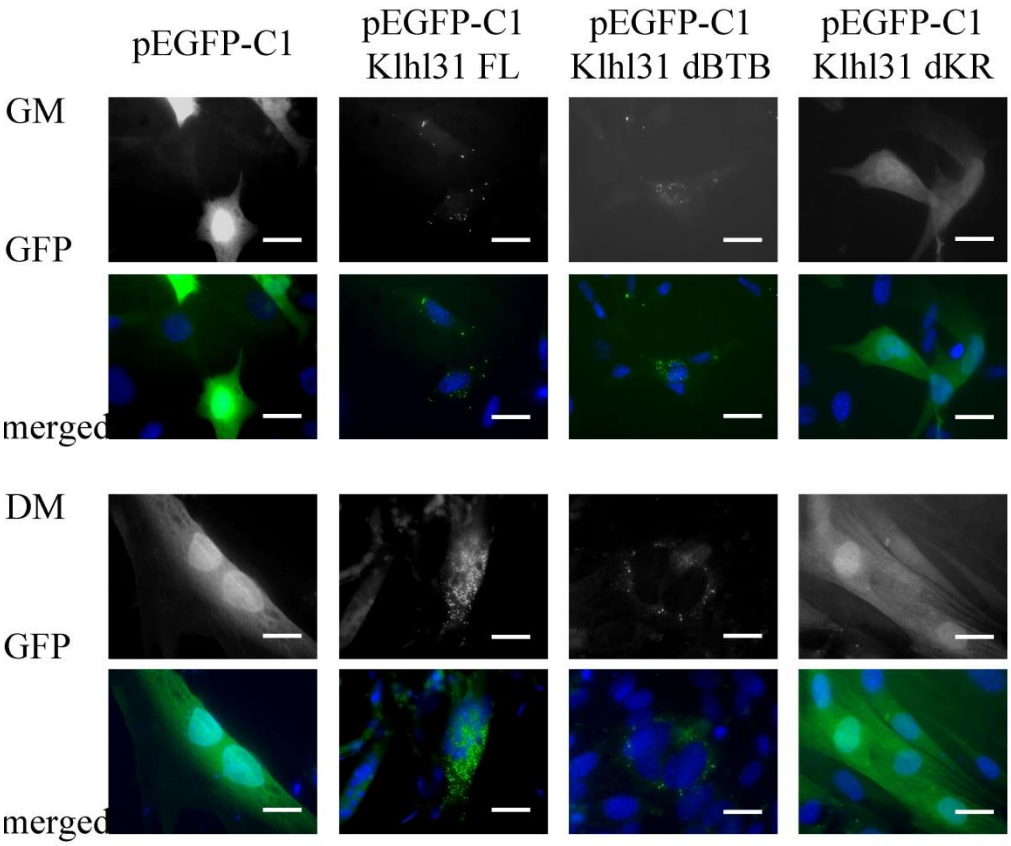

Figure 4.3: Overexpression of pEGFP-C1 Klhl31 constructs in C2C12

C2C12 were transfected with either pEGFP-C1 (a, e), pEGFP-C1 Klhl31 FL (b, f), pEGFP-C1 Klhl31 ΔBTB (c, g) or pEGFP-C1 Klhl31 ΔKR (d, h), respectively. Transfected cells were either fixed after 24 h in growth medium (GM, a-d) or left to differentiate for 5 days in differentiation medium (DM, e-h). Figure showing grayscale images for Klhl31 only (a-h) and merged with DAPI to further visualize cellular localisation (a'-h').

Scale bar (a – h') – 10 µm

The N-terminal pEGFP-C1 Fusion-protein of Klhl31 did not recapitulate the observed localisation of endogenous Klhl31 to the Actin-cytoskeleton (figure 3.7). Instead, EGFP-Klhl31 FL and EGFP-Klhl31 ΔBTB protein (see figure 4.3: b, c, f and g) both showed a localisation that is similar to that described for inclusion bodies (Goldberg, 2003) or lysosomes (Chimote and others, 2012), which contain misfolded proteins. The potential vesicular localisation can observed strongly for EGFP-Klhl31 FL in C2C12 myotubes, where the accumulation of GFP-fluorescent protein was seen to localise around multiple nuclei, which themselves are close together (figure 4.3; f). Furthermore,

nuclei appeared to be enlarged in transfected C2C12, which might be due to increased stress on cultured cells or might indicate diminished health of used C2C12 myoblasts.

Non-functional proteins stored in vesicles are usually subsequently degraded by the proteasome (Goldberg, 2003; Tyedmers and others, 2010). Observing both the full length Klhl31 protein as well as the BTB mutant of Klhl31 in structures resembling vesicles potentially containing misfolded proteins, suggested the possibility that our fusion-proteins are non-functional and therefore degraded by the cell. The ΔKR mutant could be seen to be mainly cytosolic (figure 4.3: d, h). As the Kelch-repeats have been shown to be responsible for the binding of Kelch-like proteins to Actin (Adams and others, 2000; Aromolaran and others, 2009; Aromolaran and others, 2012; Kelso and others, 2002), it might be that the loss of the kelch-propeller is responsible for the diffuse cytosolic localisation.

To test the functionality of the fusion proteins, we then used a Luciferase assay approach.

It has been shown in our laboratory that Klhl31 can antagonize β-catenin dependant Wnt-signalling (Abou-Elhamd). In a Luciferase reporter assay, it was shown that Klhl31 full length and Klhl31 ΔKR can both inhibit the Wnt-3a mediated induction of a LEF/TCF responsive promoter (TOPFLASH, kindly given to us by R. Moon), which drives luciferase expression. Klhl31 ΔBTB was not able to do so. Inducing LEF/TCF luciferase reporter vectors by β-catenin also induced the expression of luciferase, which was inhibited by around 20% by both Klhl31 FL, as well as Klhl31 ΔKR. Klhl31 ΔBTB was again not able to antagonize β-catenin induced luciferase activity (see figure 1.13).

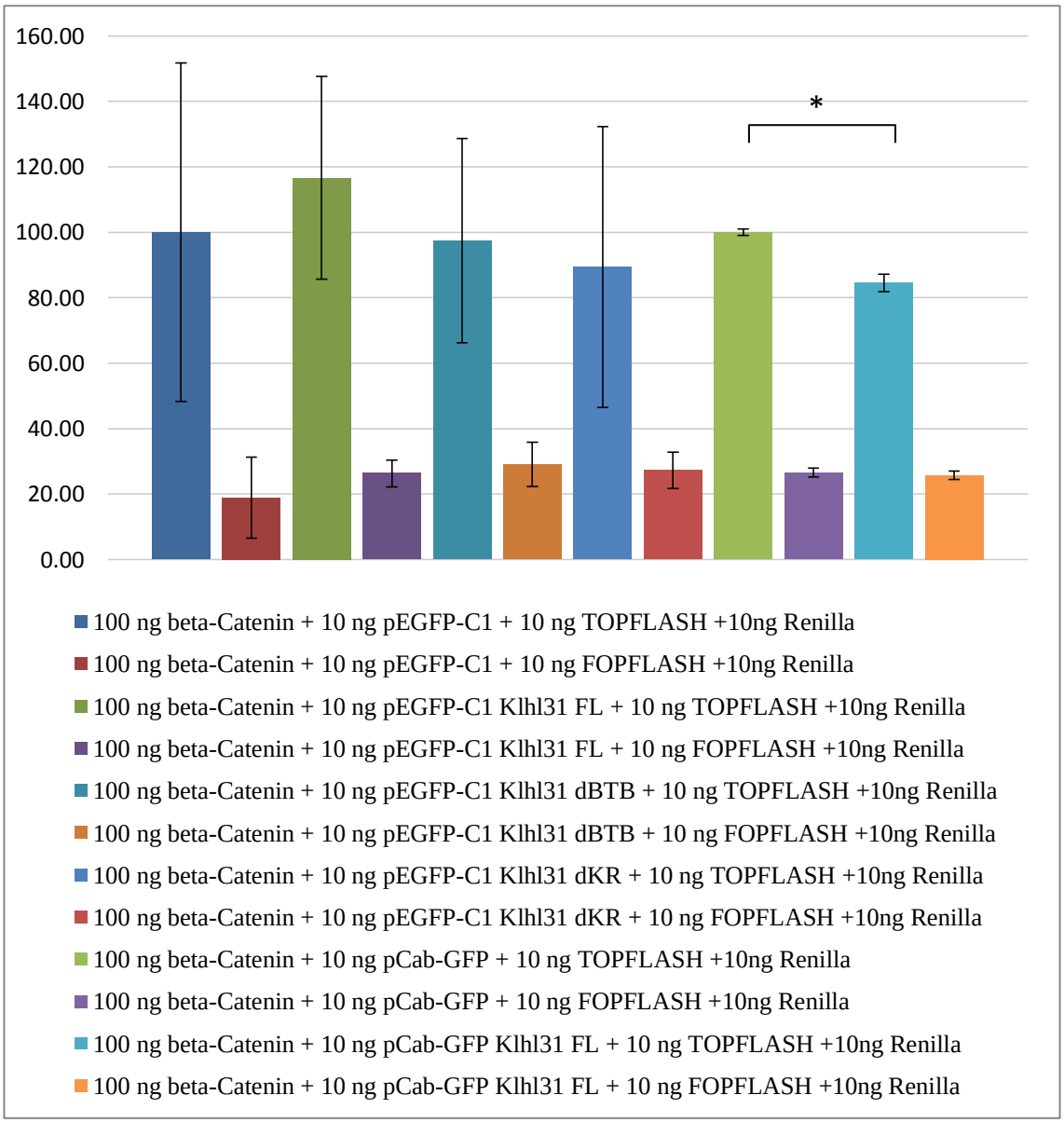

Figure 4.4: Analysing the pEGFP-C1 Klhl31 constructs by Luciferase assay

3T3 cells were transfected with either pEGFP-C1, pEGFP-C1 Klhl31 FL, pEGFP-C1 Klhl31 ΔBTB, pEGFP-C1 Klhl31 ΔKR, as well as either TOPFLASH or FOPFLASH vector, β-catenin and Renilla as internal control. Error bars were calculated based on the standard deviation. Signal strength is indicated in % compared to Luciferase signal of 3T3 cell transfected with vector only (set as 100%). As a positive control we used pCaβ-GFP (as vector only) and pCaβ-GFP Klhl31FL encoding for an untagged Klhl31 FL protein. Luciferase reporter activity was inhibited by 18% by pCaβ-GFP Klhl31 FL, which was shown to be statistically significant (*).This experiments was carried out three times, which each sample being prepared and measured as triplicates (n=9)

Compared to the results of Luciferase assays for Klhl31 carried out previously (Abou-Elhamd), the pEGFP-C1 constructs did not reproduce inhibition of β-catenin induced

Luciferase activity. In fact, pEGFP-Klhl31 FL seemed to enhance the Luciferase signal and pEGFP-Klhl31 ΔKR and pEGFP-Klhl31 ΔBTB were both not able to inhibit β-catenin induced Luciferase reading to a statistical significance (see figure 4.4). Unfortunately the Luciferase reading varied extensively between experiments, which could potentially be explained by contamination or other issues related to the used pEGFP-C1 vector. Therefore obtained data is preliminary and issues associated with the plasmids need further investigation. The BTB domain has previously been described to be the mediator of the biological function of Kelch-like proteins (Albagli and others, 1995; Geyer and others, 2003; Perez-Torrado and others, 2006; Pintard and others, 2003; Xu and others, 2003). It is possible that this might also be the case for Klhl31. This would be consistent with the finding that the loss of the BTB-domain after deletion renders the protein unable to inhibit canonical Wnt signalling (Abou-Elhamd). The sub-cellular localisation of EGFP-Klhl31 fusion proteins did not recapitulate the localization of endogenous Klhl31 protein (compare figure 4.4 and 3.5), indicating that the GFP may interfere with the function of Klhl31, potentially by interfering with the BTB domain.

In summary, both the overexpression experiment in C2C12 as well as the results obtained from the Luciferase Assay indicated that the pEGFP-C1 Klhl31 Fusion constructs did not produce a functional Klhl31 protein and could therefore not be used to investigate potential interaction partners.

4.2.2 Cloning and Analysis of carboxy-terminal DsRed- or GFP-Klhl31 Fusion-protein

Next, we decided to generate fusion-proteins with the tag placed at the carboxy terminus of Klhl31 adjacent to the kelch repeats (unless deleted). We used pEGFP-N1 or pDsRed-N1 vectors (Clontech Laboratories Inc., Mountain View, CA, USA) to construct plasmids encoding the following proteins : Klhl31 FL-GFP/DsRed, Klhl31 ΔBTB-GFP/DsRed or Klhl31 ΔKR-GFP/DsRed (see figure 4.5). We amplified the constructs from cDNA (for Klhl31 FL, Klhl31 ΔKR) or from pCaβ Klhl31 ΔBTB IRES-GFP, as described in chapter 2.2.16.

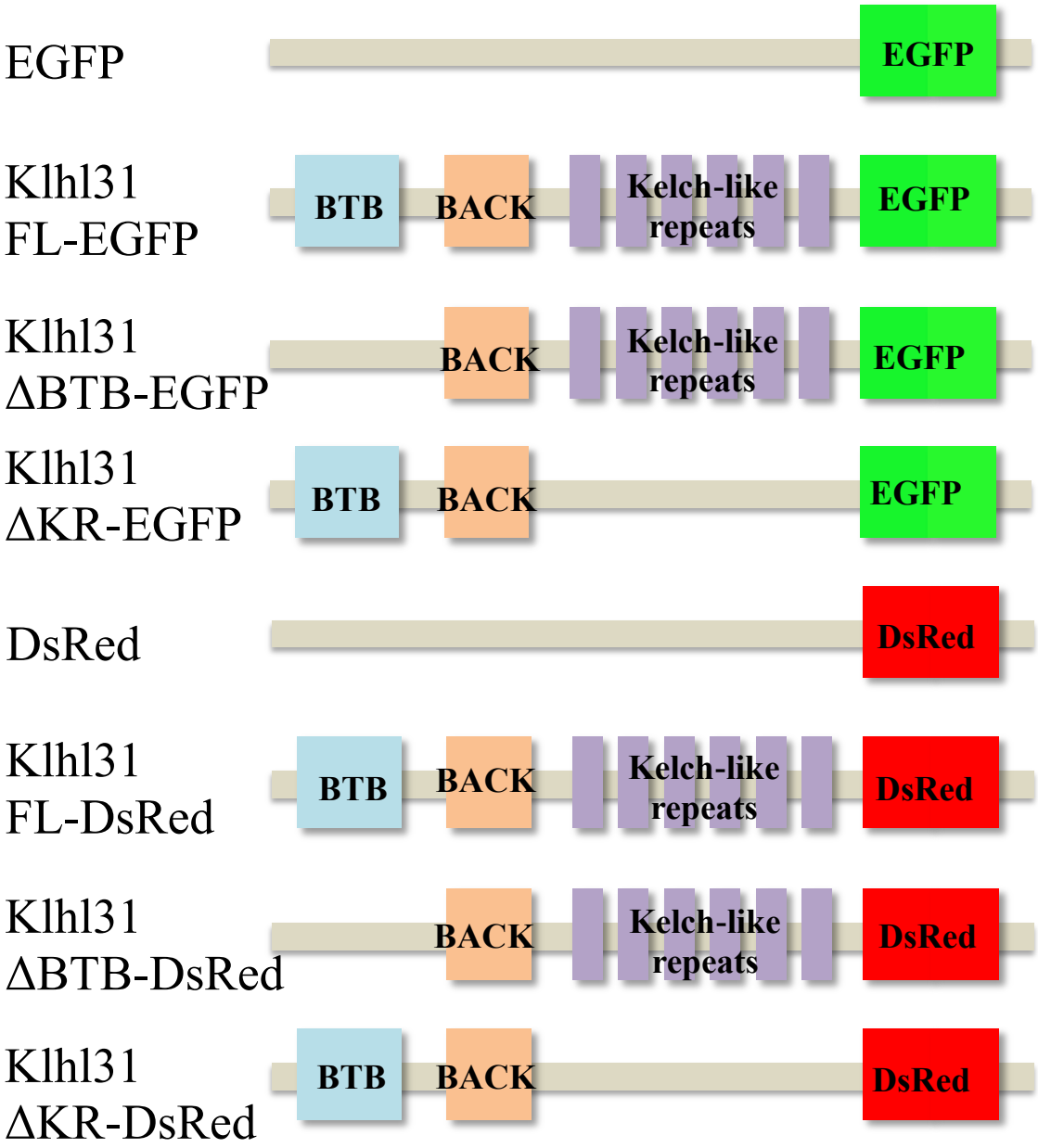

Figure 4.5: Schematic representation of C-terminal EGFP or DsRed Klhl31 fusion proteins

Klhl31 Fusions proteins were generated comprising an EGFP or DsRed tag at the carboxy terminus of the Klhl31 protein. Klhl31FL-EGFP/DsRed contains all binding domains of Klhl31, whilst Klhl31ΔBTB-EGFP/DsRed is lacking the N-terminal BTB domain. Deletion of the C-terminal Kelch-repeats leads to the generation of Klhl31ΔKR-EGFP/DsRed.

The functionality of the C-terminal fusion proteins was examined by Luciferase assay.

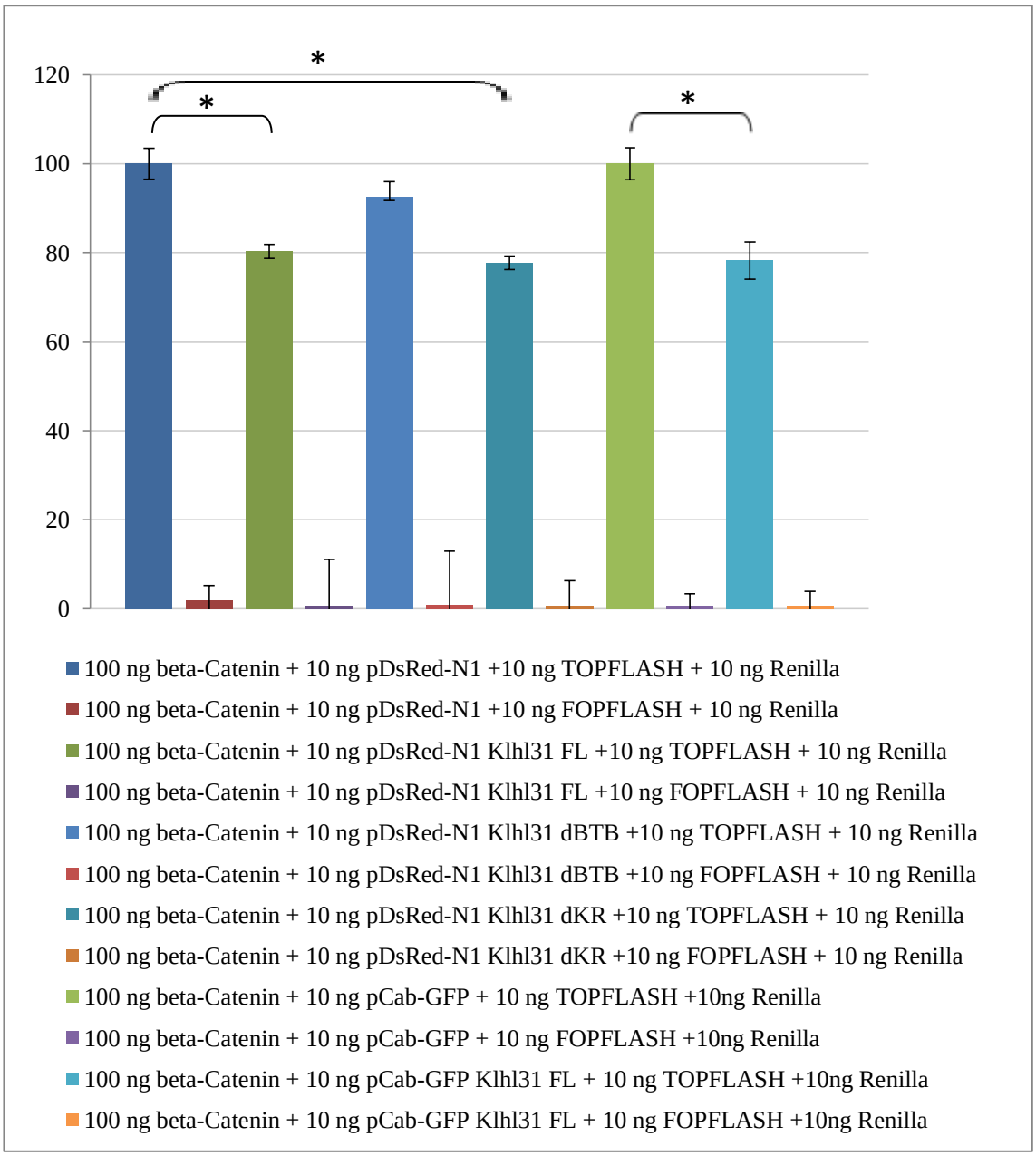

Figure 4.6: Analysing the pDsRed-N1 Klhl31 constructs by Luciferase assay

3T3 cells were transfected with either pDsRed-N1, pDsRed-N1Klhl31 FL, pDsRed-N1Klhl31 ΔKR, pDsRed-N1 Klhl31 ΔBTB, as well as either TOPFLASH or FOPFLASH vector, β-catenin and Renilla as internal control. As a positive control we used pCaβ-GFP (as vector only) and pCaβ-GFP Klhl31FL encoding for an untagged Klhl31 FL protein. Luciferase reporter activity was normalised against pCaβ-GFP and was shown to be inhibited by 22% by pCaβ-GFP Klhl31 FL, which was statistically significant (*)

The data shown is based on four experiments each carried out in triplicates (n=12). Error bars were calculated based on the standard deviation. Signal strength is indicated in % compared to Luciferase signal of 3T3 cell transfected with β-catenin and vector only (set as 100%).

Klhl31 FL-DsRed was able to inhibit β-catenin induced Luciferase signal by around 20%. The observed inhibition was statistically significant (* $p<0.05$). Data shown is similar to previous data obtained with pCaβ Klhl31 FL IRES-GFP, which does not generate a fusion protein (see figure 1.13). A similar inhibition could be observed when transfecting 3T3 cells with β-catenin, TOPFLASH vector and pDsRed-N1 Klhl31 ΔKR, again consistent with results obtained with non-tagged Klhl31 ΔKR. Klhl31 ΔBTB-DsRed was not able to reduce β-catenin induced Luciferase signal significantly, as previously described (Abou-Elhamd). This indicated that C-terminal fusion did not negatively affect Klhl31 functionality.

We therefore transfected C2C12 myocytes with these constructs to analyse the localisation of fusion proteins in the cells (see figure 4.7).

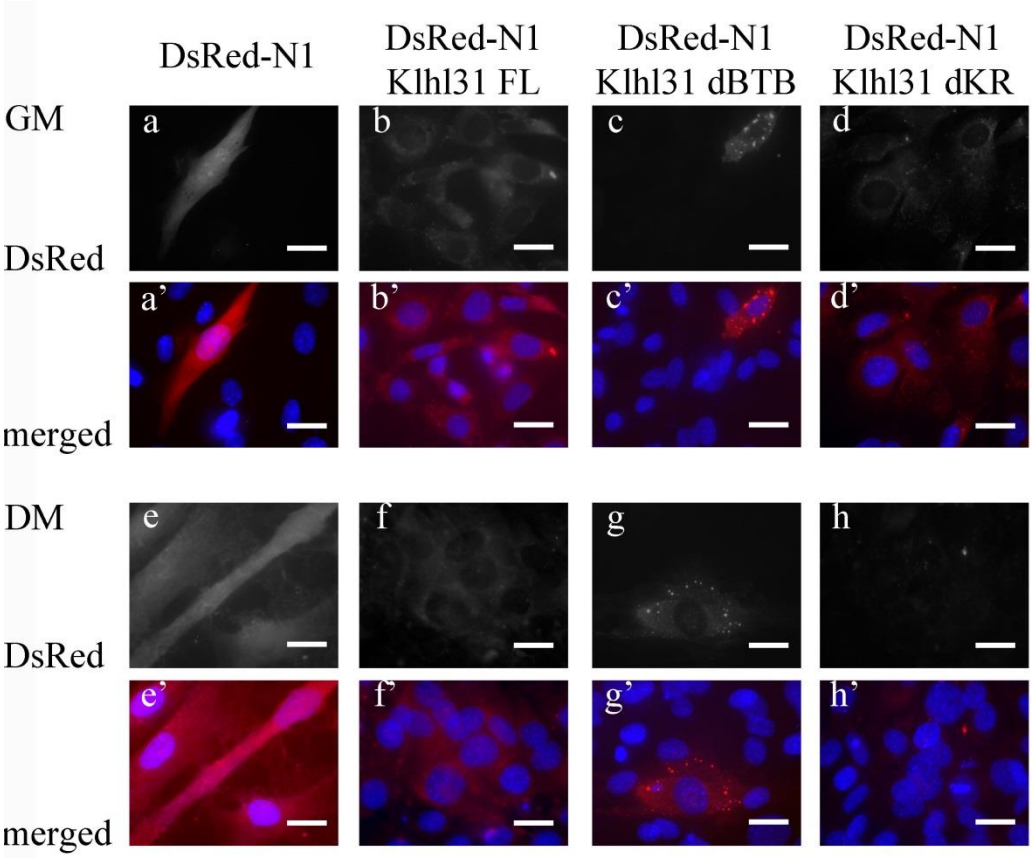

Figure 4.7: Overexpression of pDsRed-N1 Klhl31 constructs in C2C12

C2C12 were transfected with either pDsRed-N1 (a, e), pDsRed-N1 Klhl31 FL (b, f), pDsRed-N1 Klhl31 ΔBTB (c, g) or pDsRed-N1 Klhl31 ΔKR (d, h), respectively. Transfected cells were either fixed after 24 h in growth medium (GM) or left to differentiate for 5 days in differentiation medium (DM). Images a'-h' show localisation of the fusion proteins in relation to the nuclei (DAPI, blue).

Scale bar (a - h') – 10 µm

Although the dsRed-N1 Klhl31 constructs were shown to be active in Luciferase assay, they could only partially reproduce the localisation of Klhl31 in C2C12 when compared to localisation of endogenous Klhl31 in C2C12 myoblasts. Non-transfected C2C12 cells used as a negative control during the imaging process showed a moderately strong red background signal (as described in section 2.2.26 making it rather difficult to distinguish between real DsRed-signal and auto-fluorescence. Although the red fluorescence for Klhl31 FL-DsRed and Klhl31 ΔKR-DsRed was barely stronger then C2C12 auto-fluorescence, Klhl31 FL-DsRed in undifferentiated C2C12 could be observed to display a cytosolic localisation (figure 4.7; b and d, respectively) similar to the one observed of endogenous Klhl31 (see figure 3.6). Klhl31 ΔKR-DsRed was also

observed to be localised in the cytosol of the myoblast similar to Klhl31 FL-DsRed. Interestingly the localisation pattern of Klhl31 ΔBTB-DsRed resembled strongly the localisation observed for pEGFP-C1 Klhl31 FL (figure 4.3; b). Protein expressed by the DsRed-N1 Klhl31 ΔBTB construct seemed to be accumulated in vesicles surrounding the nucleus (figure 4.7; c).

Overexpression of the pDsRed-N1 Klhl31 constructs in differentiating C2C12 myocytes was even harder to analyse, as the red auto-fluorescence of C2C12 was even stronger in myocytes than in myoblasts. Also, it had previously been shown that expression of plasmid DNA decreases significantly after three days of C2C12 differentiation (Dodds and others, 1998). No fluorescence signal above background level was observed for Klhl31 FL-DsRed and Klhl31 ΔKR-DsRed (figure 4.7; f, h), whilst Klhl31 ΔBTB-DsRed was still observed to be accumulated in vesicles around nuclei (figure 4.7; g).
Not only could the lack of signal be due to a very strong background signal, the DsRed-N1 vector itself can lead to some extent to diminished fluorescence, as it has been shown that the folding itself of the DsRed-tag takes significantly longer compared to a GFP tag, which might have also been a cause for the absent Klhl31-DsRed signal.

The characterisation of the cloned pDsRed-N1 Klhl31 constructs using Luciferase reporter assays indicated the production of functional Klhl31 proteins with a C-terminal DsRed tag, either as a full length protein or as a Klhl31 mutant lacking the Kelch-repeats (figure 4.6). Also proteins encoded by the pDsRed-N1 Klhl31 FL and pDsRed-N1 Klhl31 ΔKR plasmids displayed a cytosolic, punctate localisation in the cytosol of C2C12 myoblasts (figure 4.7; b, d) comparable to the localisation of endogenous Klhl31 (figure 3.8).
Transfection of pDsRed-N1 Klhl31 ΔBTB expressing a protein lacking the BTB-domain was not able to inhibit β-catenin induced Luciferase activity (see figure 4.7) and seemed to accumulate into vesicles (figure 4.7; c, g) both in C2C12 myoblasts, as well as after induced differentiation for about 5 days. Klhl31 FL-DsRed or Klhl31 ΔKR-DsRed was never detected in differentiating C2C12 myocytes.

As we could not investigate the localisation of Klhl31-DsRed tagged proteins in C2C12, we decided to analyze generated Klhl31-GFP expressing constructs.
The pEGFP-N1 Klhl31 constructs were first examined by the luciferase assay.

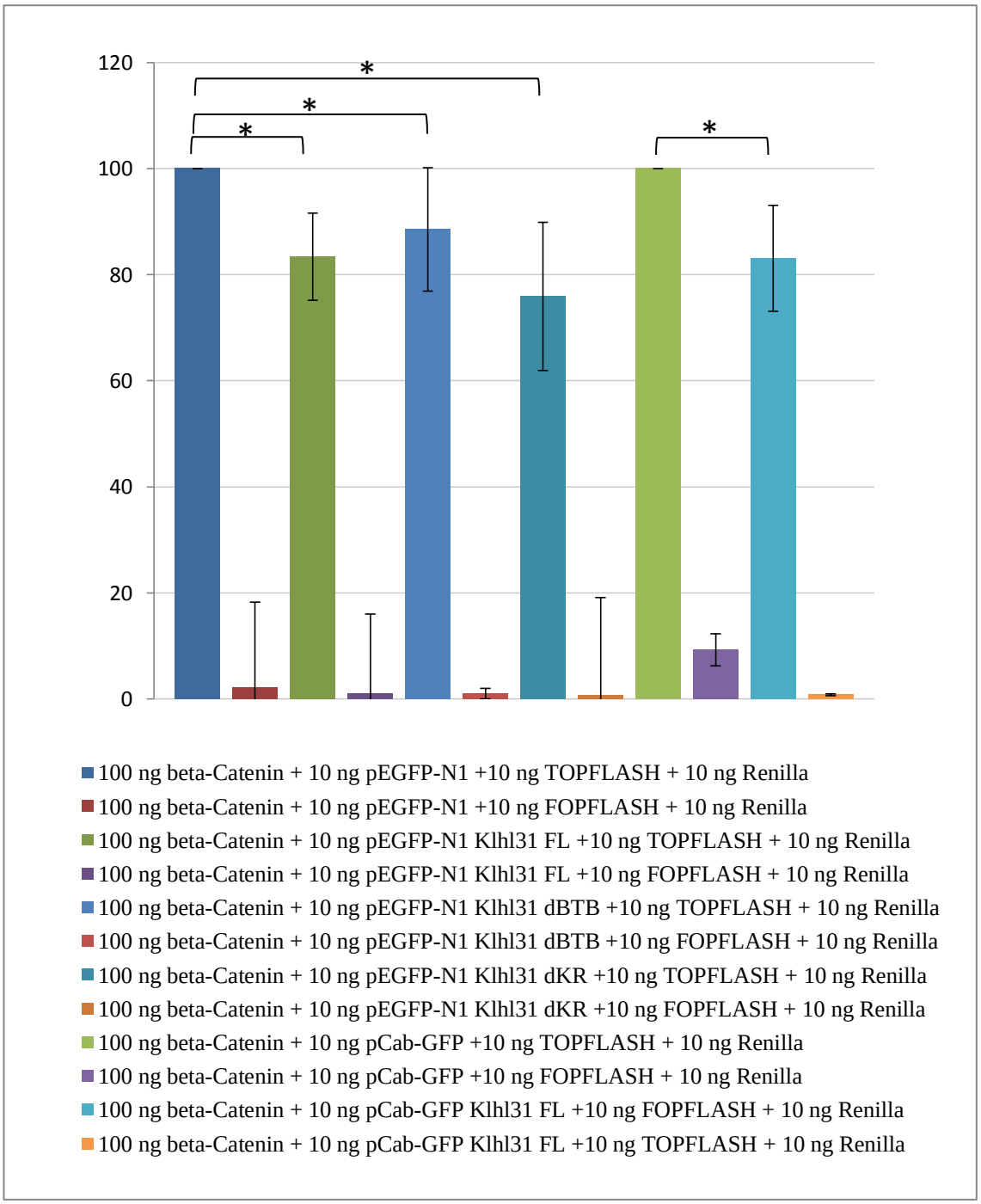

Figure 4.8: Analysing the pEGFP-N1 Klhl31 constructs by Luciferase assay

3T3 cells were transfected with either pEGFP-N1, pEGFP-N1Klhl31 FL, pEGFP-N1 Klhl31 ΔKR, pEGFP-N1 Klhl31 ΔBTB, as well as either TOPFLASH or FOPFLASH vector, β-catenin and Renilla as internal control. As a positive control we used pCaβ-GFP (as vector only) and pCaβ-GFP Klhl31FL encoding for an untagged Klhl31 FL protein. Luciferase reporter activity was normalised against pCaβ-GFP and was shown to be inhibited by 18% by pCaβ-GFP Klhl31 FL, which was statistically significant (*). Data is based on three experiments each carried out in triplicates (n=9). Error bars were calculated

based on the standard deviation. Signal strength is indicated in % compared to Luciferase signal of 3T3 cell transfected with pEGFP –N1 vector and β-catenin only (set as 100%).

The obtained data from the Luciferase assay showed the expression of potential active proteins for all three cloned constructs (figure 4.8). Klhl31 FL-GFP, as well as Klhl31 ΔKR-GFP inhibited β-catenin induced Luciferase activity by around 20%. Again this inhibition was statistically significant (*p <0.05).
Similar percentage of inhibition have been described previously for Klhl31 FL-DsRed and Klhl31-DsRed ΔKR (see figure 4.6), as well as for untagged Klhl31 full length protein and Klhl31 ΔKR protein (Abou-Elhamd).
Surprisingly, pEGFP-N1 Klhl31 ΔBTB was also shown to inhibit β-catenin by around 12%. This inhibition was shown to be statistically significant as well ($p<0.05$). However, this experiment is still consistent with the previous observations, which indicated that loss of the BTB-domain leads to the potential loss of function of Klhl31.

As we could verify the activity of all our pEGFP-N1 Klhl31 constructs, we then transfected C2C12 with these constructs and analysed the localisation of the GFP-Fusion proteins in myoblasts and myocytes.

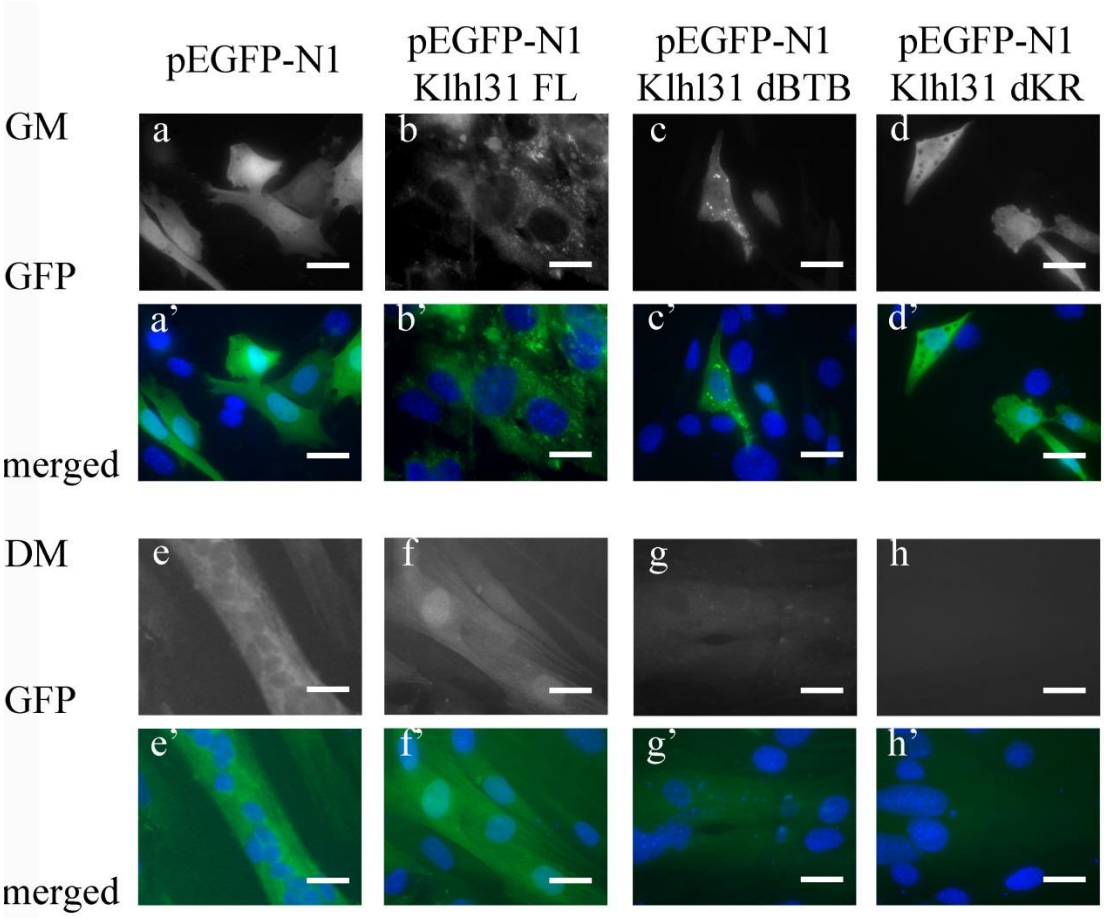

Figure 4.9: Overexpression of pEGFP-N1 Klhl31 constructs in C2C12

C2C12 myoblasts were transfected with either pEGFP-N1 (a, e), pEGFP-N1 Klhl31 FL (b, f), pEGFP-N1 Klhl31 ΔBTB (c, g) or pEGFP-N1 Klhl31 ΔKR (d, h), respectively. Transfected cells were either fixed after 24 h culturing in growth medium (GM) or left to differentiate for 5 days in differentiation medium (DM). Images a'-h' show the localisation of the Fusionprotein in comparison to nuclear staining (DAPI, blue).

Scale bar (a -h') – 10 µm

Overexpression studies of the pEGFP-N1 constructs revealed a similar localisation as described for the dsRed-N1 constructs. Klhl31 FL-GFP could be observed as having a punctate localisation pattern in C2C12 myoblasts (figure 4.9; b). However, the puncta appear larger compared to endogenous Klhl31 (figure 3.7). Klhl31 ΔKR-GFP (figure 4.9; d) was observed to display a cytosolic localisation in C2C12 myoblasts comparable to localisation of GFP expressed from the parental vector (figure 4.9; a), whilst Klhl31 ΔBTB was again observed in to localise into vesicular structures surrounding the nucleus (figure 4.9; c), as previously described for Klhl31 ΔBTB-DsRed (figure 4.7; c).

In differentiating myocytes a diffused punctate localisation was observed for Klhl31 FL-GFP (figure 4.9; f), again unlike the localisation described for endogenous Klhl31 (figure 3.7). However, most of the times differentiating C2C12 myocytes did not reveal any GFP signal indicating the absence of GFP-tagged Klhl31 protein, as seen for Klhl31 ΔBTB-GFP and Klhl31 ΔKR-GFP (figure 4.9; g and h, respectively).

4.3 Biochemical analysis of the Klhl31-GFP/DSRED Fusion proteins

4.3.1 Investigating the stability of Klhl31 Fusion proteins

It was not clear why we could only see a weak signal of overexpressed fusion-proteins in proliferating C2C12 myoblasts. Next, we wanted to analyze if we could detect Klhl31 protein on a western blot, which would help us to investigate a possible degradation of Klhl31 when over-expressed in C2C12 myoblasts. We transfected C2C12 with the pEGFP-N1 Klhl31 FL construct as the encoded protein was shown to be functionally active and seemed to resemble the localisation pattern as observed for endogenous Klhl31. Also, we would then be able to detect proteins on a western blot with either a GFP antibody or Klhl31 antibody. Unfortunately we were not able to detect Klhl31 proteins on a western blot (data not shown), neither when using a polyclonal anti-GFP antibody or with a polyclonal anti-Klhl31 antibody. This was surprising as we could test the constructs for their functionality and were able to look at their localisation in C2C12 myoblasts. To increase the transfection efficiency and hopefully be able to express a higher amount of proteins, we then decided to use a different cell line to transfect Klhl31 overexpression constructs into; 3T3 mouse fibroblasts cells. These cells do not express endogenous Klhl31 (figure 3.3). But again, we could not detect the fusion-proteins on a western blot, although GFP only was detected (see figure 4.10).

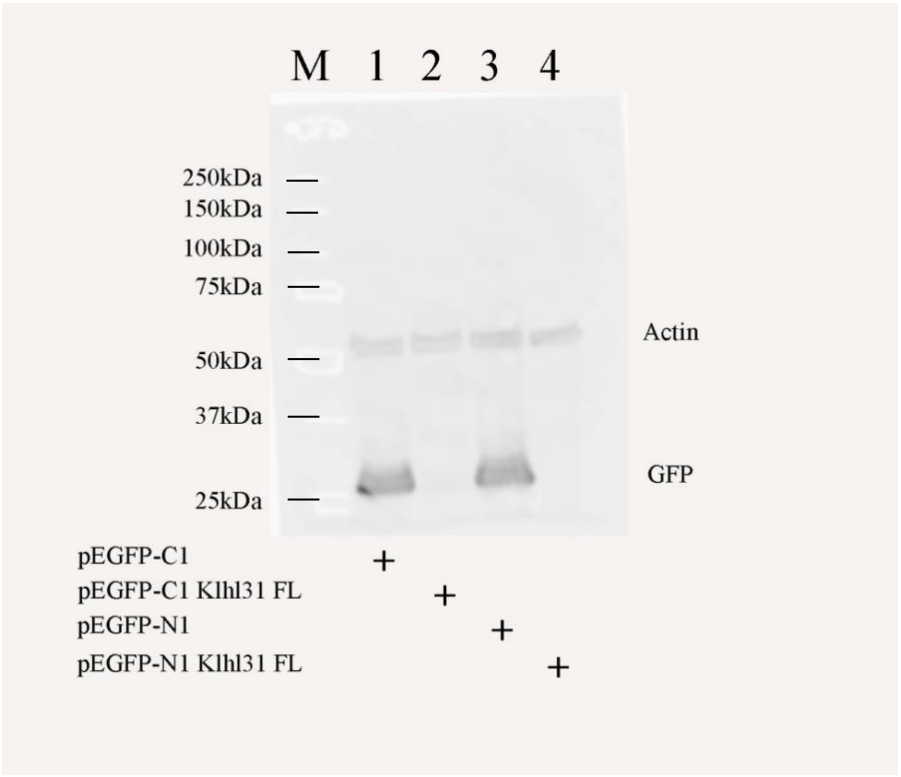

Figure 4.10: Western blot of cell lysates obtained from 3T3 cells transfected with plasmids encoding GFP-Klhl31 FL and Klhl31 FL-GFP

Protein lysates were obtained from cells transfected with pEGFP-C1, pEGFP-C1 Klhl31 FL, pEGFP-N1 or pEGFP-N1 Klhl31 FL and run on a PAA-Gel, transferred to a PVDF membrane and blotted with a GFP polyclonal antibody.

Legend: M- Marker, lane 1-4; Protein lysates: 1 – 3T3 cells transfected with pEGFP-C1, 2 – 3T3 cells transfected with pEGFP-C1 Klhl31, 3-3T3 cells transfected with pEGFP-N1, 4 – 3T3 cells transfected with pEGFP-N1 Klhl31 FL. The Actin band (loading control) can be observed at around 50 kDa.

Analysing proteins lysates from 3T3 mouse fibroblasts overexpressing GFP only (pEGFP-C1 and pEGFP-N1), GFP-Klhl31 FL or Klhl31 FL-GFP revealed that GFP was detected in both cell lines transfected with the empty vectors, while GFP was never detected in cells transfected with any of the GFP-Klhl31 Fusion proteins (figure 4.10).
It has been shown that Kelch-like proteins form homodimers (Geyer and others, 2003), but could Klhl31 dimerize with another Klhl31 protein? And could this homodimers be involved in targeting Klhl31 for degradation?

4.3.2 Klhl31 could initially be degraded via a proteasome-independent process

To investigate a potential degradation of Klhl31 after overexpression, we transfected HEK293 cells with pEGFP-N1 Klhl31 FL and treated the transfected cells with a proteasome inhibitor, MG 132 (Lee and Goldberg, 1998). MG 132 has been described to reduce the degradation of ubiquitin-conjugated proteins (Arora and others, 2005).

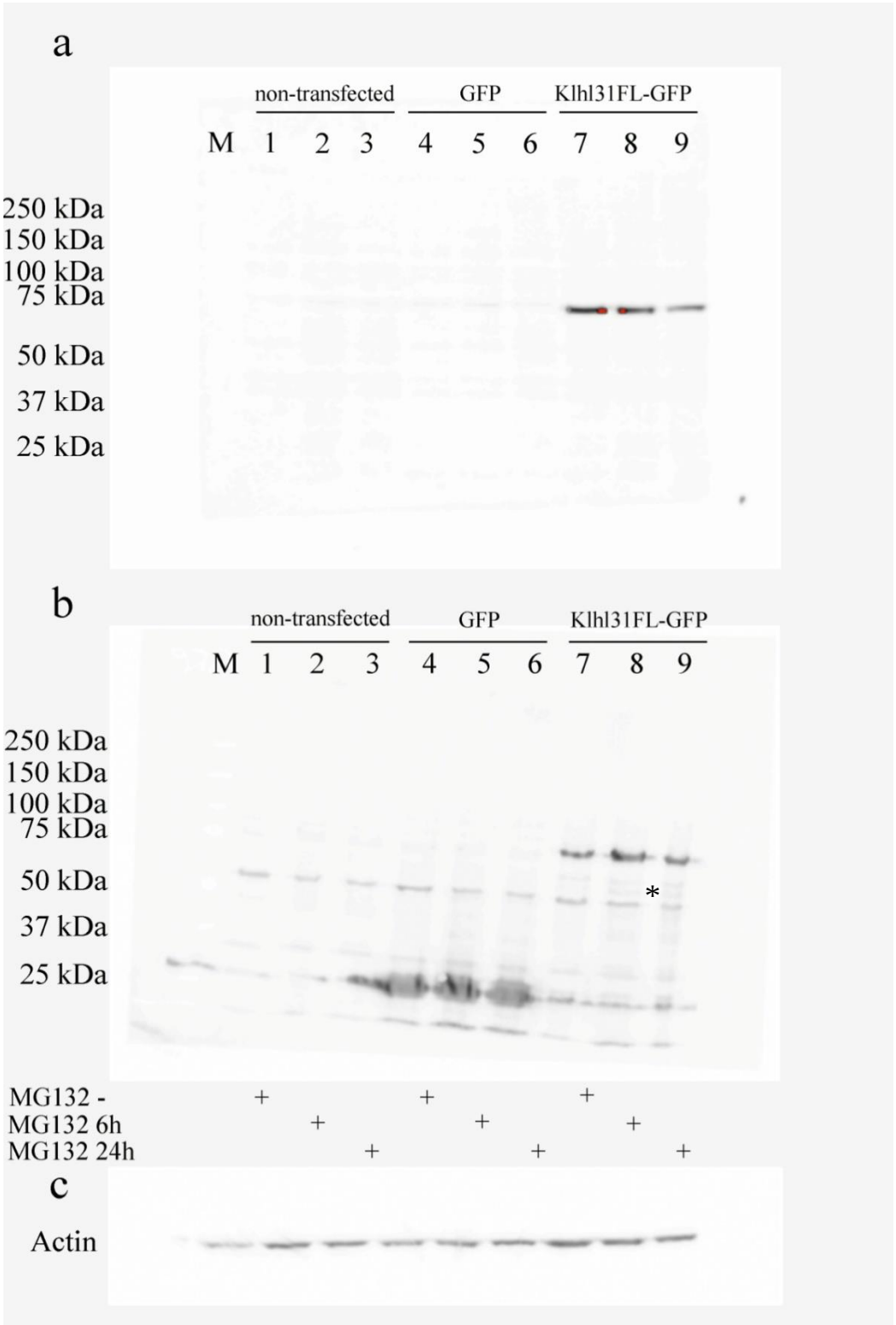

Figure 4.11: Treatment of cells with proteasome inhibitors allows the detection of Klhl31 FL-GFP with a) an antibody against Klhl31 and b) an antibody against GFP

Western blot showing the effect of treatment with MG 132 on the expression of pEGFP-Klhl31 fusion proteins. 50 µg of total protein was loaded per sample and proteins were either detected by blotting against Klhl31 (a) or GFP (b). An antibody raised against Actin was used as a protein loading control (c).

As a negative control, non-transfected HEK293 cells were either incubated for 48 h in DMEM (lane 1), or cultured in DMEM with the addition of MG 132 for either 6h (lane 2) or 24h (lane3). As a GFP-control, HEK 293 cells were transfected with pEGFP-N1. Cells were left to recover for 24h and then incubated in fresh medium for further 24h (lane 4) or cells were incubated in fresh medium with added MG 132 for either 6 h or 24 h, (lane 5 and 6) respectively. To investigate possible degradation of Klhl31 FL-GFP, HEK 293 cells were transfected with pEGFP-N1-Klhl31 FL. Transfected cells were also left to recover for 24h followed by incubation in fresh medium for further 24h (lane 7). To inhibit the proteasome, transfected HEK293 cells were cultured in fresh medium with added MG 132 for either 6 h or 24 h, (lane 8 and 9) respectively.

The visualisation of Actin showed a consistent protein amount loaded for each sample.

Legend: M- Marker

HEK293 cells were transfected with either pEGFP-N1 or pEGFP-N1 Klhl31 FL and treated with MG 132 (see figure 4.11).

The treatment with MG 132 had no obvious effect on GFP levels, as can be seen in figure 4.11, blot b, lanes 4-6. Interestingly we were able to detect a GFP Klhl 31 fusion protein with both, the Klhl31 antibody, as well as the GFP antibody in protein lysates obtained from untreated and treated HEK293 cells (see figure 4.11, blot a and blot b, lanes 7-9). However, the size of the fusion protein was smaller than expected. A full length Klhl31-GFP protein should have the size of 96 kDa; 70 kDa for Klhl31 plus 26 kDa for the GFP tag.

Furthermore, when using the GFP antibody we were able to identify additional protein bands smaller than 75 kDa (figure 4.11, blot b, lanes 7-9, *). Observed bands were not detected by using the anti-Klhl31 antibody.

Interestingly, the strength of the smaller bands seemed to increase slightly with longer incubation time in medium containing an additional proteasome inhibiting drug.

Based on our obtained data, it seemed that initial degradation of Klhl31 might not be mediated by the proteasome, as we could never observe a 96 kDa Klhl31 FL-GFP protein, not even when inhibiting the proteasome, but the additional, smaller protein bands seemed to appear stronger in the samples treated with MG 132, indicating that the treatment with the proteasome-inhibiting drug might prevent further degradation. We

therefore suggested that although the first cleavage might not be mediated by the proteasome, subsequent degradation might however be proteasome dependant.

5. Investigating interaction partners of Klhl31 during myogenesis

5.1 Introduction

5.1.1 Candidate interaction partners for Klhl31

We know from previous data, that some members of the Kelch-like family have been shown to bind to Actin (Adams and others, 2000; Kelso and others, 2002; Robinson and Cooley, 1997; Xue and Cooley, 1993). This also could be the case for Klhl31, as immuno-histochemistry revealed a close correlation of Klhl31 with Actin-fibres in differentiated C2C12 (see chapter 3.3.2). Results obtained from our Luciferase assays (see chapter 4.1.1 and chapter 4.2.1) suggest that additional potential interacting partners for Klhl31 may be found in the canonical Wnt-signalling pathway. In addition to TOPFLASH luciferase assays, there is supporting evidence previously obtained in our laboratory. In the African clawed frog, *Xenopus laevis*, a secondary body axis can be induced by overexpressing components of the β-catenin dependent Wnt-pathway (Guger and Gumbiner, 1995; Sokol and others, 1991). When injecting Wnt-ligands or β-catenin together with Klhl31 into *Xenopus laevis* embryos, formation of the secondary axis could be inhibited (Abou-Elhamd and Garcia-Morales). Based on these experiments and our Luciferase assays, we can conclude that an inhibition of canonical Wnt-signalling by Klhl31 potentially takes place at the level of β-catenin or downstream of it. Our next aim was to identify interaction partners for Klhl31.

5.1.2 Designing a Yeast-2-Hybrid screen to find interaction partners for Klhl31

As our cloned pEGFP-N1 and pEGFP-C1 Klhl31 Fusion constructs have been shown to be either non-active (for pEGFP-C1 Klhl31, see chapter 4.1) or degraded (pEGFP-N1 Klhl31, see chapter 4.2 and chapter 4.3), it was clear that we would not be able to use them to pull down interaction partners as originally planned via a GFP-binding protein (GBP), also called GBP-Nanotrap (Rothbauer and others, 2008).

We therefore chose a different approach, the Yeast-2-Hybrid screen, which would enable us to screen specific libraries, without actually using mammalian cells (Fields and Song, 1989).

The Yeast-2-Hybrid system was developed around the properties of the yeast transcriptional factor, GAL4. In general, eukaryotic transcriptional activators, including GAL4, contain two distinct domains, the DNA binding domain (DB) at the amino-terminus and the C-terminal transcription activation domain (AD). When the DB binds to its recognized DNA sequence, the AD will subsequently enable transcription of a reporter gene downstream of the DB domain by assembling a RNA polymerase II transcription complex (Chien and others, 1991; Fields and Song, 1989). This system was modified by Fields and Song to generate two specific hybrid proteins, one of which was fused to the GAL4 DNA binding domain, whilst the other protein was tagged with the GAL4 activation domain. As protein-protein interaction occurred, both domains came into close proximity leading to the transcription of a reporter gene (Fields and Song, 1989) (for a schematic overview of the Yeast-2-Hybrid screen see figure 5.1).

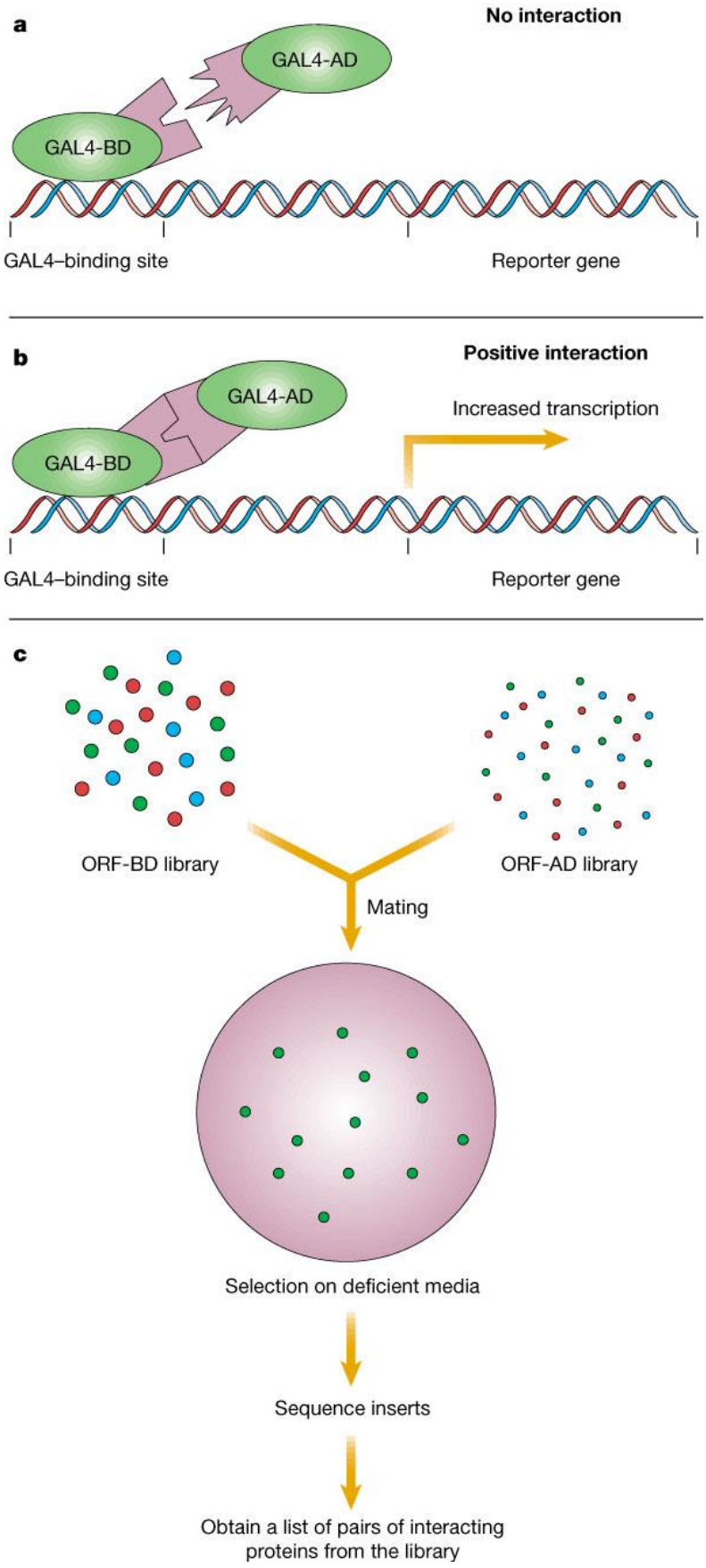

Figure 5.1: The Yeast-2-Hybrid system: a schematic overview

The Yeast-2-Hybrid allows the detection of potential interaction partners for a protein of interest. When a bait-protein X labelled with a GAL4-binding domain does not interact with a bait-protein Y fused to an activation domain, the reporter gene will not be expressed (a). However, when two proteins interact with each other and their BD and AD come into close vicinity, the transcription of the reporter gene is activated (b). Positive clones obtained from mating yeast cells expressing the bait-DB protein with a library of proteins tagged with an AD can grow on substrate deficient media (c). Positive clones can then be analysed by PCR and subsequently sequenced.

Figure taken from Pandey and Mann, 2000

Since then, the method has advanced further and can nowadays be used to screen cDNA libraries to detect potential novel interaction partners for proteins of interest (Bruckner and others, 2009). The detection of protein-interaction is carried out in living yeast cells. One set of yeast cell will be expressing the protein of interest, also called the bait protein, which is fused to the DNA binding domain, whilst the activation domain is fused to a library of other proteins, called prey proteins. As for the cDNA library approach, prey proteins can contain a pool of proteins, as well as fragments of proteins, all derived from cDNA from a specific tissue or a mixture of specific tissues (Auerbach and others, 2002). It was suggested that the inclusion of full length ORFs, as well as fragmented cDNA sequences would increase the possibility to cover the full transcriptome, therefore reducing the chance of false negatives. However, it was also shown that screening libraries would increase the chances of detecting false positives or wrongly identified proteins (Bruckner and others, 2009).

The bait protein is usually introduced to the prey proteins by mating of yeast cells, although transformation of yeast cells have also been described (Bruckner and others, 2009). Once interaction between a bait protein and a prey protein is established, i.e. when the protein of interest has bound to a potential interacting partner, the close proximity of the BD and the AD will allow transcription of a reporter gene. This reporter gene can either be used to mediate a colour reaction, allow growth on a substrate deficient media or induce a specific antibiotic resistance (Bruckner and others, 2009), enabling the selection of potential positive clones. However, these clones need to be analysed by PCR and sequencing.

The early Yeast-2-Hybrid screens were limited in their approach due to technical limitations (Fields and Song, 1989), but In recent years, the Yeast-2-Hybrid screens have been modified and developed to cater for different types of proteins and screening properties (for a list of current Y-2-H approaches, see (Bruckner and others, 2009).

The Yeast-2-Hybrid system is now an established tool to analyse protein-protein interactions.

For our Yeast-2-Hybrid screen, we decided to use Hybrigenics services, a company that claimed to be a leader in the field of protein interaction studies, as well as being the most reliable protein interaction service (http://www.hybrigenics-services.com/). We decided to screen a library for human muscle specific tissues derived from adult and 18-19 week fetal tissue using a full-length human Klhl31 as our bait protein (Image clone 9021264 obtained from Source BioScience LifeSciences, UK). Based on our previous experience with tagged Klhl31 proteins, we decided that the GAL4 binding domain should be fused to the carboxy-terminus of the Klhl31 protein, as this did not seem to affect the functionality of the protein or the BTB domain. Our previous data suggested that fusing a tag, in our case GFP, to the N-terminus of the Klhl31 protein would create a dysfunctional Klhl31 protein, which may be due to blockage of the BTB-domain (see chapter 4.1.2).

In summary, we decided to use a C-terminal fusion of the GAL4-binding domain to the human full length-Klhl31 protein. Possible interaction partners should be pulled out from a library containing protein or protein fragments derived from the transcriptome/ cDNA of fetal and adult muscle tissues.

5.1.3 Analysing the data obtained from the Yeast-2-Hybrid screen

Unfortunately for us, our Yeast-2-Hybrid screen did not progress completely without problems. The first more stringent approach did apparently fail and the second screen at reduced stringency did not reveal many positive interactions either.

Global PBS (for Interactions represented in the Screen)	
A	Very high confidence in the interaction
B	High confidence in the interaction
C	Good confidence in the interaction
D	Moderate confidence in the interaction This category is the most difficult to interpret because it mixes two classes of interactions : - False-positive interactions - Interactions hardly detectable by the Y2H technique (low representation of the mRNA in the library, prey folding, prey toxicity in yeast)
E	Interactions involving highly connected (or relatively highly connected) prey domains, warning of non-specific interaction. The total number of screens performed on each organism is taken into account to set this connectivity threshold: 20 interactions to different bait proteins in our entire database for Human, 10 for Mouse, Drosophila and Arabidopsis and 6 for all other organisms. They can be classified in different categories: - Prey proteins that are known to be highly connected due to their biological function - Proteins with a prey interacting domain that contains a known protein interaction motif or a biochemically promiscuous motif
F	Experimentally proven technical artifacts

Figure 5.2: The Yeast-2-Hybrid system: how to read your results

Hybrigenics services classified potential protein interactions based on protein structure predictions, toxicity and previous experiences. Classes A-C can usually be established as being true interaction, whilst interaction partners classified as group D have to be analysed with caution, as they might contain false-positives. Interaction partners classified in group E and F can usually be described at non-relevant, most likely false positives, either due to high connectivity of the prey protein itself or due to technical artefacts.

Picture modified from Hybrigenics Services.

As mentioned previously, we did not find a lot "most likely" real interaction partners as classified by Hybrigenics Services under groups A-C (see figure 5.2). Only one out of 37 predicted interactions was classified as B claiming high confidence in the interaction (see Appendix, A.3). When we analysed the DNA sequence of the interacting protein, it was shown to be a non-protein coding RNA sequence transcribing for JPX, a Xist activator. Xist, a non-coding RNA is involved in X chromosome inactivation (Brockdorff, 2011). It has been shown to coat the X-chromosome and recruits polycomb protein to its interacting site with the X-chromosome. Jpx is encoded by the X-inactivation centre and has been shown to be an activator for Xist (Tian and others, 2010).

Why we pulled out a non-coding RNA in protein-protein interaction screen is somehow puzzling and cannot really be described as a valid positive interaction between two proteins, one of which being Klhl31, the other one being a artificial creation based on a non coding RNA sequence. Also we were only given the short 5' sequence of the

fragment without any further information about the length of the sequence or the complete sequence of the fragment, which might limit us in terms of finding an open reading frame within the sequence, which might be translated into a protein fragment in yeast. However, we still tried to analyse the amino acid sequence to find clues with respect to structural properties or specific binding sites of Klhl31 binding partners. When we translated the given sequence into amino acids, a further problem occurred. We had no information about the frame of translation of the nucleotide sequence. So we looked at the amino acid sequence for all three possibilities. No matter what translation frame was used (reading frame 1, 2 or 3), we never found a continuous amino acid sequence. Sequences were always fragmented by stop-codons. Blasting a human protein data base against the different amino acid sequences revealed hundreds of hits, some known protein, some unknown, most of them with rather small similarity (for an example, see Appendix: blast of frame 1 of nc RNA (Jpx) transcribed into amino acid sequence). The longest non-disrupted amino acid chain was obtained from transcription in frame one. Although many proteins that were found in the screen had only around 50-70 % similarity with the blasted amino acid sequence (see Appendix), a potential binding domain was detected containing the highly conserved GVQW motif (Marchler-Bauer and others, 2011). The GVQW motif has been found so far in around 300 known proteins (Gerhard and others, 2004; Kanehori and others, 2003), but its functionality still needs to be verified. Examples of proteins obtained from the blast that contain the GVQW motif are the ubiquitously transcribed tetratricopeptide repeat protein Y-linked (UTY) (Accession number ABC87286.1) (Laaser and others, 2005) and the ubiquitin-conjugating enzyme E2D 4 (Accession number EAW94179.1) (David and others, 2010).

Proteins of the Kelch-like family have been described as being part of the E3 ubiquitin ligase complex (Furukawa and others, 2003; Geyer and others, 2003; Xu and others, 2003). Before the ubiquitin is bound to the target protein, it has to be activated first by an E1 or ubiquitin-activating enzyme, followed by transfer to an E2 ubiquitin-conjugating enzyme and subsequently attachment to the target protein via the E3 ubiquitin ligase (Neutzner and Neutzner, 2012). Therefore an interaction with an E2 ubiquitin-conjugating enzyme would make sense in terms of protein ubiquitinylation.

UTY as mentioned before is not as well described. *UTY* has a homologue on the X-Chromosome called *UTX* (Greenfield and others, 1998). Whilst UTX has been shown to demethylate trimethylated lysine-residue on position 27 on histone 3 ($H3K27^{me3}$)

(Agger and others, 2007; Lan and others, 2007) reversing repression of gene activity (Lee and others, 2007; Martin and Zhang, 2005), UTY is not a functional demethylase for H3K27^{me3} (Hong and others, 2007; Lan and others, 2007; Shpargel and others, 2012). Recent publications have indicated a role for UTX and UTY in transcriptional regulation independent of the function as a demethylase (Shpargel and others, 2012). Also recently heart defects were reported in UTX-deficient mice and embryonic stem cells (Lee and others, 2012). Whilst ESCs lacking UTX did not acquire rhythmic contraction when cultured in cardiac differentiation inducing medium, *UTX* null mice displayed severe heart defects and died before birth. It was also shown that demethylation of H3K27^{me3} is activated by binding of cardiac-specific enhancer genes to UTX (Lee and others, 2012). Further evidence for a role of UTX and UTY in heart development has been collected in co-immunoprecipitation studies. It was shown that both UTY and UTX can form complexes with BRG1, a chromatin remodelling factor, and various heart transcription factors, e.g. Tbx5 and Nkx2.5 (Lee and others, 2012; Shpargel and others, 2012).

Although both of the genes containing the GVQW motif could be interesting in terms of binding to Klhl31, as they both have been described to be involved in heart development or the ubiquitinylation process of target proteins, the evidence based for this interaction from the Yeast-2-Hybrid screen is too faint to consider a real interaction. The chances that the short amino acid fragments, which we analysed in the blast against a human protein database, would actually be a true interaction partner for Klhl31 is very small. The amino acid fragment was very small in size and identity to potential similar protein was not very high either (63% overall identity for UTY and 67% identity to E2D4), making it unlikely that we have identified a potential interacting partner based on a nc RNA sequence, even if the interaction was classified as highly likely by the company, which conducted our Yeast-2-Hybrid screen.

As we had to rule out our main best hit for a potential Klhl31 interaction partner, we then went on to analyse the hits from the screen classified as members of group D: to be analyzed with cautions, due to the possibility of false positives or toxicity issues (see figure 5.2).

5.2 Results

5.2.1 Background research on potential novel interaction partners for Klhl31

Although we obtained only one highly likely interaction partner for Klhl31 (class B interaction see Appendix), 35 interactions found were grouped into class D.

Class D interactions could contain false-positives as well as artificial products due to toxic side effects created by the overexpression of the bait-protein. We analysed all 35 interactions for the possibility to bind to Klhl31 on the basis of their verified DNA sequence. When searching a human genome database, 27 out of these 35 interaction partners were shown to be derived from introns of different genes. One further sequence was shown to span an intron-exon site within a gene, whilst two sequences were shown to be non-coding RNA and another nucleotide fragment was unidentifiable. These results were unexpected as the muscle library was based on cDNA derived from mRNA. It is possible that the screened library was contaminated with genomic DNA.

As we could not pursue any of these findings any further, we decided to investigate the three hits that were representing actual proteins.

5.2.2 NEDD9 has been identified as a potential interaction partner for Klhl31

Neural precursor expressed, developmentally down-regulated 9 (*NEDD9)* encodes for a protein called enhancer of filamentation 1, also known as HEF-1 or CAS-L. It is a member of the Cas-protein family based on a conserved structure of its protein-protein binding domain (Astier and others, 1997; Singh and others, 2007). Proteins of the Cas family have been shown to be adhesion docking proteins involved in cell migration and other cellular processes (Zhong and others, 2012). Recently NEDD9 became a protein of interest based on evidences that its expression is increased in metastatic cancers (Donninger and others, 2004; Iwata and others, 2005; O'Neill and others, 2007). Furthermore, it has been suggested that NEDD9 itself is a marker for metastasis, as increased NEDD9 expression was reported in human and mouse melanoma cells lines (Kim and others, 2006), in lung and breast cancer (Minn and others, 2005) and in

glioblastomas (Natarajan and others, 2006). In colorectal cancer NEDD9 has also been described in mediating cancer migration (Li and others, 2011).

Recently it has been shown that metastasis in WM1361 melanoma cell is increased by elevated NEDD9 expression (Ahn and others, 2012). It was also reported, that NEDD9 protein levels were depending on integrin β3 signalling and led to phosphorylation of the integrin β3, subsequently activating Scr and FAK, as well as reducing ROCK activity (Ahn and others, 2012).

That NEDD9 mediates cell migration by promoting integrin β1 receptor activity has also been reported in mouse embryonic fibroblasts (Zhong and others, 2012). Integrin signalling has been shown to regulate cell movement by binding to ligands of the extracellular matrix, such as fibronectin and collagen and by coupling the extracellular signals to the intracellular microfilaments. However, integrin receptors do not contain Actin-binding properties and changes in Actin cytoskeleton are therefore mediated by interaction of integrins with various Actin-binding proteins and the focal adhesion kinase (FAK) (Carragher and Frame, 2004; Hynes, 2002; Lo, 2006; Schlaepfer and others, 1999; Sieg and others, 1999; Wehrle-Haller, 2012).

Although we could detect a close proximity of Klhl31 to Actin fibres, this co-localisation was seen along the whole Actin filaments across the whole myotube (see figure 3.7 in chapter 3.3.2). Furthermore, we were never able to detect Actin Klhl31 co-localisation in myoblasts, which also are migrating cells. Klhl31 expression did not seem specific to focal adhesion sites. Also, NEDD9 has never been reported to have a direct link to Actin fibres, rather it seems to influence cytoskeletal changes by enhancing signals from the integrin receptors (Zhong and others, 2012).

However we have not looked in more detail at localisation of components of the focal adhesions, such as FAK and integrin receptors in relation to Klhl31. As these components are associated to the cell membrane and we detected Klhl31 either in the cytosol or associated to Actin fibres along myotubes, we did not gather any obvious evidence for association of Klhl31 to focal adhesion sites.

We concluded that with respect to this project, the function of Klhl31 during myogenesis, NEDD9 would not be investigated any further. Also, advice given by the specialist from Hybrigenics Services, suggested that NEDD9 is a protein, which is

pulled out quite often in Yeast-2-Hybrid screens and therefore might indicate the possibility of being a false-positive.

Based on our data, we decided not to pursue further experiments to validate a potential interaction for NEDD9 with Klhl31 at this stage.

5.2.3 FKPB15 has been identified as a potential interaction partner for Klhl31

FKBP15, also known as FKBP133, was first identified in mouse as a homologue of the FK506-binding proteins (Nakajima and others, 2006). FK506-binding proteins belong to immunophilins (Kawashima and others, 1988; Warty and others, 1988), a highly conserved family of proteins, which can bind immunosuppressive drugs, such as FK506 and rapamycin (for an overview of FKBP proteins see (Kang and others, 2008). Members of the FKBP protein family display two distinct domains, the FKBP domain and the tetratricopeptide repeats (TPR) (Kang and others, 2008). The FKBP domain contains peptidylprolyl isomerase (PPIase) activity (Maki and others, 1990), which catalyzes *cis-trans* isomerisation of peptidylprolyl bonds and is involved in assisting protein folding (Fischer and Aumuller, 2003; Fruman and others, 1994). The C-terminal TPR domain has been shown to mediate protein-protein interactions (Scheufler and others, 2000). Although, as mentioned before, members of the FKBP family all contain the FKBP and the TRP domain (Kang and others, 2008), the number of the domains varies from protein to protein. For example FKBP38 contains one FKBP domain, but three TRP domains (Lam and others, 1995), whilst FKBP52 contains two tandem FKBP domains and also three TRP domains (Davies and Sanchez, 2005). Other members of the family can also contain additional different protein binding domains (Kay, 1996) determining their function and localisation in the cell.

FK506-binding proteins have been shown to be involved in various intracellular events. For example, the best described member of the FKBP family, FK506-binding protein 51 (also known as FKBP5) is expressed in various cancers, where hyperexpression of FKBP51 has been shown to sustain malignancy, whilst also promoting resistance to medical treatments (Romano and others, 2011). FKBP38, however, has got a completely different function. It has been shown to be involved in apoptosis, as well as regulation of the formation of the neural tube (Edlich and Lucke, 2011).

FKBP15, also known as FKBP133 due to its size of 133 kDa, has been described to be expressed in the developing nervous system of mice. It contains a domain, which is similar to Wiskott-Aldrich syndrome protein (WASP) homology region 1 (WH1) at the N-terminus, as well as the FK506-binding protein domain (Nakajima and others, 2006) in the centre of the protein. This protein does not contain a TRP domain, but a further Band4.1-Ezrin-Radixin-Moesin (FERM) domain (Nakajima and others, 2006). Based on the presence of the FKBP domain and homology to FKBP12, FKBP15 was termed being a member of the FKBP protein family (Nakajima and others, 2006). Enzymatic test revealed that FKBP15 does not display PPIase activity unlike many other FKBP family members and it also is not able to bind to FK506 (Nakajima and others, 2006). Interestingly though, it has been shown to localise to F-Actin in growth cones of neurons in the dorsal root ganglion. It has also been described that overexpression of FKBP133 led to increased size of the growth cones, as well as leading to elevating numbers of filopodia. These changes were potentially mediated by the WH1 domain, as overexpression of a deletion mutant for the WH1 domain led to a reduced growth cone size and less filopodia (Nakajima and others, 2006). Furthermore, Nakajima et al. reported that FKBP15 does not influence changes in the Actin fibres of the growth cones directly, instead it stabilises the F-Actin cytoskeleton by preventing Semaphorin 3A induced Actin depolymerisation.

Recently, a different protein also containing the WH1 domain and the FKBP domain has been identified from biopsies taken from colons of patients with inflammatory bowel diseases (Viklund and others, 2008). Just as FKBP15, the discovered protein has been described to be transcribed by the DNA of the gene KIAA0674 (see http://www.ncbi.nlm.nih.gov/gene/23307).

Based on its similarity to both proteins of the WASP family and the FKBP family, the described newly discovered protein was named WAFL (WASP and FKBP-like).

As previously mentioned, WAFL also shows high structural similarity with FKBP15 as both proteins contain the WH1 and the FKBP domain at their N-termini (Nakajima and others, 2006; Viklund and others, 2009; Viklund and others, 2008). Alignment of the amino acid sequences for WAFL and FKBP15 revealed that both proteins share 75% identity and within the WH1 and FKBP domain the identity is even higher (82%). Also both proteins contain the predicted Klhl31 binding site. Therefore we can assume that Klhl31 could interact with both, FKBP15 and WAFL.

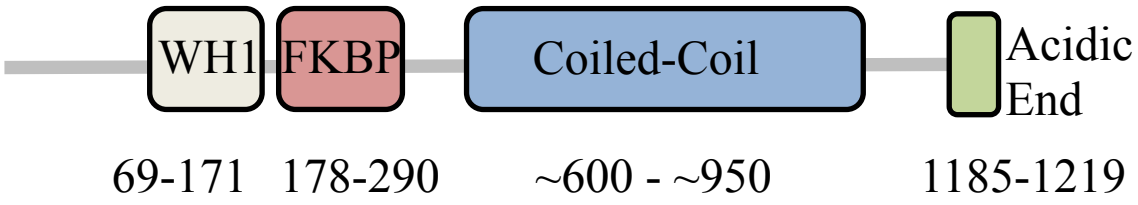

Figure 5.3: Structural organisation of WAFL

The WASP and FKBP-like (WAFL) protein contains 4 distinct domains. Close together at the N-terminus it contains a WH1 and FKBP domain. In the centre of the protein it reveals a Coiled-coil domain, whilst C-terminal it contains a stretch of acidic amino-acids.
Figure redrawn after Viklund and others, 2008

Further studies revealed a role of WAFL in endocytosis as a GFP-WAFL –fusion protein has been shown to interact with endosomes, as well as being localised along microtubules (Viklund and others, 2009). Movement of WAFL along microtubules was inhibited by treatment with nocodazole, which prevents polymerisation of microtubules. But when treated with Latrunculin A, movement was not decreased revealing that trafficking of WAFL-linked endosomes did mainly take place along microtubules (Viklund and others, 2009). Co-immunoprecipitation studies, however, revealed a direct interaction of WAFL with Actin and the WASP-interacting protein, suggesting a role for WAFL in the Actin polymerization during vesicle motility (Viklund and others, 2009).

The alignment of the Hybrigenics clone protein sequence of FKBP15, which was said to interact with Klhl31, to the amino-acid sequence of FKBP15/WAFL revealed that the Hybrigenics fragment overlaps with amino acids 336 to 559 of full length FKBP15/WAFL. The WH1 domain would contain amino-acid 71-159 (or 69-171), whilst amino-acids 178-289 (or 178-290) make up the FK506-binding domain as described by Nakajima et al., 2008 (or Viklund et al., 2008). Therefore the binding fragment for Klhl31 does not seem to be part of the published conserved binding domains.

As WAFL has been described to interact directly with Actin (Viklund and others, 2009) and as we have observed punctate localisation of Klhl31 along Actin fibres in C2C12

myotubes (see figure 3.7; section 3.3.2), Klhl31 might interact with WAFL to promote Actin polymerization as described by Viklund et al., 2009. A real interaction between FKBP15/WAFL and Klhl31 needs to be verified first and more evidence needs to be gathered about functions of Klhl31 and FKBP15/WAFL before a potential role for Klhl31 together with WAFL can be hypothesised. However, as Klhl31 expression seems to be restricted to striated muscles and FKBP15/WAFL expression has not been reported in muscular tissue so far, it seems unlikely that Klhl31 and FKBP15/WAFL could interact.

Based on the differences in their expression patterns, we did not investigate a potential role of Klhl31 together with FKBP15/ WAFL any further.

5.3 Nebulin as a novel interaction partner for Klhl31

5.3.1 The giant protein Nebulin and its role in striated muscle

Nebulin seemed to be the most promising protein being discovered in the Yeast-2-Hybrid screen. Not only did we identify two different isoforms of Nebulin, isoform 2 and isoform 3 as potential interaction candidates for Klhl31; Nebulin has also been described to play important roles in embryonic and adult muscle tissues.

Nebulin was firstly seen in rabbit skeletal myofibrils in 1980 and described as band 3 protein, which remains near the Z-discs (Wang and Williamson, 1980). Later it was shown to be a giant protein between 600 – 900 kDa large, which was eventually termed Nebulin due to its nebulous size and the fact that it was difficult to purify (Wang, 1982). Further studies revealed that Nebulin would potentially make up between 3-4% of total myofibrillar proteins in striated muscles (Locker and Wild, 1986). Since its identification, *Nebulin* has been studied extensively. Members of the *Nebulin* family can be found in invertebrates, such as chordates, and vertebrates, such as chimpanzee and humans and PCR data from various species led to the suggestion that the *Nebulin* gene family has expanded from a chordate ancestor gene during evolution (Bjorklund and others, 2010; Hanashima and others, 2009).

The Nebulin gene has so far been best described for humans (Donner and others, 2004; Jin and Wang, 1991a) and mice (Kazmierski and others, 2003).

Human *Nebulin* spans a genomic sequence of 249 kb and contains 183 exons (Donner and others, 2004), whilst the mouse *Nebulin* contains 165 exons spanning 202 kb of genomic DNA. In human *Nebulin* the translation initiation codon has been described to be in exon 3, whilst exon 183 contains the stop codon and the 3'UTR (Donner and others, 2004). Donner et al also identified alternatively spliced exons. Alternative splicing sites have been described for exons 63-66, exons 82-105 and exons 166-167, which alone can give rise to at least 20 different transcripts in the human adult tibialis anterior muscle (Donner and others, 2004). Exon 143 and exon 144 also contain an alternative splice site and only one of these exons seems to be present in each Nebulin isoform (Donner and others, 2006; Donner and others, 2004). Expression studies for exon 143/ 144 revealed that expression varies between muscle isoforms, but more

interestingly for us between developmental stages of muscles (Donner and others, 2004) with exon 144 being expressed more often in muscles of older mice. In mouse *Nebulin*, exons 127/ 128 have been described to be homologues to human *Nebulin* exons 143/ 144 (Donner and others, 2006). It was further speculated that mouse *Nebulin* exons 127/128 (or human 143/ 144) might function as developmental regulators mediating progression from growing muscle fibres (expressing exon 127 or 143) to mature muscles (expressing exon 128 or 144) (Buck and others, 2011; Donner and others, 2006).

Although there is a high homology between mouse and human *Nebulin*, mouse *Nebulin* displays a few differences when compared to human *Nebulin*. It has been reported that the mouse *Nebulin* contains 16 exons, which have no homologue in the human gene, as well as containing a protein binding domain similar to human protein ZO-1 in the 16th of the novel exons (Kazmierski and others, 2003).

As mentioned in the previous section, alternative splicing sites have been reported for *Nebulin* across different species (Donner and others, 2004; Joo and others, 2004; Kazmierski and others, 2003). This alternative splicing leads to the translation of proteins with different sizes. It was thought for a long time that the size of Nebulin might serve as a ruler for thin filament length specification, as different types of muscles had different length of thin filaments, which in turn was proportional to the size of the Nebulin protein present in the muscle's sarcomere (Kruger and others, 1991; Labeit and others, 1991; Wang, 1996). It was further reported that a single molecule of Nebulin spans the whole length of the thin filaments in sarcomeres with its C-terminus being localised to the Z-disc (Millevoi and others, 1998; Wang and Wright, 1988) (see figure 5.5). The N-terminus of Nebulin has been described to extend and potentially interact with the thin filament pointed ends via binding to tropomodulin (McElhinny and others, 2001). Recently the interaction of the C-terminus of Nebulin with the (thin filament) barbed end capping protein CapZ has been reported (Pappas and others, 2008; Witt and others, 2006) giving even more evidence of a role for Nebulin in thin filament length regulation. But Nebulin has also been shown to interact with the Actin monomers as part of the thin filament directly (Labeit and others, 1991).

Nebulin displays a highly repetitive protein structure, in which the central polypeptides are arranged in 153 modules (M9-M162) consisting of between 30 – 35 amino acids each (Jin and Wang, 1991b; Labeit and others, 1991; Labeit and Kolmerer, 1995a).

Each module contains a conserved SDXXYK Actin binding domain, so that each of the central modules can bind one Actin monomer (Jin and Wang, 1991b; Labeit and others, 1991). An overview to the structural organisation of Nebulin and its localisation in the sarcomere can be seen in figure 5.4.

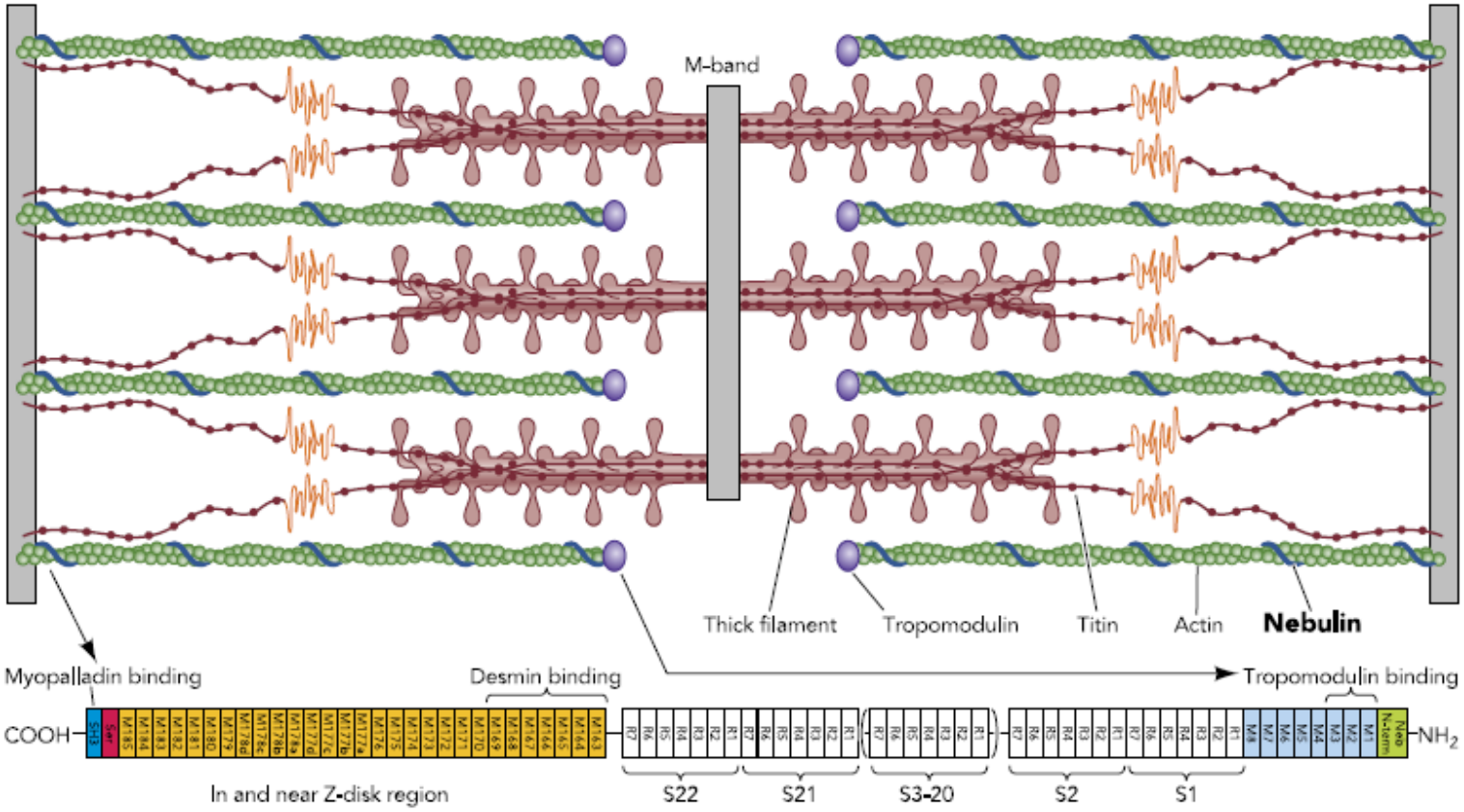

Figure 5.4: Structural organisation of Nebulin and its localisation in sarcomeres

Figure 5.4: Structural organisation of Nebulin and its localisation in sarcomeres

The giant protein Nebulin is associated to thin filaments in sarcomeres (top section). Nebulin binds to Actin via its central super repeats. With its C-terminus Nebulin has been shown to interact with titin and myopalladin, as well as CapZ and Desmin. The N-terminus of Nebulin contains binding sites for tropomodulin.

Figure taken from Ottenheijm and Granzier, 2010

Recent work by Pappas et al. (2010) described a more indirect role for Nebulin in length specification of the thin filament, as overexpression of a designed small protein of Nebulin, called Mini-Nebulin, was unable to restrict the length of the Actin filament (Pappas and others, 2010). Treatment of Nebulin-deficient myocytes and control myocytes with the Actin depolymerising toxin Latrunculin A, revealed that the presence of Nebulin prevents the binding of Latrunculin A to Actin monomers, which in turn prevents depolymerisation of the thin filament (Pappas and others, 2010). It was therefore suggested that Nebulin stabilises Actin-Actin monomer bonds in the thin filament rather than regulating its association and length (Pappas and others, 2010). It was also shown by Pappas et al. (2010) that the Actin monomers were more prone to substitution, when Nebulin was depleted using siRNA in the myocytes, again revealing a lack of Actin-polymer stabilisation. Also far earlier then Pappas et al. a stabilisation mechanism of Actin polymers has been indicated by work from Gonsior et al. It was reported that a recombinant human Nebulin fragment generated based on 5-6 modules from the N-terminal region was able to crosslink Actin monomers (Gonsior and others, 1998). It was also suggested that binding of Actin monomers by Nebulin can be used as a scaffold along which further addition of Actin monomers can occur. Strong evidence against a role of Nebulin as thin filament length regulator was published in 2009 by Castillo et al. It was reported that Nebulin does not extend to the pointed ends of the thin filament and would therefore not be able to interact with tropomodulin (Castillo and others, 2009). It was also reported that the length of the thin filament correlated with the size of the present titin isoform rather than Nebulin, thereby further highlighting that Nebulin does not regulate Actin filament length in striated muscles (Castillo and others, 2009)

As previously mentioned, Nebulin contains 153 Actin-binding modules. These modules themselves are further clustered into 22 super repeats (SR), each one consisting of a conserved binding domain comprising the motif WLKGIGW (Jin and Wang, 1991b; Labeit and others, 1991; Labeit and Kolmerer, 1995a). These binding domains have been implicated to associate with the troponin/tropomyosin complex (Labeit and Kolmerer, 1995a; Wang and others, 1996). As the troponin/tropomyosin complex is involved in regulating muscle contraction (Farah and Reinach, 1995) and Nebulin had been shown to inhibit actomyosin ATPase activity in an in vitro motility assay (Root and Wang, 1994), it was thought that Nebulin might also be involved in muscle contraction regulation. Further evidence for a role in Nebulin during muscle movement came from data obtained from Nebulin knock-out mice. It was shown that in Nebulin KO mice thin filament sizes are reduced (Bang and others, 2006; Witt and others, 2006). As contraction is based on the length of the filaments (Gordon and others, 1966; Granzier and others, 1991), as well as the ratio of overlapping of the thin filament with the thick filament, also known as the cross-bridge theory (Huxley and Simmons, 1971), shorter thin filaments meant that the active tension was highly reduced in Nebulin KO mice (Gokhin and others, 2009; Witt and others, 2006). Furthermore it was reported that Nebulin might regulate muscle contraction by changing cross-bridge activity between Actin and myosin (Bang and others, 2009; Chandra and others, 2009).

The C-terminus of Nebulin contains a serine-rich domain as well as a SRC homology 3 (SH3) domain (Labeit and Kolmerer, 1995a). It has been shown that the C-terminus of Nebulin aligns to the Z-disc of the sarcomere (Millevoi and others, 1998; Wang and Wright, 1988). Recent data revealed the association of the SH3 domain with myopalladin linking Nebulin directly to the Z-disc (Bang and others, 2001; Ma and Wang, 2002). Interestingly, it was also shown that the SH3 domain does not only bind to the PEVK domain in myopalladin, it can also link Nebulin to another giant protein, Titin (otherwise known as Connectin ;(Ma and Wang, 2002). Based on their finding, Ma and Wang proposed that Titin together with myopalladin would be able to localise Nebulin to the Z-disc during myofibrillogenesis. Analysing the C-terminal Serine-rich domain of Nebulin, led to the speculation, that Nebulin could be involved in signalling pathways taking place close to the Z-disc due to the presence of potential phosphorylation sites in the serine-rich domain (Bang and others, 2006). The C-terminus of Nebulin has also recently been implied to interact with the intermediate filament Desmin (Bang and others, 2002).

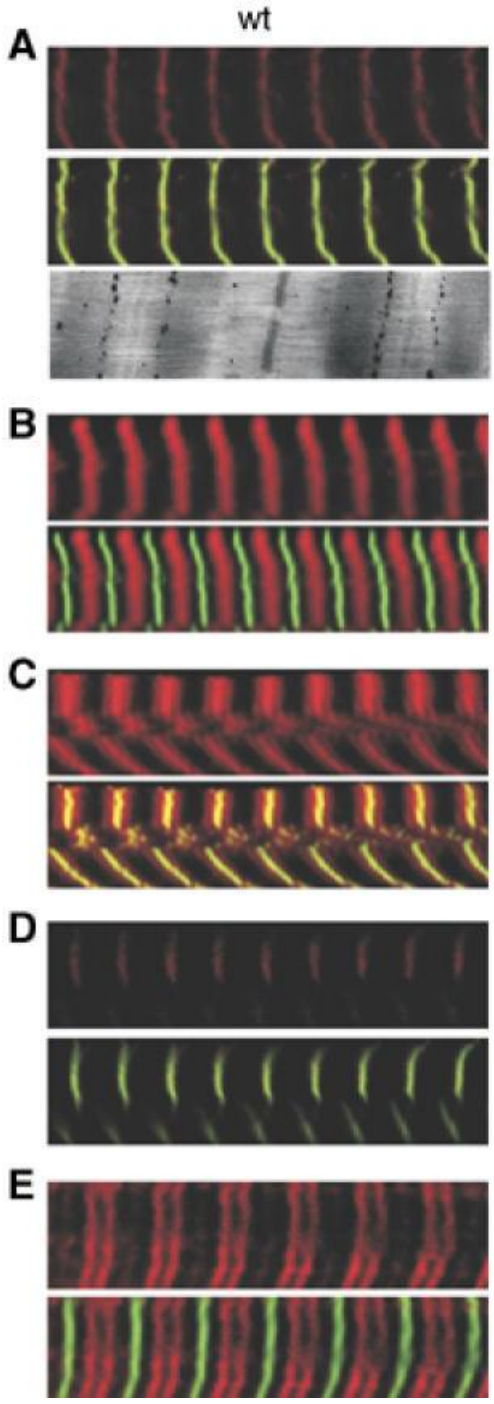

Figure 5.5: Localisation of Nebulin and interacting proteins

Sections of myofibrils from quadriceps muscle fibres from wt-mice have been labelled for α-actinin (green) as a marker for Z-discs and various other proteins (red); (A) Nebulin, (B) myosin heavy chain, (C) myopalladin, (D) CapZ and (E) tropomodulin 1. Nebulin is detected at the Z-disc, where it potentially localises to α-actinin, myopalladin and CapZ. Also (A) lower picture, electron microscopy of muscle section labelled for Nebulin.

Figure modified from Witt and others, 2006

5.3.2 A role for Nebulin during myofibrillogenesis

Nebulin is not only expressed in adult muscles, it has also been reported that Nebulin plays an important role during muscle development.

Data obtained for a function of Nebulin during myofibrillogenesis has been obtained by experiments using Nebulin knock-out mice and also by using cell culture.

Evidence that Nebulin might play a role in myofibrillogenesis came from immuno-fluorescence studies using primary cultures of skeletal muscle cells dissected out of pectoralis muscle from 10-12 days old chicken embryos. Firstly, Moncman and Wang (1996) analysed the temporal expression and assembly of sarcomeric proteins during myofibrillogenesis. Desmin was expressed first, followed by α-Actin, myosin, titin and Nebulin (Moncman and Wang, 1996). However, looking at the assembly of expressed protein it was described that Myosin was shown to align first followed by titin, Nebulin, Actin and Desmin (Moncman and Wang, 1996).

Nebulin was firstly detected in the cytoplasm of chick skeletal myocytes at the time point when cells started to differentiate and its localisation was described to be diffused, similar to that of muscular myosin and titin (Moncman and Wang, 1996). However, whilst muscle specific myosin and titin eventually became associated to nascent myofibrils and displayed striated patterns, Nebulin was still seen to be mainly cytoplasmic (Moncman and Wang, 1996). Nebulin was shown to be added to the myofibrils once myosin and titin had assembled in striations, but before the organisation of Actin into defined thin filaments with uniform lengths (Moncman and Wang, 1996). Moncman and Wang (1996) therefore concluded that the assembly of Nebulin requires the formation of the nascent I-Z-I complex containing the Z-disc as well as premature thin and thick filaments. They suggested that Nebulin is involved in organising Actin into the thin filaments as well as restricting the length of the Actin fibres (Moncman and Wang, 1996). Similar observations were also published by (Shimada and others, 1996). Furthermore, Shimada et al. also claimed that Nebulin is not needed in establishing a scaffold for other sarcomeric proteins to locate to during formation of myofibrils, but is potentially involved in the organisation of Actin to the premature sarcomeres (Shimada and others, 1996).

This is inconsistent with observations by Gonsior et al. (1998), who reported that Nebulin could potentially act as a scaffold for Actin polymerization. It was also reported that Nebulin did display a low affinity to bind to Actin monomers (Gonsior and others, 1998). Based on their observation that Nebulin crosslinks Actin monomers, as well as Actin bundles and based on previously described expression patterns for Nebulin after the formation of primitive Z-discs, Gonsior et al. (1998) speculated that Nebulin would not be able to assemble on its own into thin filament associated striations. They suggested that either a peritranslational assembly mechanism is involved in Nebulin localisation to Actin fibres or that another protein, similar to a chaperone, would assist Nebulin during incorporation into sarcomeric thin filaments (Gonsior and others, 1998).

Further evidence for Nebulin as a scaffold for Actin polymerization was published by Nwe et al. in 1999. It was reported that in premyofibrils Nebulin located along linear Actin filaments in a punctate fashion, although some Nebulin puncta were also observed to be scattered between the filament (Nwe and others, 1999). In developing myofibrils however Actin was shown to localise to the Z-disc and the edges of I-Z-I regions, whilst Nebulin was strongly expressed overlapping with Actin at the Z-disc (Nwe and others, 1999). Once the myofibril had fully developed, Actin was still seen to display strong fluorescence at the Z-disc, while Nebulin proteins were found on either side of the Actin-staining flanking the Z-disc (Nwe and others, 1999). Based on observed localisation of Nebulin to Actin, it was suggested that the punctate, but also linear Nebulin structures might build a scaffold upon which actin monomers can assemble to form non-striated Actin bundles in the first instance (Nwe and others, 1999). Furthermore, Nwe et al. studied the kinetics of Actin-assembly by Nebulin. During early myofibrillogenesis Actin filaments were not closely linked to Nebulin, as the exchange rate of Actin monomers was reported as being rapid in comparison to mature myofibrils, whilst in mature myofibrils Actin was tightly associated to Nebulin (Nwe and others, 1999). Nwe and co-workers therefore distinguished between different types of Nebulin during myofibrillogenesis. The first type of Nebulin, the immature Nebulin, has a role in attaching the Actin monomers to the Z-disc (Nwe and others, 1999). As the bond between Nebulin and Actin is not very strong in premyofibrillar cells, the fluent exchange rates allow the incorporation of Actin monomers into the Z-disc (Nwe and others, 1999). As myofibrillogenesis progresses, the link between Nebulin and Actin becomes tighter, which leads to the stabilisation of Actin fibres by Nebulin in the striations of mature sarcomeres (Nwe and others, 1999).

Recently, Nebulin-silencing experiments also revealed a role for Nebulin during myofibrillogenesis. During differentiation, the foetal rat skeletal myocytes were treated with siRNA to reduce Nebulin levels in the cells (McElhinny and others, 2005). In comparison to non-treated myocytes, Nebulin depleted rat muscle cells differentiated slower and fusion was delayed (McElhinny and others, 2005). When comparing the assembly of myofibrils in control myocytes with siRNA treated myocytes during a 5-day time course of differentiation, it was shown that the Z-disc did not form properly, nor in fact had the striated pattern of the thin and thick filaments been established (McElhinny and others, 2005).

Myofibrillogenesis was also studied in Nebulin knock-out mice. Although mouse embryos and new born rodents showed fully assembled myofibrils, the sarcomeric structure was shown to dissociate under muscle contraction (Bang and others, 2006; Gokhin and others, 2009; Witt and others, 2006).

Nebulin knock-out rodents displayed normal myofibrils, the thin filament capping proteins, CapZ and Tropomodulin (Tmod1), as well as myopalladin were affected by the absence of Nebulin (Witt and others, 2006). Labelling of myopalladin at the Z-disc revealed a reduced and diffused localisation compared to wt myopalladin labelling (Witt and others, 2006). Similar data was also obtained for CapZ and Tmod1 (Witt and others, 2006). Furthermore Tmod1 was also shown to be located closer to the Z-disc when compared to wt-Tmod1 (Witt and others, 2006). It was also shown that the length of the thin filament was greatly reduced (Witt and others, 2006). Based on their data, Witt et al. (2006) confirmed the suggested role for Nebulin in thin filament length specification. Similar observation were also made by (Bang and others, 2006), who reported that Nebulin would not be needed for the assembly of sarcomeres (Bang and others, 2006). But as they found shorter thin filaments in Nebulin deficient mice, misaligned Z-discs and the degradation of sarcomeric structures in active muscles, they also described a role for Nebulin in the stabilisation and maintenance of myofibrils (Bang and others, 2006)

In summary, Nebulin plays an important part in the organisation and stabilisation of myofibrils, as well as in mediating muscle contraction.

Recently, Nebulin has also been shown to be expressed in the heart, stomach and brain in adult chicken (Joo and others, 2004). Nebulin expression in cardiomyocytes was further reported in other species, but protein levels are significantly less for cardiac

Nebulin compared to skeletal muscle Nebulin (Donner and others, 2004; Fock and Hinssen, 1999; Kazmierski and others, 2003). It was thought that the role of Nebulin in striated muscle was carried out in heart musculature by Nebulette, a 107 kDa homologue of Nebulin (Moncman and Wang, 1995). Further data seemed to confirm an essential role for Nebulette in cardiomyocytes, as a knock-down of Nebulette in cardiomyocytes lead to a thin filament phenotype similar to that of thin filament in Nebulin depleted skeletal muscle (Moncman and Wang, 2002). It was shown that Nebulette also interacts with thin filament capping proteins indicating that Nebulette might stabilize the length of the Actin filament in a similar way to Nebulin (Bonzo and others, 2008).

5.3.3 Analysis of Nebulin as a potential new binding partner for Klhl31

As mentioned earlier, the Yeast-2-Hybrid screen identified two Nebulin isoforms as potential binding partners for Klhl31. When the amino-acid sequences of both Nebulin fragments (Isoform 2 and Isoform 3) were aligned, we discovered that both amino acid sequences contained a similar, potential conserved binding site for Klhl31 (see alignment below). The protein alignment was done by using the software Clustal2W (EMBL-EBI tools).

```
----------------------------------------------DTVSDVKYKEDLT 13
DALDIVYHRKVTDDISKIKYKENYMSQLGIWRSIPDRPEHFHHRAVTDTVSDVKYKEDLT 60
                                             **************

WLKGIGCYAYDTPDFTLAEKNKTLYSKYKYKEVFERTKSDFKYVADSPINRHFKYATQLM 73
WLKGIGCYAYDTPDFTLAEKNKTLYSKYKYKEVFERTKSDFKYVADSPINRHFKYATQLM 120
************************************************************

NERKYKSSAKMFLQHGCNEILRPDMLTALYNSHMWSQIKYRKNYEKSKDKFTSIVDTPEH 133
NEKKYRADYEQRKDKYHLVVDEPRHLLAKTAGDQISQIKYRKNYEKSKDKFTSIVDTPEH 180
**:**::. :   ::    : .*  * *   ..  *************************

LRTTKVNKQISDILYK 149
LRTTKVNKQISDILYK 196
****************
```

Legend: Fragment **Nebulin Variation 2**, Fragment **Nebulin Variation 3**.

Potential Actin binding domains (SDXXYK) are underlined.

Also, both Nebulin isoforms are substantially different from each other due to alternative splicing, with for example Nebulin isoform 3 being significantly smaller than isoform 2. Some of these differences can also be seen in the sequences of the fragments. However, when aligning the fragments to the full length DNA or amino acid sequence and comparing the obtained data to the already known DNA organisation of the Nebulin genes, it became clear that both fragments, which were identified to be a potential Klhl31 binding partner, are located in a mRNA sequence, which contains exon 144 (for alignment and additional information, see Appendix).

Exon 144 has been described to be a marker for adult muscle tissues (Buck and others, 2011; Donner and others, 2006). As we have screened a library which contained proteins from adult and foetal muscular tissues, it was possible to detect proteins that might link Klhl31 to mature rather than developing muscles. We knew from previous

studies that Klhl31 was expressed in nearly all striated muscles in chick embryos, as well as in embryonic heart and skeletal muscle tissues of humans (Abou-Elhamd and others, 2009; Yu and others, 2008), but we have not analysed Klhl31 protein levels in adult muscle tissues. Nebulin has been very well described in muscle fibres, where it has been detected in striations localising to actin fibres along the Z-disc (see figure 5.7; (Pappas and others, 2008)and figure 5.6; (Witt and others, 2006)

5.3.4 Nebulin partially co-localises with Klhl31 in mouse muscles

To find out, whether Klhl31 is actually expressed in adult muscles and if it would co-localise to Nebulin, we decided to use an immuno-staining approach on mouse adult muscle sections.

Localisation of both, Nebulin and Klhl31, were analysed by immuno-staining for both proteins in mouse tibialis anterior muscle. The preparation of mouse sections, as well as the immuno-staining was done in collaboration with Christina Stratford.

Nebulin localisation in myofibrils has been very well described for different types of muscles and species (Millevoi and others, 1998; Pappas and others, 2008; Wang and Wright, 1988; Witt and others, 2006). Klhl31 localisation however has not been analysed in adult muscle so far.

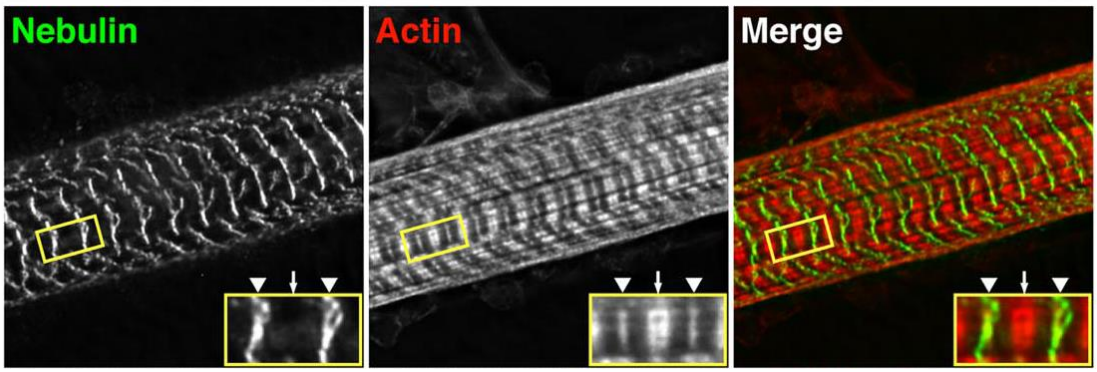

Figure 5.6: Nebulin in chick skeletal myotubes

Chick skeletal myotubes were stained with an antibody against Nebulin or were stained with Phalloidin to visualise Actin. Nebulin can be seen close to the Z-disc, where it co-localises to actin.

Figure taken from Pappas and others, 2008

Immuno-staining for Klhl31 in adult mouse muscle revealed its presence in mature muscles.

In transverse sections of mouse tibialis anterior, Klhl31 was shown to display a punctate localisation in muscle fibres (see figure 5.8, b and c).

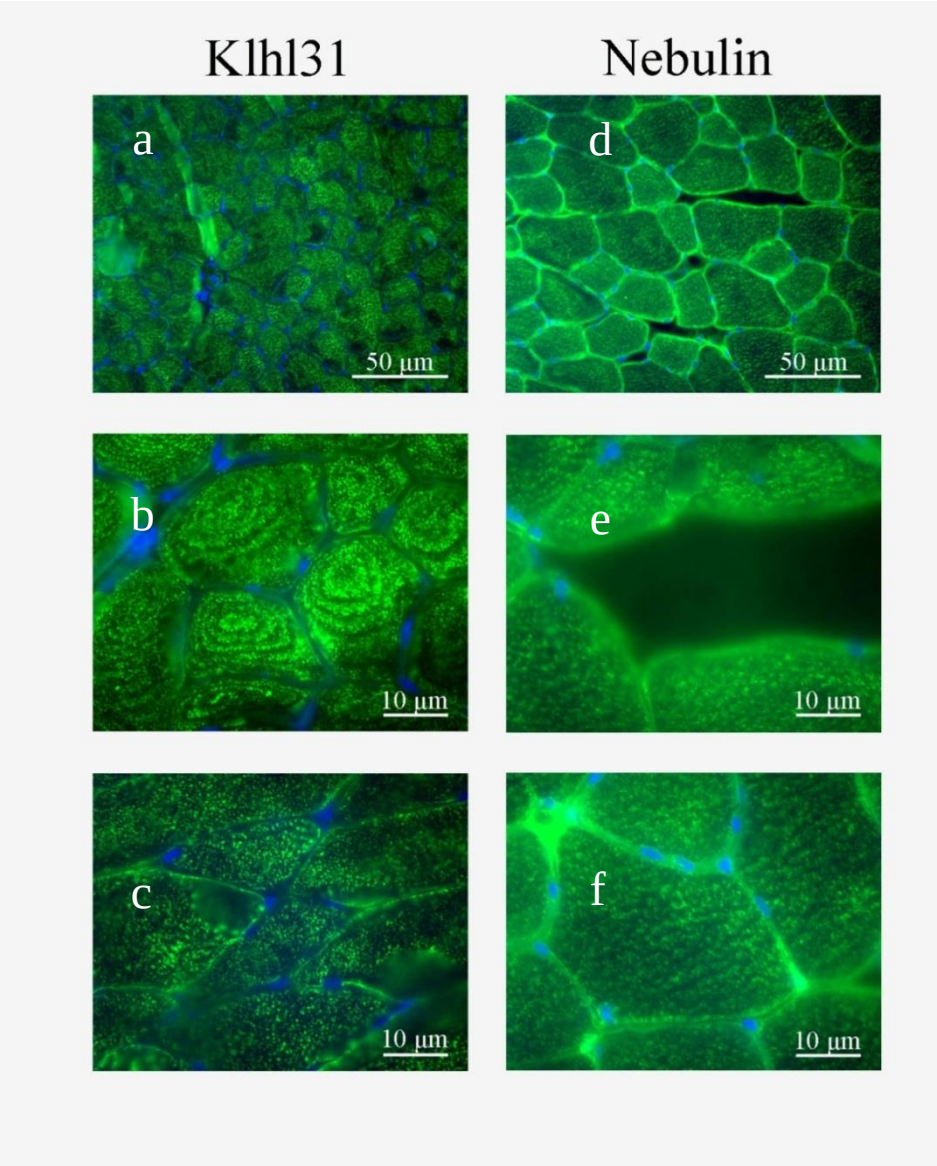

*

Figure 5.7: Expression of Nebulin and Klhl31 in mouse tibialis anterior

Immuno-staining for Klhl31 (a-c) and Nebulin (d-f) was carried out on transverse sections of wildtype mouse tibialis anterior. Images a and d were taken with a 20x objective, whilst images b-c and e-f were taken by using a 63x objective. Nuclei stained blue with Hoechst are visualized at the periphery of the muscle fibres.

Therefore we found that Klhl31 is not only expressed during development (Abou-Elhamd and others, 2009), but also in adult muscle tissues. Comparing Immuno-staining for Klhl31 with Phalloidin-staining of frozen muscle biopsies from either rectus abdominus or quadriceps (see figure 5.8; (Ilkovski and others, 2004), it could be shown that both localisation pattern for Klhl31 and Actin are very similar. Although we have not analysed Actin and Klhl31 co-localisation in adult muscle ourselves, the similar localisation of Klhl31 to Actin (as seen in mouse tibialis anterior (figure 5.6) and human rectus abdominus or quadriceps (figure 5.8)) together with the evidence for partial co-localisation of Klhl31 with actin fibres in C2C12 myotubes (chapter 3.3.2, figure 3.8) might indicate a possible interaction for both proteins in mature muscles. Each punctate expression signal of Klhl31 is potentially labelling a single myofibril, as up to 1000 myofibrils can make up a single muscle fibre (Martini, 2005). Sometimes Klhl31 expression seemed to look a bit circular or wave-like (as seen in figure 5.7, b). This might be due to shifting of the muscle tissue during the embedding process. Therefore the muscle might not have been sectioned in a transverse fashion, but slightly changed towards longitudinal section. This would mean that we would detect Klhl-31 localisation as a mixture of punctate staining (transverse section) and linear staining (longitudinal section).

Immuno-labelling for Nebulin in tibialis anterior (figure 5.7, d-f) showed a similar localisation of Nebulin when compared to the localisation of Klhl31 in the muscle fibres. Nebulin also displayed a punctate localisation, potentially labelling single myofibrils in a single muscle fibre. Unfortunately, the immuno-staining for Nebulin in transverse sections of human muscles as reported by (Ilkovski and others, 2004) (see figure 5.8) appears diffuse and can therefore not be used for a comparison with the Nebulin localisation in tibialis anterior (figure 5.7).

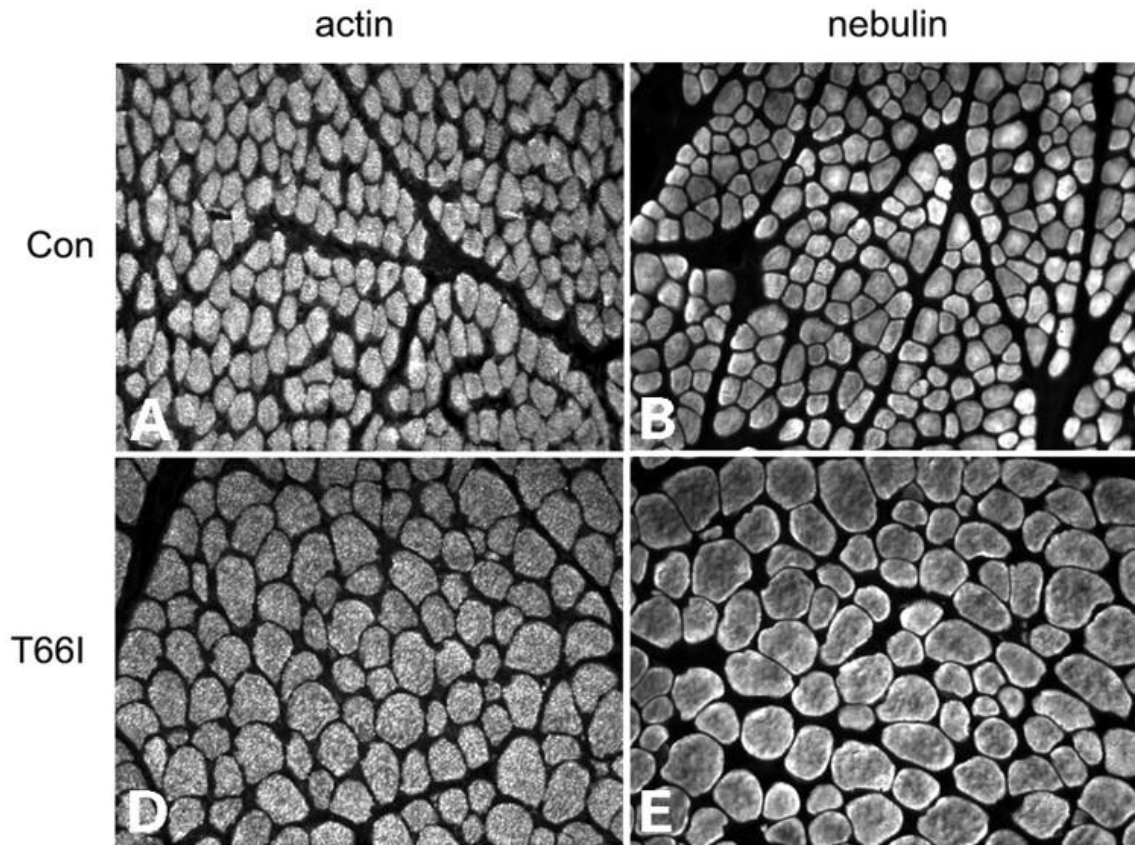

Figure 5.8: Expression of Nebulin and Actin in human muscle

Immuno-labelling for Actin (A and D) and Nebulin (B and E) of frozen biopsies from healthy human beings from either a quadriceps (A and B) or rectus abdominalis (D and E) revealed a punctate localisation for Actin in muscle fibres. The localisation for Nebulin appears diffuse, but was described as normal myofibril labelling.

Figure modified from Ilkovski and others, 2004

We could show that Klhl31 is expressed in mature muscle tissues in mice. But would Klhl31 co-localise with Nebulin in the muscle, too?

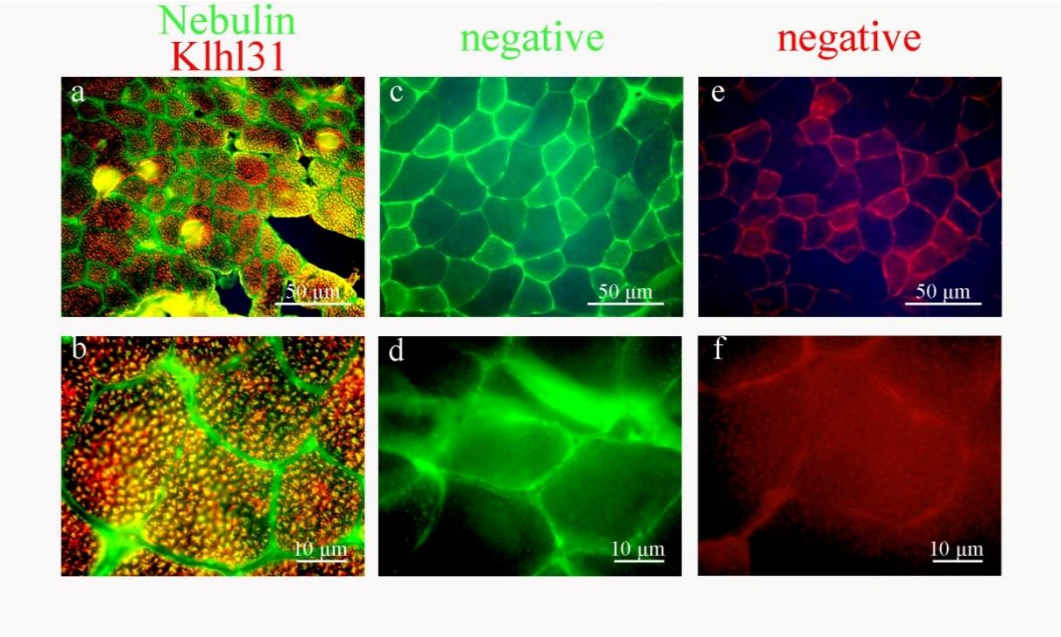

Figure 5.9: Nebulin and Klhl31 partially co-localise in mouse tibialis anterior

Double immuno-staining for Klhl31 and Nebulin was carried out on sections of wildtype mouse tibialis anterior as described previously. Images were taken with a 20x objective (a) or a 63x objective (b). Klhl31 was visualised by using an α-rabbit Alexa fluor 568 conjugated secondary antibody (red), whilst Nebulin was labelled with a α-mouse Alexa fluor 488 secondary antibody (green). Negative samples were prepared as described in section 2.2.26. Strong fluorescence in the skeletal muscle basement membrane is possibly due to accumulation of the secondary antibodies, as it was also observed in the negative controls.

Double immuno-histochemistry for Klhl31 and Nebulin on mouse tibialis anterior sections revealed that Klhl31 and Nebulin are closely localised at or along myofibrils in muscle fibres (see figure 5.9; b, yellowish coloured spots).

The NB2 antibody we used to detect Nebulin was characterised in 1988 by Furst et al. The antibody recognises an epitope in the Nebulin protein, which localises to the N2 lines in the sarcomere, a region which is not part of the alternative splicing sites of the Nebulin gene (Furst and others, 1988). Therefore we assumed we would be able to detect all present Nebulin isoforms in the muscle section.

However, we observed staining exclusively for either Nebulin or Klhl31 as single green or single red puncta. Muscles have been shown to express different isoforms of Nebulin (Donner and others, 2004; Joo and others, 2004; Kazmierski and others, 2003). For human tibialis anterior alone over 20 different transcripts have been predicted due to alternative splicing (Donner and others, 2004). We can therefore assume that mouse anterior tibialis also expresses different isoforms of Nebulin. As Klhl31 seems to be binding to an amino acid motif between super repeat 20 and super repeat 21 found in exon 128 (mouse) or exon 144 (human) in genomic DNA, we have to consider the presence of Nebulin isoforms lacking exon 128 in mouse tibialis anterior muscle. This could explain why we could see Nebulin staining on myofibrils, which do not localise with Klhl31.

Based on observed co-localisation of Klhl31 to Nebulin in myofibrils, we suggested that Klhl31 might co-localise with Nebulin in adult musculature.

5.3.5 Nebulin is expressed in differentiating C2C12 myoblasts

Nebulin has various important functions in adult muscle tissues and during myofibrillogenesis (as described in the chapter 5.3.1 and 5.3.2).

We have shown that Klhl31 localises close to Nebulin in adult muscles. Next we wanted to study potential interaction of Klhl31 and Nebulin in developing muscles.

To analyze a potential association of Klhl31 with Nebulin during C2C12 differentiation in more detail, we firstly wanted to identify the presence of Nebulin during C2C12 myotube formation. We collected total protein lysates during a 5 day time course of differentiation of mouse myoblasts as described in chapter 3.1.3. By using a 10% PAA gel, we could detect a band using a Nebulin antibody, but only on one day during the 5 days of differentiation, between day one and day two (figure 5.10).

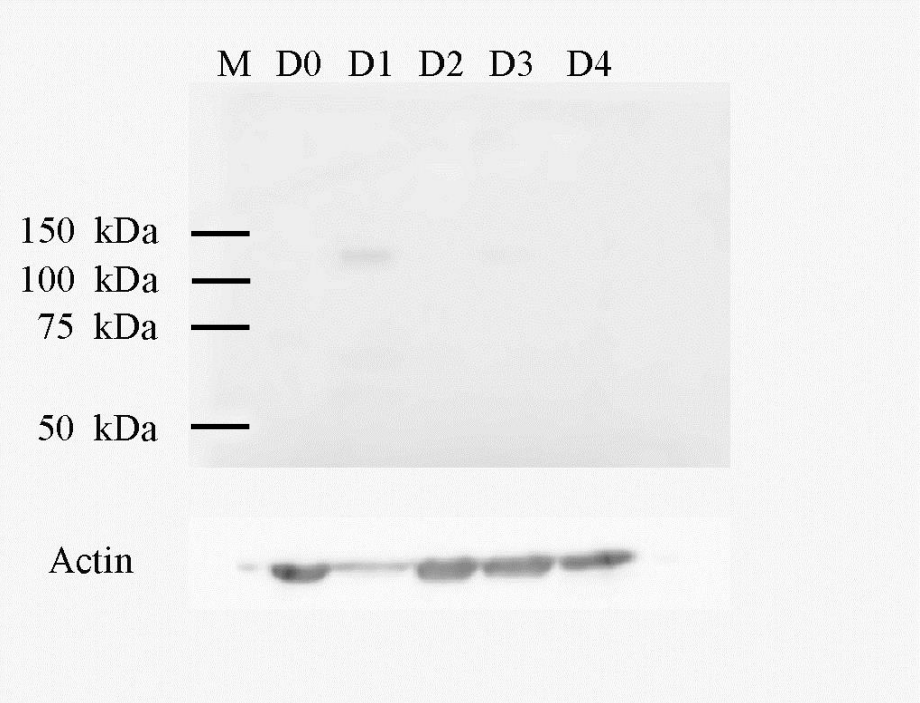

Figure 5.10: Nebulin is expressed on the onset of C2C12 differentiation

The expression of Nebulin during C2C12 differentiation was analysed by western blotting using a mouse monoclonal antibody against Nebulin. A band was detected of approximately 130kDa was detected at day 1 of C2C12 differentiation. An Actin antibody was used to detect the total Actin levels as a loading control.

Legend: M - marker, D0- Day 0, D1 – Day1, D2 – Day2, D3 – Day3, D4 – Day4

The protein band, which was detected with the NB2 Nebulin antibody, was only observed at the beginning of elongation of myocytes around day one during the differentiation time course of C2C12 cells. Comparing the expression of a potential Nebulin-protein with Klhl31 expression it was observed that the detected 130kDa protein seemed to be expressed before the expression of Klhl31 is upregulated (around day 2, see chapter 3.1.3). The published larger Nebulin protein bands (~700 kDa as described in the review by (McElhinny and others, 2003) could not be detected as the acrylamide percentage of the gel used for SDS-PAGE was not high enough to permit separation of large proteins.

As we have seen that a protein detectable with a Nebulin antibody is expressed in C2C12 during differentiation we wanted to analyse its localisation during C2C12 myotube formation.

5.3.6 Nebulin localises to Actin fibres in differentiating myocytes

A potential Nebulin-protein was shown to be expressed at the onset of myofibrillogenesis in differentiating C2C12 myocytes, slightly before Klhl31 expression was elevated (as described in the previous chapter). We wanted to know if Klhl31 could co-localise with the Nebulin-protein just as we had seen in adult muscle tissue (chapter 5.3.3). But before investigating Klhl31 and potential Nebulin localisation in C2C12 cells we wanted to compare Nebulin localisation to a well described part of myofibrils, the Actin cytoskeleton.

In adult muscle Nebulin has been described to align to the whole thin filament by binding Actin-monomers via its central modules (Jin and Wang, 1991b; Labeit and others, 1991; Labeit and Kolmerer, 1995a) and cell culture experiments led to the suggestion that Nebulin assists Actin monomers during the organisation of the thin filaments during myofibrillogenesis (Moncman and Wang, 1996; Nwe and others, 1999; Shimada and others, 1996)

Using a double immuno-staining approach we could show that Nebulin aligns to Actin fibres exclusively in differentiating C2C12 myocytes (see figure 5.11).

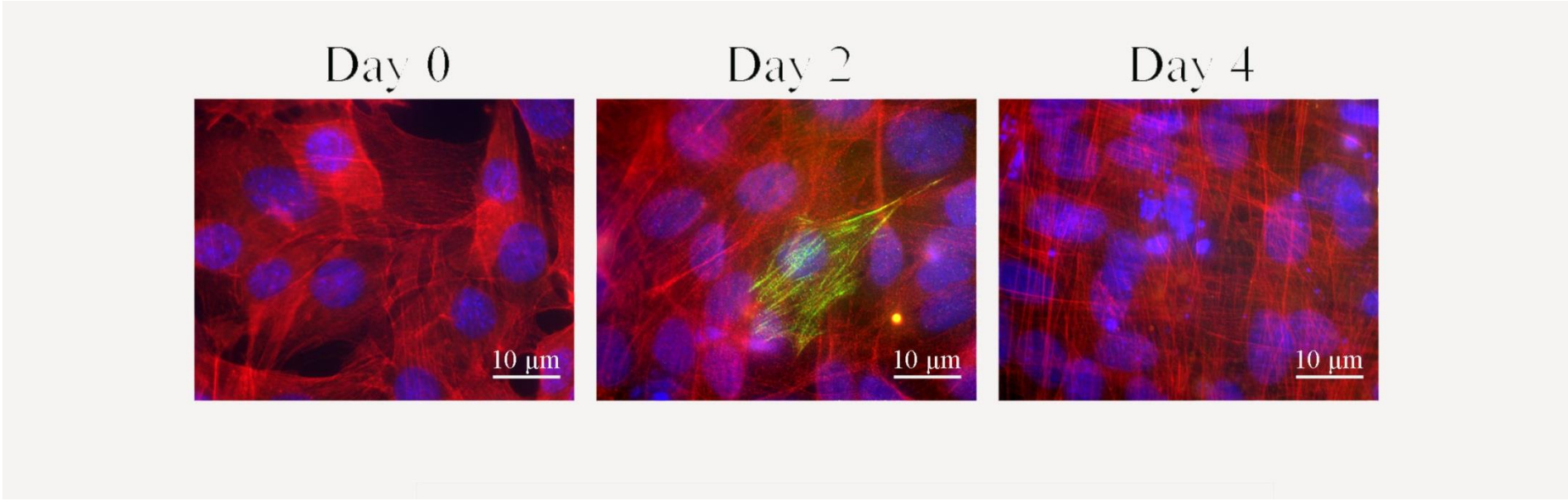

Figure 5.11: Nebulin localises to Actin fibres during the differentiation of C2C12 myocytes

Figure 5.11: Nebulin localises to Actin fibres during the differentiation of C2C12 myocytes

C2C12 myocytes (Day 0), early differentiating myocytes (Day 2) and late differentiating myocytes (Day 4) were labelled for Nebulin (green, Alexa-Fluor 488 secondary antibody) and Actin (red, Texas-red phalloidin).

We observed that Nebulin again was only present in early differentiating C2C12 myocytes, where it displayed a fibrillar localisation pattern, closely associated to Actin fibres (figure 5.11, day 2). Nebulin was not detected in undifferentiated or late differentiating C2C12.

As described previously for chick skeletal myocytes (Moncman and Wang, 1996; Nwe and others, 1999; Shimada and others, 1996), Nebulin was also shown to localise to Actin fibres in differentiating mouse myocytes.

Comparing our localisation data to previously described western blotting data for a protein detectable with a Nebulin antibody, Nebulin again was only detected between day 1 and day 2 of incubation of C2C12 cells in differentiation medium (DM).

Based on this narrow time frame of expression, we therefore decided to look in more detail at Nebulin expression during differentiation of C2C12.

As not all C2C12 cells did respond to DM at the same time and therefore differentiated differently we wanted to characterise the time frame of Nebulin expression in differentiating C2C12 more closely. Culturing and starving mouse myoblasts as described before (in chapter 5.3.5), we detected expression of a potential Nebulin-protein during a 24 hour time frame between day 1.5 and day 2.5 of C2C12 differentiation (see figure 5.12).

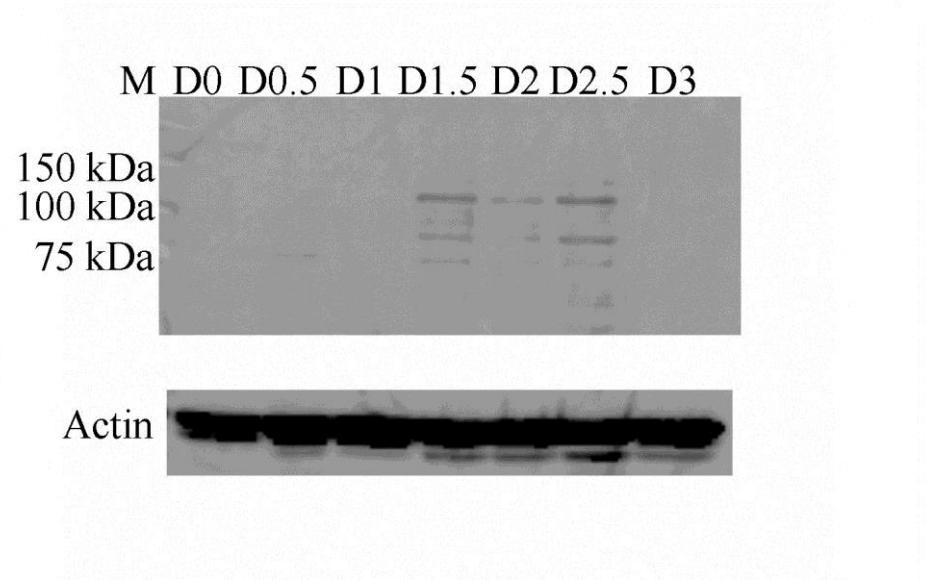

Figure 5.12: Nebulin is expressed between day 1.5 and day 2.5 of differentiation of C2C12

The expression of a potential Nebulin-protein during C2C12 differentiation was analysed by western blotting using a mouse monoclonal antibody against Nebulin. A protein band was detected between day 1.5 and day 2.5 of the differentiation time course. The strongest band displayed a proximal size of 130 kDa, whilst other lower bands were also detected. Actin levels were to compare loaded protein samples.

Legend: M - marker, D0- Day 0, D0.5- Day 0.5, D1 – Day1, D1.5 – Day1.5, D2 – Day2, D2.5 – Day 2.5 and D3 – Day 3

Analysing samples taken every 12 hours during C2C12 myotube formation revealed that a protein detectable with a Nebulin antibody was expressed between day 1.5 and day 2.5 during a time course of C2C12 differentiation (see figure 5.12). Observed protein expression was therefore consistent with previous described data from western blotting and immuno-histochemistry (as reported in chapters 5.3.5 and 5.3.6) revealing a timeframe of potential Nebulin expression of 24 hours at during early C2C12 differentiation. Furthermore, the protein detected was again to small in its size (compared with the published size of Nebulin of around 700 kDa; (McElhinny and others, 2003), raising the question whether the detected protein might be unspecific or whether it could be a degradation product of Nebulin. Again, we were not able to detect full-length Nebulin as the PAA Gel used in the experiments did not have the needed acrylamide concentration to allow protein separation for Nebulin.

Next we wanted to compare localisation of Klhl31 to localisation of Nebulin during C2C12 differentiation, as Nebulin was identified as an interaction partner for Klhl31 in the Yeast-2-Hybrid screen (see chapter 5.1). Also we had already shown that Klhl31 co-localised to Actin in adult musculature (see figure 5.9).

Therefore, we decided again to use a double-immuno staining approach to compare the expression and localisation of Klhl31 with Nebulin during myotube formation.

5.3.7 Nebulin and Klhl31 are both expressed in the differentiating myoblasts

C2C12 mouse myoblasts were cultured on coverslips, differentiated as described previously and stained for Klhl31 and Nebulin, Nebulin and Actin or Actin and Klhl31. We decided to immuno-label C2C12 cells during a 5 day time course of differentiation, with samples taken every 12 hours between day one and day three based on our previous expression data obtained for a potential Nebulin protein.

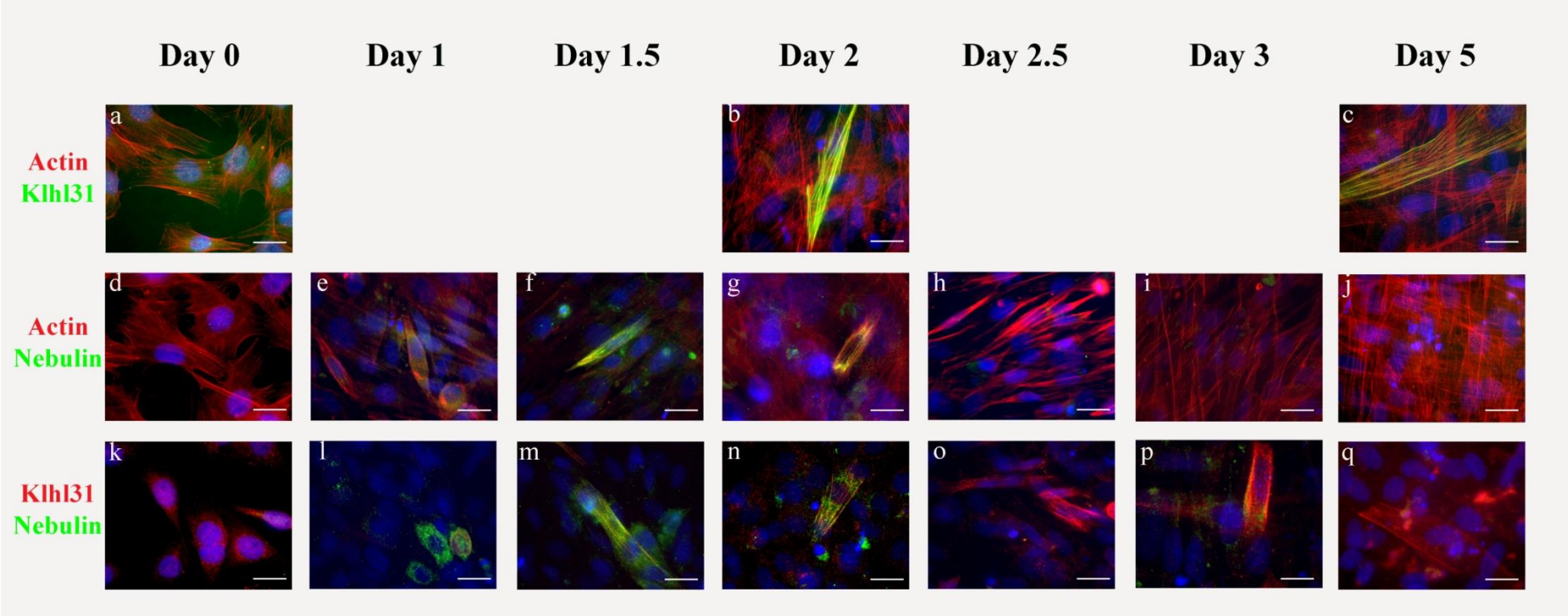

Figure 5.13: Nebulin and Klhl31 are expressed in the same differentiating myoblasts

Figure 5.13: Nebulin and Klhl31 are expressed in the same differentiating myoblasts

(a,b,c) Double immuno-staining for Klhl31 (green, Alexa-Fluor 488) and Actin (red, Texas-red Phalloidin) during a 5-day time course of C2C12 differentiation

(d-j) Double immuno-staining for Nebulin (green, Alexa-Fluor 488) and Actin (red, Texas-red Phalloidin) during a 5-day time course of C2C12 differentiation

(k-q) Double immuno-staining for Nebulin (green, Alexa-Fluor 488) and Klhl31 (red, Alexa-Fluor 568) during a 5-day time course of C2C12 differentiation

Nuclear DNA was stained with DAPI

Images were taken with a 63x objective. Legend: scale bar – 10 µm

We could observe upregulation of Klhl31 expression during C2C12 differentiation, as well as co-localisation of Klhl31 to Actin fibres in early differentiating and late differentiating C2C12, which is consistent with the expression profile for Klhl31 as described in previously (figure 3.8 and figure 5.13; a-c).

The double Immuno-staining approach further revealed a potential Nebulin expression firstly detected around day 1 (figure 5.13; e and l, similar to previous obtained data for Nebulin expression, see figure 5.12) displaying a diffused and punctate localisation in the cytosol. Nebulin exhibited the diffused localisation until approximately day 2 when it aligned to Actin fibres still displaying puncta (figure 5.13; g). A potential Nebulin expression was not detected after day 3 of C2C12 differentiation (figure 5.13; h,i,j and q). Furthermore, potential Nebulin expression was mostly observed in cells with elevated protein levels of Klhl31 (figure 5.13; l,m,n and p), although occasional Nebulin positive cells were observed during early differentiation (figure 5.13; l). Klhl31 protein levels stayed elevated whilst detected Nebulin protein levels decreased (figure 5.13; q) consistent with previously described data for potential Nebulin expression and Klhl31 expression (figure 5.12 and 3.4, respectively). During later stages of differentiation Nebulin seemed to be localised at the edges of elongated pre-fusion myoblasts close to enriched Klhl31 levels (figure 5.13; p)

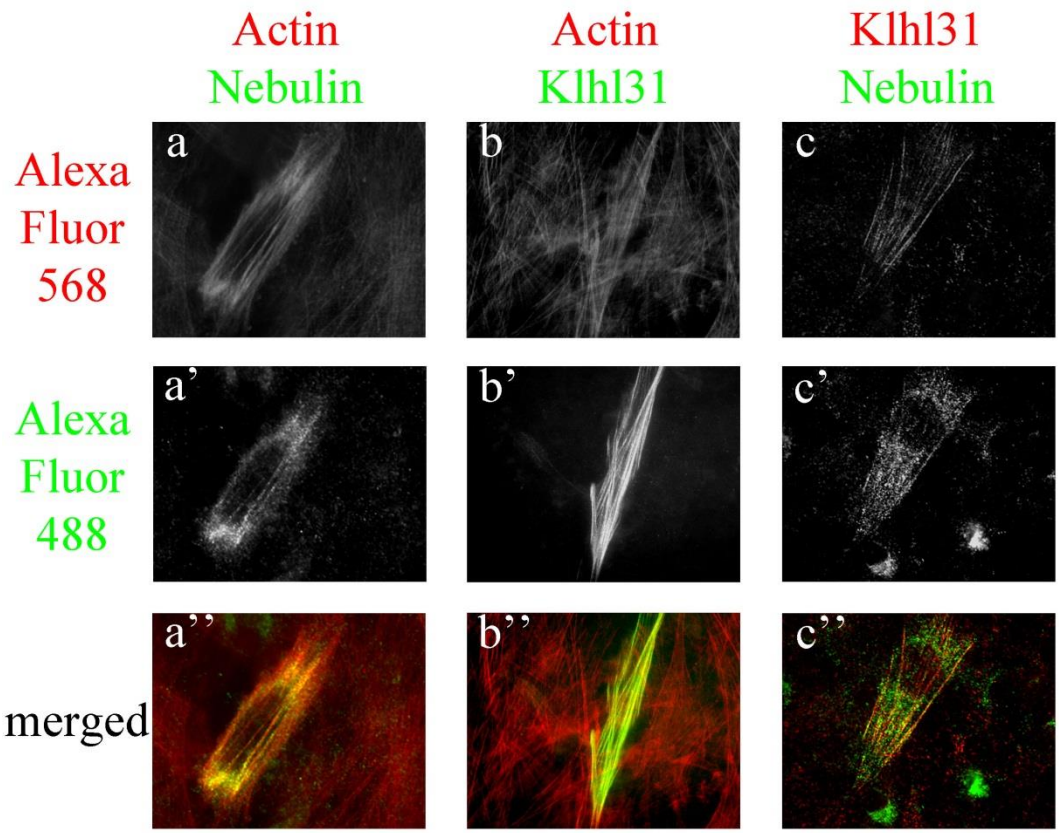

Figure 5.14: Nebulin aligns to actin fibres in elongated myoblasts

Higher magnification image of C2C12 cells during early differentiation.

Images are as shown in figure 5.13, but were further magnified using image processing software.

Further magnifying images obtained from the double immuno-staining approach (figure 5.13, g,b and n) were used to analyse a potential co-localisation of Klhl31 to Nebulin. Nebulin was observed to align to Actin fibres in pre-fusion mouse myoblasts (figure 5.14; a'') in a punctate fashion, where it also seemed to be accumulated at the edges of the cell. As previously described, Klhl31 aligned along the whole length of Actin fibres in differentiating C2C12 cells (figure 5.14; b''). Higher magnified images also revealed a partial localisation of a possible Nebulin-protein with Klhl31 (figure 5.14; c'')

As reported previously by other groups (Moncman and Wang, 1996; Shimada and others, 1996), we also observed that Nebulin displayed a diffused localisation in the cytosol before eventually aligning into a fibrillar structure closely associated to the actin fibres (figure 5.13; e-g, figure 5.14; a'). However, co-localisation of Nebulin with Klhl31 was not as clear, which is partially due to a rapidly fading Alexa Fluor 568 secondary antibody, which made it difficult to visualise Klhl31. When Nebulin

expression was observed first, it seemed to be expressed prior to enhanced Klhl31 expression (figure 5.13; l) displaying a diffused localisation in the cytosol of C2C12 myoblasts. After day 1.5 of the differentiation time course all Nebulin positive cells also showed elevated Klhl31 staining (figure 5.13; m, n, p and figure 5.14; c). Once myoblasts became elongated Nebulin partially co-localised or aligned close to fibrillar Klhl31 structures (figure 5.13; m, figure 5.14; c). We could see Nebulin puncta, which did not localise to Klhl31 fibrillar structures (figure 5.14; c''). This might be due to either the fading signal of the Alexa-Fluor 568 antibody or due to the loss of weaker Alexa-fluor 568 signal during image processing (e.g. subtracting the background obtained with Alexa-Fluor 568 secondary antibody in absence of a primary antibody, as described in materials and methods, section 2.2.26). Very rarely we observed Nebulin staining after day 2.5 of C2C12 differentiation. However, later during C2C12 differentiation (day 2+), we observed that Nebulin expression was although diffused confined to the edges of the elongated cell close to strong levels of Klhl31 (figure 5.13; p).

During later stages of C2C12 differentiation, when C2C12 cells started to fuse into myotubes, Nebulin was not detected anymore.

Although there seemed to be a close proximity between Klhl31 and Nebulin, we have so far not verified a potential direct interaction between the two proteins. We therefore decided to use a GST-pull down approach to investigate if Klhl31 can bind to Nebulin.

5.3.8 Klhl31 can bind to Actin and form homodimers

When we decided which approach to use to investigate interaction partners for Klhl31 we had the issue that it had been difficult to create fusion-proteins for Klhl31, as the added protein tags seemed to impair function of the fusion-protein (chapter 4.1.2). Furthermore we found that overexpressed Klhl31 fusion-proteins seemed to be degraded in mammalian cells (see chapter 4.3.2).

The GST approach would enable us to overexpress a GST-Klhl31 protein in a bacterial environment using low expression temperatures, which would make it possible to generate stable Klhl31 fusion proteins by preventing degradation.

We created an N-terminal GST-Klhl31 protein by cloning human Klhl31 (image clone 9021264) into a pGEX-5X-I vector. The gene expression was induced by IPTG. Using different induction temperatures revealed that we could produce stable GST-Klhl31 proteins in sufficient amounts at low temperatures (see figure 5.15). We observed the best results when inducing GST-Klhl31 expression at 21 °C for 3 hours.

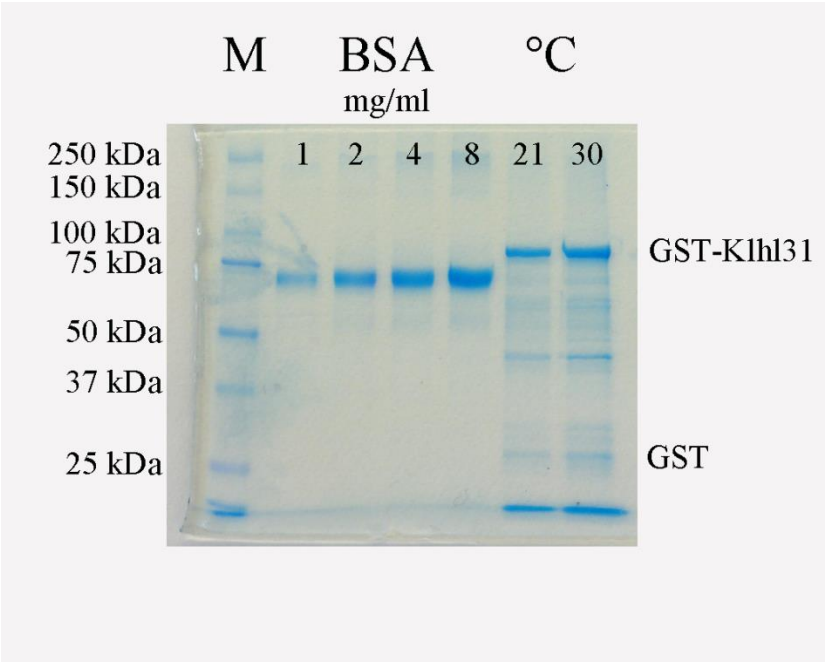

Figure 5.15: Stable overexpression of GST-Klhl31fusion protein

Samples of GST-Klhl31 expressing bacteria lysates were run on a 10% PAA Gel and stained with Coomassie brilliant blue. Approximate protein concentration for GST-Klhl31 was estimated by comparison to a BSA protein standard. Stable GST-Klhl31 was successfully expressed in E.coli at lower temperatures which prevented degradation of the fusion protein.

Legend: M – marker

Once we had purified the GST-Klhl31 proteins (as described in chapter 2.2.36), we used them to carry out pull-down experiments using C2C12 lysates from different time points of differentiation (see chapter 2.2.36). GST only served as control for these experiments.

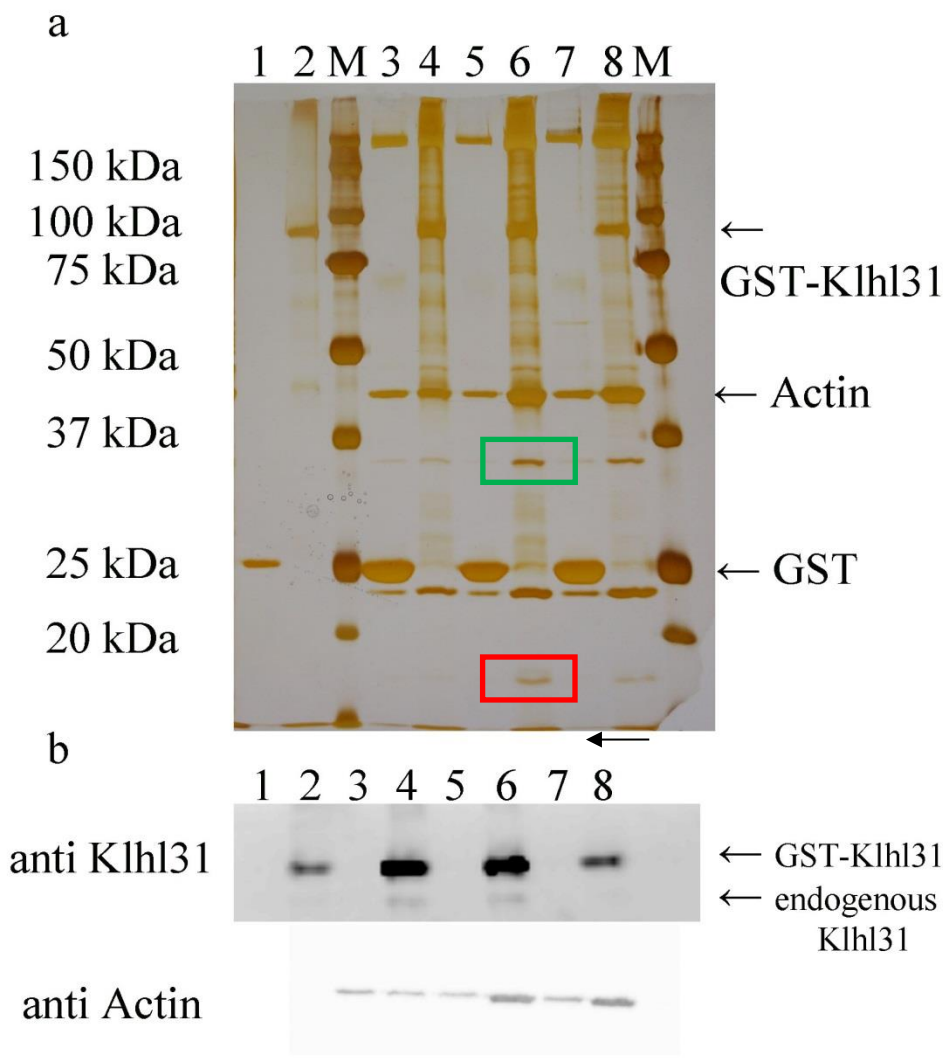

Figure 5.16: Finding interaction partner for Klhl31 using a GST-pull down approach

(a) Silver staining of a 10 % PAA gel. Pull downs with GST Beads (1,3,5,7) and GST-Klhl31 (2,4,6,8) incubated with either PBS (1,2) or in C2C12 lysates (3-8) are shown. A band potentially containing endogenous Klhl31 (←, lane 4 and 6) was pulled out by GST-Klhl31 from C2C12 lysates of early differentiation time points. Actin however seemed enriched in samples obtained during late differentiation (lane 6 and 8). Bands surrounded by coloured rectangles were analysed by mass spectrometry.

(b) Western blot against Klhl31 (upper blot) or Actin (lower blot) further identify some of the bands seen in the silver staining. Endogenous Klhl31 was pulled out of lysates from myoblasts or differentiating C2C12 cells (lanes 4 and 6), whilst Actin was shown to be enriched in samples obtained from differentiated C2C12 myotubes (lane 6 and 8)

Legend: M – marker, 1 - GST in PBS (negative control for GST only), 2 - GST-Klhl31 in PBS (negative control for GST-Klhl31), 3 - GST in C2C12 lysate (Day 0), 4 - GST-Klhl31 in C2C12 lysate (Day 0), 5 - GST in C2C12 lysate (Day 2), 6 - GST-Klhl31 in C2C12 lysate (Day 2), 7 - GST in C2C12 lysate (Day 4), 8 - GST-Klhl31 in C2C12 lysate (Day 4).

After running the samples acquired from the GST-pull downs on a PAA gel and subsequently staining with silver stain as a more sensitive staining compared to Coomassie, we could see that we were able to extract bands from C2C12 lysates when using the GST-Klhl31 fusion protein (see figure 5.16, a; lanes 4,6 and 8). More interestingly for us was that the pulled out protein bands showed variations between day 0, day 2 and day 4 of myoblast differentiation, suggesting that Klhl31 interacts with different proteins at the onset of differentiation compared to later stages of C2C12 differentiation (figure 5.16, a).

Furthermore we saw an enrichment of a protein displaying the size of endogenous Klhl31 pulled down by GST-Klhl31 (figure 5.16, a; ←), but only during the early stages of C2C12 differentiation (between day 0 and day 2). The binding of GST-Klhl31 to endogenous Klhl31 was verified by western blot (figure 5.16, b; ←). In summary, we could show that endogenous Klhl31 seems to be an interaction partner for GST-Klhl31 during early differentiation. It has been reported that proteins of the Kelch-like family can form homodimers (Geyer and others, 2003; Stogios and others, 2005). Our pull-down assays suggest that Klhl31 is also able to form homodimers during early differentiation of C2C12, before Klhl31 aligns completely to Actin fibres (see chapter 3.3.2).

Using the GST-pull down we also observed that Actin was enriched with GST-Klhl31, indicating that it may interact with Actin directly (figure 5.16, a and b; lane 6 and 8). However, as Actin was also enriched in the GST only samples, although weaker when compared to GST-Klhl31, this result needs to be interpreted with caution. Interaction with the Actin cytoskeleton has previously been reported for various members of the Kelch-like protein family as well (Adams and others, 2000; Kelso and others, 2002; Robinson and Cooley, 1997; Xue and Cooley, 1993). GST-Klhl31 pull-down did not lead to enrichment of Actin in undifferentiated C2C12 (figure 5.16, and b; lane 4) in agreement with our localisation studies (chapter 3.3.2). Only once C2C12 had passed the intermediate state of differentiation as defined by (Burattini and others, 2004), Klhl31 localised to Actin filaments. As we only pulled-down Actin bands from C2C12

lysates of day 2 or day 4 (resembling later stages of C2C12 differentiation), we can assume that localisation of Klhl31 to Actin also involves a direct interaction between Klhl31 and Actin.

5.3.9 Mass spectrometry analysis of excised bands

Next, we tried to identify additional proteins of interest pulled down using GST-Klhl31. Some of the clearer protein bands were excised from silver stained gels obtained from GST-pull down assays and the samples indicated by green and red rectangles in figure 5.16 were analysed by mass spectrometry at the FingerPrints Proteomics facility (University of Dundee). Hits were identified by using the Mascot database.

Interestingly, the verified hits indicate that Klhl31 can bind to various other proteins of the contractile muscle apparatus. The excised bands contained proteins, which were not pulled down from undifferentiated C2C12 lysates (Day 0). The bands were only observed during C2C12 differentiation (Day 2) and in late differentiating C2C12 myocytes (Day 4).

Table 5.1: Proteins identified in the excised protein bands from the GST-pull down

The table shows the top 5 hits identified by mass spectrometry from the <17 kDa excised protein band (red rectangular) and the ~35 kDa excised protein band (green rectangular) as seen in figure 5.16.

	Protein	size (kDa)			Protein	size (kDa)
~ band size		15-17		~ band size		~ 35
	myosin regulatory light chain, B-like	~20			Isoform 1 of Tropomyosin alpha-1 chain	32
	Myl12b	~20			Isoform 2 of Tropomyosin alpha-1 chain	32
	Myl9	~20			F-actin-capping protein subunit alpha-2 (Capza2)	~32
	Calmodulin	17			Annexin	36
	Actin-related protein 2/3 complex subunit 3 (Arpc3)	21			F-actin-capping protein subunit alpha-1 (Capza1)	~32

First, an excised protein band displaying a size of approximately 15-17 kDa was analysed (figure 5.16; a - red box). Calmodulin (17kDa) and myosin regulatory light chain isoforms (around 20 kDa large, e.g. myosin regulatory light chain (homo sapiens), myosin regulatory light chain B-like, Myl12b, Myl9 (all mus musculus). Myosin regulatory light chains are involved in mediating muscle contraction in adult muscle and in myofibrillogenesis in developing muscle fibres (Du and others, 2003; Gordon and others, 2000; Kamm and Stull, 2011). Also a subunit of the Actin-related protein 2/3 complex was identified. The Arp2/3 complex mediates the nucleation of Actin, the first step during de-novo Actin polymerisation by assisting the formation of Actin dimers or trimers (Soderling, 2009). The Arp2/3 complex consists of 7 subunits, two of which, Arp2 and Arp3 (identified in the GST-pull down), can mimic Actin dimers when aligning to already existing Actin fibres (Pollard, 2007). Addition of further Actin monomers by the Arp2/3 complex has been described to stimulate Actin polymerisation (Robinson and others, 2001; Volkmann and others, 2001). Also interesting, the Arp2/3 complex is activated by members of the Wiskott-Aldrich syndrome protein (WASP) family (Panchal and others, 2003). Furthermore, in striated muscle the Arp2/3 complex is also involved in Actin polymerization along the edges of the myoblast prior to fusion (Blanchoin and others, 2001; Richardson and others, 2007).

Identified proteins from a ~35 kDa band (figure 5.16, a – green box) revealed the presence of tropomyosin α-chain (32 kDa). Tropomyosin α and tropomyosin β are mainly expressed in skeletal and cardiac muscle, where they form dimers and associate to the actin filament (Bailey, 1948; Kalyva and others, 2012; Perry, 2001). The formed tropomyosin dimer in association with troponin has been shown to mediate muscle contraction (for an overview of muscle contraction and function of tropomyosin see chapter 1.9 or (Farah and Reinach, 1995; Gordon and others, 2000). Furthermore it had been reported that tropomyosin can interact with tropomodulin in regulating actin filament lengths by capping the slow growing end of Actin fibres (Casella and others, 1986; Gregorio and others, 1995; Kostyukova, 2008; Weber and others, 1994). Also by mass spectrometry analysis of the ~35 kDa protein band, CapZ had been identified to be pulled out of C2C12 lysates by Klhl31. CapZ is also a capping protein for the Actin filament, however it caps the fast-growing or barbed ends of Actin fibres (Caldwell and others, 1989).

Annexin was also identified by mass spectrometry. Annexins are involved in various cellular processes, such as membrane organisation, membrane traffic and the regulation of the activity of ion channels (Gerke and Moss, 2002). Furthermore, some Annexins have been described to be Actin-binding proteins and were thought to be involved in regulating changes to the membrane-associated cytoskeleton (Alvarez-Martinez and others, 1997; Gerke and Moss, 2002). Recently, a role for Annexin in skeletal muscle differentiation and membrane repair has been described (Bizzarro and others, 2010a; Bizzarro and others, 2010b). It was shown that Annexin 1 enhanced myoblast cell proliferation by promoting satellite cell migration (Bizzarro and others, 2010b).

We also identified NEDD8-conjugating enzyme Ubc12 (21 kDa), an E2 ubiquitin-conjugating enzyme as a potential interaction partner for Klhl31 in the GST-pull down.

Further experiments are needed in order to determine whether Nebulin is a direct interaction partner for Klhl31 in the GST pull down assays.

6. Klhl31 expression during heart development

6.1 Introduction to early cardiogenesis

6.1.1 Formation of the primary heart tube

The heart is the first organ to form during the development of vertebrates. It is important as its contractions transport nutrients and oxygen throughout the embryo. Cardiac progenitor cells are derived from the mesoderm (Garcia-Martinez and Schoenwolf, 1992; Kinder and others, 1999) and emerge from the anterior part of the primitive streak during gastrulation (Garcia-Martinez and Schoenwolf, 1993). These cells eventually give rise to all layers of the heart tube: the endocardium, myocardium and the parietal pericardium (Garcia-Martinez and Schoenwolf, 1993; Schoenwolf and others, 1992).
Recent studies showed that the prospective heart cells ingress through the primitive streak to form a bilateral heart field on the left and the right side of the axial midline (Garcia-Martinez and Schoenwolf, 1993; Rawles, 1943; Rosenquist, 1970). This cell population was termed the lateral plate mesoderm, also known as the bilateral cardiogenic mesoderm (Garcia-Martinez and Schoenwolf, 1993; Munsterberg and Yue, 2008; Yang and others, 2002). The lateral plate mesoderm will eventually split into two layers, the splanchnic and the somatic mesoderm (Linask, 1992; Linask and others, 1997). Myocardial progenitor cells originate exclusively from the splanchnic mesoderm and form the cardiogenic mesoderm in the bilateral heart fields (Linask and others, 1997).

Cells residing in the bilateral heart field eventually move medially to the ventral midline of the embryo, where they fuse to form the primitive heart tube (Moorman and others, 2003; Stalsberg and DeHaan, 1969). The group of cells that contribute to the primary heart tube are called the primary heart field (Abu-Issa and others, 2004; De La Cruz and others, 1989).

6.1.2 Cells from the secondary heart field contribute to the outflow tract

After the primary heart tube in chick has formed at HH stage 9 and the heart continues to grow, it was reported that further heart progenitor cells from the splanchnic mesoderm are recruited to the anterior pole of the primary heart (de la Cruz and others, 1977). This population of cells was named the secondary source of myocardium or secondary heart field and was shown to add to the outflow tract myocardium, as well as the right ventricle and both, the right and left atrium (Abu-Issa and others, 2004; Kelly, 2012; Waldo and others, 2001) (for a scheme of the location of cells of the secondary heart field in the heart see figure 6.1).

It was further reported that cells contributing to the outflow tract have also been derived from the pharyngeal mesenchyme or prepharyngeal mesoderm (Kelly and others, 2001; Mjaatvedt and others, 2001; Waldo and others, 2001).

Further data revealed that cardiac neural crest cells also contributed to the outflow tract (Kirby and others, 1983). These cells migrate through the pharyngeal mesoderm before addition to the outflow tract (for a review see (Keyte and Hutson, 2012).

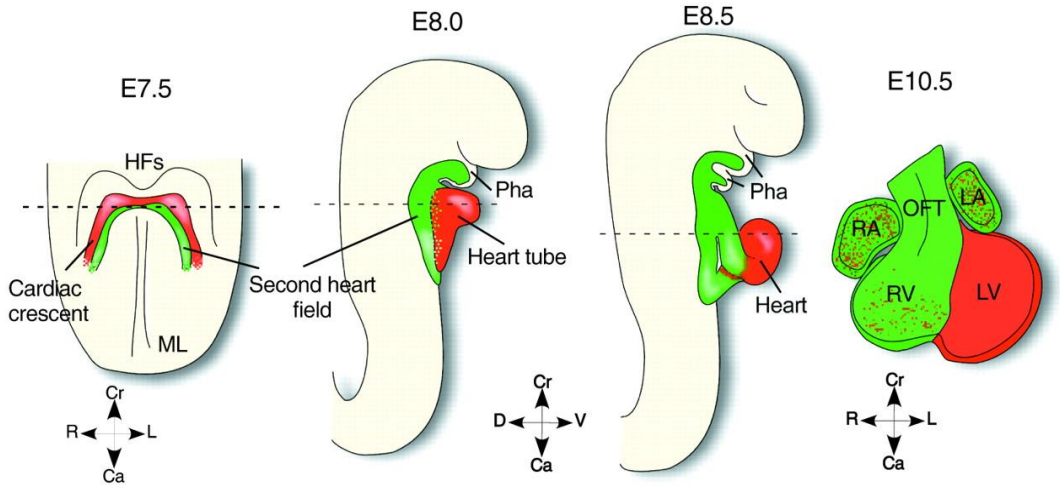

Figure 6.1: The secondary heart field during heart development

The scheme shows the localisation of cells from the secondary heart field in the mature chick heart as described by (Kelly, 2012) . The secondary heart field is labelled in green and cells of the primary heart field are labelled in red. At the cardiac crescent stage cells from the primary and secondary heart field reside in close proximity. At E8.0 cells from the secondary heart field reside close to the pharyngeal Arches (Pha) next to the primitive heart tube. In the mature heart (E10.5) cells of the secondary heart field

can be found in the outflow tract (OFT), the right ventricle (RV), as well as the left and right atrium (LA, RA). Figure modified from Laugwitz and others, 2008 .

Recently it was shown that both the primary and the secondary heart field are part of a single heart cell population, which migrate towards the midline in two distinct waves (Camp and others, 2012; Meilhac and others, 2003).

After the formation of the primary heart and addition of cells from the secondary heart field to the tube, the heart undergoes further growth and development to eventually form a contracting four-chambered heart (Anderson and others, 2003; Wagner and Siddiqui, 2007).

6.1.3 Signalling pathways involved in early cardiogenesis

Heart development is an important and highly complex process during vertebrate development. Many well known signal pathways have significant roles during early cardiac development. Ablation of the anterior endoderm has been shown to lead to incomplete specification of the myocardium in *Xenopus* (Nascone and Mercola, 1995). A role in inducing cardiogenesis has also been described for the endoderm in chick embryogenesis (Alsan and Schultheiss, 2002), revealing that a member of the fibroblast growth factor (FGF) family *FGF8* secreted from the endoderm is important for inducing and maintaining the cardiogenic fate. Also secreted from the anterior endoderm is the *bone morphogenetic protein (BMP)-2*, which was shown to be able to induce heart formation (Andree and others, 1998). A similar role has been described for *BMP-4*, *BMP-5* and *BMP-7* (Schultheiss and others, 1997; Solloway and Robertson, 1999). *Noggin* was identified as an inhibitor to BMPs in cardiogenesis, thereby preventing myocardial differentiation (Schlange and others, 2000). *BMP-2* and *FGF-10* as well as *Sonic Hedgehog (Shh)* have not only been described to be involved in the activation of cardiogenic mesoderm, but have also significant roles in the induction of the secondary heart field (Kelly and others, 2001; Waldo and others, 2001). A further important signal pathway in cardiac development is the pathway of the wingless-int (Wnt) family, which has been said to be the earliest signalling affecting the cardiac induction (Dyer and Kirby, 2009).

Studies in the primary heart field of chick embryos suggested a role for Wnt-signalling during differentiation of the myocardium. Inhibition of *Wnt3a* or *Wnt8c* signalling in the anterior lateral mesoderm led to the formation of a heart, whilst overexpression of *Wnt* in the posterior lateral mesoderm promoted blood formation (Marvin and others, 2001). Further data proved a function of *Wnt* in heart induction, showing that inhibition of Wnt signalling in explants of paraxial mesoderm led to the development of beating cardiac mesoderm (Tzahor and Lassar, 2001). Inhibitions of *Wnt* in the ventral marginal zone in *X. laevis* have also been shown to induce heart formation in non-cardiac specific tissues (Schneider and Mercola, 2001). Further analysis showed that *Wnt3a* and *Wnt8* are responsible for the promotion of cardiogenesis in *X. laevis*, revealing similarities between frog and chick heart development. When focusing on the role of *β*-catenin during cardiogenesis, Schneider and Mercola showed that a deletion of *β*-catenin via expression of GSK3 *β*, a part of the degradation complex of *β*-catenin, also was able to promote heart formation in the ventral mesoderm. Ablation of *β*-catenin in the endoderm of mouse embryos led to a phenotype displaying ectopic heart formation (Lickert and others, 2002). It was described that the cells lacking *β*-catenin developed into cardiac mesodermal cells instead of being endodermal. It was therefore suggested that β-Catenin dependent Wnt signalling must be inhibited in order for cardiogenesis to occur. Inhibition of Wnt signalling has been found to be caused by binding of the secreted Wnt-antagonist Crescent to several Wnt-proteins (Marvin and others, 2001). *Crescent* is predominantly expressed in the anterior mesendoderm and therefore able to inhibit Wnt in the mesodermal cells. A role for *Dikkopf-1 (Dkk-1)*, being expressed in the posterior lateral mesoderm, has also been described in antagonizing Wnt signalling during heart formation. However inhibition of Wnt alone is not sufficient enough to induce cardiogenesis. *BMP*2 expressed in the anterior endoderm together with the inhibition of Wnt signalling has been shown induce heart formation (Andree and others, 1998; Schultheiss and others, 1997)

As described before the inhibition of β-Catenin mediated Wnt pathway is needed for the induction of cardiogenesis in the primary heart field. Recent data showed that cells of the secondary heart field, especially their differentiation and proliferation, seem to be affected by β-catenin dependent Wnt signalling as well. Conditional knock-out of *β*-catenin in the secondary heart field of the cardiac crescent in mouse embryos led to a disruption of looping of the primary heart and the formation of a shortened outflow tract (Klaus and others, 2007). Atria and left ventricle seemed to have been developed

correctly, while the right ventricle somehow was reduced in size. Expression of *Islet-1 (Isl1)*, a marker for the secondary heart field, in the *β-Catenin* knock-out mice has been analysed further to examine the role of *β*-catenin during differentiation of the cells. *Isl1* was significantly lower expressed in knock-out embryos in comparison to wildtype embryos, especially in the outflow tract and the splanchnic mesoderm. Overexpression of *β*-catenin also revealed disruptions in the primary heart tube leading to the formation of two separate clusters of cardiomyocytes (Klaus and others, 2007). It was suggested that the observed phenotype is due to a wrong or incomplete migration of both the primary and the secondary heart field. Nevertheless, *Isl1* expression was enhanced upon *β*-catenin overexpression. Taking all described data together, *β*-catenin/Wnt signalling seem to be involved in the correctly induction of *Isl1*-positive cells and therefore in the induction of the secondary heart field.

6.1.4 Expression of marker genes during cardiogenesis

To be able to define and compare separate phases of heart development, expression of marker genes involved in cardiogenesis have been described.
The first marker for cells with a cardiac fate is *mesoderm posterior 1* (*Mesp1*) labelling early heart cells already in the primitive streak (Saga and others, 2000; Saga and others, 1999). *Mesp1* expression is switched off once cardiogenic cells populate the lateral plate mesoderm and subsequently *NK2 transcription factor related, locus 5* (*Nkx2.5*) expression is switched on (Lints and others, 1993; Pandur and others, 2013; Schultheiss and others, 1995). *Nkx2.5* expressing cells have now committed irreversibly to become heart cells (Pandur and others, 2013). Also *Nkx2.5* labels cardiac progenitor cells both from the primary and secondary heart field (Chen and Schwartz, 1996; Lints and others, 1993; Schultheiss and others, 1995), as well as endodermal and mesodermal cells (Lints and others, 1993; Lopez-Sanchez and others, 2009). However, after the primary heart tube has formed *Nkx2.5* expression is restricted to the myocardium (Lints and others, 1993; Schultheiss and others, 1995).

Several heart markers have been described to label either the primary heart field or the secondary heart field. Two of those markers are *Tbx5* and *Isl1*. *Tbx5* (*T-box transcription factor 5*) is a marker for cells of the primary heart field and is first expressed in the cardiac crescent stage (mouse E 7.5 and chick HH 7) (Bruneau and

others, 1999; Chapman and others, 1996). Later *Tbx5* expression is observed in the posterior heart tube, the left ventricle and atria (see figure 6.2), which are all structures derived from the primary heart field (Bruneau and others, 1999; Chapman and others, 1996; Liberatore and others, 2000). *LIM-homeodomain transcription factor Islet 1* (*Isl1*) however is a marker for the secondary heart field, which also can be seen to be expressed in the cardiac crescent or crescent shaped bilateral heart fields depending on developing organism (Watanabe and Buckingham, 2010). In chick *Isl1* is expressed around HH stage 4 onwards in the rostrolateral mesoderm but expression is lost in cells which fuse to form the primary heart tube (Yuan and Schoenwolf, 2000). At later stages of heart development *Isl1* expression is restricted both in mouse and chick to the right ventricle, parts of both atria and more prominent the outflow tract (Pandur and others, 2013; Watanabe and Buckingham, 2010), which all derive from the secondary heart field (figure 6.1).

As the heart loops rightwards after the formation of the primary heart tube (Brand, 2003; Manasek and others, 1972), several genes have been described in establishing the left-right asymmetry of the heart. *Paired-like homeodomain transcription factor 2* (*Pitx2*) has been shown to be expressed exclusively in the left side of the bilateral heart field around the cardiac crescent stage (Campione and others, 2001). After the formation of the primary heart tube *pitx2* expression was observed only in the left part of the heart tube and after looping *pitx2* was shown to be expressed in the left atrium, the ventral part of the ventricles and the left side of the outflow tract (Campione and others, 2001). Further expression studies revealed that *pitx2* is also a marker for mesodermal cell populations (Lopez-Sanchez and others, 2009).

So far all previously mentioned heart marker genes label cells derived from the mesoderm, but there are also genes, which are specifically expressed in the endoderm.
One of these markers is *Hex*. *Hex* expressing cells can firstly be observed around HH stage 7+ in the cardiac crescent (Lopez-Sanchez and others, 2009) and mark endodermal cells adjacent to the mesoderm in the bilateral heart field (Lopez-Sanchez and others, 2009). After fusion of the primary heart tube, *Hex* is still expressed in the underlying endoderm (Lopez-Sanchez and others, 2009).

Ventricular myosin heavy chain (*vMHC*) is a marker for later phases of heart development. *vMHC* was shown to be expressed in the entire myocardium of the

primary heart tube (Bisaha and Bader, 1991; Somi and others, 2006). From around HH 16 onwards the expression of *vMHC* becomes restricted to the ventricles as the expression levels for *vMHC* in the atria decrease (Somi and others, 2006)

6.2 Expression pattern for Klhl31 during early cardiogenesis

6.2.1 Klhl31 is expressed in heart progenitor cells during cardiogenesis

When *Klhl31* was first described it was shown to be strongly expressed in embryonic muscle and heart tissue (Yu and others, 2008). In-situ hybridisation studies on chick embryos carried out in our laboratory revealed that *Klhl31* is expressed in cardiogenic progenitor cells from HH stage 8 onwards (Abou-Elhamd and others, 2009), see figure 6.2). It was also shown that *Klhl31* is expressed in the primary heart tube (around HH 10) and in heart tissue throughout embryonic development (Abou-Elhamd and others, 2009), as seen in figure 6.2).

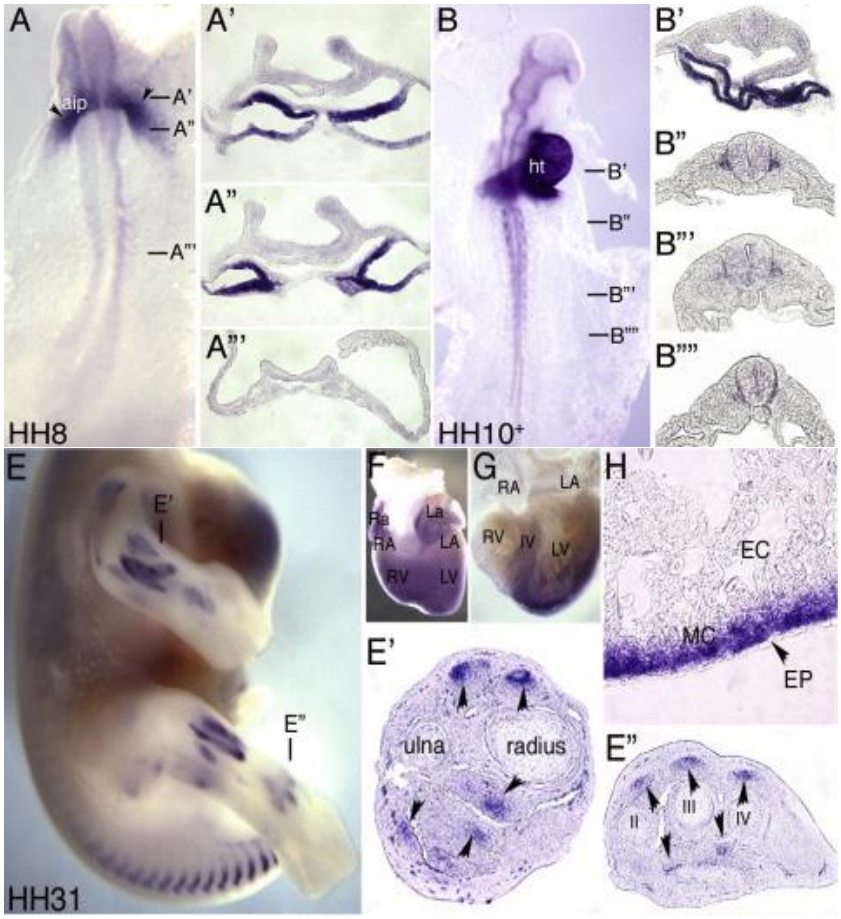

Figure 6.2: The expression of Klhl31 during chick development

In situ hybridisation for Klhl31 in chick embryos revealed that Klhl31 is expressed predominantly in skeletal and cardiac muscle tissues.

Legend: aip - anterior intestinal portal, ht - heart; EC - endocardium; MC - myocardium; EP - epicardium; R - right auricle; RA - right atrium; La - left auricle; LA - left atrium; RV - right ventricle; IV - interventricular septum; LV - left ventricle

Figure modified from Abou-Elhamd and others, 2009

6.2.2 Klhl31 expression during early heart development

Based on our evidence that *Klhl31* is expressed in heart muscle tissues, we wanted to examine *Klhl31* expression during cardiogenesis in more detail. We therefore carried out in situ hybridisations for *Klhl31* during different stages of heart development in chick embryos and compared the expression pattern of *Klhl31* to expression pattern of heart markers, such as *Isl1*, *Nkx2.5*, *Hex*, *vMHC* and *pitx2*.

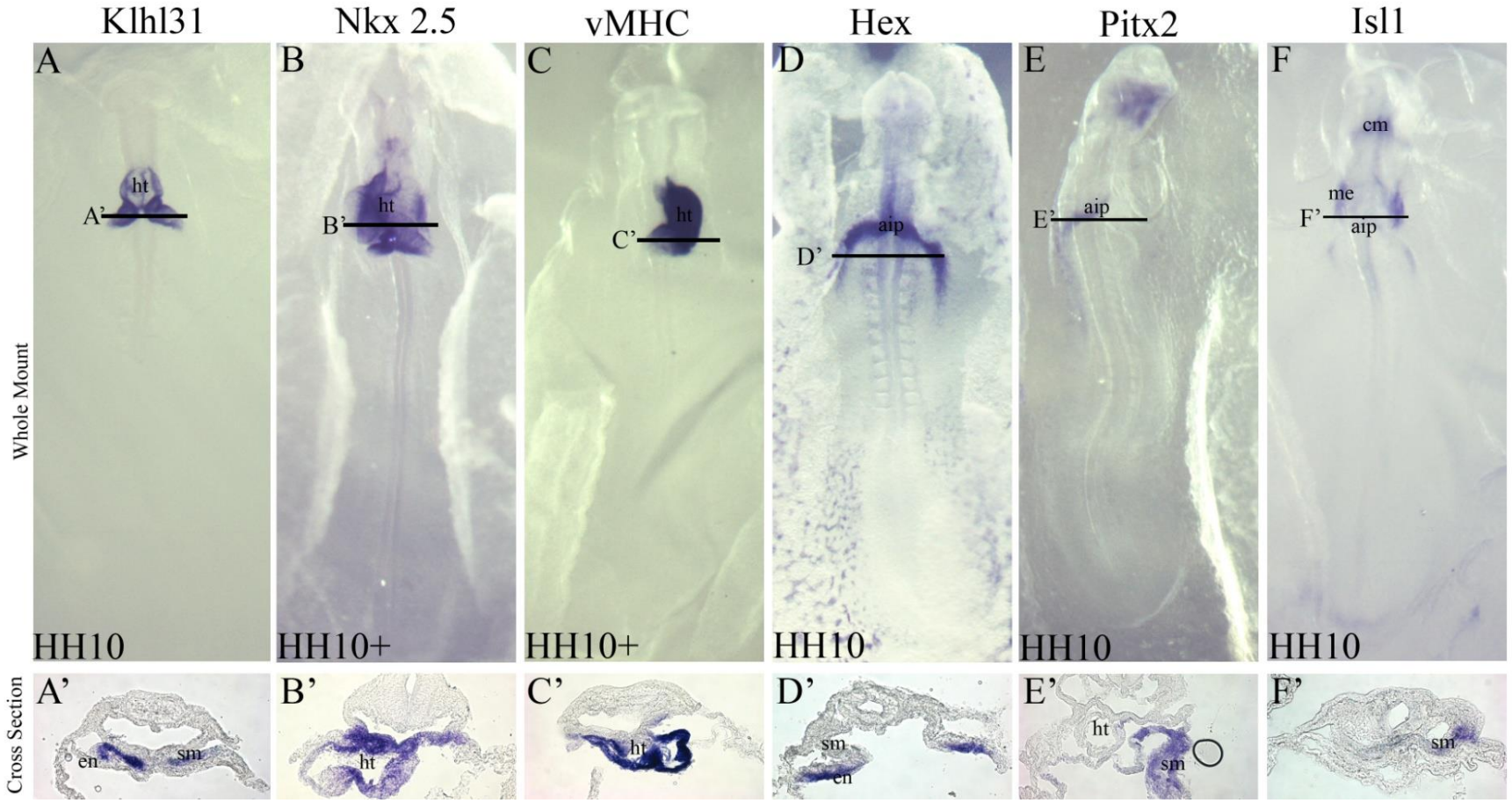

Figure 6.3: Expression of Klhl31 to the expression of heart markers at HH stage 10 of chick development

Figure 6.3: Expression of Klhl31 compared to the expression of heart markers at HH stage 10 of chick development

Whole mount in situ hybridisation for Klhl31 mRNA compared to mRNA expression of heart markers during early heart development. Nkx2.5 and vMHC expression was observed throughout the whole myocardium (B' and C', respectively). Hex was expressed in the adjacent endoderm (D'), while pitx2 expression in whole mount pictures was observed in the left omphalomesenteric vein close to the anterior intestinal portal (E). Cryosections also revealed the expression of pitx2 in the vitelline vein (E'). Expression for Isl1 was observed in mesenchymal structures to the left and to the right of the primary heart tube (F). Sectioning further specified Isl1 expression in the splanchnopleuric mesenchyme (F'). Klhl31 expression was observed in the heart (A) and the splanchnic mesoderm of chick embryos prior to fusion of the primary heart tube (A')

Legend: aip - anterior intestinal portal, ht - heart; en – endoderm; sm - splanchnic mesoderm; cm-cephalic mesenchyme; me – mesenchyme

We first analysed the expression of *Klhl31* during early cardiogenesis around HH stage 10, when the primary heart tube is formed (Stalsberg and DeHaan, 1969). We observed the known expression pattern for *Nkx2.5* (figure 6.3, B and B') and *vMHC* (figure 6.3, C and C') in the myocardium of the primary heart tube in chick embryos (Schultheiss and others, 1995; Somi and others, 2006). *Hex* was expressed in the endoderm underlying the two heart primordia prior to fusion (figure 6.3, D'). *Hex* has previously been reported to be a marker for adjacent endoderm during heart development (Lopez-Sanchez and others, 2009). Therefore our findings for *Hex* are in agreement with published data. *Pitx2* has been reported to be expressed in the left side of the primary heart tube (Campione and others, 2001). However, we were not able to reproduce the published expression pattern. Using in situ labelling for *pitx2* we detected restricted *pitx2* expression to the left part of the omphalomesenteric vein (figure 6.3, E), which is connected to the primary heart tube and originates from the same cell population as the primary heart tube (Moreno-Rodriguez and others, 2006; van den Berg and Moorman, 2011). When sectioning the embryo along the anterior intestinal portal, we could also observe *pitx2* expression in the left side of the vitelline vein (figure 6.3, E'). The reason for this discrepancy is currently unresolved.

Isl1 expression was observed as previously reported (Pandur and others, 2013). In our in situ hybridisation study *Isl1* expression was restricted to the splanchnic mesoderm adjacent to the primary heart tube (figure 6.3, F and F'). In comparison to observed

heart marker expression, *Klhl31* was expressed in the primary heart tube and in the splanchnic mesoderm prior to the fusion of the primary heart tube (figure 6.3, A and A' respectively), similar to the expression of *Nkx2.5*.

6.2.3 Klhl31 expression during later heart development (HH 17-18)

After the primary heart tube is formed cells from the secondary heart field are added to the primary heart tube and the heart undergoes morphological changes (Buckingham and others, 2005; Christoffels and others, 2000). We therefore analysed *Klhl31* expression during later cardiogenesis.

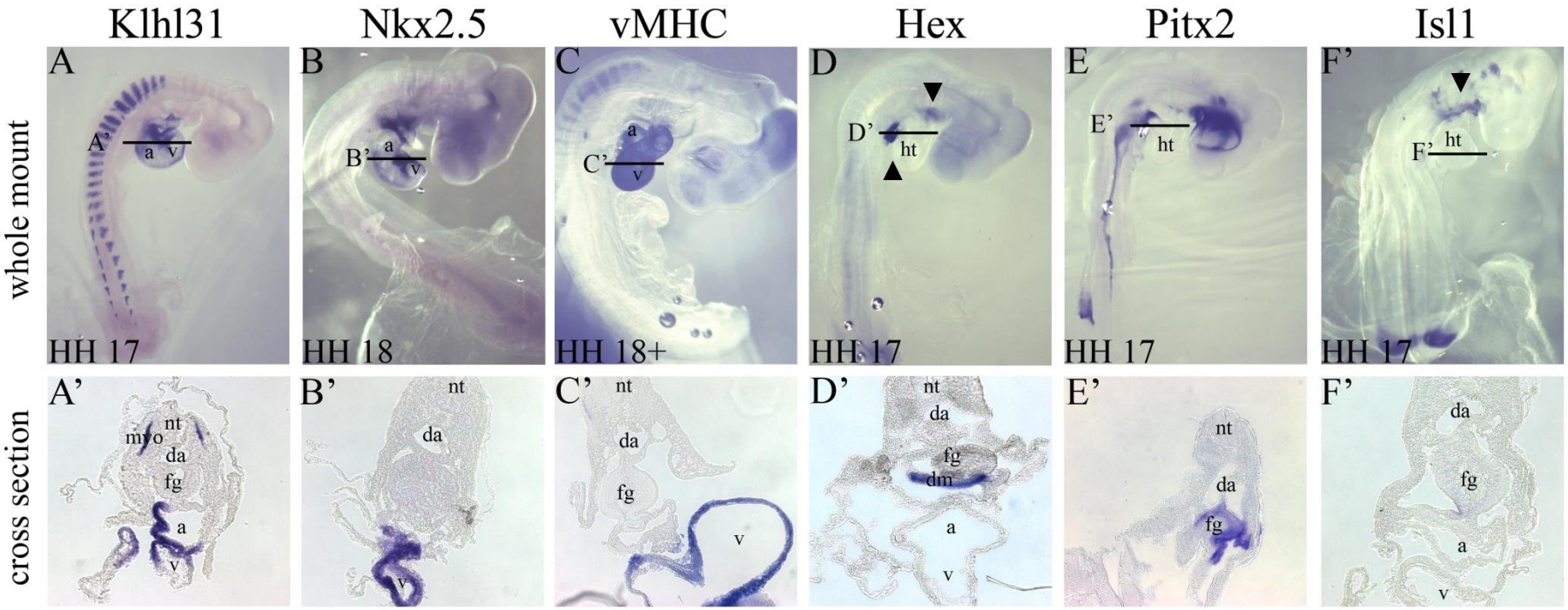

Figure 6.4: Expression of Klhl31 to the expression of heart markers at HH stage 17-18 of chick development

Figure 6.4: Expression of Klhl31 compared to the expression of heart markers at HH stage 17-18 of chick development

Whole mount in situ hybridisation for Klhl31 mRNA compared to mRNA expression of heart markers during later heart development. Nkx2.5 was still expressed in the whole myocardium (B and B') whilst vMHC expression was only observed in the ventricle of the heart (C'). Hex expression was observed in liver progenitor cells (D▲) as well as in cells that will contribute to the thyroid (D▼). In cryosections of chick embryos Hex expression was shown to be close to cells that belong to the dorsal mesocardium underlying the foregut (D'). Pitx2 expression was observed in tissue surrounding the foregut (E'), but not in the heart (E). Isl1 expression was also not observed in the heart (F, F'), but was expressed in tissues belonging to the aortic arches and the pharyngeal arches (F▼). Klhl31 expression was detected in the myotome of the somites (A) and in the myocardium (A and A')

Legend: nt – neural tube, myo – myotome, fg – forgut, da – dorsal aorta, a – atrium, v – ventricle, dm – dorsal mesocardium, ht - heart

At HH stage 17-18 chick embryos have turned to the left and have early limb buds, as well as showing a fully formed optic cup (Hamburger and Hamilton, 1992). The heart has looped rightwards and a distinct atrium and ventricle can be observed (Martinsen, 2005). *Klhl31* expression was still very similar to *Nkx2.5* expression as described by Schultheiss et al. (1995). Transcripts for both genes were detected in the myocardium (see figure 6.4; A and A' for Klhl31 and figure 6.4; B and B' for Nkx2.5). *Klhl31* expression could also be observed in the myotome (figure 6.4; A') as previously reported (Abou-Elhamd and others, 2009). Furthermore, *Klhl31* expression seems to be confined to the developing atrioventricular canal. *vMHC* expression is now restricted to the ventricle (figure 6.4; C') in conclusion with other published expression patterns for *vMHC*, which described a decrease of *vMHC* levels in the atrium and stable expression levels in the ventricle (Bisaha and Bader, 1991; Somi and others, 2006). As mentioned before, during early heart development *Hex* is a marker for underlying endoderm (Lopez-Sanchez and others, 2009). However in later stages of chick and mouse development (from mouse E9.5 onwards and in chick from HH stage 12 onwards) *Hex* is a marker for the hepatic progenitor cell population and the thyroid primordium (Crompton and others, 1992; Keng and others, 1998; Thomas and others, 1998; Yanai and others, 2005). *Hex* is expressed throughout the development of the liver and the thyroid and is also shown to be expressed in the foetal lung (Keng and others, 1998; Yanai and others, 2005). We could observe *Hex* expression in the thyroid primordium (figure 6.4; D▼) and the hepatic anlage (figure 6.4; D▲), but when we looked at

cryosections (figure 6.4; D') we did see expression of *Hex* in cells underlying the foregut close to the dorsal mesocardium. *Hex* expression has been published by many groups and although all of them describe expression for *Hex* in the thyroid and the liver, some report additional expression patterns for *Hex*. Thomas et al. (1998) reported expression of *Hex* in the ventral foregut endoderm, the allantois and in the posterior lateral mesoderm in chick embryos at HH stage 9-10 (Thomas and others, 1998). At HH stage 15-16 Hex expression was observed in the thyroid and liver primordia, as well as in the roof of the dorsal aorta and the ventral gut endoderm (Thomas and others, 1998). Our probe against *Hex* might therefore as well have labelled endodermal cells of the foregut. However, the probe we used has to be characterised further to be able to analyse the expression of *Hex* in more detail. In situ staining for different stages of chick development between HH 12-HH18 would give us more data to analyse *Hex* expression over a distinct period of development and would help us identify the cells which are expressing *Hex*. *Pitx2* was observed to be expressed predominately on the left side of the embryo (figure 6.4; E). However, pitx2 expression was not seen in the heart as reported previously (Campione and others, 2001). Furthermore we observed expression of *pitx2* in the foregut (figure 6.4; E'), which is unlike to any previous described *pitx2* expression pattern. The reason for this is unclear at present and it will need to be confirmed whether our probe detects pitx2 mRNA. Comparing *Isl1* expression as observed in our in-situ hybridisation study to *Isl1* expression as published on GEISHA (Id ISL1.UApcr and Id Islet2.UApcr, GEISHA Gallus Expression In Situ Hybridisation Analytics, University of Arizona, USA), we could observe expression of *Isl1* in the cranial ganglion and the pharyngeal arches (figure 6.4; F) as described by GEISHA. *Islet1* expression was not observed in the chick heart at HH stage 17-18.

6.2.4 Klhl31 expression during later heart development (HH 20-21)

Chick embryos at Hamburger Hamilton stage 20 are defined by the segmentation of nearly the whole embryo (somites can be seen along the dorsal side of the embryo except for the tip of the tail), enlarged limb buds and the presence of the allantois. Pigmentation in the eye is starting (Hamburger and Hamilton, 1992). The lung buds are formed, both atrium and ventricle grow in size and the conus arteriosus and sinus

venosus are formed (Martinsen, 2005). However, at this time during development the heart chambers have so far not been separated.

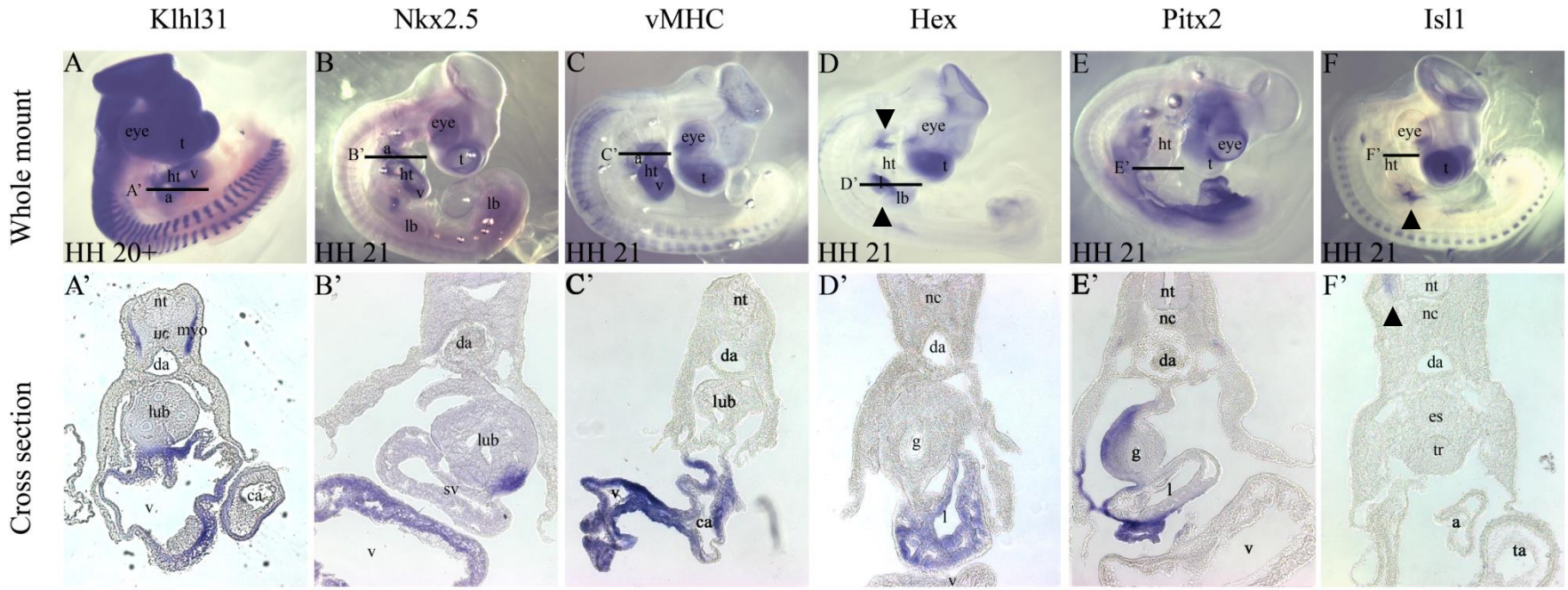

Figure 6.5: Expression of Klhl31 compared to the expression of heart markers at HH stage 20-21 of chick development

Figure 6.5: Expression of Klhl31 compared to the expression of heart markers at HH stage 20-21 of chick development

Whole mount in situ hybridisation for Klhl31 mRNA compared to mRNA expression of heart markers during later heart development. Nkx2.5 was shown to be expressed in the myocardium of the ventricle and the heart (B' and B, respectively). vMHC expression could be observed in the ventricle of the heart (C') and weak in the atrium (C) and conus arteriosus (C'). Hex expression was still observed in liver primordia (D▲, D') and in the thyroid progenitor cells (D▼). Pitx2 expression was seen along the left side of the embryo (E). The cryosection of a pitx2 labelled chick embryo revealed pitx2 expression in the left side of the gut and the liver (E'), but not in the heart (E and E'). Isl1 expression was again not observed in the heart (F, F'), but was expressed in the pharyngeal arches (F). In the corresponding cryosection expression of Isl1 was observed in the spinal cord labelling motor neurons (F'▲). Klhl31 was expressed in the myotome of the somites (A) and in the heart (A), as well as in the myocardium of the ventricle and conus arteriosus (A')

Legend: nt – neural tube, nc – notochord, lub – lung buds, myo – myotome, da – dorsal aorta, v – ventricle, ca – conus arteriosus, sv – sinus venosus, g – gut, es – esophagus, t – trachea, a – atrium, l – liver, ta – truncus arteriosus, ht - heart, lb – limb buds, t - telencephalon

Expression of *Nkx2.5* was observed in the heart (figure 6.5; B) and in the myocardium of the ventricle (figure 6.5; B'). As *Nkx2.5* has been described to be a marker for the myocardium throughout heart development (Lints and others, 1993; Schultheiss and others, 1995), our observed expression pattern is comparable to published data. At HH stage 20-21 *Klhl31* expression still resembles expression of *Nkx2.5* and *Klhl31* was also shown to be expressed in the myocardium of the ventricle (figure 6.5: A'). As previously described (Abou-Elhamd and others, 2009) *Klhl31* is also expressed in the myotome of the somites (figure 6.5; A and A'). Strong *vMHC* expression was detected in the ventricle and weak *vMHC* expression was seen in the adjacent conus arteriosus (figure 6.5; C') matching published expression patterns for *vMHC* (Bisaha and Bader, 1991; Somi and others, 2006). The observed expression for *Hex* further highlighted the role for *Hex* as a marker for liver and thyroid development (Keng and others, 1998; Yanai and others, 2005). In situ hybridisation for *Hex* in HH stage 20 chick embryos revealed labelling for Hex mRNA in the liver and thyroid primordia (figure 6.5; D) A strong signal for Hex mRNA was also noted in the liver in cryosections of chick embryos analysed for *Hex* expression (figure 6.5; D'). In situ hybridisation for *pitx2* of HH stage 20 chick embryos was again not able to reproduce published gene expression pattern marking the left side of the heart (Campione and others, 2001). We were only

able to detect pitx2 mRNA in the left part of the gut and tissues surrounding the liver (figure 6.5; E') leaving us questioning the reliability of the probe. *Isl1* expression was again observed to be similar to published data (Id ISL1.UApcr and Id Islet2.UApcr, GEISHA, University of Arizona, USA). *Islet 1* was shown to be expressed in the pharyngeal arches in whole mount chick embryos, as well as in the pancreas (figure 6.5; F▲), but not in the heart. Interestingly *Isl1* has been described to be a marker for motor neurons in the spinal cord (Tsuchida and others, 1994; Wang and others, 2011). We were able to reproduce the described expression pattern for *Isl1* in motor neurons (figure 6.5, F'▲).

In summary, by comparing the expression of *Klhl31* to the expression of other well described marker genes, we could show that *Klhl31* is a potential marker for the myocardium during cardiogenesis.

7. Discussion

7.1 A novel role for Klhl31 during myogenesis

7.1.1 Klhl31 as a potential mediator of myogenesis

We previously have reported a potential role for Klhl31 during myogenesis (Abou-Elhamd and others, 2009).

Here we provide some evidence supporting the hypothesis that Klhl31 has a role during de novo myofibrillogenesis. Further experiments are needed to substantiate this idea and I will discuss some of these below.

7.1.2 Klhl31 expression is linked to Actin filament changes during C2C12 differentiation

Differentiation of C2C12 cells involves similar processes as occurring during the differentiation of the myotome in the somite.

C2C12 differentiation is dependent on canonical Wnt-signalling, which has also been shown to activate myogenesis in somites (Tajbakhsh and others, 1998; Tanaka and others, 2011). Furthermore, both C2C12 differentiation and myotome differentiation is marked by MRFs expression. Undifferentiated C2C12 myoblasts already express Myf 5 and MyoD (Braun and others, 1989; Yoshida and others, 1998) and myogenin expression is activated in C2C12 myocytes around 20 hours of differentiation (Andres and Walsh, 1996) followed by MRF4 expression (Janot and others, 2009). Once the cells have entered the differentiation process, cultured mouse myoblasts and muscle cells in the myotome start to express p21 and withdraw from the cell cycle (Andres and Walsh, 1996; Braun and Gautel, 2011; Manceau and others, 2008). Furthermore, the

cells then elongate, fuse and eventually form multinucleated myotubes. Also, both in the myotome and in C2C12 myocytes expression of sarcomeric proteins is activated and de-novo myofibrillogenesis occurs (Andres and Walsh, 1996; Buckingham, 2001; Kontrogianni-Konstantopoulos and others, 2006; Pownall and others, 2002; Sanger and others, 2002; Sanger and others, 2010).

Analysis of C2C12 differentiation on cellular levels revealed the temporal and spatial organisation of myofibrillogenesis from premyofibrils to mature myofibrils in more detail (Burattini and others, 2004; Kontrogianni-Konstantopoulos and others, 2006). Premature Z-discs and M-bands already assembled after only 24h in differentiation medium, whilst after 48h of differentiation an early organisation of mature myofibrils was observed (Burattini and others, 2004; Kontrogianni-Konstantopoulos and others, 2006). After 72 h, C2C12 myocytes have begun to accumulate muscular myosin into their myofibrils and after 96 hours the myotubes contained mature myofibrils (Burattini and others, 2004; Kontrogianni-Konstantopoulos and others, 2006) (see figure 3.7).

Using immuno-staining experiments in differentiating C2C12 myocytes, we were able to reproduce the actin filament staining during early differentiation as described by Burattini et al (2004). We therefore assumed that changes in Actin and other Actin-associated proteins we observed were directly affected by de-novo myofibrillogenesis in C2C12 myocytes. However, our used C2C12 cell line was substantially older and less reliable then the cell line used in described publication by Burratini et al. (2004), which resulted in low differentiation potential. Unfortunately, we therefore were only able to culture our C2C12 myoblasts for a short amount of time, which restricted the experiments we aimed to do in terms of lengths of time course and expression studies. Also our C2C12 experiments cannot be completely be compared to Burratinis work, as their cell line already displayed mature myotubes after 96 hours in differentiation medium, whilst we never saw mature myotubes in our cultures in the same timeframe. We therefore need to assume that myofibrillogenesis occurred slower in our cell lines compared to published data for C2C12.

We studied Klhl31 expression and localisation during differentiation of C2C12 mouse myoblasts. The first interesting observation was that Klhl31 mRNA levels as well as protein levels were low in myoblasts, but increased around day 2 – day 3 during C2C12 differentiation (figure 3.4 and figure 3.5, respectively). Furthermore Klhl31 localisation

also changed during differentiation of mouse myoblasts from a punctate and cytosolic localisation to a fibrillar, but still punctate pattern (figure 3.6).

Further experiments revealed that the observed puncta of Klhl31 in C2C12 myotubes was closely localised with Actin fibres (figure 3.8, c and f, figure 3.9), but not with microtubules (figure 3.10).

Co-localisation of Klhl31 with Actin fibres was established around day 2 of C2C12 differentiation (figure 3.8; b, e and e') correlating with the observed increase in transcript and protein levels for Klhl31 and potentially linking enhanced Klhl31 expression with early myofibrillogenesis (Kontrogianni-Konstantopoulos and others, 2006; Sanger and others, 2002; Sanger and others, 2010).

Various members of the Kelch-like family have already been described to directly interact with Actin; Kelch, Klhl20 (KLEIP) and Klhl17 (Actinfilin) amongst others (Hara and others, 2004; Robinson and Cooley, 1997; Salinas and others, 2006; Stogios and Prive, 2004; Xue and Cooley, 1993). We therefore analysed if Klhl31 was also able to bind directly to Actin.

We used Latrunculin B to further test a potential direct interaction between Klhl31 and the Actin filament (as explained in section 3.3.3). Klhl31 localisation was affected by Latrunculin B treatment, as we observed diffused Klhl31 accumulations in the cytosol of treated C2C12 cells (see figure 3.12; b and b'). Furthermore, Klhl31 localisation to Actin fibres could also not been recovered (see figure 3.12; c'-e'). We therefore suggested that Klhl31 might associate directly to Actin fibres.

A potential direct interaction between Klhl31 and Actin fibres was found by using a GST-pull down approach. Actin was isolated from C2C12 lysates by using a GST-Klhl31 fusion protein and visualised both on a silver stained PAA Gel (figure 5.17, a) and on a western blot (figure 5.17, b). The actin bands in the GST-Klhl31 lanes are stronger than in the GST control lanes indicating that the observed interaction might be true. This would be consistent with the localisation studies for Klhl31 and Actin, thus strengthening the idea that the interaction between Klhl31 and the Actin filament was established during early myofibrillogenesis in C2C12 myocytes. However, it might also be that Actin is bound to a protein, which forms a complex with Klhl31 and therefore the observed interaction is an indirect one. A crucial experiment, which needs to be

done in order to prove that Klhl31 is involved in myofibrillogenesis is the verification of published expression patterns and expression timeframes relating to myofibrillogenesis. This should include the analysis and comparison of the sarcomeric Z-line protein α-actinin and other key sarcomeric proteins with the expression pattern for Klhl31. To further analyse a potential function for Klhl31 during myofibrillogenesis, we decided to use fluorescence-labelled Klhl31 fusion proteins.

7.1.3 The BTB domain and the Kelch-repeats of Klhl31 have specific cellular functions

Proteins of the Kelch-like family contain two highly conserved binding sites, the BTB domain and the Kelch-repeats (as described in chapter 1.12; (Stogios and others, 2005; Stogios and Prive, 2004). We carried out molecular and biochemical experiments to further analyse the function of both domains for Klhl31. We found that both Klhl31 FL, as well as Klhl31 ΔKR can significantly inhibit β-catenin induced luciferase reporter activity, while Klhl31 lacking the BTB domain did not show inhibition in the luciferase assays (see figure 4.6). The data is consistent with data previously obtained in our lab (Abou-Elhamd), see figure 1.13). It was suggested that substrates bound to the BTB-domain in Klhl31 might be targeted for degradation, possibly as part of an E3 ubiquitin ligase complex, as has been described for many other substrates targeted by members of the Kelch-like family (Geyer and others, 2003; Xu and others, 2003). Furthermore it was also described that β-catenin itself is targeted for proteasomal degradation by an E3 ubiquitin ligase, β-Transducin repeats-containing protein (β-Trcp) (Hart and others, 1999; Marikawa and Elinson, 1998). We have gathered information that Klhl31 could be associated with E3 ubiquitin ligase complexes, as we extracted an E2 ubiquitin conjugating enzyme, NEDD8-conjugating enzyme Ubc12, in our GST-pull down experiment. However, we have to be cautious as we do not know how likely this interaction is, as NEDD8-conjugating enzyme Ubc12 was not under the top 10 hits of the mass spectrometry data of proteins identified from the excised band. It is unlikely though that Klhl31 could interact with β-Trcp as well, as β-Trcp belongs to the Skp1-Cullin-1-F-box-type E3 ubiquitin ligase, whilst Kelch-like proteins have been shown to mainly associate to Cullin3-RING ubiquitin ligases (Canning and others, 2013; Fuchs and others, 2004). However finding that Klhl31 could interact with an E2 ubiquitin conjugating enzyme might indicate a role for Klhl31 in protein turnover regulations not only during Wnt-signalling but also during myofibrillogenesis.

Further experiments need to be carried out to analyse a potential role for Klhl31 as part of an E3 ubiquitin ligase complex. Determining whether Klhl31 can interact directly with associated ubiquitin-ligase complex proteins, such as Cullin3, could shed more light on potential functions of Klhl31. Nonetheless comparison of published literature together with the identification of an E2 ubiquitin-conjugating enzyme as potential interaction partner could suggest that Klhl31 could also play a part in ubiquitin-mediated proteasomal degradation and could therefore target components of the canonical Wnt-pathway, as well as sarcomeric proteins for ubiquitinylation and subsequent degradation.

To analyse potential Klhl31 functions, we created GFP and DsRed fusion proteins of Klhl31. We were able to reproduce previously described functionality for Klhl31 in inhibiting β-Catenin mediated Wnt-signalling (Abou-Elhamd), but only for fusion proteins for Klhl31 tagged at the carboxy terminus (see chapter 4.2.1). We therefore assumed that we had generated functional Klhl31-fusion proteins. Furthermore it was again shown that the loss of the BTB domain led to limited functionality of the protein.

N-terminal tagged Klhl31 fusion proteins did not inhibit β-Catenin induced luciferase signalling (see luciferase assay for pEGFP-C1 Klhl31, figure 4.3). We observed similar decrease in functionality when using an N-terminal tagged fusion protein for Klhl31 as compared to luciferase readings for Klhl31 ΔBTB-GFP/DsRed. We therefore wondered if a GFP-tag at the N-term of Klhl31 would disturb or block the structure of the Klhl31 protein, especially the BTB-domain. Circular dichroism analysis for an N-terminal tagged Klhl31 fusion protein could reveal if and to what extent GFP-tag could interact with the BTB-domain and would also shed light on whether this interaction could inhibit functionality of the fusion protein, as our data suggests.

Furthermore, we observed that the N-terminal tagged Klhl31 fusion proteins displayed a vesicular localisation in C2C12 cells (as described and discussed in sections 4.2.1 and 4.2.2), indicating that these Fusion-proteins might be degraded by the cell. However, we need to carry out lysosome-labelling experiments together with overexpression of the Klhl31-fusion proteins to be able to verify co-localisation. Also staining for ubiquitinylation could be used to validate a potential Klhl31 degradation.

Based on our data from the luciferase assays we could conclude that structural disturbances of the BTB domain potentially lead to a non functional Klhl31 protein.

As mentioned previously, Klhl31 fusion proteins tagged at the carboxy-terminus were active in our luciferase assays. However, we were not able to successfully overexpress most of the Klhl31 constructs in C2C12 myoblasts. Transfection efficiency for the used pEGFP-N1 or pDsRed-N1 constructs was never observed to be higher than 20% (consistent with a described optimal transfection efficiency of a maximum of around 25% by(Dodds and others, 1998) and signals for the C-terminal GFP tagged Kelch-like proteins only displayed very weak fluorescence (figure 4.9) making it difficult to observe real fluorescence of the fusion proteins. Only Klhl31-FL-GFP displayed a cellular localisation in C2C12 myoblasts, although different to the localisation observed for endogenous Klhl31 (figure 4.9, b). Klhl31-FL-GFP was not seen in C2C12 myotubes (figure 4.9, f). Klhl31 ΔKR-GFP was also only detected in C2C12 myoblasts revealing a diffused cytosolic localisation (figure 4.9, d) similar to the observed localisation for EGFP-Klhl31 ΔKR (figure 4.4; d). Similar cytosolic localisation of EGFP-Klhl31 ΔKR was also observed in myotubes (figure 4.4; h), but not for Klhl31 ΔKR-GFP (figure 4.9; h). It was reported that members of the Kelch-like family bind cellular Actin fibres via its Kelch-repeats (Hara and others, 2004; Robinson and Cooley, 1997; Salinas and others, 2006; Stogios and Prive, 2004). As Klhl31 seems to bind to Actin in C2C12 myotubes, a cytosolic localisation of EGFP-Klhl31 ΔKR can be explained by the loss of association to Actin fibres due to a lack of the C-terminal Kelch-propellers. However, endogenous Klhl31 in C2C12 myoblasts displayed a punctate localisation in the cytosol (figure 3.8), which could not be reproduced by overexpression of pEGFP-C1 Klhl31 ΔKR (figure 4.4; d) and pEGFP-N1 Klhl31 ΔKR (figure 4.9; d). It might be that localisation of Klhl31 is also mediated by the Kelch-repeats in undifferentiated C2C12 cells, but might not involve the Actin fibres. Proteins containing Kelch-repeats have been shown to localise to membranes, the cytosol and sperm acrosomal vesicles without being directly associated to Actin (for a review see (Adams and others, 2000). It could be possible that Klhl31 is associated to other cellular components in C2C12 myoblasts compared to myotubes. Another possibility might be that the plasmid DNA used for transfection was contaminated, which either led to less expression and therefore non-observable fluorescence or overexpression of only the fluorophore. This could explain why overexpressed Klhl31ΔKR-GFP localisation and

signal strength seemed to be highly similar to localisation and fluorescence signal of GFP expressed from the parental vector (figure 4.9, a).

As we were able to detect a similar localisation for Klhl31 FL GFP in myoblasts compared to endogenous Klhl31, we expected to also be able to visualise C-terminal DsRed-tagged Klhl31 (see figure 4.7). But unfortunately, we could not observe fluorescence signal for any of the constructs except for Klhl31 ΔBTB-DsRed, which again displayed a vesicular pattern, both in myoblasts and myotubes (figure 4.7, c and g). This could partially be explained by known problems of DsRed-constructs in terms of correct folding of generated fusion-proteins.

A further possibility why we did not observe our overexpression constructs, either Klhl31-GFP or Klhl31-DsRed could be that the fusion proteins were degraded over the differentiation time-course of C2C12 starvation. During differentiation of C2C12 myocytes apoptosis is occurring (Cerone and others, 2000; Wang and Walsh, 1996), keeping up the right balance between proliferating and differentiating cells (Burattini and others, 2004). Apoptosis is only affecting myoblasts, differentiated C2C12 do not undergo programmed cell death (Wang and Walsh, 1996). As we only transfected a low percentage of cells (~20%) followed by the induction of apoptosis in some myoblasts by promoting C2C12 differentiation, we potentially loose more protein expression over the 5 days of differentiation time course. We therefore have to assume that by the end of our time-course of C2C12 differentiation fusion-protein levels are too low to be detectable in myotubes, which did negatively affect both, DsRed and GFP-tagged Klhl31 fusion proteins.

7.1.4 Klhl31 is downregulated in mammalian cell cultures possibly by targeting itself for degradation

We could show that overexpression of Klhl31 fusion proteins in C2C12 was possible, but the levels of transcribed fusion proteins seemed to be very low.

Although we were not able to detect GFP-Fusion proteins on a western blot, we were able to see GFP on its own (figure 4.10) revealing that the transfection of C2C12 should have been successful. A further interesting clue regarding Klhl31 overexpression in

C2C12 was observed by Dr. Katarzyna Goljanek-Whysall in our laboratory. It was previously reported that expression of canonical Wnt-ligands in C2C12 keep C2C12 cells in a proliferative state and that inhibition of β-catenin mediated Wnt-signalling is a prerequisite for the induction of C2C12 differentiation (Nakashima and others, 2005; Tanaka and others, 2011; Zhang and others, 2012). Previous work from our group had already indicated that Klhl31 can inhibit canonical Wnt-signalling (Abou-Elhamd and Garcia-Morales).

When Dr. Katarzyna Goljanek-Whysall silenced Klhl31 expression in C2C12 myoblasts she observed that proliferation was increased and differentiation delayed. This observation was supporting the suggestion that Klhl31 is an inhibitor for β-catenin dependent Wnt-signalling. However, C2C12 cells were also observed to proliferate more when transfected with Klhl31. C2C12 myoblast expressing ectopic Klhl31 did not differentiate as efficiently compared to controls.

Based on our findings, that Klhl31 levels in C2C12 myoblasts were very low, only increasing during the intermediate phase of differentiation and that overexpression of Klhl31 did surprisingly not induce myotube formation, we were wondering if Klhl31 levels need to be low and therefore might be regulated by the cellular environment. Another possibility could be that Klhl31 mediates its own downregulation in C2C12 myoblasts, as a negative feed-back, to prevent increased Klhl31 protein levels.

If Klhl31 is in fact downregulated by targeted degradation, we might be able to prevent degradation by inhibiting the proteasome. First we decided to increase our transfection efficiency by choosing HEK293 cells, which do not endogenously express Klhl31. We overexpressed Klhl31 FL-GFP in HEK293 cells and treated transfected cells with MG 132. We observed a 75 kDa protein band in HEK293 cells, both treated and untreated with MG132. However, this protein band was smaller than expected for a full-length Klhl31 FL-GFP protein. As we could detect the C-terminal tagged GFP-fusion protein with a GFP-antibody, we assumed that a full length protein was produced in the cell. The smaller size may therefore indicate that the fusion protein was cleaved near the amino-terminus. Using MG132 did not seem to prevent this reduction in size and presumed cleavage. However, after MG132 treatment, we observed a weak stabilisation of some smaller fragments of the cleaved Klhl31 fusion protein, which ran below the main band (figure 4.11 and figure 4.12, lanes 7-9).

It has recently been shown that other members of the Kelch-like family have also been initially degraded by a so far unknown process which does not involve the proteasome (Zhang and others, 2005). KEAP-1 (Klhl19) degradation is due to the formation of homodimers, which triggers the ubiquitinylation of KEAP-1 and subsequently leads to the degradation of this Kelch-like protein (Zhang and others, 2005). Zhang et al. (2005) also claimed that the switch from substrate to substrate adaptor ubiquitinylation is important for the regulation and control of steady-state protein levels of both, substrates and adaptor proteins, in the cellular environment.

Could Klhl31 also not only control protein levels of its substrates, but also its own protein levels based on potentially self-targeted or self-induced degradation? It has been suggested that in theory all members of the Kelch-like family should be able to form homodimers (Geyer and others, 2003).

We used a GST-pull down approach to find interaction partners for Klhl31 specifically in C2C12 cells and we found that GST-Klhl31 was detected together with a protein band displaying the size of endogenous Klhl31 on a PAA gel (figure 5.17, a; ←). Furthermore, the potential interaction of Klhl31 with itself was further verified by detection of both endogenous Klhl31 and GST-Klhl31 with a Klhl31-antibody on a western blot (figure 5.17, b; ←).

Being able to show that Klhl31 can eventually interact with itself, possibly as homodimers, further highlights a function for a self-regulation of protein levels of Klhl31.

7.1.5 Identifying interaction partners for Klhl31

To identify potential interactions for Klhl31 in skeletal muscle tissues, we commissioned a Yeast-2-Hybrid screen (see chapter 5.1.2). The Yeast-2-Hybrid screen in general has not been very successful and included sequences derived from non protein-coding RNA or intronic DNA sequences (chapter 5.1.3) suggesting contaminations with genomic DNA in the screened libraries.

All four proteins identified as potential interaction partners were classified as category D, which contains potentially false positives (figure 5.2). We had designed our bait construct for Klhl31 in consultation with Hybrigenics. Based on our GFP/DSRed fusion proteins, it seemed likely that a tag at the BTB domain would impair function (as discussed in chapter 7.1.3). We therefore decided to use a C-terminal LexA/GAL4-Klhl31 fusion protein for Klhl31. C-terminal tagged fusion proteins were shown to be functional and seemed to localise similar to endogenous Klhl31 in C2C12 myoblasts. Thus we were confident that a C-terminal tagged bait protein could successfully be used in a Yeast-2-Hybrid screen. However, we have also seen that overexpressed Klhl31 in cell culture was potentially degraded, potentially initiated by the cellular environment and maybe even targeted by itself (chapter 7.1.4). To what extent this might have been an issue in Yeast cells we do not know.

The screen identified three potential new interaction partners for Klhl31. NEDD9 (described in chapter 5.2.2), FKBP15 (described in chapter 5.2.3) and two isoforms of Nebulin (chapter 5.3). NEDD9 and FKBP15 have been discussed previously (section 5.2.2 and 5.2.3, respectively) and will not be analysed any further. The possible interaction with Nebulin will be discussed in the following chapter (7.2).

We wondered why the Yeast-2-Hybrid screen did not identify a possible interaction of Klhl31 with Actin. We had previously shown that Klhl31 localises closely to Actin fibres and we were able to verify a direct interaction by a GST-pull down approach. We questioned if the GAL4/LexA domain fused to the carboxy terminus in Klhl31 for the Yeast-2-Hybrid Screen might have diminished the binding capacity of the Kelch-repeats. Also we wondered if a potential structural blockage or rearrangement of the C-terminus might also have had an impact on the N-terminus of the Klhl31 fusion protein again speculating that the Yeast-2-Hybrid screen might have missed some interactions for Klhl31.

7.2 Nebulin and Klhl31 might both be involved in mediating myofibrillogenesis

7.2.1 Nebulin and Klhl31 co-localise in adult muscle tissues

As the Y-2-H had identified two isoforms of the giant sarcomeric protein Nebulin and as it was reported that Nebulin has function both in embryonic and adult muscle tissues, we decided to further investigate Nebulin as a potential new interacting partner for Klhl31. First we compared both fragments of the Nebulin isoforms with each other. We found that both isoforms contained the same amino acid sequence, which potentially could be a conserved binding site for Klhl31 (see alignment of both fragments in chapter 5.3.1).

Using an immuno-histochemistry approach we showed that both Klhl31 and Nebulin are expressed in adult mouse striated muscles (see figure 5.7). Both Klhl31 and Nebulin could be observed to label punctate structures in myofibres, potentially single myofibrils. Using double immuno-staining for Klhl31 and Nebulin on tibialis anterior sections revealed a close association of Nebulin and Klhl31, as both proteins were detected in the majority of myofibrils (yellow staining, see figure 5.8; b). Observing this close localisation suggested that Klhl31 and Nebulin might be able to interact directly with each other, as predicted by the Yeast-2-Hybrid screen. However, we have also observed myofibrils that were either Nebulin positive (green), but not Klhl31 positive, as well as myofibrils, which were only labelled for Klhl31 (red), but not for Nebulin. Various isoforms for Nebulin have been reported to be expressed in different muscle tissues and during different developmental stages (Donner and others, 2004; Joo and others, 2004; Kazmierski and others, 2003). It was predicted that over 20 different Nebulin transcripts could be generated by alternative splicing in the human tibialis anterior muscle alone (Donner and others, 2004) and therefore we have to assume that the tibialis anterior muscle in mice also expresses various Nebulin isoforms. Having observed Nebulin-positive myofibrils, which were negative for Klhl31, we could assume that Klhl31 does not interact with all of the potential present Nebulin isoforms.

This observation would be in line with the data analysis for a potential binding domain for Klhl31 within the super-repeat domain of Nebulin, which is different for each isoform due to alternative splicing sites within the Nebulin gene. We know that the antibody, which we used to detect Nebulin was raised against an epitope found in the conserved C-terminal region of Nebulin, which is localised close to the Z-disc in the sarcomere and which is not affected by alternative splicing (Furst and others, 1988). The Nebulin antibody should therefore label all present Nebulin isoforms within the mouse muscle. Having observed Klhl31 expressing myofibrils, which were not labelled for Nebulin leads to the question whether Klhl31 is closely associated to Nebulin and whether Klhl31 could also associate to other sarcomeric proteins, which are not located in the Nebulin-containing area of the sarcomere. We therefore have to consider that Nebulin and Klhl31 might not associate with each other along the whole myofibrillar structure. We know that Nebulin is associated to thin filaments, but not the thick filaments (Millevoi and others, 1998; Wang and Wright, 1988). It could be that Klhl31 also aligns to specific parts of the myofibrils. We propose that Klhl31 is associated to Actin (see figure 5.16) and an interaction with Nebulin was predicted in the Yeast-2-Hybrid screen (chapter 5.3.1), leading to the suggestion that Klhl31 is localised to the thin filaments, maybe also associated to Nebulin. However, we need to undertake more experiments to identify localisation and function for Klhl31 in mature muscles, potentially by using longitudinal sections. Immuno-staining for Nebulin, Actin and Klhl31 could further clarify if Klhl31 is only found along the thin filament, whilst comparing the localisation of further sarcomeric proteins (such as α-actinin or proteins of the M-band) with the localisation of Klhl31 could also shed more light on a potential function for Klhl31 in adult muscle.

Unfortunately we were not able to verify Nebulin-Klhl31 interaction by using a GST-Klhl31 fusion protein in pull-down assays in C2C12 lysates during C2C12 differentiation.

This could be explained in that observed Nebulin levels were very low in the C2C12 lysates. Also we still have to remember that we could not detect full length Nebulin by Western blotting, as we have chosen to use a too low concentrated PAA gel. We therefore cannot confirm nor deny a potential interaction of Klhl31 with Nebulin. Another possibility is that Klhl31 could target Nebulin for degradation as part of a potential E3-Ubiquitin-ligase complex. When we analysed Nebulin protein expression by western blotting, the antibody against Nebulin detected a protein band of 130 kDa

(see section 5.3.7). This is far too small to be a full length Nebulin protein, as Nebulin has been described to be between 600-900 kDa large (Labeit and Kolmerer, 1995a; McElhinny and others, 2003). At this moment we cannot confirm, whether Klhl31 could potentially assist in the ubiquitinylation of Nebulin. We firstly need to identify full-length Nebulin protein on an appropriate SDS-PAGE, followed by characterisation of the observed 130 kDa protein band, before we can investigate this suggestion any further. Ubiquitination assays could further help highlighting if Nebulin is degraded during myofibrillogenesis. At this moment, we probably have to assume that the detected protein band might only be an unspecific protein, which cross-reacted with our used Nebulin antibody. We could use other anti-Nebulin antibodies to further clarify the identity of the detected protein band.

7.2.2 Nebulin and Klhl31 might function in myofibrillogenesis in C2C12 mouse myoblasts

Nebulin has also been described to play an important role during myofibrillogenesis (as explained in chapter 5.3.2).

As described previously, Nebulin during C2C12 differentiation was only expressed for approximately 24 h between day 1.5 and day 2.5 (see figure 5.10 and figure 5.12).

Comparing the expression of Nebulin to the expression of Klhl31 during C2C12 differentiation, it was seen that Nebulin expression seemed to be expressed before or at the same time that Klhl31 protein levels increased (as described in chapter 3.1.3) at the time point during differentiation that was marked by the formation of primitive Z-discs and was described as the onset of C2C12 myofibrillogenesis (Burattini and others, 2004; Kontrogianni-Konstantopoulos and others, 2006).

However, previous data reported a constant expression of Nebulin during myofibrillogenesis and in adult muscle tissues (McElhinny and others, 2005; Moncman and Wang, 1996; Nwe and others, 1999). Therefore we were wondering, why we were not able to detect Nebulin throughout differentiation of mouse myocytes. It could be that the antibody we used to label Nebulin with does not detect all Nebulin isoforms. Therefore we maybe had only detected one specific isoform of Nebulin, which only

functions during early myogenesis. But as mentioned before, the Nebulin antibody used is very well characterised and should not selectively detect specific Nebulin-isoforms.

Also it seemed like that the C2C12 cell culture used was unhealthy and maybe even a bit too old. Therefore we cannot exclude that the differentiation potential of the used C2C12 cells was diminished, especially towards later stages of differentiation, so that a lack of constant Nebulin expression is not due to a real absence of Nebulin, it might be rather be due to undefined cellular processes within the C2C12 myocytes originating from high stress levels or diminished health.

This problem could also have affected the observations made in our Latrunculin B experiments (as described in chapter 3.3.3) to some extend. In published literature, it has been reported that Actin filaments associated to Nebulin cannot be depolymerised under Latrunculin B treatment (Pappas and others, 2010). However differentiated C2C12, which were treated with Latrunculin B in our experiments, lost all their Actin filaments and eventually the cell structure collapsed (see figure 3.11) raising the possibility that the Actin filament was not stabilised by Nebulin or that again due to poor health our C2C12 cells were not able to recover from additional stress caused by treatment with the drug.

Also, we could not test C2C12 myotubes, which have differentiated for more than 5 days, for expression of Nebulin. This was due to technical problems with the C2C12 cell culture. Mature myotubes in culture tend to detach and reform constantly leading to a huge number of cells being lost from the plates or coverslips (already after 5-6 days in differentiation medium), which might also have been increased in our cell culture due to mentioned age and health-related issues. Published data for Nebulin expression during C2C12 differentiation stated a constant expression of Nebulin from early myofibrillogenesis on and even in fully mature myotubes (Burattini and others, 2004; Sanger and others, 2010). In fully mature C2C12 myotubes (around day 10 of differentiation) Nebulin was even shown to display striations in myofibrils just as described for adult muscles (Cooper and others, 2004). We have tested whether our C2C12 myoblasts could differentiate into striated myofibrils. However, as this was not the case, we have to assume that our C2C12 cells were potentially not healthy enough to undergo a normal differentiation process compared to healthy myoblasts.

Further expression data, for both Nebulin mRNA and protein, needs to be obtained in healthy C2C12 myoblasts in order to be able to clearly indentify the time frame of Nebulin expression, as well as Klhl31 expression during C2C12 differentiation.

Following the analysis of Nebulin expression in C2C12, we studied the localisation of Nebulin in elongating C2C12 cells. In conclusion with published literature, we also found that Nebulin aligns to Actin fibres during differentiation of muscle cells (figure 5.11 and figure 5.13) (Moncman and Wang, 1996; Shimada and others, 1996). Although Nebulin seemed to form fibrillar structures, it could be seen that some of this fibrillar structures displayed a punctate pattern. Also punctate staining was observed in the cytosol and not attached to Actin fibres (figure 5.11, day 2). A similar pattern was observed by Nwe et al. (1999).

As differentiation of C2C12 cells progressed, we could observe Nebulin staining in a punctate and accumulated pattern restricted to the edges of the elongating cells (see figure 5.13; g and p) with few puncta still observed along Actin fibres (see also figure 5.14, a). Nwe et al. (1999) published that Actin during later myocyte differentiation localised to Z-discs, where it overlapped with high levels of Nebulin. As we were able to observe accumulation of Actin and Nebulin at the edges of the cell we were wondering if this localisation could be close to primitive Z-discs in C2C12. Co-staining for Nebulin with sarcomeric α-actinin would clarify if we have Nebulin localisation along the Z-discs in differentiating C2C12 cells. Based on our obtained data for Nebulin during C2C12 differentiation and published literature for Nebulin, we could assume that Nebulin is involved in C2C12 mouse myoblasts, potentially by assisting the association of Actin filaments to the primitive Z-discs.

Unfortunately, once Nebulin staining has been refined to the edges of the cells expression decreases and was not detected anymore during the subsequent days of C2C12 differentiation. This observation has not been made in any other cell line or model organism (as described previously) leaving us again wondering whether the health or age of our C2C12 cell line was inhibiting our ability to investigate the late differentiation of mouse myoblasts.

Having analysed Nebulin and Actin, as well as Klhl31 and Actin localisation during C2C12 differentiation, we then compared Klhl31and Nebulin localisation.

Klhl31 and Nebulin both aligned to Actin fibres in similar stages of C2C12 myotube formation (see figure 5.13; k-q), from day 1 until around day 2. We were also able to show a weak, partial co-localisation of Nebulin puncta to Klhl31 fibres (see figure 5.14; c) but only in elongated myocytes after day 1.5 of C2C12 differentiation. However, we also detected a higher number of Nebulin puncta that did not align to Klhl31 structures (figure 5. 14; c), which is likely to be observed due to the instability of the red signal from the secondary antibody (as described in material and methods, section 2.2.26). Compared to previous Klhl31 staining (see figure 3.8), we only observed a few Klhl31 fibres in differentiating mouse myoblasts indicating that we had potentially detected less Klhl31 than were actually present in the cell. Based on previous immuno-staining in C2C12 for Actin and Klhl31, as well as for Actin and Nebulin, we have to assume that Klhl31 and Nebulin would be in close proximity in elongating myoblasts. However again, we need to repeat the experiment in young, healthy mouse myoblasts and we also need to co-stain for other well defined sarcomeric proteins, like α-actinin to further clarify the regions within the premyofibril the proteins, especially Klhl31 and Nebulin, localise to.

We also need to repeat some of the expression profiling experiments, so we can further clarify the temporal expression pattern, both on mRNA and protein level) of Klhl31 compared to other well-described sarcomeric genes during C2C12 differentiation in order to be able to describe a potential function for Klhl31 during myofibrillogenesis.

Our data obtained from the cell culture experiments can also not be used to explain why Klhl31 is still localised to Actin fibres during late myofibrillogenesis and in adult muscles, as well as that we also have no idea what the function of Klhl31 is both in developing and mature muscles. We have evidence from in-situ hybridisation in chick embryo (Abou-Elhamd and others, 2009), as well as from our data obtained in myoblasts that Klhl31 could play a key part during myofibrillogenesis in the myotome, which requires association with the Actin filament. But so far we have not gathered enough evidence to specify this role.

We have identified CapZ and tropomyosin as potential interacting partners for Klhl31 in differentiating C2C12 myoblasts. Various publications had suggested a role for Nebulin in stabilisation of the thin filament in striated muscles (Kruger and others, 1991; Labeit and others, 1991; McElhinny and others, 2005; Moncman and Wang, 1996; Pappas and others, 2010). As we could observed an association between Nebulin and Klhl31 and as

we have identified CapZ, as well as tropomyosin (both, tropomyosin, by binding to tropomodulin, and CapZ are involved in capping of the Actin filament in striated muscles (Bailey, 1948; Caldwell and others, 1989; Kostyukova, 2008; Perry, 2001; Weber and others, 1994)) as being able to bind to Klhl31, as well as being able to bind to Nebulin (McElhinny and others, 2001; Pappas and others, 2008), we could hypothesise that Klhl31 might be involved in thin filament assembly and stabilisation (probably in association with Nebulin), maybe even in length specification. This might be a potential function for Klhl31, as we also have identified the Arp2/3 complex as a potential interaction partner for Klhl31 during C2C12 differentiation and potential myofibrillogenesis. Nebulin was recently shown to form a complex with N-WASP, which was able to induce Actin nucleation without the assistance of the Arp2/3 complex (Takano and others, 2010). We have identified FKBP15/WAFL, a member of the Wiskott–Aldrich Syndrome protein (WASP) family as a potential interaction partner for Klhl31 in the Yeast-2-Hybrid screen. Although a direct interaction between Klhl31 and FKBP15/WAFL needs to be verified, it could be interesting to test, whether a member of the WASP family is involved in Actin polymerization together with potentially Nebulin and Klhl31.

Furthermore, we pulled down the myosin regulatory light chains Myl9 and Myl12b. Myl9 and Myl12 b are be part of Myosin II in non-muscle cell tissues, where they play a crucial role in cell adhesion, cell division and migration (Park and others, 2011). Furthermore, Myl9 has also been reported to be expressed in smooth muscle (Kumar and others, 1989). Myl9 and Myl12b have not been reported to be expressed in adult skeletal muscle.

However, immuno-histochemistry studies and protein extraction studies revealed the presence of both Myl9 and Myl12b in C2C12 cells (http://www.scbt.com/datasheet-19848-p-MYL9-thr-18-antibody.html, (Sharma and others, 2012), which could mean that both RLCs have actual functions in the sarcomeric structures of C2C12 cells. During myofibrillogenesis it was reported that non-muscular myosin II is initially assembled into premyofibrils and is later replaced by muscle-specific myosins (Sanger and others, 2002; Sanger and others, 2010). This also includes the associated non-muscle myosin regulatory light chains (Du and others, 2003). It was reported that myosin II and its associated myosin regulatory light chain Myl12b are expressed during early myofibrillogenesis. Furthermore phosphorylation of non-muscle myosin regulatory light chains is essential for premyofibril assembly, as the inhibition of non-

muscle myosin regulatory light chain led to the complete loss of premyofibrils in precardiac mesoderm explants (Du and others, 2003). Having observed that Klhl31 might bind to components of non-muscle myosin II during early myofibrillogenesis might reveal a role for Klhl31 during myofibril assembly, not only for the thin filament, but also for the thick filament. However, we can only speculate here, as we do not have enough evidence to support our idea. Our immuno-staining for Klhl31 during C2C12 differentiation contradicts the idea of a potential role for Klhl31 during thin and thick filament assembly, as we have only observed an interrupted staining for Klhl31, whilst we probably would expect a continuous staining inside the myocytes if Klhl31 would associate to both the actin and the myosin filament. Again, we need to carry out further experiments directed towards the question whether Klhl31 might be involved in myofibrillogenesis, assisting both the thin and the thick filament to assemble.

The data from the mass spectrometry might also give clues towards a role for Klhl31 in mature sarcomeres. Based on having identified CapZ and tropomyosin as interaction partners for Klhl31 by GST-pull down and co-localisation of both proteins, Klhl31 and Nebulin in adult muscle, we could suggested that Klhl31 together with Nebulin might be involved in stabilising the Actin thin filament in mature muscles.

Furthermore, tropomyosin as an interacting partner for Klhl31 could also link Klhl31 to muscle contraction, as troponin/tropomyosin complexes have been reported to mediate muscle contraction by translating elevated Ca^{2+} signals into actomyosin interactions and subsequent movement (Catterall, 1995; Farah and Reinach, 1995; Gordon and others, 2000; Zhi and others, 2005). This idea could furthermore be emphasized by the identification of Calmodulin from the GST-pull down. However, we have no clear evidence or in fact any supporting material for this hypothesis and I therefore emphasize here again, that this is only a speculation of what Klhl31 might be involved in at this point in time.

So far we have only analysed the low sized proteins from the silver stained PAA-Gel by mass spectrometry. Further bands have been excised and are still kept at – 80 °C. We could possibly find other interesting candidates in the other excised protein bands.

7.2.3 Nebulin, Actin and tropomyosin mutations in nemaline myopathy

Nemaline myopathies are congenital, inheritable neuromuscular disorders characterized by the presence of rod-like structures in skeletal muscle fibres.

Patients with nemaline myopathies show signs of hypotonia and biopsies of affected muscles reveal unusual rod-shaped structures or myogranules, also known as nemaline bodies (Conen and others, 1963; Sanoudou and Beggs, 2001; Shy and others, 1963).

Most nemaline myopathies originate during development caused by mutations of various sarcomeric proteins (Wallgren-Pettersson and others, 2011).

Mutation in *ACTA1*, encoding skeletal muscle α-Actin, *Nebulin*, *TPM2*, expressing β-tropomyosin, *TPM3*, which encodes α-tropomyosin, *TNNT1*, expressing slow skeletal muscle troponin T as well as *CFL2*, encoding muscle specific cofilin have been shown to be responsible for nemaline myopathies (Agrawal and others, 2007; Donner and others, 2002; Johnston and others, 2000; Laing and others, 1995; Nowak and others, 1999; Pelin and others, 1999). More recently a gene of the Kelch/BTB family has been described to also be mutated in patients displaying nemaline myopathy, KBTBD13 (Sambuughin and others, 2010).

In comparison to the other genes affected in nemaline myopathies, Actin and Nebulin mutations seem to be the most common mutations ***(Wallgren-Pettersson and others, 2011).*** How mutations in sarcomeric proteins lead to a myopathy, remains unclear. Based on present knowledge, two hypotheses have been formulated. The first one being that mutations in sarcomeric proteins interfere directly with muscle contractile apparatus or that, claimed in hypothesis two, the presence of nemaline bodies would decrease the number of functional sarcomeres (Ravenscroft and others, 2011a; Ravenscroft and others, 2011b)

Components and structure of nemaline bodies have been analyzed in biopsies and by using transgenic mice. It was shown that nemaline bodies are extensions of Z-discs and mainly consist of α-actinin, myotilin and sarcomeric α-Actin (Jockusch and others, 1980; Schroder and others, 2003; Wallgren-Pettersson and others, 1995; Witt and others, 2006; Yamaguchi and others, 1982). Accumulations of filamentous proteins and desmin have also been described (Ravenscroft and others, 2011b).

In the context of this project, we were wondering if mutations in Klhl31 could also cause nemaline myopathy or otherwise if mutations in Actin, Nebulin and other sarcomeric proteins could alter Klhl31 expression during nemaline myopathy. Our obtained data indicated a potential role for Klhl31 during myofibril assembly as it has been predicted to bind to Nebulin and has been shown to interact with Actin and tropomyosin. However, a mutation in Klhl31 in nemaline myopathy has not been reported so far. Interestingly though, a mutation in a different member of the Kelch-BTB protein family, KBTBD13, causing nemaline myopathy has been published recently (Sambuughin and others, 2010). KBTBD13 similar to Klhl31 is mainly expressed in skeletal and cardiac muscle. Furthermore it was shown that mutations in KBTBD13 that promote nemaline myopathy were found in the kelch-propeller domain potentially changing the structure of the carboxy-terminus of KBTBD13. We were wondering if KBTBD13 might have similar function like Klhl31. However, a function for KBTBD13 has not been described so far. Recently it was reported that KBTBD13 might function as a E3 ubiquitin ligase (Sambuughin and others, 2012). Based on known data, we were wondering if Klhl31 and KBTBD13 could be structurally related. However, when aligned KBTBD13 and Klhl31 do not share a high homology on DNA and protein level (see Appendix A.6).

We therefore cannot compare Klhl31 with KBTBD13. However, based on predicted and observed interactions of Klhl31 with Actin, tropomyosin and Nebulin, it would be interesting to see if mutations of Klhl31 could also play a role in nemaline myopathies. Analysing Klhl31 expression and localisation in fibres affected by nemaline myopathy could potentially also give further insight into the role of Klhl31 in sarcomeres and maybe further clarify a role of Klhl31 during myofibrillogenesis.

7.3 Klhl31 expression and potential function during cardiogenesis

7.3.1 Klhl31 is expressed in the myocardium during chick development

We compared expression of Klhl31 to the expression patterns for published heart marker genes during early heart development of chick embryos.

We observed that Klhl31 was expressed in the same tissues as the myocardium-marker Nkx2.5 throughout all analysed stages of chick development. However, in contrast to Nkx2.5, Klhl31 was not expressed in cardiac progenitor cells prior to fusion of the primary heart tube. Fusion of the primary heart tube in chick correlates with the differentiation of myocytes (Colas and others, 2000; Yuan and Schoenwolf, 2000). It is therefore possible that Klhl31 might have similar function as proposed for C2C12 skeletal myocytes.

Sarcomeres in cardiac muscle display similar organisation to skeletal muscle myofibrils (thick and thin filaments, Z-discs, M-bands) and are comprised of some of the same structural proteins (e.g. Actin, myosin, tropomyosin, and troponin). Furthermore processes regulating cardiac myofibril assembly and stability seem to be similar (Rudy and others, 2001; Sanger and others, 2010), also explained in chapter 1.3).

However, cardiomyocytes express Nebulette, a relatively small homologue of the *Nebulin* gene family (Moncman and Wang, 1995). Just as Nebulin, Nebulette also contains the central repeat domain through which Nebulette can associate with Actin monomers (Jin and Wang, 1991a; Jin and Wang, 1991b; Millevoi and others, 1998; Moncman and Wang, 1995; Moncman and Wang, 1999). Also similar to Nebulin, Nebulette contains a C-terminal SH3 domain and has been shown to interact via the C-terminus with α-actinin, titin, myopalladin and desmin (Bang and others, 2001; Esham and others, 2007; Grunewald and Butt, 2008; Wang and others, 2002). Recently the interaction of the central repeat domain of Nebulette with the tropomyosin/troponin complex has also been revealed (Bonzo and others, 2008; Ogut and others, 2003). Based on the similarity of Nebulin and Nebulette, it was suggested that Nebulette carries out the role that Nebulin mediates in skeletal muscle (Bonzo and others, 2008; Moncman and Wang, 1995).

Evidence that Nebulette might be involved in myofibrillogenesis in heart muscle was reported by Moncman and Wang (1995, 1999). It was shown that Nebulette binds to sarcomeric α-actinin already in premature myofibrils and stays associated to the Z-disc in mature myofibrils, leading to the suggestion that Nebulette might be involved in myofibrillogenesis by connecting the Actin filament to the Z-disc (Moncman and Wang, 1995; Moncman and Wang, 1999).

It was furthermore described that Nebulette might also stabilise the thin filament in a similar way as described for Nebulin (Moncman and Wang, 2002; Pappas and others,

2010). Although Nebulette in comparison to Nebulin seems to be too small to be able to span the whole Actin filament and Nebulette only associates to Actin-fibres in the Z-disc, silencing studies in cardiomyocytes have been reported to generate a reduced size of the thin filament revealing that Nebulette can stabilise thin filaments longer then Nebulette itself (Moncman and Wang, 2002). Further data seemed to confirm an essential role for Nebulette in thin filament length specification, as a knock-down of Nebulette in cardiomyocytes lead to a thin filament phenotype similar to that of reduced thin filament seen in Nebulin depleted skeletal muscle (Bang and others, 2006; Bonzo and others, 2008; Witt and others, 2006).

Nebulette does also interact with the thin filament capping protein tropomyosin (Bonzo and others, 2008), which might further indicate a role for Nebulette in thin filament length specification.

Furthermore, Nebulette also seems to be involved in muscle contraction, as Nebulette deficient cardiomyocytes display weaker heart beats compared to wt cardiomyocytes (Moncman and Wang, 2002).

Based on published data, we can assume that Nebulette functions as Nebulin counterpart in cardiomyocytes. However, Nebulin is also expressed in the heart, but its expression levels are lower compared to levels in skeletal muscle (Bang and others, 2006; Kazmierski and others, 2003).

It was therefore suggested that Nebulin and Nebulette have overlapping functions in cardiomyocytes (Pappas and others, 2011).

Based on our observation of Klhl31 expression in the myocardium exclusively during myogenic differentiation and based on data that Klhl31 might interact with Nebulin and that Klhl31 does interact with Actin, Actin-capping proteins and components of myosin II, we assume that Klhl31 might also be involved in myofibril assembly and thin filament stabilisation during heart development. But we do not know yet, if Klhl31 can also interact with Nebulette. Based on sequence analysis of Nebulette, we did not find the potential binding site for Klhl31, but we were not able to further investigate the structural organisation of this domain. It was reported that both Nebulin and Nebulette display structural similarities in their super-repeat domains (Bjorklund and others, 2010). It might be that the Klhl31 binding site contains a specific structural motif, which would allow Klhl31 to associate with it, both in Nebulin and Nebulette. As the

Klhl31 binding site lies within the boundary of two super-repeat domains, which has been reported to contain conserved binding sites for Actin and tropomyosin/troponin complexes (Labeit and Kolmerer, 1995a; Pfuhl and others, 1996), we wondered if the Klhl31 binding domain or structure could also be found in other domains, both in Nebulin and Nebulette proteins other than predicted super-repeat 20 and 21. Although we have no direct evidence at present, it might be interesting to see if Klhl31 could interact with Nebulette during heart development.

8. Conclusion

Klhl31 has previously been described as a novel protein involved in myogenesis (Abou-Elhamd and others, 2009).

In this report we suggest a potential role for Klhl31 during myocyte differentiation and myofibrillogenesis.

We studied Klhl31 expression in C2C12 mouse myoblast and found increasing expression levels for Klhl31 during the intermediate stage of differentiation, potentially correlating with myofibrillogenesis in mouse myoblasts. We also observed that Klhl31 closely aligned to Actin fibres during C2C12 differentiation. This interaction was later verified by GST-pull down approaches. Nebulin, a giant sarcomeric protein, which binds and stabilises Actin polymers in striated muscles (Pappas and others, 2011), was identified as a potential binding partner for Klhl31 in a Yeast-2-Hybrid screen. Furthermore a close localisation for both Nebulin and Klhl31 was observed in differentiating C2C12 mouse myoblasts and mouse tibialis anterior muscles. Possible interactions of Klhl31 with Nebulin and Actin indicated a potential novel role for Klhl31 within the thin filament of striated muscles. More information about the potential novel function was obtained by the identification of further interaction partners for Klhl31. Thin filament capping protein CapZ and tropomyosin (Fowler, 1996) were pulled down by GST-Klhl31. Taking together our observed localisation pattern for Klhl31 during C2C12 differentiation, the identified possible binding partners for Klhl31, as well as published data for Nebulin, we hypothesised that Klhl31 might be involved in myofibrillogenesis, potentially by either regulating the thin filament length in collaboration with Nebulin or by assisting the assembly of the thin filament to the Z-discs. Klhl31 might even be involved in the assembly of premyofibrils as it also seems to interact with non-muscle myosin II.

Further interacting proteins identified in the GST-pull downs could shed a light of a role for Klhl31 in mature striated muscles. Calmodulin and tropomyosin were found to associate with Klhl31. Together with the observed interaction of Klhl31 with Actin, this data indicates that Klhl31 might be associated to the contractile apparatus in fully developed sarcomeres.

As Klhl31 was shown to be expressed both in the somite after the commitment towards a myogenic fate and in cardiac progenitor cells at the onset of differentiation, we could assume, that Klhl31 might have similar roles in cardiac and skeletal muscle.

9. Bibliography

Abou-Elhamd A. unpublished data.

Abou-Elhamd A, Cooper O, Munsterberg A. 2009. Klhl31 is associated with skeletal myogenesis and its expression is regulated by myogenic signals and Myf-5. Mech Dev 126(10):852-862.

Abou-Elhamd A, Garcia-Morales C. unpublished data.

Abu-Issa R, Waldo K, Kirby ML. 2004. Heart fields: one, two or more? Dev Biol 272(2):281-285.

Adams J, Kelso R, Cooley L. 2000. The kelch repeat superfamily of proteins: propellers of cell function. Trends Cell Biol 10(1):17-24.

Adams JC, Seed B, Lawler J. 1998. Muskelin, a novel intracellular mediator of cell adhesive and cytoskeletal responses to thrombospondin-1. EMBO J 17(17):4964-4974.

Agarkova I, Auerbach D, Ehler E, Perriard JC. 2000. A novel marker for vertebrate embryonic heart, the EH-myomesin isoform. The Journal of biological chemistry 275(14):10256-10264.

Agarkova I, Perriard JC. 2005. The M-band: an elastic web that crosslinks thick filaments in the center of the sarcomere. Trends Cell Biol 15(9):477-485.

Agger K, Cloos PA, Christensen J, Pasini D, Rose S, Rappsilber J, Issaeva I, Canaani E, Salcini AE, Helin K. 2007. UTX and JMJD3 are histone H3K27 demethylases involved in HOX gene regulation and development. Nature 449(7163):731-734.

Agrawal PB, Greenleaf RS, Tomczak KK, Lehtokari VL, Wallgren-Pettersson C, Wallefeld W, Laing NG, Darras BT, Maciver SK, Dormitzer PR and others. 2007. Nemaline myopathy with minicores caused by mutation of the CFL2 gene encoding the skeletal muscle actin-binding protein, cofilin-2. Am J Hum Genet 80(1):162-167.

Ahmad KF, Melnick A, Lax S, Bouchard D, Liu J, Kiang CL, Mayer S, Takahashi S, Licht JD, Prive GG. 2003. Mechanism of SMRT corepressor recruitment by the BCL6 BTB domain. Mol Cell 12(6):1551-1564.

Ahn J, Sanz-Moreno V, Marshall CJ. 2012. The metastasis gene NEDD9 product acts through integrin beta3 and Src to promote mesenchymal motility and inhibit amoeboid motility. J Cell Sci 125:1814-1826.

Albagli O, Dhordain P, Deweindt C, Lecocq G, Leprince D. 1995. The BTB/POZ domain: a new protein-protein interaction motif common to DNA- and actin-binding proteins. Cell Growth Differ 6(9):1193-1198.

Alberts B, Bray D, Lewis J, Raff M, Roberts K, Watson J. 1994. molecular biology of the cell.

Alberts BJ, Alexander: Lewis, Julian: Raff, Martin 2008. molecular biology of the cell. 5th edition.

Alsan BH, Schultheiss TM. 2002. Regulation of avian cardiogenesis by Fgf8 signaling. Development 129(8):1935-1943.

Alvarez-Martinez MT, Porte F, Liautard JP, Sri Widada J. 1997. Effects of profilin-annexin I association on some properties of both profilin and annexin I: modification of the inhibitory activity of profilin on actin polymerization and inhibition of the self-association of annexin I and its interactions with liposomes. Biochim Biophys Acta 1339(2):331-340.

Anderson RH, Webb S, Brown NA, Lamers W, Moorman A. 2003. Development of the heart: (2) Septation of the atriums and ventricles. Heart 89(8):949-958.

Andree B, Duprez D, Vorbusch B, Arnold HH, Brand T. 1998. BMP-2 induces ectopic expression of cardiac lineage markers and interferes with somite formation in chicken embryos. Mech Dev 70(1-2):119-131.

Andres V, Walsh K. 1996. Myogenin expression, cell cycle withdrawal, and phenotypic differentiation are temporally separable events that precede cell fusion upon myogenesis. J Cell Biol 132(4):657-666.

Angers S, Thorpe CJ, Biechele TL, Goldenberg SJ, Zheng N, MacCoss MJ, Moon RT. 2006. The KLHL12-Cullin-3 ubiquitin ligase negatively regulates the Wnt-beta-catenin pathway by targeting Dishevelled for degradation. Nat Cell Biol 8(4):348-357.

Aoyama H, Asamoto K. 1988. Determination of somite cells: independence of cell differentiation and morphogenesis. Development 104(1):15-28.

Aromolaran KA, Benzow KA, Cribbs LL, Koob MD, Piedras-Renteria ES. 2009. Kelch-like 1 protein upregulates T-type currents by an actin-F dependent increase in alpha(1H) channels via the recycling endosome. Channels (Austin) 3(6):402-412.

Aromolaran KA, Benzow KA, Cribbs LL, Koob MD, Piedras-Renteria ES. 2010. T-type current modulation by the actin-binding protein Kelch-like 1. Am J Physiol Cell Physiol 298(6):C1353-1362.

Aromolaran KA, Benzow KA, Cribbs LL, Koob MD, Piedras-Renteria ES. 2012. Elimination of the actin-binding domain in kelch-like 1 protein induces T-type calcium channel modulation only in the presence of action potential waveforms. J Signal Transduct 2012:505346.

Arora PD, Narani N, McCulloch CA. 1999. The compliance of collagen gels regulates transforming growth factor-beta induction of alpha-smooth muscle actin in fibroblasts. Am J Pathol 154(3):871-882.

Arora S, Yang JM, Hait WN. 2005. Identification of the ubiquitin-proteasome pathway in the regulation of the stability of eukaryotic elongation factor-2 kinase. Cancer Res 65(9):3806-3810.

Astier A, Avraham H, Manie SN, Groopman J, Canty T, Avraham S, Freedman AS. 1997. The related adhesion focal tyrosine kinase is tyrosine-phosphorylated after beta1-integrin stimulation in B cells and binds to p130cas. The Journal of biological chemistry 272(1):228-232.

Auber J. 1969. La myofibrillogenese du muscle stile I : Insectes. Journal of Microscopy.

Auerbach D, Thaminy S, Hottiger MO, Stagljar I. 2002. The post-genomic era of interactive proteomics: facts and perspectives. Proteomics 2(6):611-623.

Azakir BA, Di Fulvio S, Therrien C, Sinnreich M. 2010. Dysferlin interacts with tubulin and microtubules in mouse skeletal muscle. PLoS One 5(4):e10122.

Bailey K. 1948. Tropomyosin: a new asymmetric protein component of the muscle fibril. Biochem J 43(2):271-279.

Balogh J, Li Z, Paulin D, Arner A. 2005. Desmin filaments influence myofilament spacing and lateral compliance of slow skeletal muscle fibers. Biophys J 88(2):1156-1165.

Bang ML, Caremani M, Brunello E, Littlefield R, Lieber RL, Chen J, Lombardi V, Linari M. 2009. Nebulin plays a direct role in promoting strong actin-myosin interactions. FASEB J 23(12):4117-4125.

Bang ML, Gregorio C, Labeit S. 2002. Molecular dissection of the interaction of desmin with the C-terminal region of nebulin. J Struct Biol 137(1-2):119-127.

Bang ML, Li X, Littlefield R, Bremner S, Thor A, Knowlton KU, Lieber RL, Chen J. 2006. Nebulin-deficient mice exhibit shorter thin filament lengths and reduced contractile function in skeletal muscle. J Cell Biol 173(6):905-916.

Bang ML, Mudry RE, McElhinny AS, Trombitas K, Geach AJ, Yamasaki R, Sorimachi H, Granzier H, Gregorio CC, Labeit S. 2001. Myopalladin, a novel 145-kilodalton sarcomeric protein with multiple roles in Z-disc and I-band protein assemblies. J Cell Biol 153(2):413-427.

Bardwell VJ, Treisman R. 1994. The POZ domain: a conserved protein-protein interaction motif. Genes Dev 8(14):1664-1677.

Bellin RM, Sernett SW, Becker B, Ip W, Huiatt TW, Robson RM. 1999. Molecular characteristics and interactions of the intermediate filament protein synemin. Interactions with alpha-actinin may anchor synemin-containing heterofilaments. The Journal of biological chemistry 274(41):29493-29499.

Bilak SR, Sernett SW, Bilak MM, Bellin RM, Stromer MH, Huiatt TW, Robson RM. 1998. Properties of the novel intermediate filament protein synemin and its identification in mammalian muscle. Arch Biochem Biophys 355(1):63-76.

Bisaha JG, Bader D. 1991. Identification and characterization of a ventricular-specific avian myosin heavy chain, VMHC1: expression in differentiating cardiac and skeletal muscle. Dev Biol 148(1):355-364.

Bizzarro V, Belvedere R, Dal Piaz F, Parente L, Petrella A. 2010a. Annexin A1 induces skeletal muscle cell migration acting through formyl peptide receptors. PLoS One 7(10):e48246.

Bizzarro V, Fontanella B, Franceschelli S, Pirozzi M, Christian H, Parente L, Petrella A. 2010b. Role of Annexin A1 in mouse myoblast cell differentiation. J Cell Physiol 224(3):757-765.

Bjorklund AK, Light S, Sagit R, Elofsson A. 2010. Nebulin: a study of protein repeat evolution. J Mol Biol 402(1):38-51.

Blanchoin L, Pollard TD, Hitchcock-DeGregori SE. 2001. Inhibition of the Arp2/3 complex-nucleated actin polymerization and branch formation by tropomyosin. Curr Biol 11(16):1300-1304.

Bomont P, Cavalier L, Blondeau F, Ben Hamida C, Belal S, Tazir M, Demir E, Topaloglu H, Korinthenberg R, Tuysuz B and others. 2000. The gene encoding gigaxonin, a new member of the cytoskeletal BTB/kelch repeat family, is mutated in giant axonal neuropathy. Nat Genet 26(3):370-374.

Bonzo JR, Norris AA, Esham M, Moncman CL. 2008. The nebulette repeat domain is necessary for proper maintenance of tropomyosin with the cardiac sarcomere. Exp Cell Res 314(19):3519-3530.

Boriek AM, Capetanaki Y, Hwang W, Officer T, Badshah M, Rodarte J, Tidball JG. 2001. Desmin integrates the three-dimensional mechanical properties of muscles. Am J Physiol Cell Physiol 280(1):C46-52.

Bork P, Doolittle RF. 1994. Drosophila kelch motif is derived from a common enzyme fold. J Mol Biol 236(5):1277-1282.

Borycki A, Brown AM, Emerson CP, Jr. 2000. Shh and Wnt signaling pathways converge to control Gli gene activation in avian somites. Development 127(10):2075-2087.

Borycki AG, Brunk B, Tajbakhsh S, Buckingham M, Chiang C, Emerson CP, Jr. 1999. Sonic hedgehog controls epaxial muscle determination through Myf5 activation. Development 126(18):4053-4063.

Borycki AG, Mendham L, Emerson CP, Jr. 1998. Control of somite patterning by Sonic hedgehog and its downstream signal response genes. Development 125(4):777-790.

Bovolenta P, Esteve P, Ruiz JM, Cisneros E, Lopez-Rios J. 2008. Beyond Wnt inhibition: new functions of secreted Frizzled-related proteins in development and disease. J Cell Sci 121:737-746.

Bradford MM. 1976. A rapid and sensitive method for the quantitation of microgram quantities of protein utilizing the principle of protein-dye binding. Anal Biochem 72:248-254.

Brand-Saberi B, Ebensperger C, Wilting J, Balling R, Christ B. 1993. The ventralizing effect of the notochord on somite differentiation in chick embryos. Anat Embryol (Berl) 188(3):239-245.

Brand T. 2003. Heart development: molecular insights into cardiac specification and early morphogenesis. Dev Biol 258(1):1-19.

Braun T, Buschhausen-Denker G, Bober E, Tannich E, Arnold HH. 1989. A novel human muscle factor related to but distinct from MyoD1 induces myogenic conversion in 10T1/2 fibroblasts. EMBO J 8(3):701-709.

Braun T, Gautel M. 2011. Transcriptional mechanisms regulating skeletal muscle differentiation, growth and homeostasis. Nat Rev Mol Cell Biol 12(6):349-361.

Braybrook C, Warry G, Howell G, Arnason A, Bjornsson A, Moore GE, Ross MT, Stanier P. 2001. Identification and characterization of KLHL4, a novel human homologue of the Drosophila Kelch gene that maps within the X-linked cleft palate and Ankyloglossia (CPX) critical region. Genomics 72(2):128-136.

Brennan TJ, Edmondson DG, Li L, Olson EN. 1991. Transforming growth factor beta represses the actions of myogenin through a mechanism independent of DNA binding. Proc Natl Acad Sci U S A 88(9):3822-3826.

Brent AE, Schweitzer R, Tabin CJ. 2003. A somitic compartment of tendon progenitors. Cell 113(2):235-248.

Brockdorff N. 2011. Chromosome silencing mechanisms in X-chromosome inactivation: unknown unknowns. Development 138(23):5057-5065.

Bruckner A, Polge C, Lentze N, Auerbach D, Schlattner U. 2009. Yeast two-hybrid, a powerful tool for systems biology. Int J Mol Sci 10(6):2763-2788.

Bruneau BG, Logan M, Davis N, Levi T, Tabin CJ, Seidman JG, Seidman CE. 1999. Chamber-specific cardiac expression of Tbx5 and heart defects in Holt-Oram syndrome. Dev Biol 211(1):100-108.

Brunet LJ, McMahon JA, McMahon AP, Harland RM. 1998. Noggin, cartilage morphogenesis, and joint formation in the mammalian skeleton. Science 280(5368):1455-1457.

Buck D, Hudson BD, Ottenheijm CA, Labeit S, Granzier H. 2011. Differential splicing of the large sarcomeric protein nebulin during skeletal muscle development. J Struct Biol 170(2):325-333.

Buckingham M. 2001. Skeletal muscle formation in vertebrates. Curr Opin Genet Dev 11(4):440-448.

Buckingham M, Bajard L, Chang T, Daubas P, Hadchouel J, Meilhac S, Montarras D, Rocancourt D, Relaix F. 2003. The formation of skeletal muscle: from somite to limb. J Anat 202(1):59-68.

Buckingham M, Meilhac S, Zaffran S. 2005. Building the mammalian heart from two sources of myocardial cells. Nat Rev Genet 6(11):826-835.

Burattini S, Ferri P, Battistelli M, Curci R, Luchetti F, Falcieri E. 2004. C2C12 murine myoblasts as a model of skeletal muscle development: morpho-functional characterization. Eur J Histochem 48(3):223-233.

Caldwell JE, Heiss SG, Mermall V, Cooper JA. 1989. Effects of CapZ, an actin capping protein of muscle, on the polymerization of actin. Biochemistry 28(21):8506-8514.

Camp E, Dietrich S, Munsterberg A. 2012. Fate Mapping Identifies the Origin of SHF/AHF Progenitors in the Chick Primitive Streak. PLoS One 7(12):e51948.

Campione M, Ros MA, Icardo JM, Piedra E, Christoffels VM, Schweickert A, Blum M, Franco D, Moorman AF. 2001. Pitx2 expression defines a left cardiac lineage of

cells: evidence for atrial and ventricular molecular isomerism in the iv/iv mice. Dev Biol 231(1):252-264.
Campione M, Steinbeisser H, Schweickert A, Deissler K, van Bebber F, Lowe LA, Nowotschin S, Viebahn C, Haffter P, Kuehn MR and others. 1999. The homeobox gene Pitx2: mediator of asymmetric left-right signaling in vertebrate heart and gut looping. Development 126(6):1225-1234.
Canning P, Cooper CD, Krojer T, Murray JW, Pike AC, Chaikuad A, Keates T, Thangaratnarajah C, Hojzan V, Marsden BD and others. 2013. Structural basis for Cul3 protein assembly with the BTB-Kelch family of E3 ubiquitin ligases. The Journal of biological chemistry 288(11):7803-7814.
Carragher NO, Frame MC. 2004. Focal adhesion and actin dynamics: a place where kinases and proteases meet to promote invasion. Trends Cell Biol 14(5):241-249.
Casella JF, Maack DJ, Lin S. 1986. Purification and initial characterization of a protein from skeletal muscle that caps the barbed ends of actin filaments. The Journal of biological chemistry 261(23):10915-10921.
Castillo A, Nowak R, Littlefield KP, Fowler VM, Littlefield RS. 2009. A nebulin ruler does not dictate thin filament lengths. Biophys J 96(5):1856-1865.
Catterall WA. 1995. Structure and function of voltage-gated ion channels. Annu Rev Biochem 64:493-531.
Cekanova M, Yuan JS, Li X, Kim K, Baek SJ. 2008. Gene alterations by peroxisome proliferator-activated receptor gamma agonists in human colorectal cancer cells. Int J Oncol 32(4):809-819.
Cerone MA, Marchetti A, Bossi G, Blandino G, Sacchi A, Soddu S. 2000. p53 is involved in the differentiation but not in the differentiation-associated apoptosis of myoblasts. Cell Death Differ 7(5):506-508.
Chandra M, Mamidi R, Ford S, Hidalgo C, Witt C, Ottenheijm C, Labeit S, Granzier H. 2009. Nebulin alters cross-bridge cycling kinetics and increases thin filament activation: a novel mechanism for increasing tension and reducing tension cost. The Journal of biological chemistry 284(45):30889-30896.
Chapman DL, Garvey N, Hancock S, Alexiou M, Agulnik SI, Gibson-Brown JJ, Cebra-Thomas J, Bollag RJ, Silver LM, Papaioannou VE. 1996. Expression of the T-box family genes, Tbx1-Tbx5, during early mouse development. Dev Dyn 206(4):379-390.
Chau V, Tobias JW, Bachmair A, Marriott D, Ecker DJ, Gonda DK, Varshavsky A. 1989. A multiubiquitin chain is confined to specific lysine in a targeted short-lived protein. Science 243(4898):1576-1583.
Chen CY, Schwartz RJ. 1996. Recruitment of the tinman homolog Nkx-2.5 by serum response factor activates cardiac alpha-actin gene transcription. Mol Cell Biol 16(11):6372-6384.
Chen Y, Derin R, Petralia RS, Li M. 2002. Actinfilin, a brain-specific actin-binding protein in postsynaptic density. The Journal of biological chemistry 277(34):30495-30501.
Chen Y, Li M. 2005. Interactions between CAP70 and actinfilin are important for integrity of actin cytoskeleton structures in neurons. Neuropharmacology 49(7):1026-1041.
Cheney RE, Mooseker MS. 1992. Unconventional myosins. Curr Opin Cell Biol 4(1):27-35.
Cheroki C, Krepischi-Santos AC, Szuhai K, Brenner V, Kim CA, Otto PA, Rosenberg C. 2008. Genomic imbalances associated with mullerian aplasia. J Med Genet 45(4):228-232.

Chien CT, Bartel PL, Sternglanz R, Fields S. 1991. The two-hybrid system: a method to identify and clone genes for proteins that interact with a protein of interest. Proc Natl Acad Sci U S A 88(21):9578-9582.
Chimote AA, Kuras Z, Conforti L. 2012. Disruption of kv1.3 channel forward vesicular trafficking by hypoxia in human T lymphocytes. The Journal of biological chemistry 287(3):2055-2067.
Christ B, Brand-Saberi B, Grim M, Wilting J. 1992. Local signalling in dermomyotomal cell type specification. Anat Embryol (Berl) 186(5):505-510.
Christ B, Huang R, Scaal M. 2004. Formation and differentiation of the avian sclerotome. Anat Embryol (Berl) 208(5):333-350.
Christ B, Huang R, Scaal M. 2007. Amniote somite derivatives. Dev Dyn 236(9):2382-2396.
Christ B, Huang R, Wilting J. 2000. The development of the avian vertebral column. Anat Embryol (Berl) 202(3):179-194.
Christ B, Ordahl CP. 1995. Early stages of chick somite development. Anat Embryol (Berl) 191(5):381-396.
Christoffels VM, Habets PE, Franco D, Campione M, de Jong F, Lamers WH, Bao ZZ, Palmer S, Biben C, Harvey RP and others. 2000. Chamber formation and morphogenesis in the developing mammalian heart. Dev Biol 223(2):266-278.
Cirak S, von Deimling F, Sachdev S, Errington WJ, Herrmann R, Bonnemann C, Brockmann K, Hinderlich S, Lindner TH, Steinbrecher A and others. 2010. Kelch-like homologue 9 mutation is associated with an early onset autosomal dominant distal myopathy. Brain 133:2123-2135.
Colas JF, Lawson A, Schoenwolf GC. 2000. Evidence that translation of smooth muscle alpha-actin mRNA is delayed in the chick promyocardium until fusion of the bilateral heart-forming regions. Dev Dyn 218(2):316-330.
Conen PE, Murphy EG, Donohue WL. 1963. Light and Electron Microscopic Studies of "Myogranules" in a Child with Hypotonia and Muscle Weakness. Can Med Assoc J 89:983-986.
Cooke R. 1997. Actomyosin interaction in striated muscle. Physiol Rev 77(3):671-697.
Cooper JA, Schafer DA. 2000. Control of actin assembly and disassembly at filament ends. Curr Opin Cell Biol 12(1):97-103.
Cooper ST, Maxwell AL, Kizana E, Ghoddusi M, Hardeman EC, Alexander IE, Allen DG, North KN. 2004. C2C12 co-culture on a fibroblast substratum enables sustained survival of contractile, highly differentiated myotubes with peripheral nuclei and adult fast myosin expression. Cell Motil Cytoskeleton 58(3):200-211.
Coue M, Brenner SL, Spector I, Korn ED. 1987. Inhibition of actin polymerization by latrunculin A. FEBS Lett 213(2):316-318.
Craig RW, Padron R. 2004. molecular structure of the sarcomere. Myology pp. 129-166, 3rd ed., McGraw-Hill, Inc., New York.
Crawford GL, Horowits R. 2011. Scaffolds and chaperones in myofibril assembly: putting the striations in striated muscle. Biophys Rev 3(1):25-32.
Crompton MR, Bartlett TJ, MacGregor AD, Manfioletti G, Buratti E, Giancotti V, Goodwin GH. 1992. Identification of a novel vertebrate homeobox gene expressed in haematopoietic cells. Nucleic Acids Res 20(21):5661-5667.
Dabiri GA, Turnacioglu KK, Sanger JM, Sanger JW. 1997. Myofibrillogenesis visualized in living embryonic cardiomyocytes. Proc Natl Acad Sci U S A 94(17):9493-9498.
David Y, Ziv T, Admon A, Navon A. 2010. The E2 ubiquitin-conjugating enzymes direct polyubiquitination to preferred lysines. The Journal of biological chemistry 285(12):8595-8604.
Davies TH, Sanchez ER. 2005. Fkbp52. Int J Biochem Cell Biol 37(1):42-47.

de Forges H, Bouissou A, Perez F. 2012. Interplay between microtubule dynamics and intracellular organization. Int J Biochem Cell Biol 44(2):266-274.
de la Cruz MV, Sanchez-Gomez C, Arteaga MM, Arguello C. 1977. Experimental study of the development of the truncus and the conus in the chick embryo. J Anat 123:661-686.
De La Cruz MV, Sanchez-Gomez C, Palomino MA. 1989. The primitive cardiac regions in the straight tube heart (Stage 9) and their anatomical expression in the mature heart: An experimental study in the chick embryo. J Anat 165:121-131.
Deng L, Wang C, Spencer E, Yang L, Braun A, You J, Slaughter C, Pickart C, Chen ZJ. 2000. Activation of the IkappaB kinase complex by TRAF6 requires a dimeric ubiquitin-conjugating enzyme complex and a unique polyubiquitin chain. Cell 103(2):351-361.
Dequeant ML, Pourquie O. 2008. Segmental patterning of the vertebrate embryonic axis. Nat Rev Genet 9(5):370-382.
Dietrich S, Schubert FR, Lumsden A. 1997. Control of dorsoventral pattern in the chick paraxial mesoderm. Development 124(19):3895-3908.
Dlugosz AA, Antin PB, Nachmias VT, Holtzer H. 1984. The relationship between stress fiber-like structures and nascent myofibrils in cultured cardiac myocytes. J Cell Biol 99(6):2268-2278.
Dodds E, Dunckley MG, Naujoks K, Michaelis U, Dickson G. 1998. Lipofection of cultured mouse muscle cells: a direct comparison of Lipofectamine and DOSPER. Gene Ther 5(4):542-551.
Donner K, Nowak KJ, Aro M, Pelin K, Wallgren-Pettersson C. 2006. Developmental and muscle-type-specific expression of mouse nebulin exons 127 and 128. Genomics 88(4):489-495.
Donner K, Ollikainen M, Ridanpaa M, Christen HJ, Goebel HH, de Visser M, Pelin K, Wallgren-Pettersson C. 2002. Mutations in the beta-tropomyosin (TPM2) gene--a rare cause of nemaline myopathy. Neuromuscul Disord 12(2):151-158.
Donner K, Sandbacka M, Lehtokari VL, Wallgren-Pettersson C, Pelin K. 2004. Complete genomic structure of the human nebulin gene and identification of alternatively spliced transcripts. Eur J Hum Genet 12(9):744-751.
Donninger H, Bonome T, Radonovich M, Pise-Masison CA, Brady J, Shih JH, Barrett JC, Birrer MJ. 2004. Whole genome expression profiling of advance stage papillary serous ovarian cancer reveals activated pathways. Oncogene 23(49):8065-8077.
Du A, Sanger JM, Linask KK, Sanger JW. 2003. Myofibrillogenesis in the first cardiomyocytes formed from isolated quail precardiac mesoderm. Dev Biol 257(2):382-394.
Du A, Sanger JM, Sanger JW. 2008. Cardiac myofibrillogenesis inside intact embryonic hearts. Dev Biol 318(2):236-246.
du Puy L, Beqqali A, van Tol HT, Monshouwer-Kloots J, Passier R, Haagsman HP, Roelen BA. 2012. Sarcosin (Krp1) in skeletal muscle differentiation: gene expression profiling and knockdown experiments. Int J Dev Biol 56(4):301-309.
Dubrulle J, Pourquie O. 2003. Welcome to syndetome: a new somitic compartment. Dev Cell 4(5):611-612.
Duda DM, Borg LA, Scott DC, Hunt HW, Hammel M, Schulman BA. 2008. Structural insights into NEDD8 activation of cullin-RING ligases: conformational control of conjugation. Cell 134(6):995-1006.
Dyer LA, Kirby ML. 2009. The role of secondary heart field in cardiac development. Dev Biol 336(2):137-144.
Edlich F, Lucke C. 2011. From cell death to viral replication: the diverse functions of the membrane-associated FKBP38. Curr Opin Pharmacol 11(4):348-353.

Edmondson DG, Olson EN. 1989. A gene with homology to the myc similarity region of MyoD1 is expressed during myogenesis and is sufficient to activate the muscle differentiation program. Genes Dev 3(5):628-640.

Edstrom L, Thornell LE, Eriksson A. 1980. A new type of hereditary distal myopathy with characteristic sarcoplasmic bodies and intermediate (skeletin) filaments. J Neurol Sci 47(2):171-190.

Ehler E, Rothen BM, Hammerle SP, Komiyama M, Perriard JC. 1999. Myofibrillogenesis in the developing chicken heart: assembly of Z-disk, M-line and the thick filaments. J Cell Sci 112:1529-1539.

Elliott G, Lowy J, Worthington C. 1963. An x-ray and light-diffraction study of the filament lattice of striated muscle in the living state and in rigor. J Mol Biol.

Emerson CP. 1990. Myogenesis and developmental control genes. Curr Opin Cell Biol 2(6):1065-1075.

Esham M, Bryan K, Milnes J, Holmes WB, Moncman CL. 2007. Expression of nebulette during early cardiac development. Cell Motil Cytoskeleton 64(4):258-273.

Fallon JR, Nachmias VT. 1980. Localization of cytoplasmic and skeletal myosins in developing muscle cells by double-label immunofluorescence. J Cell Biol 87(1):237-247.

Fan CM, Porter JA, Chiang C, Chang DT, Beachy PA, Tessier-Lavigne M. 1995. Long-range sclerotome induction by sonic hedgehog: direct role of the amino-terminal cleavage product and modulation by the cyclic AMP signaling pathway. Cell 81(3):457-465.

Fan CM, Tessier-Lavigne M. 1994. Patterning of mammalian somites by surface ectoderm and notochord: evidence for sclerotome induction by a hedgehog homolog. Cell 79(7):1175-1186.

Farah CS, Reinach FC. 1995. The troponin complex and regulation of muscle contraction. FASEB J 9(9):755-767.

Fields S, Song O. 1989. A novel genetic system to detect protein-protein interactions. Nature 340(6230):245-246.

Fischer G, Aumuller T. 2003. Regulation of peptide bond cis/trans isomerization by enzyme catalysis and its implication in physiological processes. Rev Physiol Biochem Pharmacol 148:105-150.

Fischman DA. 1967. An electron microscope study of myofibril formation in embryonic chick skeletal muscle. J Cell Biol 32(3):557-575.

Fock U, Hinssen H. 1999. Identification and localisation of nebulin as a thin filament component of invertebrate chordate muscles. J Comp Physiol B 169(8):555-560.

Fowler VM. 1996. Regulation of actin filament length in erythrocytes and striated muscle. Curr Opin Cell Biol 8(1):86-96.

Fowler VM, Sussmann MA, Miller PG, Flucher BE, Daniels MP. 1993. Tropomodulin is associated with the free (pointed) ends of the thin filaments in rat skeletal muscle. J Cell Biol 120(2):411-420.

Friedman JS, Ray JW, Waseem N, Johnson K, Brooks MJ, Hugosson T, Breuer D, Branham KE, Krauth DS, Bowne SJ and others. 2009. Mutations in a BTB-Kelch protein, KLHL7, cause autosomal-dominant retinitis pigmentosa. Am J Hum Genet 84(6):792-800.

Fruman DA, Burakoff SJ, Bierer BE. 1994. Immunophilins in protein folding and immunosuppression. FASEB J 8(6):391-400.

Fry AC, Staron RS, James CB, Hikida RS, Hagerman FC. 1997. Differential titin isoform expression in human skeletal muscle. Acta Physiol Scand 161(4):473-479.

Fuchs SY, Spiegelman VS, Kumar KG. 2004. The many faces of beta-TrCP E3 ubiquitin ligases: reflections in the magic mirror of cancer. Oncogene 23(11):2028-2036.

Fukuda N, Granzier HL, Ishiwata S, Kurihara S. 2008. Physiological functions of the giant elastic protein titin in mammalian striated muscle. J Physiol Sci 58(3):151-159.

Fukuda N, Wu Y, Nair P, Granzier HL. 2005. Phosphorylation of titin modulates passive stiffness of cardiac muscle in a titin isoform-dependent manner. J Gen Physiol 125(3):257-271.

Furst DO, Obermann WM, van der Ven PF. 1999. Structure and assembly of the sarcomeric M band. Rev Physiol Biochem Pharmacol 138:163-202.

Furst DO, Osborn M, Nave R, Weber K. 1988. The organization of titin filaments in the half-sarcomere revealed by monoclonal antibodies in immunoelectron microscopy: a map of ten nonrepetitive epitopes starting at the Z line extends close to the M line. J Cell Biol 106(5):1563-1572.

Furst DO, Osborn M, Weber K. 1989. Myogenesis in the mouse embryo: differential onset of expression of myogenic proteins and the involvement of titin in myofibril assembly. J Cell Biol 109(2):517-527.

Furukawa M, He YJ, Borchers C, Xiong Y. 2003. Targeting of protein ubiquitination by BTB-Cullin 3-Roc1 ubiquitin ligases. Nat Cell Biol 5(11):1001-1007.

Furukawa M, Xiong Y. 2005. BTB protein Keap1 targets antioxidant transcription factor Nrf2 for ubiquitination by the Cullin 3-Roc1 ligase. Mol Cell Biol 25(1):162-171.

Furutani Y, Umemoto T, Murakami M, Matsui T, Funaba M. 2011. Role of endogenous TGF-beta family in myogenic differentiation of C2C12 cells. J Cell Biochem 112(2):614-624.

Ganay T, Boizot A, Burrer R, Chauvin JP, Bomont P. 2011 Sensory-motor deficits and neurofilament disorganization in gigaxonin-null mice. Mol Neurodegener 6:25.

Garcia-Martinez V, Schoenwolf GC. 1992. Positional control of mesoderm movement and fate during avian gastrulation and neurulation. Dev Dyn 193(3):249-256.

Garcia-Martinez V, Schoenwolf GC. 1993. Primitive-streak origin of the cardiovascular system in avian embryos. Dev Biol 159(2):706-719.

Gautel M. 1996. The super-repeats of titin/connectin and their interactions: glimpses at sarcomeric assembly. Adv Biophys 33:27-37.

Gautel M, Goulding D, Bullard B, Weber K, Furst DO. 1996. The central Z-disk region of titin is assembled from a novel repeat in variable copy numbers. J Cell Sci 109:2747-2754.

Geeves MA. 1991. The dynamics of actin and myosin association and the crossbridge model of muscle contraction. Biochem J 274:1-14.

Geeves MA, Conibear PB. 1995. The role of three-state docking of myosin S1 with actin in force generation. Biophys J 68:194S-199S; discussion 199S-201S.

Gerhard DS, Wagner L, Feingold EA, Shenmen CM, Grouse LH, Schuler G, Klein SL, Old S, Rasooly R, Good P and others. 2004. The status, quality, and expansion of the NIH full-length cDNA project: the Mammalian Gene Collection (MGC). Genome Res 14:2121-2127.

Gerke V, Moss SE. 2002. Annexins: from structure to function. Physiol Rev 82(2):331-371.

Geyer R, Wee S, Anderson S, Yates J, Wolf DA. 2003. BTB/POZ domain proteins are putative substrate adaptors for cullin 3 ubiquitin ligases. Mol Cell 12(3):783-790.

Giles LM, Li L, Chin LS. 2009. Printor, a novel torsinA-interacting protein implicated in dystonia pathogenesis. The Journal of biological chemistry 284(32):21765-21775.
Goebel SJ, Johnson GP, Perkus ME, Davis SW, Winslow JP, Paoletti E. 1990. The complete DNA sequence of vaccinia virus. Virology 179(1):247-266, 517-263.
Gokhin DS, Bang ML, Zhang J, Chen J, Lieber RL. 2009. Reduced thin filament length in nebulin-knockout skeletal muscle alters isometric contractile properties. Am J Physiol Cell Physiol 296(5):C1123-1132.
Goldberg AL. 2003. Protein degradation and protection against misfolded or damaged proteins. Nature 426(6968):895-899.
Goldman RD, Cleland MM, Murthy SN, Mahammad S, Kuczmarski ER. 2012. Inroads into the structure and function of intermediate filament networks. J Struct Biol 177(1):14-23.
Gomes AV, Potter JD, Szczesna-Cordary D. 2002. The role of troponins in muscle contraction. IUBMB Life 54(6):323-333.
Gonsior SM, Gautel M, Hinssen H. 1998. A six-module human nebulin fragment bundles actin filaments and induces actin polymerization. J Muscle Res Cell Motil 19(3):225-235.
Gordon AM, Homsher E, Regnier M. 2000. Regulation of contraction in striated muscle. Physiol Rev 80(2):853-924.
Gordon AM, Huxley AF, Julian FJ. 1966. The variation in isometric tension with sarcomere length in vertebrate muscle fibres. J Physiol 184(1):170-192.
Graham FL, Smiley J, Russell WC, Nairn R. 1977. Characteristics of a human cell line transformed by DNA from human adenovirus type 5. J Gen Virol 36(1):59-74.
Granger BL, Repasky EA, Lazarides E. 1982. Synemin and vimentin are components of intermediate filaments in avian erythrocytes. J Cell Biol 92(2):299-312.
Granzier H, Labeit S. 2002. Cardiac titin: an adjustable multi-functional spring. J Physiol 541:335-342.
Granzier HL, Akster HA, Ter Keurs HE. 1991. Effect of thin filament length on the force-sarcomere length relation of skeletal muscle. Am J Physiol 260:C1060-1070.
Greenfield A, Carrel L, Pennisi D, Philippe C, Quaderi N, Siggers P, Steiner K, Tam PP, Monaco AP, Willard HF and others. 1998. The UTX gene escapes X inactivation in mice and humans. Hum Mol Genet 7(4):737-742.
Gregorio CC, Fowler VM. 1995. Mechanisms of thin filament assembly in embryonic chick cardiac myocytes: tropomodulin requires tropomyosin for assembly. J Cell Biol 129(3):683-695.
Gregorio CC, Granzier H, Sorimachi H, Labeit S. 1999. Muscle assembly: a titanic achievement? Curr Opin Cell Biol 11(1):18-25.
Gregorio CC, Weber A, Bondad M, Pennise CR, Fowler VM. 1995. Requirement of pointed-end capping by tropomodulin to maintain actin filament length in embryonic chick cardiac myocytes. Nature 377(6544):83-86.
Gros J, Scaal M, Marcelle C. 2004. A two-step mechanism for myotome formation in chick. Dev Cell 6(6):875-882.
Grove BK, Kurer V, Lehner C, Doetschman TC, Perriard JC, Eppenberger HM. 1984. A new 185,000-dalton skeletal muscle protein detected by monoclonal antibodies. J Cell Biol 98(2):518-524.
Grunewald TG, Butt E. 2008. The LIM and SH3 domain protein family: structural proteins or signal transducers or both? Mol Cancer 7:31.
Guger KA, Gumbiner BM. 1995. beta-Catenin has Wnt-like activity and mimics the Nieuwkoop signaling center in Xenopus dorsal-ventral patterning. Dev Biol 172(1):115-125.

Hamburger V, Hamilton HL. 1992. A series of normal stages in the development of the chick embryo. 1951. Dev Dyn 195(4):231-272.
Hanashima A, Kubokawa K, Kimura S. 2009. Structure of the amphioxus nebulin gene and evolution of the nebulin family genes. Gene 443(1-2):76-82.
Hanson J, Huxley HE. 1957. Quantitative studies on the structure of cross-striated myofibrils. II. Investigations by biochemical techniques. Biochim Biophys Acta 23(2):250-260.
Hara T, Ishida H, Raziuddin R, Dorkhom S, Kamijo K, Miki T. 2004. Novel kelch-like protein, KLEIP, is involved in actin assembly at cell-cell contact sites of Madin-Darby canine kidney cells. Mol Biol Cell 15(3):1172-1184.
Hart M, Concordet JP, Lassot I, Albert I, del los Santos R, Durand H, Perret C, Rubinfeld B, Margottin F, Benarous R and others. 1999. The F-box protein beta-TrCP associates with phosphorylated beta-catenin and regulates its activity in the cell. Curr Biol 9(4):207-210.
Heidenhain M. 1913. Uber die Entstehung der quergestreiften Muskelsubstanz bei der Forelle. Archiv Mikroskopische Anatomie EntivMech.
Helmes M, Trombitas K, Centner T, Kellermayer M, Labeit S, Linke WA, Granzier H. 1999. Mechanically driven contour-length adjustment in rat cardiac titin's unique N2B sequence: titin is an adjustable spring. Circ Res 84(11):1339-1352.
Helmes M, Trombitas K, Granzier H. 1996. Titin develops restoring force in rat cardiac myocytes. Circ Res 79(3):619-626.
Hemken PM, Bellin RM, Sernett SW, Becker B, Huiatt TW, Robson RM. 1997. Molecular characteristics of the novel intermediate filament protein paranemin. Sequence reveals EAP-300 and IFAPa-400 are highly homologous to paranemin. The Journal of biological chemistry 272(51):32489-32499.
Herrmann H, Aebi U. 2000. Intermediate filaments and their associates: multi-talented structural elements specifying cytoarchitecture and cytodynamics. Curr Opin Cell Biol 12(1):79-90.
Hershko A, Ciechanover A. 1998. The ubiquitin system. Annu Rev Biochem 67:425-479.
Herzog W, Leonard T, Joumaa V, DuVall M, Panchangam A. 2012. The three filament model of skeletal muscle stability and force production. Mol Cell Biomech 9(3):175-191.
Hibbs RG. 1956. Electron microscopy of developing cardiac muscle in chick embryos. Am J Anat 99(1):17-51.
Hinz B. 2006. Masters and servants of the force: the role of matrix adhesions in myofibroblast force perception and transmission. Eur J Cell Biol 85(3-4):175-181.
Holtzer H, Hijikata T, Lin ZX, Zhang ZQ, Holtzer S, Protasi F, Franzini-Armstrong C, Sweeney HL. 1997. Independent assembly of 1.6 microns long bipolar MHC filaments and I-Z-I bodies. Cell Struct Funct 22(1):83-93.
Hong S, Cho YW, Yu LR, Yu H, Veenstra TD, Ge K. 2007. Identification of JmjC domain-containing UTX and JMJD3 as histone H3 lysine 27 demethylases. Proc Natl Acad Sci U S A 104(47):18439-18444.
Houmeida A, Holt J, Tskhovrebova L, Trinick J. 1995. Studies of the interaction between titin and myosin. J Cell Biol 131:1471-1481.
Hudson AM, Cooley L. 2010. Drosophila Kelch functions with Cullin-3 to organize the ring canal actin cytoskeleton. J Cell Biol 188(1):29-37.
Hui CC, Angers S. 2011. Gli proteins in development and disease. Annu Rev Cell Dev Biol 27:513-537.
Huxley AF. 1957. Muscle structure and theories of contraction. Prog Biophys Biophys Chem 7:255-318.

Huxley AF, Simmons RM. 1971. Proposed mechanism of force generation in striated muscle. Nature 233(5321):533-538.
Huxley HE, Hanson J. 1957. Quantitative studies on the structure of cross-striated myofibrils. I. Investigations by interference microscopy. Biochim Biophys Acta 23(2):229-249.
Hynes RO. 2002. Integrins: bidirectional, allosteric signaling machines. Cell 110(6):673-687.
I. Neeman LF, Y. Kashman. 1975. Isolation of a new toxin from the sponge Latrunculia magnifica in the Gulf of Aquaba (Red Sea). Marine Biology.
Ilkovski B, Nowak KJ, Domazetovska A, Maxwell AL, Clement S, Davies KE, Laing NG, North KN, Cooper ST. 2004. Evidence for a dominant-negative effect in ACTA1 nemaline myopathy caused by abnormal folding, aggregation and altered polymerization of mutant actin isoforms. Hum Mol Genet 13(16):1727-1743.
Ito N, Phillips SE, Yadav KD, Knowles PF. 1994. Crystal structure of a free radical enzyme, galactose oxidase. J Mol Biol 238(5):794-814.
Iwata S, Souta-Kuribara A, Yamakawa A, Sasaki T, Shimizu T, Hosono O, Kawasaki H, Tanaka H, Dang NH, Watanabe T and others. 2005. HTLV-I Tax induces and associates with Crk-associated substrate lymphocyte type (Cas-L). Oncogene 24(7):1262-1271.
Janot M, Audfray A, Loriol C, Germot A, Maftah A, Dupuy F. 2009. Glycogenome expression dynamics during mouse C2C12 myoblast differentiation suggests a sequential reorganization of membrane glycoconjugates. BMC Genomics 10:483.
Jin JP, Wang K. 1991a. Cloning, expression, and protein interaction of human nebulin fragments composed of varying numbers of sequence modules. The Journal of biological chemistry 266(31):21215-21223.
Jin JP, Wang K. 1991b. Nebulin as a giant actin-binding template protein in skeletal muscle sarcomere. Interaction of actin and cloned human nebulin fragments. FEBS Lett 281(1-2):93-96.
Jin L, Pahuja KB, Wickliffe KE, Gorur A, Baumgartel C, Schekman R, Rape M. 2012. Ubiquitin-dependent regulation of COPII coat size and function. Nature 482(7386):495-500.
Jin L, Williamson A, Banerjee S, Philipp I, Rape M. 2008. Mechanism of ubiquitin-chain formation by the human anaphase-promoting complex. Cell 133(4):653-665.
Jockusch BM, Veldman H, Griffiths GW, van Oost BA, Jennekens FG. 1980. Immunofluorescence microscopy of a myopathy. alpha-Actinin is a major constituent of nemaline rods. Exp Cell Res 127(2):409-420.
Johnson RL, Laufer E, Riddle RD, Tabin C. 1994. Ectopic expression of Sonic hedgehog alters dorsal-ventral patterning of somites. Cell 79(7):1165-1173.
Johnston JJ, Kelley RI, Crawford TO, Morton DH, Agarwala R, Koch T, Schaffer AA, Francomano CA, Biesecker LG. 2000. A novel nemaline myopathy in the Amish caused by a mutation in troponin T1. Am J Hum Genet 67(4):814-821.
Joo YM, Lee MA, Lee YM, Kim MS, Kim SY, Jeon EH, Choi JK, Kim WH, Lee HC, Min BI and others. 2004. Identification of chicken nebulin isoforms of the 31-residue motifs and non-muscle nebulin. Biochem Biophys Res Commun 325(4):1286-1291.
Kabsch W, Mannherz HG, Suck D, Pai EF, Holmes KC. 1990. Atomic structure of the actin:DNase I complex. Nature 347(6288):37-44.
Kabsch W, Vandekerckhove J. 1992. Structure and function of actin. Annu Rev Biophys Biomol Struct 21:49-76.

Kalyva A, Schmidtmann A, Geeves MA. 2012. In vitro formation and characterization of the skeletal muscle alpha.beta tropomyosin heterodimers. Biochemistry 51(32):6388-6399.
Kamm KE, Stull JT. 2011. Signaling to myosin regulatory light chain in sarcomeres. The Journal of biological chemistry 286(12):9941-9947.
Kanehori K, Ishibashi T, Chiba Y, Tanai H, Watanabe S. 2003. NEDO human cDNA sequencing project. EMBL/GenBank/DDBJ databases.
Kang CB, Hong Y, Dhe-Paganon S, Yoon HS. 2008. FKBP family proteins: immunophilins with versatile biological functions. Neurosignals 16(4):318-325.
Kang MI, Kobayashi A, Wakabayashi N, Kim SG, Yamamoto M. 2004. Scaffolding of Keap1 to the actin cytoskeleton controls the function of Nrf2 as key regulator of cytoprotective phase 2 genes. Proc Natl Acad Sci U S A 101(7):2046-2051.
Kapitein LC, Hoogenraad CC. 2011. Which way to go? Cytoskeletal organization and polarized transport in neurons. Mol Cell Neurosci 46(1):9-20.
Kaplan Y, Gibbs-Bar L, Kalifa Y, Feinstein-Rotkopf Y, Arama E. 2010. Gradients of a ubiquitin E3 ligase inhibitor and a caspase inhibitor determine differentiation or death in spermatids. Dev Cell 19(1):160-173.
Katagiri T, Yamaguchi A, Komaki M, Abe E, Takahashi N, Ikeda T, Rosen V, Wozney JM, Fujisawa-Sehara A, Suda T. 1994. Bone morphogenetic protein-2 converts the differentiation pathway of C2C12 myoblasts into the osteoblast lineage. J Cell Biol 127:1755-1766.
Kawashima H, Fujino Y, Mochizuki M. 1988. Effects of a new immunosuppressive agent, FK506, on experimental autoimmune uveoretinitis in rats. Invest Ophthalmol Vis Sci 29(8):1265-1271.
Kay JE. 1996. Structure-function relationships in the FK506-binding protein (FKBP) family of peptidylprolyl cis-trans isomerases. Biochem J 314:361-385.
Kazmierski ST, Antin PB, Witt CC, Huebner N, McElhinny AS, Labeit S, Gregorio CC. 2003. The complete mouse nebulin gene sequence and the identification of cardiac nebulin. J Mol Biol 328(4):835-846.
Kelly RG. 2012. The second heart field. Curr Top Dev Biol 100:33-65.
Kelly RG, Brown NA, Buckingham ME. 2001. The arterial pole of the mouse heart forms from Fgf10-expressing cells in pharyngeal mesoderm. Dev Cell 1(3):435-440.
Kelso RJ, Hudson AM, Cooley L. 2002. Drosophila Kelch regulates actin organization via Src64-dependent tyrosine phosphorylation. J Cell Biol 156(4):703-713.
Keng VW, Fujimori KE, Myint Z, Tamamaki N, Nojyo Y, Noguchi T. 1998. Expression of Hex mRNA in early murine postimplantation embryo development. FEBS Lett 426(2):183-186.
Kerenyi L, Gallyas F. 1973. [Errors in quantitative estimations on agar electrophoresis using silver stain]. Clin Chim Acta 47(3):425-436.
Keyte A, Hutson MR. 2012. The neural crest in cardiac congenital anomalies. Differentiation 84(1):25-40.
Kigoshi Y, Tsuruta F, Chiba T. 2011. Ubiquitin ligase activity of Cul3-KLHL7 protein is attenuated by autosomal dominant retinitis pigmentosa causative mutation. The Journal of biological chemistry 286(38):33613-33621.
Kim IF, Mohammadi E, Huang RC. 1999. Isolation and characterization of IPP, a novel human gene encoding an actin-binding, kelch-like protein. Gene 228(1-2):73-83.
Kim M, Gans JD, Nogueira C, Wang A, Paik JH, Feng B, Brennan C, Hahn WC, Cordon-Cardo C, Wagner SN and others. 2006. Comparative oncogenomics identifies NEDD9 as a melanoma metastasis gene. Cell 125(7):1269-1281.
Kinder SJ, Tsang TE, Quinlan GA, Hadjantonakis AK, Nagy A, Tam PP. 1999. The orderly allocation of mesodermal cells to the extraembryonic structures and the

anteroposterior axis during gastrulation of the mouse embryo. Development 126(21):4691-4701.
Kirby ML, Gale TF, Stewart DE. 1983. Neural crest cells contribute to normal aorticopulmonary septation. Science 220(4601):1059-1061.
Klaus A, Saga Y, Taketo MM, Tzahor E, Birchmeier W. 2007. Distinct roles of Wnt/beta-catenin and Bmp signaling during early cardiogenesis. Proc Natl Acad Sci U S A 104(47):18531-18536.
Kobayashi A, Kang MI, Okawa H, Ohtsuji M, Zenke Y, Chiba T, Igarashi K, Yamamoto M. 2004. Oxidative stress sensor Keap1 functions as an adaptor for Cul3-based E3 ligase to regulate proteasomal degradation of Nrf2. Mol Cell Biol 24(16):7130-7139.
Komander D, Rape M. 2012. The ubiquitin code. Annu Rev Biochem 81:203-229.
Kontrogianni-Konstantopoulos A, Catino DH, Strong JC, Bloch RJ. 2006. De novo myofibrillogenesis in C2C12 cells: evidence for the independent assembly of M bands and Z disks. Am J Physiol Cell Physiol 290(2):C626-637.
Kostyukova AS. 2008. Capping complex formation at the slow-growing end of the actin filament. Biochemistry (Mosc) 73(13):1467-1472.
Kostyukova AS, Choy A, Rapp BA. 2006. Tropomodulin binds two tropomyosins: a novel model for actin filament capping. Biochemistry 45(39):12068-12075.
Kostyukova AS, Rapp BA, Choy A, Greenfield NJ, Hitchcock-DeGregori SE. 2005. Structural requirements of tropomodulin for tropomyosin binding and actin filament capping. Biochemistry 44(12):4905-4910.
Krek W. 2003. BTB proteins as henchmen of Cul3-based ubiquitin ligases. Nat Cell Biol 5(11):950-951.
Kroll J, Shi X, Caprioli A, Liu HH, Waskow C, Lin KM, Miyazaki T, Rodewald HR, Sato TN. 2005. The BTB-kelch protein KLHL6 is involved in B-lymphocyte antigen receptor signaling and germinal center formation. Mol Cell Biol 25(19):8531-8540.
Kruger M, Mennerich D, Fees S, Schafer R, Mundlos S, Braun T. 2001. Sonic hedgehog is a survival factor for hypaxial muscles during mouse development. Development 128(5):743-752.
Kruger M, Wright J, Wang K. 1991. Nebulin as a length regulator of thin filaments of vertebrate skeletal muscles: correlation of thin filament length, nebulin size, and epitope profile. J Cell Biol 115(1):97-107.
Kulikowski RR, Manasek FJ. 1979. Myosin localization in cultured embryonic cardiac myocytes. Motility in Cell Function.
Kumar CC, Mohan SR, Zavodny PJ, Narula SK, Leibowitz PJ. 1989. Characterization and differential expression of human vascular smooth muscle myosin light chain 2 isoform in nonmuscle cells. Biochemistry 28(9):4027-4035.
Kurahashi H, Akagi K, Inazawa J, Ohta T, Niikawa N, Kayatani F, Sano T, Okada S, Nishisho I. 1995. Isolation and characterization of a novel gene deleted in DiGeorge syndrome. Hum Mol Genet 4(4):541-549.
Kushmerick MJ. 1998. Energy balance in muscle activity: simulations of ATPase coupled to oxidative phosphorylation and to creatine kinase. Comp Biochem Physiol B Biochem Mol Biol 120(1):109-123.
Laaser I, Kolb HJ, Adamski J. 2005. Characterization of the UTY gene. EMBL/GenBank/DDBJ databases.
Labeit S, Gibson T, Lakey A, Leonard K, Zeviani M, Knight P, Wardale J, Trinick J. 1991. Evidence that nebulin is a protein-ruler in muscle thin filaments. FEBS Lett 282(2):313-316.
Labeit S, Kolmerer B. 1995a. The complete primary structure of human nebulin and its correlation to muscle structure. J Mol Biol 248(2):308-315.

Labeit S, Kolmerer B. 1995b. Titins: giant proteins in charge of muscle ultrastructure and elasticity. Science 270(5234):293-296.
Laezza F, Wilding TJ, Sequeira S, Coussen F, Zhang XZ, Hill-Robinson R, Mulle C, Huettner JE, Craig AM. 2007. KRIP6: a novel BTB/kelch protein regulating function of kainate receptors. Mol Cell Neurosci 34(4):539-550.
Laezza F, Wilding TJ, Sequeira S, Craig AM, Huettner JE. 2008. The BTB/kelch protein, KRIP6, modulates the interaction of PICK1 with GluR6 kainate receptors. Neuropharmacology 55(7):1131-1139.
Laing NG, Wilton SD, Akkari PA, Dorosz S, Boundy K, Kneebone C, Blumbergs P, White S, Watkins H, Love DR and others. 1995. A mutation in the alpha tropomyosin gene TPM3 associated with autosomal dominant nemaline myopathy. Nat Genet 9(1):75-79.
Lam E, Martin M, Wiederrecht G. 1995. Isolation of a cDNA encoding a novel human FK506-binding protein homolog containing leucine zipper and tetratricopeptide repeat motifs. Gene 160(2):297-302.
Lan F, Bayliss PE, Rinn JL, Whetstine JR, Wang JK, Chen S, Iwase S, Alpatov R, Issaeva I, Canaani E and others. 2007. A histone H3 lysine 27 demethylase regulates animal posterior development. Nature 449(7163):689-694.
Lassar AB, Davis RL, Wright WE, Kadesch T, Murre C, Voronova A, Baltimore D, Weintraub H. 1991. Functional activity of myogenic HLH proteins requires hetero-oligomerization with E12/E47-like proteins in vivo. Cell 66(2):305-315.
Laugwitz KL, Moretti A, Caron L, Nakano A, Chien KR. 2008. Islet1 cardiovascular progenitors: a single source for heart lineages? Development 135(2):193-205.
Lazarides E. 1975. Tropomyosin antibody: the specific localization of tropomyosin in nonmuscle cells. J Cell Biol 65(3):549-561.
Lazarides E. 1982. Intermediate filaments: a chemically heterogeneous, developmentally regulated class of proteins. Annu Rev Biochem 51:219-250.
Lazarides E, Burridge K. 1975. Alpha-actinin: immunofluorescent localization of a muscle structural protein in nonmuscle cells. Cell 6(3):289-298.
Lecuona E, Minin A, Trejo HE, Chen J, Comellas AP, Sun H, Grillo D, Nekrasova OE, Welch LC, Szleifer I and others. 2009. Myosin-Va restrains the trafficking of Na+/K+-ATPase-containing vesicles in alveolar epithelial cells. J Cell Sci 122(Pt 21):3915-3922.
Lee CS, Buttitta LA, May NR, Kispert A, Fan CM. 2000. SHH-N upregulates Sfrp2 to mediate its competitive interaction with WNT1 and WNT4 in the somitic mesoderm. Development 127(1):109-118.
Lee DH, Goldberg AL. 1998. Proteasome inhibitors: valuable new tools for cell biologists. Trends Cell Biol 8(10):397-403.
Lee MG, Villa R, Trojer P, Norman J, Yan KP, Reinberg D, Di Croce L, Shiekhattar R. 2007. Demethylation of H3K27 regulates polycomb recruitment and H2A ubiquitination. Science 318(5849):447-450.
Lee S, Lee JW, Lee SK. 2012. UTX, a histone H3-lysine 27 demethylase, acts as a critical switch to activate the cardiac developmental program. Dev Cell 22(1):25-37.
Lee YR, Yuan WC, Ho HC, Chen CH, Shih HM, Chen RH. 2010. The Cullin 3 substrate adaptor KLHL20 mediates DAPK ubiquitination to control interferon responses. EMBO J.
Lendahl U, Zimmerman LB, McKay RD. 1990. CNS stem cells express a new class of intermediate filament protein. Cell 60(4):585-595.
LeWinter MM, Granzier H. 2010. Cardiac titin: a multifunctional giant. Circulation 121(19):2137-2145.

Leyns L, Bouwmeester T, Kim SH, Piccolo S, De Robertis EM. 1997. Frzb-1 is a secreted antagonist of Wnt signaling expressed in the Spemann organizer. Cell 88(6):747-756.
Li W, Tu D, Brunger AT, Ye Y. 2007. A ubiquitin ligase transfers preformed polyubiquitin chains from a conjugating enzyme to a substrate. Nature 446(7133):333-337.
Li X, Zhang D, Hannink M, Beamer LJ. 2004. Crystal structure of the Kelch domain of human Keap1. The Journal of biological chemistry 279(52):54750-54758.
Li Y, Bavarva JH, Wang Z, Guo J, Qian C, Thibodeau SN, Golemis EA, Liu W. 2011. HEF1, a novel target of Wnt signaling, promotes colonic cell migration and cancer progression. Oncogene 30(23):2633-2643.
Li Z, Colucci-Guyon E, Pincon-Raymond M, Mericskay M, Pournin S, Paulin D, Babinet C. 1996. Cardiovascular lesions and skeletal myopathy in mice lacking desmin. Dev Biol 175(2):362-366.
Liberatore CM, Searcy-Schrick RD, Yutzey KE. 2000. Ventricular expression of tbx5 inhibits normal heart chamber development. Dev Biol 223(1):169-180.
Lickert H, Kutsch S, Kanzler B, Tamai Y, Taketo MM, Kemler R. 2002. Formation of multiple hearts in mice following deletion of beta-catenin in the embryonic endoderm. Dev Cell 3(2):171-181.
Linask KK. 1992. N-cadherin localization in early heart development and polar expression of Na+,K(+)-ATPase, and integrin during pericardial coelom formation and epithelialization of the differentiating myocardium. Dev Biol 151(1):213-224.
Linask KK, Knudsen KA, Gui YH. 1997. N-cadherin-catenin interaction: necessary component of cardiac cell compartmentalization during early vertebrate heart development. Dev Biol 185(2):148-164.
Linke WA, Granzier H. 1998. A spring tale: new facts on titin elasticity. Biophys J 75(6):2613-2614.
Lints TJ, Parsons LM, Hartley L, Lyons I, Harvey RP. 1993. Nkx-2.5: a novel murine homeobox gene expressed in early heart progenitor cells and their myogenic descendants. Development 119(3):969.
Littlefield R, Almenar-Queralt A, Fowler VM. 2001. Actin dynamics at pointed ends regulates thin filament length in striated muscle. Nat Cell Biol 3(6):544-551.
Littlefield R, Fowler VM. 1998. Defining actin filament length in striated muscle: rulers and caps or dynamic stability? Annu Rev Cell Dev Biol 14:487-525.
Lo SH. 2006. Focal adhesions: what's new inside. Dev Biol 294(2):280-291.
Locker RH, Wild DJ. 1986. A comparative study of high molecular weight proteins in various types of muscle across the animal kingdom. J Biochem 99(5):1473-1484.
Lopez-Sanchez C, Garcia-Masa N, Ganan CM, Garcia-Martinez V. 2009. Movement and commitment of primitive streak precardiac cells during cardiogenesis. Int J Dev Biol 53(8-10):1445-1455.
Louis-Dit-Picard H, Barc J, Trujillano D, Miserey-Lenkei S, Bouatia-Naji N, Pylypenko O, Beaurain G, Bonnefond A, Sand O, Simian C and others. 2012. KLHL3 mutations cause familial hyperkalemic hypertension by impairing ion transport in the distal nephron. Nat Genet 44(4):456-460, S451-453.
Lowey S, Benefield PA, Silberstein L, Lang LM. 1979. Distribution of light chains in fast skeletal myosin. Nature 282(5738):522-524.
Lowey S, Slayter HS, Weeds AG, Baker H. 1969. Substructure of the myosin molecule. I. Subfragments of myosin by enzymic degradation. J Mol Biol 42(1):1-29.

Lowey S, Waller GS, Bandman E. 1991. Neonatal and adult myosin heavy chains form homodimers during avian skeletal muscle development. J Cell Biol 113(2):303-310.

Lu S, Carroll SL, Herrera AH, Ozanne B, Horowits R. 2003. New N-RAP-binding partners alpha-actinin, filamin and Krp1 detected by yeast two-hybrid screening: implications for myofibril assembly. J Cell Sci 116:2169-2178.

Luther PK. 1991. Three-dimensional reconstruction of a simple Z-band in fish muscle. J Cell Biol 113(5):1043-1055.

Ma K, Wang K. 2002. Interaction of nebulin SH3 domain with titin PEVK and myopalladin: implications for the signaling and assembly role of titin and nebulin. FEBS Lett 532(3):273-278.

MacDonald BT, Tamai K, He X. 2009. Wnt/beta-catenin signaling: components, mechanisms, and diseases. Dev Cell 17(1):9-26.

Maerki S, Olma MH, Staubli T, Steigemann P, Gerlich DW, Quadroni M, Sumara I, Peter M. 2009. The Cul3-KLHL21 E3 ubiquitin ligase targets aurora B to midzone microtubules in anaphase and is required for cytokinesis. J Cell Biol 187(6):791-800.

Mahajan-Miklos S, Cooley L. 1994. Intercellular cytoplasm transport during Drosophila oogenesis. Dev Biol 165(2):336-351.

Maki N, Sekiguchi F, Nishimaki J, Miwa K, Hayano T, Takahashi N, Suzuki M. 1990. Complementary DNA encoding the human T-cell FK506-binding protein, a peptidylprolyl cis-trans isomerase distinct from cyclophilin. Proc Natl Acad Sci U S A 87(14):5440-5443.

Manasek FJ, Burnside MB, Waterman RE. 1972. Myocardial cell shape change as a mechanism of embryonic heart looping. Dev Biol 29(4):349-371.

Manceau M, Gros J, Savage K, Thome V, McPherron A, Paterson B, Marcelle C. 2008. Myostatin promotes the terminal differentiation of embryonic muscle progenitors. Genes Dev 22(5):668-681.

Manes G, Hebrard M, Bocquet B, Meunier I, Coustes-Chazalette D, Senechal A, Bolland-Auge A, Zelenika D, Hamel CP. 2011. A novel locus (CORD12) for autosomal dominant cone-rod dystrophy on chromosome 2q24.2-2q33.1. BMC Med Genet 12:54.

Marcelle C, Ahlgren S, Bronner-Fraser M. 1999. In vivo regulation of somite differentiation and proliferation by Sonic Hedgehog. Dev Biol 214(2):277-287.

Marchler-Bauer A, Lu S, Anderson JB, Chitsaz F, Derbyshire MK, DeWeese-Scott C, Fong JH, Geer LY, Geer RC, Gonzales NR and others. 2011. CDD: a Conserved Domain Database for the functional annotation of proteins. Nucleic Acids Res 39:D225-229.

Marikawa Y, Elinson RP. 1998. beta-TrCP is a negative regulator of Wnt/beta-catenin signaling pathway and dorsal axis formation in Xenopus embryos. Mech Dev 77(1):75-80.

Maroto M, Bone RA, Dale JK. 2012. Somitogenesis. Development 139(14):2453-2456.

Martin C, Zhang Y. 2005. The diverse functions of histone lysine methylation. Nat Rev Mol Cell Biol 6(11):838-849.

Martini FH. 2005. Fundamentals of Anatomy and Physiology.

Martinsen BJ. 2005. Reference guide to the stages of chick heart embryology. Dev Dyn 233(4):1217-1237.

Maruyama K. 1976. Connectin, an elastic protein from myofibrils. J Biochem 80(2):405-407.

Maruyama K, Kurokawa H, Oosawa M, Shimaoka S, Yamamoto H, Ito M. 1990. Beta-actinin is equivalent to Cap Z protein. The Journal of biological chemistry 265(15):8712-8715.

Maruyama K, Natori R, Nonomura Y. 1976. New elastic protein from muscle. Nature 262(5563):58-60.
Marvin MJ, Di Rocco G, Gardiner A, Bush SM, Lassar AB. 2001. Inhibition of Wnt activity induces heart formation from posterior mesoderm. Genes Dev 15(3):316-327.
Matsumoto ML, Wickliffe KE, Dong KC, Yu C, Bosanac I, Bustos D, Phu L, Kirkpatrick DS, Hymowitz SG, Rape M and others. 2010. K11-linked polyubiquitination in cell cycle control revealed by a K11 linkage-specific antibody. Mol Cell 39(3):477-484.
McElhinny AS, Kazmierski ST, Labeit S, Gregorio CC. 2003. Nebulin: the nebulous, multifunctional giant of striated muscle. Trends Cardiovasc Med 13(5):195-201.
McElhinny AS, Kolmerer B, Fowler VM, Labeit S, Gregorio CC. 2001. The N-terminal end of nebulin interacts with tropomodulin at the pointed ends of the thin filaments. The Journal of biological chemistry 276(1):583-592.
McElhinny AS, Schwach C, Valichnac M, Mount-Patrick S, Gregorio CC. 2005. Nebulin regulates the assembly and lengths of the thin filaments in striated muscle. J Cell Biol 170(6):947-957.
McGarrity G, Kotani H, Butler G. 1992. Mycoplasmas and tissue culture cells.
McKillop DF, Geeves MA. 1993. Regulation of the interaction between actin and myosin subfragment 1: evidence for three states of the thin filament. Biophys J 65(2):693-701.
McMahon JA, Takada S, Zimmerman LB, Fan CM, Harland RM, McMahon AP. 1998. Noggin-mediated antagonism of BMP signaling is required for growth and patterning of the neural tube and somite. Genes Dev 12(10):1438-1452.
Meilhac SM, Kelly RG, Rocancourt D, Eloy-Trinquet S, Nicolas JF, Buckingham ME. 2003. A retrospective clonal analysis of the myocardium reveals two phases of clonal growth in the developing mouse heart. Development 130(16):3877-3889.
Mermelstein CS, Rebello MI, Amaral LM, Costa ML. 2003. Changes in cell shape, cytoskeletal proteins and adhesion sites of cultured cells after extracellular Ca2+ chelation. Braz J Med Biol Res 36(8):1111-1116.
Miller CJ, Cheung P, White P, Reisler E. 1995. Actin's view of actomyosin interface. Biophys J 68(4 Suppl):50S-54S.
Millevoi S, Trombitas K, Kolmerer B, Kostin S, Schaper J, Pelin K, Granzier H, Labeit S. 1998. Characterization of nebulette and nebulin and emerging concepts of their roles for vertebrate Z-discs. J Mol Biol 282(1):111-123.
Milner DJ, Weitzer G, Tran D, Bradley A, Capetanaki Y. 1996. Disruption of muscle architecture and myocardial degeneration in mice lacking desmin. J Cell Biol 134(5):1255-1270.
Miner JH, Wold B. 1990. Herculin, a fourth member of the MyoD family of myogenic regulatory genes. Proc Natl Acad Sci U S A 87(3):1089-1093.
Minn AJ, Gupta GP, Siegel PM, Bos PD, Shu W, Giri DD, Viale A, Olshen AB, Gerald WL, Massague J. 2005. Genes that mediate breast cancer metastasis to lung. Nature 436(7050):518-524.
Minor DL, Lin YF, Mobley BC, Avelar A, Jan YN, Jan LY, Berger JM. 2000. The polar T1 interface is linked to conformational changes that open the voltage-gated potassium channel. Cell 102(5):657-670.
Mittal B, Sanger JM, Sanger JW. 1987. Visualization of myosin in living cells. J Cell Biol 105(4):1753-1760.
Mjaatvedt CH, Nakaoka T, Moreno-Rodriguez R, Norris RA, Kern MJ, Eisenberg CA, Turner D, Markwald RR. 2001. The outflow tract of the heart is recruited from a novel heart-forming field. Dev Biol 238(1):97-109.

Moghe S, Jiang F, Miura Y, Cerny RL, Tsai MY, Furukawa M. 2011. The CUL3-KLHL18 ligase regulates mitotic entry and ubiquitylates Aurora-A. Biol Open 1(2):82-91.

Moncman CL, Wang K. 1995. Nebulette: a 107 kD nebulin-like protein in cardiac muscle. Cell Motil Cytoskeleton 32(3):205-225.

Moncman CL, Wang K. 1996. Assembly of nebulin into the sarcomeres of avian skeletal muscle. Cell Motil Cytoskeleton 34(3):167-184.

Moncman CL, Wang K. 1999. Functional dissection of nebulette demonstrates actin binding of nebulin-like repeats and Z-line targeting of SH3 and linker domains. Cell Motil Cytoskeleton 44(1):1-22.

Moncman CL, Wang K. 2002. Targeted disruption of nebulette protein expression alters cardiac myofibril assembly and function. Exp Cell Res 273(2):204-218.

Monsoro-Burq AH. 2005. Sclerotome development and morphogenesis: when experimental embryology meets genetics. Int J Dev Biol 49(2-3):301-308.

Moorman A, Webb S, Brown NA, Lamers W, Anderson RH. 2003. Development of the heart: (1) formation of the cardiac chambers and arterial trunks. Heart 89(7):806-814.

Moreno-Rodriguez RA, Krug EL, Reyes L, Villavicencio L, Mjaatvedt CH, Markwald RR. 2006. Bidirectional fusion of the heart-forming fields in the developing chick embryo. Dev Dyn 235(1):191-202.

Morimoto K, Harrington WF. 1972. Isolation and physical chemical properties of an M-line protein from skeletal muscle. The Journal of biological chemistry 247(10):3052-3061.

Morris MR, Ricketts CJ, Gentle D, McRonald F, Carli N, Khalili H, Brown M, Kishida T, Yao M, Banks RE and others. 2011. Genome-wide methylation analysis identifies epigenetically inactivated candidate tumour suppressor genes in renal cell carcinoma. Oncogene 30(12):1390-1401.

Morton WM, Ayscough KR, McLaughlin PJ. 2000. Latrunculin alters the actin-monomer subunit interface to prevent polymerization. Nat Cell Biol 2(6):376-378.

Mudry RE, Perry CN, Richards M, Fowler VM, Gregorio CC. 2003. The interaction of tropomodulin with tropomyosin stabilizes thin filaments in cardiac myocytes. J Cell Biol 162(6):1057-1068.

Munsterberg A, Yue Q. 2008. Cardiac progenitor migration and specification: The dual function of Wnts. Cell Adh Migr 2(2):74-76.

Munsterberg AE, Kitajewski J, Bumcrot DA, McMahon AP, Lassar AB. 1995. Combinatorial signaling by Sonic hedgehog and Wnt family members induces myogenic bHLH gene expression in the somite. Genes Dev 9(23):2911-2922.

Munsterberg AE, Lassar AB. 1995. Combinatorial signals from the neural tube, floor plate and notochord induce myogenic bHLH gene expression in the somite. Development 121(3):651-660.

Nagalla S, Shaw C, Kong X, Kondkar AA, Edelstein LC, Ma L, Chen J, McKnight GS, Lopez JA, Yang L and others. 2011. Platelet microRNA-mRNA coexpression profiles correlate with platelet reactivity. Blood 117(19):5189-5197.

Nakajima O, Nakamura F, Yamashita N, Tomita Y, Suto F, Okada T, Iwamatsu A, Kondo E, Fujisawa H, Takei K and others. 2006. FKBP133: a novel mouse FK506-binding protein homolog alters growth cone morphology. Biochem Biophys Res Commun 346(1):140-149.

Nakashima A, Katagiri T, Tamura M. 2005. Cross-talk between Wnt and bone morphogenetic protein 2 (BMP-2) signaling in differentiation pathway of C2C12 myoblasts. The Journal of biological chemistry 280(45):37660-37668.

Nam S, Min K, Hwang H, Lee HO, Lee JH, Yoon J, Lee H, Park S, Lee J. 2009. Control of rapsyn stability by the CUL-3-containing E3 ligase complex. The Journal of biological chemistry 284(12):8195-8206.

Nascone N, Mercola M. 1995. An inductive role for the endoderm in Xenopus cardiogenesis. Development 121(2):515-523.

Natarajan M, Stewart JE, Golemis EA, Pugacheva EN, Alexandropoulos K, Cox BD, Wang W, Grammer JR, Gladson CL. 2006. HEF1 is a necessary and specific downstream effector of FAK that promotes the migration of glioblastoma cells. Oncogene 25(12):1721-1732.

Neutzner M, Neutzner A. 2012. Enzymes of ubiquitination and deubiquitination. Essays Biochem 52:37-50.

Ngai J, Capetanaki YG, Lazarides E. 1985. Expression of the genes coding for the intermediate filament proteins vimentin and desmin. Ann N Y Acad Sci 455:144-157.

Noden DM. 1991. Vertebrate craniofacial development: the relation between ontogenetic process and morphological outcome. Brain Behav Evol 38(4-5):190-225.

Nowak KJ, Wattanasirichaigoon D, Goebel HH, Wilce M, Pelin K, Donner K, Jacob RL, Hubner C, Oexle K, Anderson JR and others. 1999. Mutations in the skeletal muscle alpha-actin gene in patients with actin myopathy and nemaline myopathy. Nat Genet 23(2):208-212.

Nowak SJ, Nahirney PC, Hadjantonakis AK, Baylies MK. 2009. Nap1-mediated actin remodeling is essential for mammalian myoblast fusion. J Cell Sci 122(Pt 18):3282-3293.

Nwe TM, Maruyama K, Shimada Y. 1999. Relation of nebulin and connectin (titin) to dynamics of actin in nascent myofibrils of cultured skeletal muscle cells. Exp Cell Res 252(1):33-40.

O'Brien E, Dickens M. 1983. Actin and thin filaments. Electron Microscopy of Proteins.

O'Neill GM, Seo S, Serebriiskii IG, Lessin SR, Golemis EA. 2007. A new central scaffold for metastasis: parsing HEF1/Cas-L/NEDD9. Cancer Res 67(19):8975-8979.

Oberg EA, Nifoussi SK, Gingras AC, Strack S. 2012. Selective proteasomal degradation of the B'beta subunit of protein phosphatase 2A by the E3 ubiquitin ligase adaptor Kelch-like 15. The Journal of biological chemistry 287(52):43378-43389.

Obermann WM, Gautel M, Steiner F, van der Ven PF, Weber K, Furst DO. 1996. The structure of the sarcomeric M band: localization of defined domains of myomesin, M-protein, and the 250-kD carboxy-terminal region of titin by immunoelectron microscopy. J Cell Biol 134(6):1441-1453.

Obermann WM, Plessmann U, Weber K, Furst DO. 1995. Purification and biochemical characterization of myomesin, a myosin-binding and titin-binding protein, from bovine skeletal muscle. Eur J Biochem 233(1):110-115.

Offer G, Moos C, Starr R. 1973. A new protein of the thick filaments of vertebrate skeletal myofibrils. Extractions, purification and characterization. J Mol Biol 74(4):653-676.

Ogut O, Hossain MM, Jin JP. 2003. Interactions between nebulin-like motifs and thin filament regulatory proteins. The Journal of biological chemistry 278(5):3089-3097.

Ohta A, Schumacher FR, Mehellou Y, Johnson C, Knebel A, Macartney TJ, Wood NT, Alessi DR, Kurz T. 2013. The CUL3-KLHL3 E3 ligase complex mutated in Gordon's hypertension syndrome interacts with and ubiquitylates WNK

isoforms; disease-causing mutations in KLHL3 and WNK4 disrupt interaction. Biochem J.
Ohtake Y, Tojo H, Seiki M. 2006. Multifunctional roles of MT1-MMP in myofiber formation and morphostatic maintenance of skeletal muscle. J Cell Sci 119(Pt 18):3822-3832.
Ottenheijm CA, Granzier H. 2010. Lifting the nebula: novel insights into skeletal muscle contractility. Physiology (Bethesda) 25(5):304-310.
Panchal SC, Kaiser DA, Torres E, Pollard TD, Rosen MK. 2003. A conserved amphipathic helix in WASP/Scar proteins is essential for activation of Arp2/3 complex. Nat Struct Biol 10(8):591-598.
Pandey A, Mann M. 2000. Proteomics to study genes and genomes. Nature 405(6788):837-846.
Pandur P, Sirbu IO, Kuhl SJ, Philipp M, Kuhl M. 2013. Islet1-expressing cardiac progenitor cells: a comparison across species. Dev Genes Evol 223(1-2):117-129.
Papa I, Astier C, Kwiatek O, Raynaud F, Bonnal C, Lebart MC, Roustan C, Benyamin Y. 1999. Alpha actinin-CapZ, an anchoring complex for thin filaments in Z-line. J Muscle Res Cell Motil 20(2):187-197.
Pappas CT, Bhattacharya N, Cooper JA, Gregorio CC. 2008. Nebulin interacts with CapZ and regulates thin filament architecture within the Z-disc. Mol Biol Cell 19(5):1837-1847.
Pappas CT, Bliss KT, Zieseniss A, Gregorio CC. 2011. The Nebulin family: an actin support group. Trends Cell Biol 21(1):29-37.
Pappas CT, Krieg PA, Gregorio CC. 2010. Nebulin regulates actin filament lengths by a stabilization mechanism. J Cell Biol 189(5):859-870.
Park I, Han C, Jin S, Lee B, Choi H, Kwon JT, Kim D, Kim J, Lifirsu E, Park WJ and others. 2011. Myosin regulatory light chains are required to maintain the stability of myosin II and cellular integrity. Biochem J 434(1):171-180.
Paulin D, Li Z. 2004. Desmin: a major intermediate filament protein essential for the structural integrity and function of muscle. Exp Cell Res 301(1):1-7.
Paxton CW, Cosgrove RA, Drozd AC, Wiggins EL, Woodhouse S, Watson RA, Spence HJ, Ozanne BW, Pell JM. 2011. BTB-Kelch protein Krp1 regulates proliferation and differentiation of myoblasts. Am J Physiol Cell Physiol 300(6):C1345-1355.
Pelin K, Hilpela P, Donner K, Sewry C, Akkari PA, Wilton SD, Wattanasirichaigoon D, Bang ML, Centner T, Hanefeld F and others. 1999. Mutations in the nebulin gene associated with autosomal recessive nemaline myopathy. Proc Natl Acad Sci U S A 96(5):2305-2310.
Pellegrin S, Mellor H. 2007. Actin stress fibres. J Cell Sci 120(Pt 20):3491-3499.
Perconti G, Ferro A, Amato F, Rubino P, Randazzo D, Wolff T, Feo S, Giallongo A. 2007. The kelch protein NS1-BP interacts with alpha-enolase/MBP-1 and is involved in c-Myc gene transcriptional control. Biochim Biophys Acta 1773(12):1774-1785.
Perez-Torrado R, Yamada D, Defossez PA. 2006. Born to bind: the BTB protein-protein interaction domain. Bioessays 28(12):1194-1202.
Perry SV. 2001. Vertebrate tropomyosin: distribution, properties and function. J Muscle Res Cell Motil 22(1):5-49.
Petroski MD, Deshaies RJ. 2005a. Function and regulation of cullin-RING ubiquitin ligases. Nat Rev Mol Cell Biol 6(1):9-20.
Petroski MD, Deshaies RJ. 2005b. Mechanism of lysine 48-linked ubiquitin-chain synthesis by the cullin-RING ubiquitin-ligase complex SCF-Cdc34. Cell 123(6):1107-1120.

Pfuhl M, Winder SJ, Castiglione Morelli MA, Labeit S, Pastore A. 1996. Correlation between conformational and binding properties of nebulin repeats. J Mol Biol 257(2):367-384.

Pintard L, Willems A, Peter M. 2004. Cullin-based ubiquitin ligases: Cul3-BTB complexes join the family. EMBO J 23(8):1681-1687.

Pintard L, Willis JH, Willems A, Johnson JL, Srayko M, Kurz T, Glaser S, Mains PE, Tyers M, Bowerman B and others. 2003. The BTB protein MEL-26 is a substrate-specific adaptor of the CUL-3 ubiquitin-ligase. Nature 425(6955):311-316.

Pollard TD. 1990. Actin. Curr Opin Cell Biol 2(1):33-40.

Pollard TD. 2007. Regulation of actin filament assembly by Arp2/3 complex and formins. Annu Rev Biophys Biomol Struct 36:451-477.

Pollard TD, Cooper JA. 2009. Actin, a central player in cell shape and movement. Science 326(5957):1208-1212.

Pourquie O. 2003. Vertebrate somitogenesis: a novel paradigm for animal segmentation? Int J Dev Biol 47(7-8):597-603.

Pownall ME, Gustafsson MK, Emerson CP, Jr. 2002. Myogenic regulatory factors and the specification of muscle progenitors in vertebrate embryos. Annu Rev Cell Dev Biol 18:747-783.

Price MG, Gomer RH. 1993. Skelemin, a cytoskeletal M-disc periphery protein, contains motifs of adhesion/recognition and intermediate filament proteins. The Journal of biological chemistry 268(29):21800-21810.

Qiu QM, Liu G, Li WN, Shi QW, Zhu FX, Lu GX. 2009. [Mutation of KLHL-10 in idiopathic infertile males with azoospermia, oligospermia or asthenospermia]. Zhonghua Nan Ke Xue 15(11):974-979.

Rahighi S, Ikeda F, Kawasaki M, Akutsu M, Suzuki N, Kato R, Kensche T, Uejima T, Bloor S, Komander D and others. 2009. Specific recognition of linear ubiquitin chains by NEMO is important for NF-kappaB activation. Cell 136(6):1098-1109.

Ravenscroft G, Jackaman C, Bringans S, Papadimitriou JM, Griffiths LM, McNamara E, Bakker AJ, Davies KE, Laing NG, Nowak KJ. 2011a. Mouse models of dominant ACTA1 disease recapitulate human disease and provide insight into therapies. Brain 134:1101-1115.

Ravenscroft G, Jackaman C, Sewry CA, McNamara E, Squire SE, Potter AC, Papadimitriou J, Griffiths LM, Bakker AJ, Davies KE and others. 2011b. Actin nemaline myopathy mouse reproduces disease, suggests other actin disease phenotypes and provides cautionary note on muscle transgene expression. PLoS One 6(12):e28699.

Rawles ME. 1943. The heart-forming areas of the early chick blastoderm. Physiol Zool 16:22-42.

Rayment I, Holden HM, Whittaker M, Yohn CB, Lorenz M, Holmes KC, Milligan RA. 1993. Structure of the actin-myosin complex and its implications for muscle contraction. Science 261(5117):58-65.

Rhee D, Sanger JM, Sanger JW. 1994. The premyofibril: evidence for its role in myofibrillogenesis. Cell Motil Cytoskeleton 28(1):1-24.

Rhodes SJ, Konieczny SF. 1989. Identification of MRF4: a new member of the muscle regulatory factor gene family. Genes Dev 3(12B):2050-2061.

Richardson BE, Beckett K, Nowak SJ, Baylies MK. 2007. SCAR/WAVE and Arp2/3 are crucial for cytoskeletal remodeling at the site of myoblast fusion. Development 134(24):4357-4367.

Richardson MK, Allen SP, Wright GM, Raynaud A, Hanken J. 1998. Somite number and vertebrate evolution. Development 125(2):151-160.

Robinson DN, Cant K, Cooley L. 1994. Morphogenesis of Drosophila ovarian ring canals. Development 120(7):2015-2025.
Robinson DN, Cooley L. 1997. Drosophila kelch is an oligomeric ring canal actin organizer. J Cell Biol 138(4):799-810.
Robinson RC, Turbedsky K, Kaiser DA, Marchand JB, Higgs HN, Choe S, Pollard TD. 2001. Crystal structure of Arp2/3 complex. Science 294(5547):1679-1684.
Romano S, Sorrentino A, Di Pace AL, Nappo G, Mercogliano C, Romano MF. 2011. The emerging role of large immunophilin FK506 binding protein 51 in cancer. Curr Med Chem 18(35):5424-5429.
Rondou P, Skieterska K, Packeu A, Lintermans B, Vanhoenacker P, Vauquelin G, Haegeman G, Van Craenenbroeck K. 2011. KLHL12-mediated ubiquitination of the dopamine D4 receptor does not target the receptor for degradation. Cell Signal 22(6):900-913.
Root DD, Wang K. 1994. Calmodulin-sensitive interaction of human nebulin fragments with actin and myosin. Biochemistry 33(42):12581-12591.
Rosenquist GC. 1970. Location and movements of cardiogenic cells in the chick embryo: the heart-forming portion of the primitive streak. Dev Biol 22(3):461-475.
Rothbauer U, Zolghadr K, Muyldermans S, Schepers A, Cardoso MC, Leonhardt H. 2008. A versatile nanotrap for biochemical and functional studies with fluorescent fusion proteins. Mol Cell Proteomics 7(2):282-289.
Rudy DE, Yatskievych TA, Antin PB, Gregorio CC. 2001. Assembly of thick, thin, and titin filaments in chick precardiac explants. Dev Dyn 221(1):61-71.
Saga Y, Kitajima S, Miyagawa-Tomita S. 2000. Mesp1 expression is the earliest sign of cardiovascular development. Trends Cardiovasc Med 10(8):345-352.
Saga Y, Miyagawa-Tomita S, Takagi A, Kitajima S, Miyazaki J, Inoue T. 1999. MesP1 is expressed in the heart precursor cells and required for the formation of a single heart tube. Development 126(15):3437-3447.
Saha A, Deshaies RJ. 2008. Multimodal activation of the ubiquitin ligase SCF by Nedd8 conjugation. Mol Cell 32(1):21-31.
Salinas GD, Blair LA, Needleman LA, Gonzales JD, Chen Y, Li M, Singer JD, Marshall J. 2006. Actinfilin is a Cul3 substrate adaptor, linking GluR6 kainate receptor subunits to the ubiquitin-proteasome pathway. The Journal of biological chemistry 281(52):40164-40173.
Sambrook J, Fritsch, E.F., Maniatis, T. 1989. Molecular Cloning A laboratory manual: Cold Spring Harbor Laboratory Press.
Sambuughin N, Swietnicki W, Techtmann S, Matrosova V, Wallace T, Goldfarb L, Maynard E. 2012. KBTBD13 interacts with Cullin 3 to form a functional ubiquitin ligase. Biochem Biophys Res Commun 421(4):743-749.
Sambuughin N, Yau KS, Olive M, Duff RM, Bayarsaikhan M, Lu S, Gonzalez-Mera L, Sivadorai P, Nowak KJ, Ravenscroft G and others. 2010. Dominant mutations in KBTBD13, a member of the BTB/Kelch family, cause nemaline myopathy with cores. Am J Hum Genet 87(6):842-847.
Sandbo N, Dulin N. 2011. Actin cytoskeleton in myofibroblast differentiation: ultrastructure defining form and driving function. Transl Res 158(4):181-196.
Sanger JM, Mittal B, Pochapin MB, Sanger JW. 1986. Myofibrillogenesis in living cells microinjected with fluorescently labeled alpha-actinin. J Cell Biol 102(6):2053-2066.
Sanger JW, Chowrashi P, Shaner NC, Spalthoff S, Wang J, Freeman NL, Sanger JM. 2002. Myofibrillogenesis in skeletal muscle cells. Clin Orthop Relat Res:S153-162.

Sanger JW, Mittal B, Sanger JM. 1984a. Analysis of myofibrillar structure and assembly using fluorescently labeled contractile proteins. J Cell Biol 98(3):825-833.
Sanger JW, Mittal B, Sanger JM. 1984b. Formation of myofibrils in spreading chick cardiac myocytes. Cell Motil 4(6):405-416.
Sanger JW, Sanger JM. 2001. Fishing out proteins that bind to titin. J Cell Biol 154(1):21-24.
Sanger JW, Wang J, Fan Y, White J, Sanger JM. 2010. Assembly and dynamics of myofibrils. J Biomed Biotechnol 2010:858606.
Sanoudou D, Beggs AH. 2001. Clinical and genetic heterogeneity in nemaline myopathy--a disease of skeletal muscle thin filaments. Trends Mol Med 7(8):362-368.
Sasagawa K, Matsudo Y, Kang M, Fujimura L, Iitsuka Y, Okada S, Ochiai T, Tokuhisa T, Hatano M. 2002. Identification of Nd1, a novel murine kelch family protein, involved in stabilization of actin filaments. The Journal of biological chemistry 277(46):44140-44146.
Sax CM, Farrell FX, Zehner ZE. 1989. Down-regulation of vimentin gene expression during myogenesis is controlled by a 5'-flanking sequence. Gene 78(2):235-242.
Schaefer H, Rongo C. 2006. KEL-8 is a substrate receptor for CUL3-dependent ubiquitin ligase that regulates synaptic glutamate receptor turnover. Mol Biol Cell 17(3):1250-1260.
Schafer DA, Hug C, Cooper JA. 1995. Inhibition of CapZ during myofibrillogenesis alters assembly of actin filaments. J Cell Biol 128(1-2):61-70.
Scheufler C, Brinker A, Bourenkov G, Pegoraro S, Moroder L, Bartunik H, Hartl FU, Moarefi I. 2000. Structure of TPR domain-peptide complexes: critical elements in the assembly of the Hsp70-Hsp90 multichaperone machine. Cell 101(2):199-210.
Schlaepfer DD, Hauck CR, Sieg DJ. 1999. Signaling through focal adhesion kinase. Prog Biophys Mol Biol 71(3-4):435-478.
Schlange T, Andree B, Arnold HH, Brand T. 2000. BMP2 is required for early heart development during a distinct time period. Mech Dev 91(1-2):259-270.
Schmid MF, Agris JM, Jakana J, Matsudaira P, Chiu W. 1994. Three-dimensional structure of a single filament in the Limulus acrosomal bundle: scruin binds to homologous helix-loop-beta motifs in actin. J Cell Biol 124(3):341-350.
Schmidt M, Tanaka M, Munsterberg A. 2000. Expression of (beta)-catenin in the developing chick myotome is regulated by myogenic signals. Development 127(19):4105-4113.
Schneider VA, Mercola M. 2001. Wnt antagonism initiates cardiogenesis in Xenopus laevis. Genes Dev 15(3):304-315.
Schoenwolf GC, Garcia-Martinez V, Dias MS. 1992. Mesoderm movement and fate during avian gastrulation and neurulation. Dev Dyn 193(3):235-248.
Schroder R, Reimann J, Salmikangas P, Clemen CS, Hayashi YK, Nonaka I, Arahata K, Carpen O. 2003. Beyond LGMD1A: myotilin is a component of central core lesions and nemaline rods. Neuromuscul Disord 13(6):451-455.
Schulman BA, Harper JW. 2009. Ubiquitin-like protein activation by E1 enzymes: the apex for downstream signalling pathways. Nat Rev Mol Cell Biol 10(5):319-331.
Schultheiss T, Lin ZX, Lu MH, Murray J, Fischman DA, Weber K, Masaki T, Imamura M, Holtzer H. 1990. Differential distribution of subsets of myofibrillar proteins in cardiac nonstriated and striated myofibrils. J Cell Biol 110(4):1159-1172.
Schultheiss TM, Burch JB, Lassar AB. 1997. A role for bone morphogenetic proteins in the induction of cardiac myogenesis. Genes Dev 11(4):451-462.

Schultheiss TM, Xydas S, Lassar AB. 1995. Induction of avian cardiac myogenesis by anterior endoderm. Development 121(12):4203-4214.
Schupbach T, Wieschaus E. 1991. Female sterile mutations on the second chromosome of Drosophila melanogaster. II. Mutations blocking oogenesis or altering egg morphology. Genetics 129(4):1119-1136.
Schweitzer SC, Klymkowsky MW, Bellin RM, Robson RM, Capetanaki Y, Evans RM. 2001. Paranemin and the organization of desmin filament networks. J Cell Sci 114:1079-1089.
Seeger M, Hartmann-Petersen R, Wilkinson CR, Wallace M, Samejima I, Taylor MS, Gordon C. 2003. Interaction of the anaphase-promoting complex/cyclosome and proteasome protein complexes with multiubiquitin chain-binding proteins. The Journal of biological chemistry 278(19):16791-16796.
Sellers JR. 2000. Myosins: a diverse superfamily. Biochim Biophys Acta 1496(1):3-22.
Sharma N, Medikayala S, Defour A, Rayavarapu S, Brown KJ, Hathout Y, Jaiswal JK. 2012. Use of quantitative membrane proteomics identifies a novel role of mitochondria in healing injured muscles. The Journal of biological chemistry 287(36):30455-30467.
Shimada Y, Komiyama M, Begum S, Maruyama K. 1996. Development of connectin/titin and nebulin in striated muscles of chicken. Adv Biophys 33:223-233.
Shiraishi I, Takamatsu T, Fujita S. 1993. 3-D observation of N-cadherin expression during cardiac myofibrillogenesis of the chick embryo using a confocal laser scanning microscope. Anat Embryol (Berl) 187(2):115-120.
Shiraishi I, Takamatsu T, Fujita S. 1995. Three-dimensional observation with a confocal scanning laser microscope of fibronectin immunolabeling during cardiac looping in the chick embryo. Anat Embryol (Berl) 191(3):183-189.
Shitani M, Sasaki S, Akutsu N, Takagi H, Suzuki H, Nojima M, Yamamoto H, Tokino T, Hirata K, Imai K and others. 2012. Genome-wide analysis of DNA methylation identifies novel cancer-related genes in hepatocellular carcinoma. Tumour Biol 33(5):1307-1317.
Shpargel KB, Sengoku T, Yokoyama S, Magnuson T. 2012. UTX and UTY demonstrate histone demethylase-independent function in mouse embryonic development. PLoS Genet 8(9):e1002964.
Shy GM, Engel WK, Somers JE, Wanko T. 1963. Nemaline Myopathy. A New Congenital Myopathy. Brain 86:793-810.
Sieg DJ, Hauck CR, Schlaepfer DD. 1999. Required role of focal adhesion kinase (FAK) for integrin-stimulated cell migration. J Cell Sci 112:2677-2691.
Simeonova I, Lejour V, Bardot B, Bouarich-Bourimi R, Morin A, Fang M, Charbonnier L, Toledo F. 2012. Fuzzy tandem repeats containing p53 response elements may define species-specific p53 target genes. PLoS Genet 8(6):e1002731.
Singh M, Cowell L, Seo S, O'Neill G, Golemis E. 2007. Molecular basis for HEF1/NEDD9/Cas-L action as a multifunctional co-ordinator of invasion, apoptosis and cell cycle. Cell Biochem Biophys 48(1):54-72.
Soderling SH. 2009. Grab your partner with both hands: cytoskeletal remodeling by Arp2/3 signaling. Sci Signal 2(55):pe5.
Sokol S, Christian JL, Moon RT, Melton DA. 1991. Injected Wnt RNA induces a complete body axis in Xenopus embryos. Cell 67(4):741-752.
Solloway MJ, Robertson EJ. 1999. Early embryonic lethality in Bmp5;Bmp7 double mutant mice suggests functional redundancy within the 60A subgroup. Development 126(8):1753-1768.

Soltysik-Espanola M, Rogers RA, Jiang S, Kim TA, Gaedigk R, White RA, Avraham H, Avraham S. 1999. Characterization of Mayven, a novel actin-binding protein predominantly expressed in brain. Mol Biol Cell 10(7):2361-2375.

Somi S, Klein AT, Houweling AC, Ruijter JM, Buffing AA, Moorman AF, van den Hoff MJ. 2006. Atrial and ventricular myosin heavy-chain expression in the developing chicken heart: strengths and limitations of non-radioactive in situ hybridization. J Histochem Cytochem 54(6):649-664.

Spector I, Shochet NR, Kashman Y, Groweiss A. 1983. Latrunculins: novel marine toxins that disrupt microfilament organization in cultured cells. Science 219(4584):493-495.

Spence HJ, Johnston I, Ewart K, Buchanan SJ, Fitzgerald U, Ozanne BW. 2000. Krp1, a novel kelch related protein that is involved in pseudopod elongation in transformed cells. Oncogene 19(10):1266-1276.

Spence HJ, McGarry L, Chew CS, Carragher NO, Scott-Carragher LA, Yuan Z, Croft DR, Olson MF, Frame M, Ozanne BW. 2006. AP-1 differentially expressed proteins Krp1 and fibronectin cooperatively enhance Rho-ROCK-independent mesenchymal invasion by altering the function, localization, and activity of nondifferentially expressed proteins. Mol Cell Biol 26(4):1480-1495.

Squire JM. 1997. Architecture and function in the muscle sarcomere. Curr Opin Struct Biol 7(2):247-257.

Stafford DA, Brunet LJ, Khokha MK, Economides AN, Harland RM. 2011. Cooperative activity of noggin and gremlin 1 in axial skeleton development. Development 138(5):1005-1014.

Stalsberg H, DeHaan RL. 1969. The precardiac areas and formation of the tubular heart in the chick embryo. Dev Biol 19(2):128-159.

Starr R, Offer G. 1983. H-protein and X-protein. Two new components of the thick filaments of vertebrate skeletal muscle. J Mol Biol 170(3):675-698.

Stehbens SJ, Akhmanova A, Yap AS. 2009. Microtubules and cadherins: a neglected partnership. Front Biosci 14:3159-3167.

Steiner F, Weber K, Furst DO. 1999. M band proteins myomesin and skelemin are encoded by the same gene: analysis of its organization and expression. Genomics 56(1):78-89.

Stogios PJ, Chen L, Prive GG. 2007. Crystal structure of the BTB domain from the LRF/ZBTB7 transcriptional regulator. Protein Sci 16(2):336-342.

Stogios PJ, Downs GS, Jauhal JJ, Nandra SK, Prive GG. 2005. Sequence and structural analysis of BTB domain proteins. Genome Biol 6(10):R82.

Stogios PJ, Prive GG. 2004. The BACK domain in BTB-kelch proteins. Trends Biochem Sci 29(12):634-637.

Streit A, Stern CD. 1999. Mesoderm patterning and somite formation during node regression: differential effects of chordin and noggin. Mech Dev 85(1-2):85-96.

Stromer MH. 1990. Intermediate filaments in muscle. Cellular and Molecular Biology of Intermediate Filaments.

Sumara I, Quadroni M, Frei C, Olma MH, Sumara G, Ricci R, Peter M. 2007. A Cul3-based E3 ligase removes Aurora B from mitotic chromosomes, regulating mitotic progression and completion of cytokinesis in human cells. Dev Cell 12(6):887-900.

Sutoh K, Ando M, Toyoshima YY. 1991. Site-directed mutations of Dictyostelium actin: disruption of a negative charge cluster at the N terminus. Proc Natl Acad Sci U S A 88(17):7711-7714.

Suzuki M, Morita H, Ueno N. 2012. Molecular mechanisms of cell shape changes that contribute to vertebrate neural tube closure. Dev Growth Differ 54(3):266-276.

Switzer RC, 3rd, Merril CR, Shifrin S. 1979. A highly sensitive silver stain for detecting proteins and peptides in polyacrylamide gels. Anal Biochem 98(1):231-237.
Tajbakhsh S, Borello U, Vivarelli E, Kelly R, Papkoff J, Duprez D, Buckingham M, Cossu G. 1998. Differential activation of Myf5 and MyoD by different Wnts in explants of mouse paraxial mesoderm and the later activation of myogenesis in the absence of Myf5. Development 125(21):4155-4162.
Tajbakhsh S, Buckingham M. 2000. The birth of muscle progenitor cells in the mouse: spatiotemporal considerations. Curr Top Dev Biol 48:225-268.
Takada F, Vander Woude DL, Tong HQ, Thompson TG, Watkins SC, Kunkel LM, Beggs AH. 2001. Myozenin: an alpha-actinin- and gamma-filamin-binding protein of skeletal muscle Z lines. Proc Natl Acad Sci U S A 98(4):1595-1600.
Takano K, Watanabe-Takano H, Suetsugu S, Kurita S, Tsujita K, Kimura S, Karatsu T, Takenawa T, Endo T. 2010. Nebulin and N-WASP cooperate to cause IGF-1-induced sarcomeric actin filament formation. Science 330(6010):1536-1540.
Tanaka S, Terada K, Nohno T. 2011. Canonical Wnt signaling is involved in switching from cell proliferation to myogenic differentiation of mouse myoblast cells. J Mol Signal 6:12.
Tassin AM, Maro B, Bornens M. 1985. Fate of microtubule-organizing centers during myogenesis in vitro. J Cell Biol 100(1):35-46.
Taylor A, Obholz K, Linden G, Sadiev S, Klaus S, Carlson KD. 1998. DNA sequence and muscle-specific expression of human sarcosin transcripts. Mol Cell Biochem 183(1-2):105-112.
Thayer MJ, Tapscott SJ, Davis RL, Wright WE, Lassar AB, Weintraub H. 1989. Positive autoregulation of the myogenic determination gene MyoD1. Cell 58(2):241-248.
Thomas PQ, Brown A, Beddington RS. 1998. Hex: a homeobox gene revealing peri-implantation asymmetry in the mouse embryo and an early transient marker of endothelial cell precursors. Development 125(1):85-94.
Tian D, Sun S, Lee JT. 2010. The long noncoding RNA, Jpx, is a molecular switch for X chromosome inactivation. Cell 143(3):390-403.
Tilney LG, Tilney MS, Guild GM. 1996. Formation of actin filament bundles in the ring canals of developing Drosophila follicles. J Cell Biol 133(1):61-74.
Tkachev VO, Menshchikova EB, Zenkov NK. 2011. Mechanism of the Nrf2/Keap1/ARE signaling system. Biochemistry (Mosc) 76(4):407-422.
Todaro GJ, Green H. 1963. Quantitative studies of the growth of mouse embryo cells in culture and their development into established lines. J Cell Biol 17:299-313.
Tojkander S, Gateva G, Lappalainen P. 2012. Actin stress fibers--assembly, dynamics and biological roles. J Cell Sci 125:1855-1864.
Tokuyasu KT. 1989. Immunocytochemical studies of cardiac myofibrillogenesis in early chick embryos. III. Generation of fasciae adherentes and costameres. J Cell Biol 108(1):43-53.
Tokuyasu KT, Maher PA. 1987a. Immunocytochemical studies of cardiac myofibrillogenesis in early chick embryos. I. Presence of immunofluorescent titin spots in premyofibril stages. J Cell Biol 105:2781-2793.
Tokuyasu KT, Maher PA. 1987b. Immunocytochemical studies of cardiac myofibrillogenesis in early chick embryos. II. Generation of alpha-actinin dots within titin spots at the time of the first myofibril formation. J Cell Biol 105:2795-2801.
Tseng LA, Bixby JL. 2011. Interaction of an intracellular pentraxin with a BTB-Kelch protein is associated with ubiquitylation, aggregation and neuronal apoptosis. Mol Cell Neurosci 47(4):254-264.

Tsuchida T, Ensini M, Morton SB, Baldassare M, Edlund T, Jessell TM, Pfaff SL. 1994. Topographic organization of embryonic motor neurons defined by expression of LIM homeobox genes. Cell 79(6):957-970.

Tullio AN, Accili D, Ferrans VJ, Yu ZX, Takeda K, Grinberg A, Westphal H, Preston YA, Adelstein RS. 1997. Nonmuscle myosin II-B is required for normal development of the mouse heart. Proc Natl Acad Sci U S A 94(23):12407-12412.

Turnacioglu KK, Mittal B, Dabiri GA, Sanger JM, Sanger JW. 1997a. An N-terminal fragment of titin coupled to green fluorescent protein localizes to the Z-bands in living muscle cells: overexpression leads to myofibril disassembly. Mol Biol Cell 8(4):705-717.

Turnacioglu KK, Mittal B, Dabiri GA, Sanger JM, Sanger JW. 1997b. Zeugmatin is part of the Z-band targeting region of titin. Cell Struct Funct 22(1):73-82.

Turner DC, Wallimann T, Eppenberger HM. 1973. A protein that binds specifically to the M-line of skeletal muscle is identified as the muscle form of creatine kinase. Proc Natl Acad Sci U S A 70(3):702-705.

Tyedmers J, Mogk A, Bukau B. 2010. Cellular strategies for controlling protein aggregation. Nat Rev Mol Cell Biol 11(11):777-788.

Tzahor E. 2007. Wnt/beta-catenin signaling and cardiogenesis: timing does matter. Dev Cell 13(1):10-13.

Tzahor E, Lassar AB. 2001. Wnt signals from the neural tube block ectopic cardiogenesis. Genes Dev 15(3):255-260.

Vaidya TB, Rhodes SJ, Taparowsky EJ, Konieczny SF. 1989. Fibroblast growth factor and transforming growth factor beta repress transcription of the myogenic regulatory gene MyoD1. Mol Cell Biol 9(8):3576-3579.

Vale RD. 2003. The molecular motor toolbox for intracellular transport. Cell 112(4):467-480.

van den Berg G, Moorman AF. 2011. Development of the pulmonary vein and the systemic venous sinus: an interactive 3D overview. PLoS One 6(7):e22055.

Van Der Ven PF, Obermann WM, Weber K, Furst DO. 1996. Myomesin, M-protein and the structure of the sarcomeric M-band. Adv Biophys 33:91-99.

Verma R, Chen S, Feldman R, Schieltz D, Yates J, Dohmen J, Deshaies RJ. 2000. Proteasomal proteomics: identification of nucleotide-sensitive proteasome-interacting proteins by mass spectrometric analysis of affinity-purified proteasomes. Mol Biol Cell 11(10):3425-3439.

Vicente-Manzanares M, Ma X, Adelstein RS, Horwitz AR. 2009. Non-muscle myosin II takes centre stage in cell adhesion and migration. Nat Rev Mol Cell Biol 10(11):778-790.

Vigoreaux JO. 1994. The muscle Z band: lessons in stress management. J Muscle Res Cell Motil 15(3):237-255.

Viklund IM, Aspenstrom P, Meas-Yedid V, Zhang B, Kopec J, Agren D, Schneider G, D'Amato M, Olivo-Marin JC, Sansonetti P and others. 2009. WAFL, a new protein involved in regulation of early endocytic transport at the intersection of actin and microtubule dynamics. Exp Cell Res 315(6):1040-1052.

Viklund IM, Kuznetsov NV, Lofberg R, Daperno M, Sostegni R, Astegiano M, Rizzetto M, von Stein O, D'Amato M, von Stein P and others. 2008. Identification of a new WASP and FKBP-like (WAFL) protein in inflammatory bowel disease: a potential marker gene for ulcerative colitis. Int J Colorectal Dis 23(10):921-930.

Villeneuve NF, Lau A, Zhang DD. 2010. Regulation of the Nrf2-Keap1 antioxidant response by the ubiquitin proteasome system: an insight into cullin-ring ubiquitin ligases. Antioxid Redox Signal 13(11):1699-1712.

Vinkemeier U, Obermann W, Weber K, Furst DO. 1993. The globular head domain of titin extends into the center of the sarcomeric M band. cDNA cloning, epitope mapping and immunoelectron microscopy of two titin-associated proteins. J Cell Sci 106:319-330.

Volkmann N, Amann KJ, Stoilova-McPhie S, Egile C, Winter DC, Hazelwood L, Heuser JE, Li R, Pollard TD, Hanein D. 2001. Structure of Arp2/3 complex in its activated state and in actin filament branch junctions. Science 293(5539):2456-2459.

von Bulow M, Heid H, Hess H, Franke WW. 1995. Molecular nature of calicin, a major basic protein of the mammalian sperm head cytoskeleton. Exp Cell Res 219(2):407-413.

Wagner J, Schmidt C, Nikowits W, Jr., Christ B. 2000. Compartmentalization of the somite and myogenesis in chick embryos are influenced by wnt expression. Dev Biol 228(1):86-94.

Wagner M, Siddiqui MA. 2007. Signal transduction in early heart development (II): ventricular chamber specification, trabeculation, and heart valve formation. Exp Biol Med (Maywood) 232(7):866-880.

Waldo KL, Kumiski DH, Wallis KT, Stadt HA, Hutson MR, Platt DH, Kirby ML. 2001. Conotruncal myocardium arises from a secondary heart field. Development 128(16):3179-3188.

Wallgren-Pettersson C, Jasani B, Newman GR, Morris GE, Jones S, Singhrao S, Clarke A, Virtanen I, Holmberg C, Rapola J. 1995. Alpha-actinin in nemaline bodies in congenital nemaline myopathy: immunological confirmation by light and electron microscopy. Neuromuscul Disord 5(2):93-104.

Wallgren-Pettersson C, Sewry CA, Nowak KJ, Laing NG. 2011. Nemaline myopathies. Semin Pediatr Neurol 18(4):230-238.

Wallimann T, Eppenberger HM. 1985. Localization and function of M-line-bound creatine kinase. M-band model and creatine phosphate shuttle. Cell Muscle Motil 6:239-285.

Wallimann T, Turner DC, Eppenberger HM. 1977. Localization of creatine kinase isoenzymes in myofibrils. I. Chicken skeletal muscle. J Cell Biol 75(2 Pt 1):297-317.

Walsh K, Perlman H. 1997. Cell cycle exit upon myogenic differentiation. Curr Opin Genet Dev 7(5):597-602.

Wang J, Sanger JM, Sanger JW. 2005a. Differential effects of Latrunculin-A on myofibrils in cultures of skeletal muscle cells: insights into mechanisms of myofibrillogenesis. Cell Motil Cytoskeleton 62(1):35-47.

Wang J, Walsh K. 1996. Resistance to apoptosis conferred by Cdk inhibitors during myocyte differentiation. Science 273(5273):359-361.

Wang K. 1982. Purification of titin and nebulin. Methods Enzymol 85 Pt B:264-274.

Wang K. 1996. Titin/connectin and nebulin: giant protein rulers of muscle structure and function. Adv Biophys 33:123-134.

Wang K, Knipfer M, Huang QQ, van Heerden A, Hsu LC, Gutierrez G, Quian XL, Stedman H. 1996. Human skeletal muscle nebulin sequence encodes a blueprint for thin filament architecture. Sequence motifs and affinity profiles of tandem repeats and terminal SH3. The Journal of biological chemistry 271(8):4304-4314.

Wang K, McClure J, Tu A. 1979. Titin: major myofibrillar components of striated muscle. Proc Natl Acad Sci U S A 76(8):3698-3702.

Wang K, Ramirez-Mitchell R. 1983. A network of transverse and longitudinal intermediate filaments is associated with sarcomeres of adult vertebrate skeletal muscle. J Cell Biol 96(2):562-570.

Wang K, Williamson CL. 1980. Identification of an N2 line protein of striated muscle. Proc Natl Acad Sci U S A 77(6):3254-3258.
Wang K, Wright J. 1988. Architecture of the sarcomere matrix of skeletal muscle: immunoelectron microscopic evidence that suggests a set of parallel inextensible nebulin filaments anchored at the Z line. J Cell Biol 107:2199-2212.
Wang M, Mominoki K, Kinutani M, Wang Z, Kobayashi N, Shimokawa T, Nabeka H, Fujiwara T, Matsuda S. 2011. Developmental delay in islet-1-positive motor neurons in chick spina bifida. J Vet Med Sci 73(4):447-452.
Wang W, Ding J, Allen E, Zhu P, Zhang L, Vogel H, Yang Y. 2005b. Gigaxonin interacts with tubulin folding cofactor B and controls its degradation through the ubiquitin-proteasome pathway. Curr Biol 15(22):2050-2055.
Wang X, Osinska H, Gerdes AM, Robbins J. 2002. Desmin filaments and cardiac disease: establishing causality. J Card Fail 8(6 Suppl):S287-292.
Warty V, Diven W, Cadoff E, Todo S, Starzl T, Sanghvi A. 1988. FK506: a novel immunosuppressive agent. Characteristics of binding and uptake by human lymphocytes. Transplantation 46(3):453-455.
Watanabe Y, Buckingham M. 2010. The formation of the embryonic mouse heart: heart fields and myocardial cell lineages. Ann N Y Acad Sci 1188:15-24.
Way M, Sanders M, Chafel M, Tu YH, Knight A, Matsudaira P. 1995. beta-Scruin, a homologue of the actin crosslinking protein scruin, is localized to the acrosomal vesicle of Limulus sperm. J Cell Sci 108:3155-3162.
Weber A, Pennise CR, Babcock GG, Fowler VM. 1994. Tropomodulin caps the pointed ends of actin filaments. J Cell Biol 127:1627-1635.
Wehrle-Haller B. 2012. Structure and function of focal adhesions. Curr Opin Cell Biol 24(1):116-124.
Weins A, Schwarz K, Faul C, Barisoni L, Linke WA, Mundel P. 2001. Differentiation- and stress-dependent nuclear cytoplasmic redistribution of myopodin, a novel actin-bundling protein. J Cell Biol 155(3):393-404.
Welte MA. 2004. Bidirectional transport along microtubules. Curr Biol 14(13):R525-537.
Williams SK, Spence HJ, Rodgers RR, Ozanne BW, Fitzgerald U, Barnett SC. 2005. Role of Mayven, a kelch-related protein in oligodendrocyte process formation. J Neurosci Res 81(5):622-631.
Witt CC, Burkart C, Labeit D, McNabb M, Wu Y, Granzier H, Labeit S. 2006. Nebulin regulates thin filament length, contractility, and Z-disk structure in vivo. EMBO J 25(16):3843-3855.
Wolff T, O'Neill RE, Palese P. 1998. NS1-Binding protein (NS1-BP): a novel human protein that interacts with the influenza A virus nonstructural NS1 protein is relocalized in the nuclei of infected cells. J Virol 72(9):7170-7180.
Woodhead JL, Lowey S. 1983. An in vitro study of the interactions of skeletal muscle M-protein and creatine kinase with myosin and its subfragments. J Mol Biol 168(4):831-846.
Wright WE, Sassoon DA, Lin VK. 1989. Myogenin, a factor regulating myogenesis, has a domain homologous to MyoD. Cell 56(4):607-617.
Wu YL, Gong Z. 2004. A novel zebrafish kelchlike gene klhl and its human ortholog KLHL display conserved expression patterns in skeletal and cardiac muscles. Gene 338(1):75-83.
Xu L, Wei Y, Reboul J, Vaglio P, Shin TH, Vidal M, Elledge SJ, Harper JW. 2003. BTB proteins are substrate-specific adaptors in an SCF-like modular ubiquitin ligase containing CUL-3. Nature 425(6955):316-321.
Xue F, Cooley L. 1993. kelch encodes a component of intercellular bridges in Drosophila egg chambers. Cell 72(5):681-693.

Yaffe D, Saxel O. 1977. Serial passaging and differentiation of myogenic cells isolated from dystrophic mouse muscle. Nature 270(5639):725-727.
Yamaguchi M, Robson RM, Stromer MH, Dahl DS, Oda T. 1982. Nemaline myopathy rod bodies. Structure and composition. J Neurol Sci 56(1):35-56.
Yanai M, Tatsumi N, Endo F, Yokouchi Y. 2005. Analysis of gene expression patterns in the developing chick liver. Dev Dyn 233(3):1116-1122.
Yang X, Dormann D, Munsterberg AE, Weijer CJ. 2002. Cell movement patterns during gastrulation in the chick are controlled by positive and negative chemotaxis mediated by FGF4 and FGF8. Dev Cell 3(3):425-437.
Yoshida N, Yoshida S, Koishi K, Masuda K, Nabeshima Y. 1998. Cell heterogeneity upon myogenic differentiation: down-regulation of MyoD and Myf-5 generates 'reserve cells'. J Cell Sci 111:769-779.
Young P, Ferguson C, Banuelos S, Gautel M. 1998. Molecular structure of the sarcomeric Z-disk: two types of titin interactions lead to an asymmetrical sorting of alpha-actinin. EMBO J 17(6):1614-1624.
Yu W, Li Y, Zhou X, Deng Y, Wang Z, Yuan W, Li D, Zhu C, Zhao X, Mo X and others. 2008. A novel human BTB-kelch protein KLHL31, strongly expressed in muscle and heart, inhibits transcriptional activities of TRE and SRE. Mol Cells 26(5):443-453.
Yuan S, Schoenwolf GC. 2000. Islet-1 marks the early heart rudiments and is asymmetrically expressed during early rotation of the foregut in the chick embryo. Anat Rec 260(2):204-207.
Yusuf F, Brand-Saberi B. 2012. Myogenesis and muscle regeneration. Histochem Cell Biol 138(2):187-199.
Zhang DD, Lo SC, Cross JV, Templeton DJ, Hannink M. 2004. Keap1 is a redox-regulated substrate adaptor protein for a Cul3-dependent ubiquitin ligase complex. Mol Cell Biol 24(24):10941-10953.
Zhang DD, Lo SC, Sun Z, Habib GM, Lieberman MW, Hannink M. 2005. Ubiquitination of Keap1, a BTB-Kelch substrate adaptor protein for Cul3, targets Keap1 for degradation by a proteasome-independent pathway. The Journal of biological chemistry 280(34):30091-30099.
Zhang L, Shi S, Zhang J, Zhou F, ten Dijke P. 2012. Wnt/beta-catenin signaling changes C2C12 myoblast proliferation and differentiation by inducing Id3 expression. Biochem Biophys Res Commun 419(1):83-88.
Zhi G, Ryder JW, Huang J, Ding P, Chen Y, Zhao Y, Kamm KE, Stull JT. 2005. Myosin light chain kinase and myosin phosphorylation effect frequency-dependent potentiation of skeletal muscle contraction. Proc Natl Acad Sci U S A 102(48):17519-17524.
Zhong J, Baquiran JB, Bonakdar N, Lees J, Ching YW, Pugacheva E, Fabry B, O'Neill GM. 2012. NEDD9 stabilizes focal adhesions, increases binding to the extra-cellular matrix and differentially effects 2D versus 3D cell migration. PLoS One 7(4):e35058.
Zimmerman ES, Schulman BA, Zheng N. 2010. Structural assembly of cullin-RING ubiquitin ligase complexes. Curr Opin Struct Biol 20(6):714-721.
Zollman S, Godt D, Prive GG, Couderc JL, Laski FA. 1994. The BTB domain, found primarily in zinc finger proteins, defines an evolutionarily conserved family that includes several developmentally regulated genes in Drosophila. Proc Natl Acad Sci U S A 91(22):10717-10721.

Appendix

A.1 Klhl31 Sequences (gallus gallus)

This chapter contains information of DNA and protein sequences for Klhl31 with a legend highlighting the functional domains. Primer information is also available for cloned Klhl31 constructs.

A1.1 Klhl31 (DNA)

atggcacctaagaagaagaacgtgaagaagaacaaagcagcagatatcagtgaaatgactatcattgtggaagatggcccc
ctcagtaaactaaatggcttgaatggactcttagatggaggcaatggtttcagctgcgtctcatctgaagtttctgacccatcatat
agcccaaatctcttggaaggtctaagcagaatgagactagaaaattttctttgtgacttgactatcagtaccaaaaccaaatctttc
agtgttcataaggtggtgatggcttcaatcagtgactactttcacaacatcttaaagaaagatccatccactcaaagagtagacct
caatgatgtatccccattgggtctagctactgttatcacctatgcttacactggaaagctcactctctcactttatacaataggtagt
attatttccaccgcgatttatcttcagattcacacccttgtaaagatgtgctgtgattttctaacccaagaaatcagtgttgagaattg
tatgtatattgccaatattgcagaaacgtacggactaaaaacaaccaaggaagctgcacacaaatttattagagacaacttcatt
gaattttcagaaacagatcagttcttaaaactcacttttgatcagattaatgaacttcttgcagatgatgacttgcagttgccttctga
aattgttgcattccagattgcaataaaatggctggaatttgaccaaaaaagagtaaagtttgctgctgatctcttaggtaacattcgt
tttggtactatctcagctcaagacctcgtcaattatgtccaaactgttccgagaatgatgcaagatgcagattgccataaactcctg
gtagatgccatgaactatcatttgcttccctatcatcagaatacacttcagtctagaagaacaaggattcgtggaggattcagagt
gttagttactgttggcggacgccctgctttaacagaaaagtctcttagcagagacatcttgtacagagatcctgaaaatggatgg
aagaagcttagtgaaatgcccgctaaaagttttaaccagtgcgtgacggtgatggatgggtttctctacgtggccggtggggaa
gaccagaatgatgccaggaaccaagccaagcatgcagtcagcaacttctgcagatacgatcctcgtttcaacacctggattca
cctggcaaatatgaatcagaagcgcacccacttcagcctgaatgtattcaatggcctccttttgcagtgggtggtcgcaacttg
gagggttgtctctcctcgatggagtgctacgtgcctgcaactaatcagtggcagatgaaggcacccctggaggtgcccaggtg
ctgccatgccagtgctgtggtggatggtaggatcctggtcacgggaggttacattaataatgcttactctcgttcagtgtgcatgt
atgaccccagcaatgatagctggcaagataagtccagtcttagcaccccacgagggtggcactgtgccgtgtccctgctgga
gagggtctatgtcatgggtgggtctcaactgggggggagaggggaaagggtcgacgttctccctgtggagtgttacagcccctt
acacagggcagtggagttatgtggcacccccttcaaactggagttagcacagccggtgcttcgatgctggatgggaaaatttact
agtgggggggctggaatgagatagagaaaaaatataagaagtgcattcagtgctataacccagatctcaatgagtggacgga
ggaagacgagctgcctgaagccactgtgggagtatcctgttgtactatatccatgcccaacaccaagacaagggagtccaga
gcaagctcagtctcttctgtaccagtcagtatt**taa**

Legend:

Start/Stop-Codon

BTB-Domain

Kelch-repeats

A1.2 Klhl31 (protein)

MAPKKKNVKKNKAADISEMTIIVEDGPLSKLNGLNGLLDGGNGFSCVSSEVSD
PSYSPNLLEG**LSRMRLENFLCDLTISTKTKSFSVHKVVMASISDYFHNILKKD**
PSTQRVDLNDVSPLGLATVITYAYTGKLTLSLYTIGSIISTAIYLQIHTLVKM
CCDFLTQEISVENCMYIANIAETYGLKTTKEAAHKFIRDNFIEFSETDQFLKLT
FDQINELLADDDLQLPSEIVAFQIAIKWLEFDQKRVKFAADLLGNIRFGTISAQD
LVNYVQTVPRMMQDADCHKLLVDAMNYHLLPYHQNTLQSRRTRIRGGFR**VL**
VTVGGRPALTEKSLSRDILYRDPENGWKKLSEMPAKSFNQCVTVMDGFLY
VAGGEDQNDARNQAKHAVSNFCRYDPRFNTWIHLANMNQKRTHFSLNVF
NGLLFAVGGRNLEGCLSSMECYVPATNQWQMKAPLEVPRCCHASAVVDG
RILVTGGYINNAYSRSVCMYDPSNDSWQDKSSLSTPRGWHCAVSLLERVYV
MGGSQLGGRGERVDVLPVECYSPYTGQWSYVAPLQTGVSTAGASMLDGK
IYLVGGWNEIEKKYKKCIQCYNPDLNEWTEEDELPEATVGVSCCTISMPNT
KTRESRASSVSSVPVSI

Legend:

Start Methionine

BTB-Domain

Kelch-repeats

A1.3 pEGFP-N1 / dsRED-N1 Klhl31 constructs

pEGFP-N1 Klhl31 FL
dsRED-N1 Klhl31 FL

pEGFP-N1 as well as dsRED-N1 share the same multiple cloning site.

All used pEGFP-N1/C1 and dsRED-N1 constructs are not manufactured anymore by Clontech.

Vector information and map for pEGFP-N1

GenBank Accession #55762

Clontech Catalog number #6085-1

Vector map and multiple cloning site for pEGFP-N1

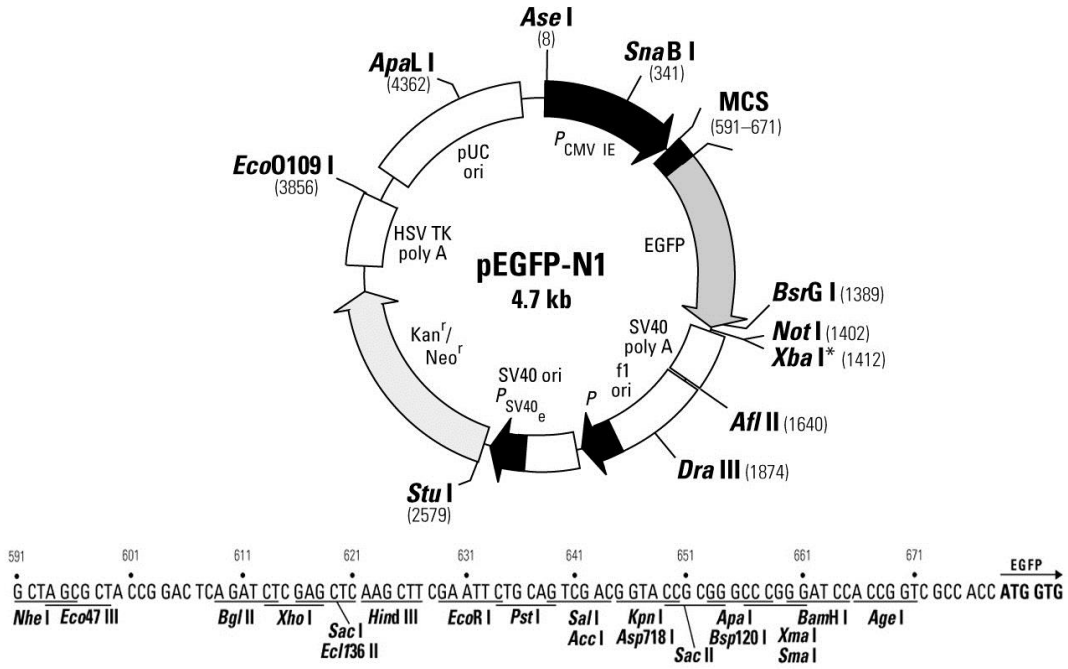

Vector information for pDsRed-Express-N1

GenBank Accession n/a

Clontech Catalog number 632429

Same multiple cloning site as for pEGFP-N1

Primer information

forward primer – ctcgag**atg**gcacctaagaagaagaac
restriction enzyme – XhoI

reverse primer - gaattccaatactgactggtacagaaga
restriction enzyme - EcoRI

ctcgag**atg**gcacctaagaagaagaacgtgaagaagaacaaagcagcagatatcagtgaaatgactatcattgtggaagatg
gccccctcagtaaactaaatggcttgaatggactcttagatggaggcaatggtttcagctgcgtctcatctgaagtttctgaccca
tcatatagcccaaatctcttggaaggtctaagcagaatgagactagaaaattttctttgtgacttgactatcagtaccaaaaccaaa
tctttcagtgttcataaggtggtgatggcttcaatcagtgactactttcacaacatcttaaagaaagatccatccactcaaagagta
gacctcaatgatgtatccccattgggtctagctactgttatcacctatgcttacactggaaagctcactctctcactttatacaatag

gtagtattatttccaccgcgatttatcttcagattcacacccttgtaaagatgtgctgtgattttctaacccaagaaatcagtgttgag
aattgtatgtatattgccaatattgcagaaacgtacggactaaaaacaaccaaggaagctgcacacaaatttattagagacaact
tcattgaattttcagaaacagatcagttcttaaaactcacttttgatcagattaatgaacttcttgcagatgatgacttgcagttgcctt
ctgaaattgttgcattccagattgcaataaaatggctggaatttgaccaaaaaagagtaaagtttgctgctgatctcttaggtaaca
ttcgttttggtactatctcagctcaagacctcgtcaattatgtccaaactgttccgagaatgatgcaagatgcagattgccataaac
tcctggtagatgccatgaactatcatttgcttccctatcatcagaatacacttcagtctagaagaacaaggattcgtggaggattca
gagtgttagttactgttggcggacgccctgctttaacagaaaagtctcttagcagagacatcttgtacagagatcctgaaaatgg
atggaagaagcttagtgaaatgcccgctaaaagttttaaccagtgcgtgacggtgatggatgggtttctctacgtggccggtgg
ggaagaccagaatgatgccaggaaccaagccaagcatgcagtcagcaacttctgcagatacgatcctcgtttcaacacctgg
attcacctggcaaatatgaatcagaagcgcacccacttcagcctgaatgtattcaatggcctccttttgcagtgggtggtcgcaa
cttggagggttgtctctcctcgatggagtgctacgtgcctgcaactaatcagtggcagatgaaggcacccctggaggtgccca
ggtgctgccatgccagtgctgtggtggatggtaggatcctggtcacgggaggttacattaataatgcttactctcgttcagtgtgc
atgtatgaccccagcaatgatagctggcaagataagtccagtcttagcaccccacgagggtggcactgtgccgtgtccctgct
ggagagggtctatgtcatgggtgggtctcaactgggggggagaggggaaagggtcgacgttctccctgtggagtgttacagc
ccttacacagggcagtggagttatgtggcacccctttcaaactggagttagcacagccggtgcttcgatgctggatgggaaaatt
tacttagtgggggctggaatgagatagagaaaaaatataagaagtgcattcagtgctataacccagatctcaatgagtggac
ggaggaagacgagctgcctgaagccactgtgggagtatcctgttgtactatatccatgcccaacaccaagacaagggagtcc
agagcaagctcagtctcttctgtaccagtcagtattggaattc

pEGFP-N1 Klhl31 ΔBTB
dsRED-N1 Klhl31 ΔBTB

Primer information

forward primer – ctcgag**atg**gcacctaagaagaagaac
restriction enzyme – XhoI

reverse primer - gaattccaatactgactggtacagaaga
restriction enzyme - EcoRI

ctcgag**atg**gcacctaagaagaagaacgtgaagaagaacaaagcagcagatatcagtgaaatgactatcattgtggaagatg
gccccctcagtaaactaaatggcttgaatggactcttagatggaggcaatggtttcagctgcgtctcatctgaagtttctgaccca
tcatatagcccaaatctcttggaaggttacggactaaaaacaaccaaggaagctgcacacaaatttattagagacaacttcattg
aattttcagaaacagatcagttcttaaaactcacttttgatcagattaatgaacttcttgcagatgatgacttgcagttgccttctgaa
attgttgcattccagattgcaataaaatggctggaatttgaccaaaaaagagtaaagtttgctgctgatctcttaggtaacattcgtt
ttggtactatctcagctcaagacctcgtcaattatgtccaaactgttccgagaatgatgcaagatgcagattgccataaactcctg
gtagatgccatgaactatcatttgcttccctatcatcagaatacacttcagtctagaagaacaaggattcgtggaggattcagagt
gttagttactgttggcggacgccctgctttaacagaaaagtctcttagcagagacatcttgtacagagatcctgaaaatggatgg
aagaagcttagtgaaatgcccgctaaaagttttaaccagtgcgtgacggtgatggatgggtttctctacgtggccggtggggaa
gaccagaatgatgccaggaaccaagccaagcatgcagtcagcaacttctgcagatacgatcctcgtttcaacacctggattca
cctggcaaatatgaatcagaagcgcacccacttcagcctgaatgtattcaatggcctccttttgcagtgggtggtcgcaacttg
gagggttgtctctcctcgatggagtgctacgtgcctgcaactaatcagtggcagatgaaggcacccctggaggtgcccaggtg
ctgccatgccagtgctgtggtggatggtaggatcctggtcacgggaggttacattaataatgcttactctcgttcagtgtgcatgt
atgaccccagcaatgatagctggcaagataagtccagtcttagcaccccacgagggtggcactgtgccgtgtccctgctgga
gagggtctatgtcatgggtgggtctcaactgggggggagaggggaaagggtcgacgttctccctgtggagtgttacagccctt
acacagggcagtggagttatgtggcacccctttcaaactggagttagcacagccggtgcttcgatgctggatgggaaaatttact
tagtgggggctggaatgagatagagaaaaaatataagaagtgcattcagtgctataacccagatctcaatgagtggacgga
ggaagacgagctgcctgaagccactgtgggagtatcctgttgtactatatccatgcccaacaccaagacaagggagtccaga
gcaagctcagtctcttctgtaccagtcagtattggaattc

pEGFP-N1 Klhl31 ΔKR
dsRED-N1 Klhl31 ΔKR

Primer information

forward primer – ctcgag**atg**gcacctaagaagaagaac
restriction enzyme – XhoI

reverse primer - gaattcctctgaatcctccacgaatcct
restriction enzyme - EcoRI

ctcgag**atg**gcacctaagaagaagaacgtgaagaagaacaaagcagcagatatcagtgaaatgactatcattgtggaagatg
gccccctcagtaaactaaatggcttgaatggactcttagatggaggcaatggtttcagctgcgtctcatctgaagtttctgaccca
tcatatagcccaaatctcttggaaggtctaagcagaatgagactagaaaattttctttgtgacttgactatcagtaccaaaaccaaa
tctttcagtgttcataaggtggtgatggcttcaatcagtgactactttcacaacatcttaaagaaagatccatccactcaaagagta
gacctcaatgatgtatccccattgggtctagctactgttatcacctatgcttacactggaaagctcactctctcactttatacaatag
gtagtattatttccaccgcgatttatcttcagattcacacccttgtaaagatgtgctgtgattttctaacccaagaaatcagtgttgag
aattgtatgtatattgccaatattgcagaaacgtacggactaaaaacaaccaaggaagctgcacacaaatttattagagacaact
tcattgaattttcagaaacagatcagttcttaaaactcacttttgatcagattaatgaacttcttgcagatgatgacttgcagttgcctt
ctgaaattgttgcattccagattgcaataaaatggctggaatttgaccaaaaaagagtaaagtttgctgctgatctcttaggtaaca
ttcgttttggtactatctcagctcaagacctcgtcaattatgtccaaactgttccgagaatgatgcaagatgcagattgccataaac
tcctggtagatgccatgaactatcatttgcttccctatcatcagaatacacttcagtctagaagaacaaggattcgtggaggattca
gaggaattc

A1.4 pEGFP-C1 Klhl31 constructs

Vector information and map for pEGFP-C1

GenBank Accession #55763

Clontech Catalog number #6084-1

Vector map and multiple cloning site for pEGFP-C1

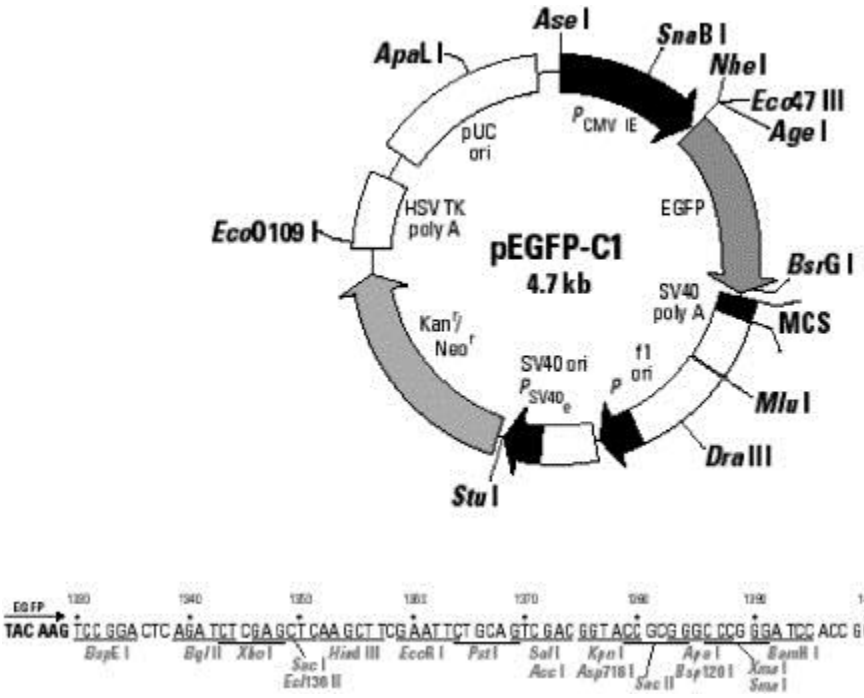

pEGFP-C1 Klhl31 FL

Primer information

forward primer – tccgga**atg**gcacctaagaagaac
restriction enzyme – BspEI

reverse primer - gaattctcaagcgtaatctggaacatcgtatgggtaaatactgactggtacagaag
restriction enzyme - EcoRI

tccgga**atg**gcacctaagaagaagaacgtgaagaagaacaaagcagcagatatcagtgaaatgactatcattgtggaagatg
gccccctcagtaaactaaatggcttgaatggactcttagatggaggcaatggtttcagctgcgtctcatctgaagtttctgaccca
tcatatagcccaaatctcttggaaggtctaagcagaatgagactagaaaatttttctttgtgacttgactatcagtaccaaaaccaaa
tctttcagtgttcataaggtggtgatggcttcaatcagtgactactttcacaacatcttaaagaaagatccatccactcaaagagta
gacctcaatgatgtatccccattgggtctagctactgttatcacctatgcttacactggaaagctcactctctcactttatacaatag
gtagtattatttccaccgcgatttatcttcagattcacacccttgtaaagatgtgctgtgattttctaacccaagaaatcagtgttgag

aattgtatgtatattgccaatattgcagaaacgtacggactaaaaacaaccaaggaagctgcacacaaatttattagagacaact
tcattgaattttcagaaacagatcagttcttaaaactcacttttgatcagattaatgaacttcttgcagatgatgacttgcagttgcctt
ctgaaattgttgcattccagattgcaataaaatggctggaatttgaccaaaaaagagtaaagtttgctgctgatctcttaggtaaca
ttcgttttggtactatctcagctcaagacctcgtcaattatgtccaaactgttccgagaatgatgcaagatgcagattgccataaac
tcctggtagatgccatgaactatcatttgcttccctatcatcagaatacacttcagtctagaagaacaaggattcgtggaggattca
gagtgttagttactgttggcggacgccctgctttaacagaaaagtctcttagcagagacatcttgtacagagatcctgaaaatgg
atggaagaagcttagtgaaatgcccgctaaaagttttaaccagtgcgtgacggtgatggatgggtttctctacgtggccggtgg
ggaagaccagaatgatgccaggaaccaagccaagcatgcagtcagcaacttctgcagatacgatcctcgtttcaacacctgg
attcacctggcaaatatgaatcagaagcgcacccacttcagcctgaatgtattcaatggcctccttttttgcagtgggtggtcgcaa
cttggagggttgtctctcctcgatggagtgctacgtgcctgcaactaatcagtggcagatgaaggcacccctggaggtgccca
ggtgctgccatgccagtgctgtggtggatggtaggatcctggtcacgggaggttacattaataatgcttactctcgttcagtgtgc
atgtatgaccccagcaatgatagctggcaagataagtccagtcttagcaccccacgagggtggcactgtgccgtgtccctgct
ggagagggtctatgtcatgggtgggtctcaactgggggggagaggggaaagggtcgacgttctccctgtggagtgttacagc
ccttacacagggcagtggagttatgtggcacccccttcaaactggagttagcacagccggtgcttcgatgctggatgggaaaatt
tacttagtgggggggctggaatgagatagagaaaaaatataagaagtgcattcagtgctataacccagatctcaatgagtggac
ggaggaagacgagctgcctgaagccactgtgggagtatcctgttgtactatatccatgcccaacaccaagacaagggagtcc
agagcaagctcagtctcttctgtaccagtcagtatttacccatacgatgttccagattacgct**tga**gaattc

pEGFP-C1 Klhl31 ΔBTB

Primer information

forward primer – tccgga**atg**gcacctaagaagaac
restriction enzyme – BspEI

reverse primer - gaattctcaagcgtaatctggaacatcgtatgggtaaatactgactggtacagaag
restriction enzyme - EcoRI

tccgga**atg**gcacctaagaagaagaacgtgaagaagaacaaagcagcagatatcagtgaaatgactatcattgtggaagatg
gccccctcagtaaactaaatggcttgaatggactcttagatggaggcaatggtttcagctgcgtctcatctgaagtttctgaccca
tcatatagcccaaatctcttggagtacggactaaaaacaaccaaggaagctgcacacaaatttattagagacaacttcattgaatt
ttcagaaacagatcagttcttaaaactcacttttgatcagattaatgaacttcttgcagatgatgacttgcagttgccttctgaaattg
ttgcattccagattgcaataaaatggctggaatttgaccaaaaaagagtaaagtttgctgctgatctcttaggtaacattcgttttgg
tactatctcagctcaagacctcgtcaattatgtccaaactgttccgagaatgatgcaagatgcagattgccataaactcctggtag
atgccatgaactatcatttgcttccctatcatcagaatacacttcagtctagaagaacaaggattcgtggaggattcagagtgtta
gttactgttggcggacgccctgctttaacagaaaagtctcttagcagagacatcttgtacagagatcctgaaaatggatggaag
aagcttagtgaaatgcccgctaaaagttttaaccagtgcgtgacggtgatggatgggtttctctacgtggccggtggggaagac
cagaatgatgccaggaaccaagccaagcatgcagtcagcaacttctgcagatacgatcctcgtttcaacacctggattcacctg
gcaaatatgaatcagaagcgcacccacttcagcctgaatgtattcaatggcctccttttttgcagtgggtggtcgcaacttggagg
gttgtctctcctcgatggagtgctacgtgcctgcaactaatcagtggcagatgaaggcacccctggaggtgcccaggtgctgc
catgccagtgctgtggtggatggtaggatcctggtcacgggaggttacattaataatgcttactctcgttcagtgtgcatgtatga
ccccagcaatgatagctggcaagataagtccagtcttagcaccccacgagggtggcactgtgccgtgtccctgctggagagg
gtctatgtcatgggtgggtctcaactgggggggagaggggaaagggtcgacgttctccctgtggagtgttacagcccttacac
agggcagtggagttatgtggcacccccttcaaactggagttagcacagccggtgcttcgatgctggatgggaaaatttacttagt
gggggggctggaatgagatagagaaaaaatataagaagtgcattcagtgctataacccagatctcaatgagtggacggaggaa
gacgagctgcctgaagccactgtgggagtatcctgttgtactatatccatgcccaacaccaagacaagggagtccagagcaa
gctcagtctcttctgtaccagtcagtatttacccatacgatgttccagattacgct**tga**gaattc

pEGFP-C1 Klhl31 ΔKR

Primer information

forward primer – tccgga**atg**gcacctaagaagaac
restriction enzyme – BspEI

reverse primer - gaattctcaagcgtaatctggaacatcgtatgggtatctgaatcctccacgaatcc
restriction enzyme - EcoRI

tccgga**atg**gcacctaagaagaagaacgtgaagaagaacaaagcagcagatatcagtgaaatgactatcattgtggaagatg
gccccctcagtaaactaaatggcttgaatggactcttagatggaggcaatggtttcagctgcgtctcatctgaagtttctgaccca
tcatatagcccaaatctcttggaaggtctaagcagaatgagactagaaaattttctttgtgacttgactatcagtaccaaaaccaaa
tctttcagtgttcataaggtggtgatggcttcaatcagtgactactttcacaacatcttaaagaaagatccatccactcaaagagta
gacctcaatgatgtatccccattgggtctagctactgttatcacctatgcttacactggaaagctcactctctcactttatacaatag
gtagtattatttccaccgcgatttatcttcagattcacacccttgtaaagatgtgctgtgattttctaacccaagaaatcagtgttgag
aattgtatgtatattgccaatattgcagaaacgtacggactaaaaacaaccaaggaagctgcacacaaatttattagagacaact
tcattgaattttcagaaacagatcagttcttaaaactcacttttgatcagattaatgaacttcttgcagatgatgacttgcagttgcctt
ctgaaattgttgcattccagattgcaataaaatggctggaatttgaccaaaaaagagtaaagtttgctgctgatctcttaggtaaca
ttcgttttggtactatctcagctcaagacctcgtcaattatgtccaaactgttccgagaatgatgcaagatgcagattgccataaac
tcctggtagatgccatgaactatcatttgcttccctatcatcagaatacacttcagtctagaagaacaaggattcgtggaggattca
gatacccatacgatgttccagattacgct**tga**gaattc

A.2 Klhl31 Sequence (homo sapiens)

Klhl31 IMAGE Clone 9021264

Clone obtained from Source BioScience Life Sciences

Plasmid Information for IMAGE Clone 9021264

Cross Reference	Gene Symbol	KLHL31
	Species	Homo sapiens
Technical Clone Data		
	Library	NIH_MGC_362
	Alternative Name	9021264 (IMAGE ID)
	Source	Homo sapiens, tissue:'pool of cerebellum, kidney, placenta, testis, lung, colon, liver, heart, thyroid, bladder, uterus', organ:'mixed'
	Host	DH10B TonA (Escherichia coli)
	Vector	pCR4-TOPO
	Cloning Sites	5s: **TA cloning**, 3s: **TA cloning**
	Growth Conditions	medium: **LB** ; antibiotics: **Amp (50 µg/ml)** ; alternative antibiotic: **Kan (30 µg/ml)**
Sequence	• accession: BC137267	

Vector information and map for pCR4-TOPO

Invitrogen Catalog number K4575-02

Vector map and multiple cloning site for pCR®4-TOPO

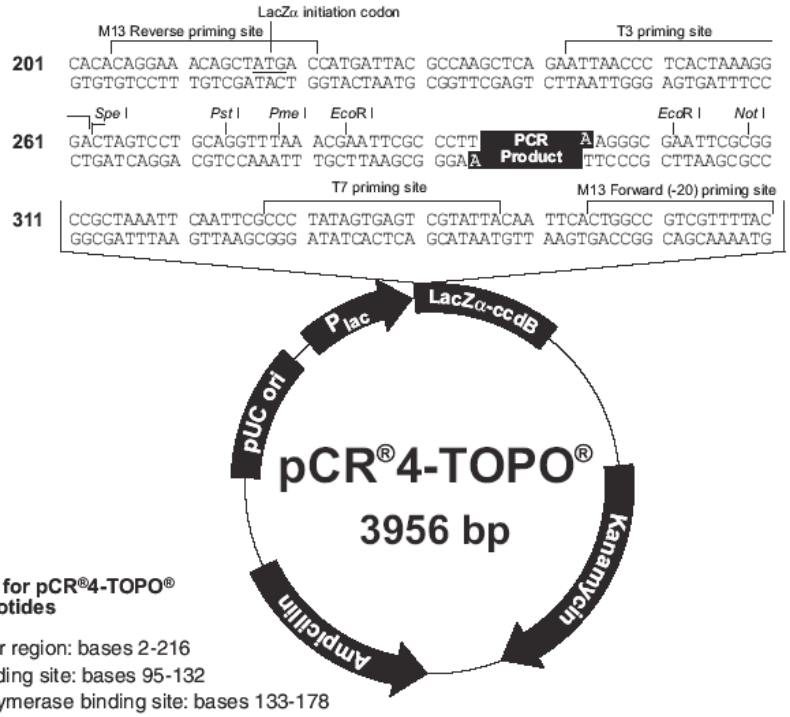

Comments for pCR®4-TOPO®
3956 nucleotides

lac promoter region: bases 2-216
CAP binding site: bases 95-132
RNA polymerase binding site: bases 133-178
Lac repressor binding site: bases 179-199
Start of transcription: base 179
M13 Reverse priming site: bases 205-221
LacZα-*ccdB* gene fusion: bases 217-810
LacZα portion of fusion: bases 217-497
*ccd*B portion of fusion: bases 508-810
T3 priming site: bases 243-262
TOPO® Cloning site: bases 294-295
T7 priming site: bases 328-347
M13 Forward (-20) priming site: bases 355-370
Kanamycin promoter: bases 1021-1070
Kanamycin resistance gene: bases 1159-1953
Ampicillin (*bla*) resistance gene: bases 2203-3063 (c)
Ampicillin (*bla*) promoter: bases 3064-3160 (c)
pUC origin: bases 3161-3834
(c) = complementary strand

Sequence (DNA)

atggcacccaaaaagaagattgtcaaaaagaacaaaggagatatcaatgagatgactataatcgtagaagatagccccctaaa
caaactgaatgctttgaatgggctcctagagggaggcaatggccttagctgcatttcttctgaactaacagatgcttcttatggcc
ccaacctcttggaaggtttaagtaaaatgcggcaggagaacttcttatgtgacttagtcattggtaccaaaaccaaatcctttgat
gttcataagtcagtcatggcttcatgcagtgagtatttttacaacatcctaaaaaaagacccgtcaattcagagggtggatctcaat
gatatctcaccactaggcctggccactgtcattgcatatgcctacactggaaagctcactctctccttgtatacaataggaagcat
tatttctgctgctgtttatcttcagatccatactcttataaagatgtgcagtgattttctgatacgggagatgagtgttgagaattgcat
gtatgttgttaatattgctgaaacatactccctaaaaaatgcaaaagcagcagcccagaaatttattcgggataacttccttgaattt
gcagaatcggatcagtttatgaaacttacatttgaacaaattaatgaacttcttatagatgatgacttacagttgccttctgagatagt
agcattccagattgcaatgaaatggttagaatttgaccaaaagagagtaaaatacgctgcagatcttttgagcaatattcgctttg
gtaccatctctgcacaagacctggtcaattatgttcaatccgtaccaagaatgatgcaagatgctgattgtcacagacttctcgta

gatgctatgaactaccacttgcttccatatcatcaaaacacattgcaatctaggcgaacaagaatccgaggtggctgccgagtc
ctcgtcactgttgggggacgcccaggccttactgagaagtcccttagcagagacatcctgtatagagaccctgaaaatggatg
gagcaagcttacggaaatgccagccaaaagttttaatcagtgtgtggctgtgatggatggatttctttatgtagccggtggtgaa
gaccagaatgatgcaagaaatcaagccaagcatgcagtcagcaatttctgcagatacgatccccgcttcaacacctggataca
cctggccagcatgaaccagaagcgcacgcacttcagcctgagcgtgttcaacgggctcgtgtacgccgcgggcggccgca
acgcagaaggaagcctggcctcgctggagtgctacgtgccctccaccaatcagtggcagccgaagacgcccctggaggtg
gcgcgctgctgccacgctagcgcggtcgccgacggccgcgtgctggtgaccggaggctacatcgccaacgcctactcgcg
ctctgtgtgcgcctacgacccggccagcgaccgtggcaggagctgccgaacctcagcacaccccggggctggcactgcgc
ggtcacgctgagcgacagagtgtacgtgatgggcggcagccagctggggccgcgcggggagcgcgtggacgtgctcacc
gtggagtgctacagccccgcgaccggccagtggagctacgcggcgccgctgcaggtgggagtgagcactgcgggcgtct
cggcgctgcatggccgcgcctacctggtgggggctggaacgagggcgagaagaagtacaagaagtgcatccagtgcttc
agccccgagctcaacgagtggacggaggacgacgagctacccgaggccactgtcggcgtgtcctgctgcaccctctcgatg
cccaacaacgtgactcgggaatcccgggccagttcggtatcttctgtgccagtcagtatctgagcccaggtagatgcagggac
gcaggaa

Sequence (Protein)

MAPKKKIVKKNKGDINEMTIIVEDSPLNKLNALNGLLEGGNGLS
CISSELTDASYGPNLLEGLSKMRQENFLCDLVIGTKTKSFDVHKSVMASCSEYF
YNILKKDPSIQRVDLNDISPLGLATVIAYAYTGKLTLSLYTIGSIISAAVYLQIHTL
IKMCSDFLIREMSVENCMYVVNIAETYSLKNAKAAAQKFIRDNFLEFAESDQFM
KLTFEQINELLIDDDLQLPSEIVAFQIAMKWLEFDQKRVKYAADLLSNIRFGTIS
AQDLVNYVQSVPRMMQDADCHRLLVDAMNYHLLPYHQNTLQSRRTRIRGGC
RVLVTVGGRPGLTEKSLSRDILYRDPENGWSKLTEMPAKSFNQCVAVMDGFLY
VAGGEDQNDARNQAKHAVSNFCRYDPRFNTWIHLASMNQKRTHFSLSVFNGL
VYAAGGRNAEGSLASLECYVPSTNQWQPKTPLEVARCCHASAVADGRVLVTG
GYIANAYSRSVCAYDPASDSWQELPNLSTPRGWHCAVTLSDRVYVMGGSQLG
PRGERVDVLTVECYSPATGQWSYAAPLQVGVSTAGVSALHGRAYLVGGWNE
GEKKYKKCIQCFSPELNEWTEDDELPEATVGVSCCTLSMPNNVTRESRASSVSS
VPVSI

A.3 Yeast-2-Hybrid Screen, Hybrigenics Services

This chapter of the Appendix contains data from the Yeast-2-Hybrid Screen, as well as an example for alignment of retrieved hits from the screen to a human protein library.

A.3.1 Yeast-2-Hybrid Result summary

HYBRIGENICS

services

Results Summary

ULTImate Y2H SCREEN
Homo sapiens - KLHL31
vs Human Adult/Fetal Skeletal Muscle_RP1

Mon, Mar 19, 2012 - 07:56 AM

Screen Parameters

Nature	cDNA
Reference Bait Fragment	Homo sapiens - KLHL31 (aa 1-634) ; hgx2966v1
Prey Library	Human Adult/Fetal Skeletal Muscle_RP1
Vector(s)	pB43 (N-bait-GAL4-C fusion)
Processed Clones	84 (pB43_A)
Analyzed Interactions	71.7 millions (pB43_A)
3AT Concentration	0.0 mM (pB43_A)

Global PBS®

	Global PBS (for Interactions represented in the Screen)	Nb	%
A	Very high confidence in the interaction	0	0.0%
B	High confidence in the interaction	1	2.7%
C	Good confidence in the interaction	0	0.0%
D	Moderate confidence in the interaction This category is the most difficult to interpret because it mixes two classes of interactions : - False-positive interactions - Interactions hardly detectable by the Y2H technique (low representation of the mRNA in the library, prey folding, prey toxicity in yeast)	35	94.6%
E	Interactions involving highly connected (or relatively highly connected) prey domains, warning of non-specific interaction. The total number of screens performed on each organism is taken into account to set this connectivity threshold: 20 interactions to different bait proteins in our entire database for Human, 10 for Mouse, Drosophila and Arabidopsis and 6 for all other organisms. They can be classified in different categories: - Prey proteins that are known to be highly connected due to their biological function - Proteins with a prey interacting domain that contains a known protein interaction motif or a biochemically promiscuous motif	1	2.7%
F	Experimentally proven technical artifacts	0	0.0%
	Non Appliable		
N/A	The PBS is a score that is automatically computed through algorithms and cannot be attributed for the following reasons : - All the fragments of the same reference CDS are antisense - The 5p sequence is missing - All the fragments of the same reference CDS are either all OOF1 or all OOF2 - All the fragments of the same reference CDS lie in the 5' or 3' UTR		

A3.2 Blast of a ncRNA Sequence transcribed into protein (based on translation frame 1)

The amino acid sequence based on the RNA Sequence for Jpx was used to search a human protein data base for matching results.

Given nucleotide sequence for Jpx-fragment (as obtained from Hybrigenics Services)

CCCGGGTTCAAGCAATTCTCCTGCTTCAGCCTCCCGAGTAGCTGGGATTACTGGTGCCCATC
ACTGCACCCAGCTCATTTTTTTGTACTTTTAGTGGAGACAGGGTTTTACCATGTTGGCCAGGC
TGGTCTTGAACTCCTGACCTCATGATCCACCCGCCTCGGCCTCCCAAAGTGCTGGGATTACA
GACGTGAGCCACTGCGCCCAGCCAATAACGCATCTTAAACATGAAATATCTCCCCATTTATT
TTGGTCTTTTAAAATTTTCTTCAACAACATTGTGTAGCTTTCTTTATACAAATCTTGCAGGTGT
TTTGTTGAATTATTCCTAAAGATTTAGTCTTTTTGGTGCTATTTTGTATGGAATTGATTTCTTA
ATTTCATTTTTGGATCATTCATTGCTAG

Translation into amino acid sequence by using ExPASy **(**SIB Bioinformatics Resource Portal) identified stop-codons and therefore fragmented proteins. Translation based on frame one (starting with nucleotide one), for example, contained 6 distinct protein fragments and one single amino acid.

Translated amino acid sequence based on Jpx-fragment (frame 1)

PGFKQFSCFSLPSSWDYWCPSLHPAHFFVLLVETGFYHVGQAGLELLTS.

STRLGLPKCWDYRREPLRPANNAS.

T.

NISPFILVF.

NFLQQHCVAFFIQILQVFC.

IIPKDLVFLVLFCMELIS.

FHFWIIHC.

When searching a human protein data base with the described amino acid sequences, various proteins have been found. They all share limited percentage of identity with the blasted amino acid fragment and seem to have no common origin. However, for the first amino acid fragment of the translated nc RNA, a conserved potential binding domain was found. The GVQW domain can usually be found incorporated into longer functional domains. However, no function has been described for this domain yet, but its highly conserved GVQW motif indicates the potential of being a binding domain. Information about the GVQW domain was collected from the NCBI Conserved Domain Database (CDD) (Marchler-Bauer and others, 2011).

Protein Sequence (128 letters)

Results for: lcl|26936 None(128aa) [?]

Your BLAST job specified more than one input sequence. This box lets you choose which input sequence to show BLAST results for.

Query ID
lcl|26936
lcl|26936
Description
None
Molecule type
amino acid
Query Length
128
Database Name
nr
Description
All non-redundant GenBank CDS translations+PDB+SwissProt+PIR+PRF excluding environmental samples from WGS projects See details
Program
BLASTP 2.2.27+ Citation

Reference
Stephen F. Altschul, Thomas L. Madden, Alejandro A. Schäffer, Jinghui Zhang, Zheng Zhang, Webb Miller, and David J. Lipman (1997), "Gapped BLAST and PSI-BLAST: a new generation of protein database search programs", Nucleic Acids Res. 25:3389-3402.
Reference - compositional score matrix adjustment
Stephen F. Altschul, John C. Wootton, E. Michael Gertz, Richa Agarwala, Aleksandr Morgulis, Alejandro A. Schäffer, and Yi-Kuo Yu (2005) "Protein database searches using compositionally adjusted substitution matrices", FEBS J. 272:5101-5109.

Graphic Summary

Show Conserved Domains

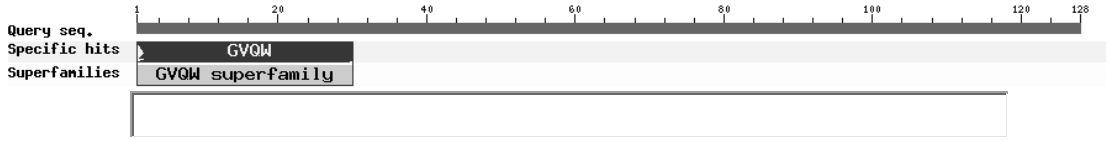

Descriptions

Accession	Description	Max score	Total score	Query coverage	E value	Max ident
BAC03563.1	unnamed protein product [Homo sapiens]	77.0	77.0	75%	2e-17	48%
AAA36776.1	transformation-related protein, partial [Homo sapiens]	79.3	79.3	50%	3e-17	64%
EAW56733.1	similar to zinc finger protein 569, isoform CRA_a [Homo sapiens]	72.8	72.8	39%	5e-16	72%
AAB49034.1	c-MYB [Homo sapiens] >gb|EAW47974.1| v-myb myeloblastosis viral oncogene homolog (avian), isoform CRA_h [Homo sapiens]	76.3	110	52%	8e-16	73%
CAF04484.1	unnamed protein product [Homo sapiens]	76.3	110	52%	9e-16	73%
CAE55174.1	v-myb myeloblastosis viral oncogene homologue (avian) [Homo sapiens]	76.3	110	52%	1e-15	73%
EAW47968.1	v-myb myeloblastosis viral oncogene homolog (avian), isoform CRA_b [Homo sapiens]	75.1	108	52%	1e-15	73%
EAW82740.1	hypothetical protein FLJ38101, isoform CRA_c [Homo sapiens]	69.3	96.7	50%	5e-15	71%
NP_001158011.1	disrupted in schizophrenia 1 protein isoform c [Homo sapiens] >gb|ACR40062.1| disrupted in schizophrenia 1 isoform 26 [Homo sapiens]	71.2	71.2	39%	5e-14	70%
EAW74756.1	hCG1820410 [Homo sapiens]	66.2	96.3	50%	6e-14	76%
EAW93409.1	hCG2039073 [Homo sapiens]	67.0	67.0	51%	8e-14	56%
BAC85397.1	unnamed protein product [Homo sapiens]	66.6	66.6	38%	1e-13	69%
AAG35515.1	PRO2550 [Homo sapiens]	65.9	94.3	54%	2e-13	70%
Q0VDF0.1	RecName: Full=Putative uncharacterized protein LOC65996 >gb|EAW72619.1| hypothetical protein MGC2752 [Homo sapiens]	66.6	99.7	54%	2e-13	67%
BAC11494.1	unnamed protein product [Homo sapiens]	68.2	68.2	38%	3e-13	67%

Accession	Description	Max score	Total score	Query coverage	E value	Max ident
EAW91517.1	hCG1820395 [Homo sapiens]	63.5	63.5	39%	8e-13	68%
BAC85329.1	unnamed protein product [Homo sapiens]	63.9	63.9	39%	9e-13	68%
CAI40721.1	emopamil binding protein-like [Homo sapiens]	64.3	93.2	52%	9e-13	67%
NP_689672.4	UPF0764 protein C16orf89 isoform 1 precursor [Homo sapiens] >sp|Q6UX73.2|CP089_HUMAN RecName: Full=UPF0764 protein C16orf89; Flags: Precursor	66.2	66.2	38%	1e-12	65%
AAQ88847.1	SARG904 [Homo sapiens] >gb|EAW85244.1| hypothetical protein MGC45438, isoform CRA_c [Homo sapiens]	66.2	66.2	38%	2e-12	65%
EAW85243.1	hypothetical protein MGC45438, isoform CRA_b [Homo sapiens]	66.2	66.2	38%	2e-12	65%
AAF69605.1	PRO1722 [Homo sapiens]	62.8	62.8	40%	2e-12	67%
BAH12031.1	unnamed protein product [Homo sapiens]	65.5	65.5	38%	2e-12	63%
BAC86633.1	unnamed protein product [Homo sapiens]	63.2	63.2	39%	3e-12	68%
BAC86261.1	unnamed protein product [Homo sapiens]	62.8	92.4	53%	4e-12	68%
BAA91131.1	unnamed protein product [Homo sapiens]	62.4	62.4	67%	4e-12	48%
EAW65573.1	hCG2039011 [Homo sapiens]	61.2	61.2	29%	5e-12	77%
EAW55887.1	hCG1742852 [Homo sapiens]	62.8	62.8	39%	6e-12	68%
ABC87286.1	ubiquitously transcribed tetratricopeptide repeat protein Y-linked transcript variant 16 [Homo sapiens]	65.1	65.1	38%	9e-12	63%
AAH07609.1	E2F2 protein [Homo sapiens]	59.7	59.7	39%	2e-11	68%
EAX08445.1	hCG2019873 [Homo sapiens]	60.1	60.1	39%	2e-11	62%
AAR84645.1	alpha 1A adrenoceptor isoform 2c [Homo sapiens] >gb|ACA05904.1| adrenergic, alpha-1A-, receptor variant 6 [Homo sapiens]	61.6	61.6	38%	4e-11	64%
EAW62752.1	hCG2039002 [Homo sapiens]	58.9	58.9	38%	6e-11	61%
Q6ZSR6.3	RecName: Full=Putative uncharacterized protein FLJ45256 >dbj|BAC86880.1|	59.7	59.7	31%	6e-11	70%

Accession	Description	Max score	Total score	Query coverage	E value	Max ident
	unnamed protein product [Homo sapiens]					
AAH33883.1	RBP7 protein, partial [Homo sapiens]	59.7	59.7	39%	6e-11	66%
CAI14684.1	retinol binding protein 7, cellular [Homo sapiens]	59.3	59.3	44%	6e-11	61%
AAY68207.1	ubiquitously transcribed tetratricopeptide repeat protein Y-linked transcript variant 6 [Homo sapiens]	61.2	61.2	38%	1e-10	58%
EAW85402.1	hCG1778978 [Homo sapiens]	57.8	57.8	39%	1e-10	66%
ABR09258.1	ubiquitously transcribed tetratricopeptide repeat protein Y-linked transcript variant 8 [Homo sapiens]	61.6	61.6	38%	1e-10	58%
EAW93800.1	hypothetical protein MGC72075, isoform CRA_c [Homo sapiens]	57.8	57.8	39%	1e-10	64%
ABR09247.1	ubiquitously transcribed tetratricopeptide repeat protein Y-linked transcript variant 9 [Homo sapiens]	61.2	61.2	38%	1e-10	58%
ABV49427.1	ubiquitously transcribed tetratricopeptide repeat protein Y-linked transcript variant 28 [Homo sapiens]	61.2	61.2	38%	1e-10	58%
ABC75708.1	ubiquitously transcribed tetratricopeptide repeat protein Y-linked transcript variant 27 [Homo sapiens]	61.2	61.2	38%	1e-10	58%
BAF85547.1	unnamed protein product [Homo sapiens]	61.2	61.2	38%	1e-10	58%
ABC87284.1	ubiquitously transcribed tetratricopeptide repeat protein Y-linked transcript variant 29 [Homo sapiens]	61.2	61.2	38%	1e-10	58%
ABC75709.1	ubiquitously transcribed tetratricopeptide repeat protein Y-linked transcript variant 24 [Homo sapiens]	61.2	61.2	38%	1e-10	58%
ABR09240.1	ubiquitously transcribed tetratricopeptide repeat protein Y-linked transcript variant 18 [Homo sapiens]	61.2	61.2	38%	1e-10	58%
ABR09243.1	ubiquitously transcribed tetratricopeptide repeat protein	61.2	61.2	38%	2e-10	58%

Accession	Description	Max score	Total score	Query coverage	E value	Max ident
	Y-linked transcript variant 22 [Homo sapiens]					
AAU87837.1	ubiquitously transcribed tetratricopeptide repeat protein Y-linked transcript variant 11 [Homo sapiens]	61.2	61.2	38%	2e-10	58%
NP_872601.1	histone demethylase UTY isoform 1 [Homo sapiens] >gb|AAC51843.1| ubiquitous TPR motif, Y isoform [Homo sapiens]	61.2	61.2	38%	2e-10	58%
Q8WTZ3.1	RecName: Full=Zinc finger protein ENSP00000375192 >gb|AAH21822.1| ZNF99 protein [Homo sapiens] >gb|EAW84927.1| hCG1796108 [Homo sapiens]	58.9	58.9	52%	2e-10	49%
ABR09242.1	ubiquitously transcribed tetratricopeptide repeat protein Y-linked transcript variant 4 [Homo sapiens]	61.2	61.2	38%	2e-10	58%
ABR09253.1	ubiquitously transcribed tetratricopeptide repeat protein Y-linked transcript variant 30 [Homo sapiens]	61.2	61.2	38%	2e-10	58%
BAC05300.1	unnamed protein product [Homo sapiens] >emb|CAH71256.1| tigger transposable element derived 1-like 2 [Homo sapiens]	58.2	58.2	39%	2e-10	69%
ABV49466.1	ubiquitously transcribed tetratricopeptide repeat protein Y-linked transcript variant 23 [Homo sapiens]	61.2	61.2	38%	2e-10	58%
ABR09257.1	ubiquitously transcribed tetratricopeptide repeat protein Y-linked transcript variant 21 [Homo sapiens]	61.2	61.2	38%	2e-10	58%
ABR09255.1	ubiquitously transcribed tetratricopeptide repeat protein Y-linked transcript variant 25 [Homo sapiens]	61.2	61.2	38%	2e-10	58%
ABR09237.1	ubiquitously transcribed tetratricopeptide repeat protein Y-linked transcript variant 12 [Homo sapiens]	60.8	60.8	38%	2e-10	58%
ABR09254.1	ubiquitously transcribed	60.8	60.8	38%	2e-10	58%

Accession	Description	Max score	Total score	Query coverage	E value	Max ident
	tetratricopeptide repeat protein Y-linked transcript variant 19 [Homo sapiens]					
EAW89455.1	hCG2039055 [Homo sapiens]	57.4	87.0	54%	3e-10	67%
BAB14371.1	unnamed protein product [Homo sapiens] >gb|EAW83838.1| ATP/GTP binding protein-like 3, isoform CRA_b [Homo sapiens]	57.0	57.0	38%	4e-10	65%
XP_003960524.1	PREDICTED: putative uncharacterized protein LOC65996-like [Homo sapiens]	55.8	55.8	37%	5e-10	63%
ABV82621.1	ubiquitously transcribed tetratricopeptide repeat protein Y-linked transcript variant 10 [Homo sapiens]	59.3	59.3	38%	7e-10	57%
EAW94179.1	ubiquitin-conjugating enzyme E2D 4 (putative), isoform CRA_b [Homo sapiens]	55.8	55.8	39%	7e-10	66%
EAW55348.1	chromosome 6 open reading frame 79, isoform CRA_c [Homo sapiens]	57.0	57.0	39%	9e-10	62%
EAW62475.1	hCG2038077 [Homo sapiens]	55.5	55.5	39%	9e-10	62%
BAB14934.1	unnamed protein product [Homo sapiens]	57.0	57.0	39%	1e-09	62%
ACP43292.1	ubiquitously transcribed tetratricopeptide repeat Y-linked isoform 3 [Homo sapiens] >gb|ACP43293.1| ubiquitously transcribed tetratricopeptide repeat Y-linked isoform 3 [Homo sapiens] >gb|ACP43294.1| ubiquitously transcribed tetratricopeptide repeat Y-linked isoform 3 [Homo sapiens]	54.3	54.3	41%	2e-09	56%
NP_001243358.1	PDZ and LIM domain protein 5 isoform i [Homo sapiens] >gb|AAR09142.1| PDZ and LIM domain 5 [Homo sapiens]	54.7	54.7	39%	2e-09	64%
BAG64432.1	unnamed protein product [Homo sapiens]	54.7	54.7	50%	2e-09	45%
XP_003846407.1	PREDICTED: putative uncharacterized protein LOC65996-like [Homo sapiens] >gb|AAF69654.1|AF119917_62 PRO2822 [Homo sapiens]	53.9	53.9	37%	2e-09	60%
EAW98491.1	hCG2042307 [Homo sapiens]	53.9	53.9	50%	2e-09	48%

Accession	Description	Max score	Total score	Query coverage	E value	Max ident
EAW53691.1	hCG1747827 [Homo sapiens]	53.9	53.9	37%	2e-09	60%
AAF77052.1	ubiquitous TPR-motif protein Y isoform [Homo sapiens]	55.5	55.5	39%	3e-09	57%
EAW51245.1	hCG2044997 [Homo sapiens]	53.5	53.5	39%	3e-09	63%
AAH28935.1	C3orf64 protein [Homo sapiens]	53.5	53.5	38%	4e-09	58%
BAC86723.1	unnamed protein product [Homo sapiens]	53.9	53.9	53%	4e-09	43%
BAC87102.1	unnamed protein product [Homo sapiens]	53.5	53.5	53%	5e-09	43%
EAW67976.1	cytoskeleton associated protein 5 [Homo sapiens]	56.2	56.2	30%	6e-09	69%
EAW49158.1	hCG1648656, isoform CRA_c [Homo sapiens] >gb|ACF23537.1| unknown [Homo sapiens]	52.4	52.4	39%	9e-09	62%
CAI12641.1	caspase 7, apoptosis-related cysteine peptidase [Homo sapiens] >emb|CAI16007.1| caspase 7, apoptosis-related cysteine peptidase [Homo sapiens]	53.1	53.1	39%	1e-08	58%
EAX11403.1	bromodomain adjacent to zinc finger domain, 2B, isoform CRA_a [Homo sapiens]	51.6	51.6	40%	2e-08	56%
ABR09248.1	ubiquitously transcribed tetratricopeptide repeat protein Y-linked transcript variant 7 [Homo sapiens]	54.3	54.3	39%	2e-08	57%
EAX07947.1	hCG1817231 [Homo sapiens]	52.0	52.0	39%	2e-08	59%
EAX09874.1	hCG1820769 [Homo sapiens]	51.6	51.6	38%	2e-08	58%
XP_003846420.1	PREDICTED: putative calcium-sensing receptor-like 1-like [Homo sapiens]	51.2	80.5	52%	2e-08	69%
XP_003403540.1	PREDICTED: uncharacterized protein LOC100652894 [Homo sapiens] >ref|XP_003960858.1| PREDICTED: uncharacterized protein LOC100652894 [Homo sapiens] >dbj|BAC87615.1| unnamed protein product [Homo sapiens]	52.8	52.8	56%	3e-08	46%
XP_003846587.1	PREDICTED: putative calcium-sensing receptor-like 1-like [Homo sapiens] >ref|XP_003960517.1|	51.2	80.5	52%	3e-08	69%

Accession	Description	Max score	Total score	Query coverage	E value	Max ident
	PREDICTED: putative calcium-sensing receptor-like 1-like [Homo sapiens] >dbj|BAC86985.1| unnamed protein product [Homo sapiens]					
XP_003846686.1	PREDICTED: LOW QUALITY PROTEIN: uncharacterized protein LOC100652894 [Homo sapiens]	52.8	52.8	56%	3e-08	46%
AAH31359.1	Unknown (protein for IMAGE:4778855), partial [Homo sapiens]	48.5	48.5	31%	9e-08	63%
EAX03685.1	hCG2000628 [Homo sapiens]	48.1	48.1	32%	1e-07	60%
EAX06532.1	hCG2031845 [Homo sapiens]	48.9	48.9	28%	1e-07	64%
EAW83901.1	hCG2014257 [Homo sapiens]	50.1	50.1	35%	2e-07	58%
BAE97422.1	decay-accelerating factor splicing variant 1 [Homo sapiens]	51.2	51.2	28%	2e-07	70%
BAB71666.1	unnamed protein product [Homo sapiens]	48.1	48.1	39%	3e-07	60%
EAW97718.1	5'-nucleotidase domain containing 3, isoform CRA_d [Homo sapiens]	48.1	48.1	51%	3e-07	46%
EAW98472.1	hCG2015876 [Homo sapiens]	48.5	48.5	39%	3e-07	58%
EAW70437.1	hCG1641896, isoform CRA_b [Homo sapiens]	48.9	48.9	39%	4e-07	52%
AAC51145.1	FAP protein, partial [Homo sapiens]	48.5	48.5	28%	9e-07	62%
EAX04784.1	chloride channel 3, isoform CRA_c [Homo sapiens]	46.6	46.6	39%	1e-06	56%

A.4 Analysis of the Nebulin Isoforms

A.4.1 Amino Acid Alignment for Nebulin Isoform 2 and Nebulin Isoform 3

The amino acid sequences for Nebulin Isoform 2 and Isoform 3 were aligned using Clustal2W software. The sequences of DNA fragments for clones from the Hybrigenics Y-2-H screen are indicated in grey (for Nebulin Isoform2) and in yellow (for Nebulin Isoform 3).

```
NebV2
MADDEDYEEVVEYYTEEVVYEEVPGETITKIYETTTTRTSDYEQSETSKPALAQPALAQP 60
NebV3
MADDEDYEEVVEYYTEEVVYEEVPGETITKIYETTTTRTSDYEQSETSKPALAQPALAQP 60

************************************************************

NebV2
ASAKPVERRKVIRKKVDPSKFMTPYIAHSQKMQDLFSPNKYKEKFEKTKGQPYASTTDTP 120
NebV3
ASAKPVERRKVIRKKVDPSKFMTPYIAHSQKMQDLFSPNKYKEKFEKTKGQPYASTTDTP 120

************************************************************

NebV2
ELRRIKKVQDQLSEVKYRMDGDVAKTICHVDEKAKDIEHAKKVSQQVSKVLYKQNWEDTK 180
NebV3
ELRRIKKVQDQLSEVKYRMDGDVAKTICHVDEKAKDIEHAKKVSQQVSKVLYKQNWEDTK 180

************************************************************

NebV2
DKYLLPPDAPELVQAVKNTAMFSKKLYTEDWEADKSLFYPYNDSPELRRVAQAQKALSDV 240
NebV3
DKYLLPPDAPELVQAVKNTAMFSKKLYTEDWEADKSLFYPYNDSPELRRVAQAQKALSDV 240

************************************************************

NebV2
AYKKGLAEQQAQFTPLADPPDIEFAKKVTNQVSKQKYKEDYENKIKGKWSETPCFEVANA 300
NebV3
AYKKGLAEQQAQFTPLADPPDIEFAKKVTNQVSKQKYKEDYENKIKGKWSETPCFEVANA 300

************************************************************

NebV2
RMNADNISTRKYQEDFENMKDQIYFMQTETPEYKMNKKAGVAASKVKYKEDYEKNKGKAD 360
NebV3
RMNADNISTRKYQEDFENMKDQIYFMQTETPEYKMNKKAGVAASKVKYKEDYEKNKGKAD 360

************************************************************

NebV2
YNVLPASENPQLRQLKAAGDALSDKLYKENYEKTKAKSINYCETPKFKLDTVLQNFSSDK 420
NebV3
YNVLPASENPQLRQLKAAGDALSDKLYKENYEKTKAKSINYCETPKFKLDTVLQNFSSDK 420

************************************************************
```

```
NebV2
KYKDSYLKDILGHYVGSFEDPYHSHCMKVTAQNSDKNYKAEYEEDRGKGFFPQTITQEYE 480
NebV3
KYKDSYLKDILGHYVGSFEDPYHSHCMKVTAQNSDKNYKAEYEEDRGKGFFPQTITQEYE 480

************************************************************

NebV2
AIKKLDQCKDHTYKVHPDKTKFTQVTDSPVLLQAQVNSKQLSDLNYKAKHESEKFKCHIP 540
NebV3
AIKKLDQCKDHTYKVHPDKTKFTQVTDSPVLLQAQVNSKQLSDLNYKAKHESEKFKCHIP 540

************************************************************

NebV2
PDTPAFIQHKVNAYNLSDNLYKQDWEKSKAKKFDIKVDAIPLLAAKANTKNTSDVMYKKD 600
NebV3
PDTPAFIQHKVNAYNLSDNLYKQDWEKSKAKKFDIKVDAIPLLAAKANTKNTSDVMYKKD 600

************************************************************

NebV2
YEKNKGKMIGVLSINDDPKMLHSLKVAKNQSDRLYKENYEKTKAKSMNYCETPKYQLDTQ 660
NebV3
YEKNKGKMIGVLSINDDPKMLHSLKVAKNQSDRLYKENYEKTKAKSMNYCETPKYQLDTQ 660

************************************************************

NebV2
LKNFSEARYKDLYVKDVLGHYVGSMEDPYHTHCMKVAAQNSDKSYKAEYEEDKGKCYFPQ 720
NebV3
LKNFSEARYKDLYVKDVLGHYVGSMEDPYHTHCMKVAAQNSDKSYKAEYEEDKGKCYFPQ 720

************************************************************

NebV2
TITQEYEAIKKLDQCKDHTYKVHPDKTKFTAVTDSPVLLQAQLNTKQLSDLNYKAKHEGE 780
NebV3
TITQEYEAIKKLDQCKDHTYKVHPDKTKFTAVTDSPVLLQAQLNTKQLSDLNYKAKHEGE 780

************************************************************

NebV2
KFKCHIPADAPQFIQHRVNAYNLSDNVYKQDWEKSKAKKFDIKVDAIPLLAAKANTKNTS 840
NebV3
KFKCHIPADAPQFIQHRVNAYNLSDNVYKQDWEKSKAKKFDIKVDAIPLLAAKANTKNTS 840

************************************************************

NebV2
DVMYKKDYEKSKGKMIGALSINDDPKMLHSLKTAKNQSDREYRKDYEKSKTIYTAPLDML 900
NebV3
DVMYKKDYEKSKGKMIGALSINDDPKMLHSLKTAKNQSDREYRKDYEKSKTIYTAPLDML 900

************************************************************
```

```
NebV2
QVTQAKKSQAIASDVDYKHILHSYSYPPDSINVDLAKKAYALQSDVEYKADYNSWMKGCG 960
NebV3
QVTQAKKSQAIASDVDYKHILHSYSYPPDSINVDLAKKAYALQSDVEYKADYNSWMKGCG 960

************************************************************


NebV2
WVPFGSLEMEKAKRASDILNEKKYRQHPDTLKFTSIEDAPITVQSKINQAQRSDIAYKAK 1020

NebV3
WVPFGSLEMEKAKRASDILNEKKYRQHPDTLKFTSIEDAPITVQSKINQAQRSDIAYKAK 1020


************************************************************

NebV2
GEEIIHKYNLPPDLPQFIQAKVNAYNISENMYKADLKDLSKKGYDLRTDAIPIRAAKAAR 1080
NebV3
GEEIIHKYNLPPDLPQFIQAKVNAYNISENMYKADLKDLSKKGYDLRTDAIPIRAAKAAR 1080

************************************************************

NebV2
QAASDVQYKKDYEKAKGKMVGFQSLQDDPKLVHYMNVAKIQSDREYKKDYEKTKSKYNTP 1140
NebV3
QAASDVQYKKDYEKAKGKMVGFQSLQDDPKLVHYMNVAKIQSDREYKKDYEKTKSKYNTP 1140

************************************************************

NebV2
HDMFNVVAAKKAQDVVSNVNYKHSLHHYTYLPDAMDLELSKNMMQIQSDNVYKEDYNNWM 1200
NebV3
HDMFNVVAAKKAQDVVSNVNYKHSLHHYTYLPDAMDLELSKNMMQIQSDNVYKEDYNNWM 1200

************************************************************

NebV2
KGIGWIPIGSLDVEKVKKAGDALNEKKYRQHPDTLKFTSIVDSPVMVQAKQNTKQVSDIL 1260
NebV3
KGIGWIPIGSLDVEKVKKAGDALNEKKYRQHPDTLKFTSIVDSPVMVQAKQNTKQVSDIL 1260

************************************************************

NebV2
YKAKGEDVKHKYTMSPDLPQFLQAKCNAYNISDVCYKRDWYDLIAKGNNVLGDAIPITAA 1320
NebV3
YKAKGEDVKHKYTMSPDLPQFLQAKCNAYNISDVCYKRDWYDLIAKGNNVLGDAIPITAA 1320

************************************************************

NebV2
KASRNIASDYKYKEAYEKSKGKHVGFRSLQDDPKLVHYMNVAKLQSDREYKKNYENTKTS 1380
NebV3
KASRNIASDYKYKEAYEKSKGKHVGFRSLQDDPKLVHYMNVAKLQSDREYKKNYENTKTS 1380

************************************************************
```

```
NebV2
YHTPGDMVSITAAKMAQDVATNVNYKQPLHHYTYLPDAMSLEHTRNVNQIQSDNVYKDEY 1440
NebV3
YHTPGDMVSITAAKMAQDVATNVNYKQPLHHYTYLPDAMSLEHTRNVNQIQSDNVYKDEY 1440

************************************************************


NebV2
NSFLKGIGWIPIGSLEVEKVKKAGDALNERKYRQHPDTVKFTSVPDSMGMVLAQHNTKQL 1500

NebV3
NSFLKGIGWIPIGSLEVEKVKKAGDALNERKYRQHPDTVKFTSVPDSMGMVLAQHNTKQL 1500

************************************************************

NebV2
SDLNYKVEGEKLKHKYTIDPELPQFIQAKVNALNMSDAHYKADWKKTIAKGYDLRPDAIP 1560
NebV3
SDLNYKVEGEKLKHKYTIDPELPQFIQAKVNALNMSDAHYKADWKKTIAKGYDLRPDAIP 1560

************************************************************

NebV2
IVAAKSSRNIASDCKYKEAYEKAKGKQVGFLSLQDDPKLVHYMNVAKIQSDREYKKGYEA 1620
NebV3
IVAAKSSRNIASDCKYKEAYEKAKGKQVGFLSLQDDPKLVHYMNVAKIQSDREYKKGYEA 1620

************************************************************

NebV2
SKTKYHTPLDMVSVTAAKKSQEVATNANYRQSYHHYTLLPDALNVEHSRNAMQIQSDNLY 1680
NebV3
SKTKYHTPLDMVSVTAAKKSQEVATNANYRQSYHHYTLLPDALNVEHSRNAMQIQSDNLY 1680

************************************************************

NebV2
KSDFTNWMKGIGWVPIESLEVEKAKKAGEILSEKKYRQHPEKLKFTYAMDTMEQALNKSN 1740
NebV3
KSDFTNWMKGIGWVPIESLEVEKAKKAGEILSEKKYRQHPEKLKFTYAMDTMEQALNKSN 1740

************************************************************

NebV2
KLNMDKRLYTEKWNKDKTTIHVMPDTPDILLSRVNQITMSDKLYKAGWEEEKKKGYDLRP 1800
NebV3
KLNMDKRLYTEKWNKDKTTIHVMPDTPDILLSRVNQITMSDKLYKAGWEEEKKKGYDLRP 1800

************************************************************

NebV2
DAIAIKAARASRDIASDYKYKKAYEQAKGKHIGFRSLEDDPKLVHFMQVAKMQSDREYKK 1860
NebV3
DAIAIKAARASRDIASDYKYKKAYEQAKGKHIGFRSLEDDPKLVHFMQVAKMQSDREYKK 1860

************************************************************
```

```
NebV2
GYEKSKTSFHTPVDMLSVVAAKKSQEVATNANYRNVIHTYNMLPDAMSFELAKNMMQIQS 1920
NebV3
GYEKSKTSFHTPVDMLSVVAAKKSQEVATNANYRNVIHTYNMLPDAMSFELAKNMMQIQS 1920

************************************************************


NebV2
DNQYKADYADFMKGIGWLPLGSLEAEKNKKAMEIISEKKYRQHPDTLKYSTLMDSMNMVL 1980

NebV3
DNQYKADYADFMKGIGWLPLGSLEAEKNKKAMEIISEKKYRQHPDTLKYSTLMDSMNMVL 1980

************************************************************

NebV2
AQNNAKIMNEHLYKQAWEADKTKVHIMPDIPQIILAKANAINMSDKLYKLSLEESKKKGY 2040
NebV3
AQNNAKIMNEHLYKQAWEADKTKVHIMPDIPQIILAKANAINMSDKLYKLSLEESKKKGY 2040

************************************************************

NebV2
DLRPDAIPIKAAKASRDIASDYKYKYNYEKGKGKMVGFRSLEDDPKLVHSMQVAKMQSDR 2100
NebV3
DLRPDAIPIKAAKASRDIASDYKYKYNYEKGKGKMVGFRSLEDDPKLVHSMQVAKMQSDR 2100

************************************************************

NebV2
EYKKNYENTKTSYHTPADMLSVTAAKDAQANITNTNYKHLIHKYILLPDAMNIELTRNMN 2160
NebV3
EYKKNYENTKTSYHTPADMLSVTAAKDAQANITNTNYKHLIHKYILLPDAMNIELTRNMN 2160

************************************************************

NebV2
RIQSDNEYKQDYNEWYKGLGWSPAGSLEVEKAKKATEYASDQKYRQHPSNFQFKKLTDSM 2220
NebV3
RIQSDNEYKQDYNEWYKGLGWSPAGSLEVEKAKKATEYASDQKYRQHPSNFQFKKLTDSM 2220

************************************************************

NebV2
DMVLAKQNAHTMNKHLYTIDWNKDKTKIHVMPDTPDILQAKQNQTLYSQKLYKLGWEEAL 2280
NebV3
DMVLAKQNAHTMNKHLYTIDWNKDKTKIHVMPDTPDILQAKQNQTLYSQKLYKLGWEEAL 2280

************************************************************

NebV2
KKGYDLPVDAISVQLAKASRDIASDYKYKQGYRKQLGHHVGFRSLQDDPKLVLSMNVAKM 2340
NebV3
KKGYDLPVDAISVQLAKASRDIASDYKYKQGYRKQLGHHVGFRSLQDDPKLVLSMNVAKM 2340

************************************************************
```

```
NebV2
QSEREYKKDFEKWKTKFSSPVDMLGVVLAKKCQELVSDVDYKNYLHQWTCLPDQNDVVQA 2400
NebV3
QSEREYKKDFEKWKTKFSSPVDMLGVVLAKKCQELVSDVDYKNYLHQWTCLPDQNDVVQA 2400

************************************************************


NebV2
KKVYELQSENLYKSDLEWLRGIGWSPLGSLEAEKNKRASEIISEKKYRQPPDRNKFTSIP 2460

NebV3
KKVYELQSENLYKSDLEWLRGIGWSPLGSLEAEKNKRASEIISEKKYRQPPDRNKFTSIP 2460

************************************************************

NebV2
DAMDIVLAKTNAKNRSDRLYREAWDKDKTQIHIMPDTPDIVLAKANLINTSDKLYRMGYE 2520
NebV3
DAMDIVLAKTNAKNRSDRLYREAWDKDKTQIHIMPDTPDIVLAKANLINTSDKLYRMGYE 2520

************************************************************

NebV2
ELKRKGYDLPVDAIPIKAAKASREIASEYKYKEGFRKQLGHHIGARNIEDDPKMMWSMHV 2580
NebV3
ELKRKGYDLPVDAIPIKAAKASREIASEYKYKEGFRKQLGHHIGARNIEDDPKMMWSMHV 2580

************************************************************

NebV2
AKIQSDREYKKDFEKWKTKFSSPVDMLGVVLAKKCQTLVSDVDYKNYLHQWTCLPDQSDV 2640
NebV3
AKIQSDREYKKDFEKWKTKFSSPVDMLGVVLAKKCQTLVSDVDYKNYLHQWTCLPDQSDV 2640

************************************************************

NebV2
IHARQAYDLQSDNLYKSDLQWLKGIGWMTSGSLEDEKNKRATQILSDHVYRQHPDQFKFS 2700
NebV3
IHARQAYDLQSDNLYKSDLQWLKGIGWMTSGSLEDEKNKRATQILSDHVYRQHPDQFKFS 2700

************************************************************

NebV2
SLMDSIPMVLAKNNAITMNHRLYTEAWDKDKTTVHIMPDTPEVLLAKQNKVNYSEKLYKL 2760
NebV3
SLMDSIPMVLAKNNAITMNHRLYTEAWDKDKTTVHIMPDTPEVLLAKQNKVNYSEKLYKL 2760

************************************************************

NebV2
GLEEAKRKGYDMRVDAIPIKAAKASRDIASEFKYKEGYRKQLGHHIGARAIRDDPKMMWS 2820
NebV3
GLEEAKRKGYDMRVDAIPIKAAKASRDIASEFKYKEGYRKQLGHHIGARAIRDDPKMMWS 2820

************************************************************
```

```
NebV2
MHVAKIQSDREYKKDFEKWKTKFSSPVDMLGVVLAKKCQTLVSDVDYKNYLHQWTCLPDQ 2880
NebV3
MHVAKIQSDREYKKDFEKWKTKFSSPVDMLGVVLAKKCQTLVSDVDYKNYLHQWTCLPDQ 2880

************************************************************


NebV2
SDVIHARQAYDLQSDNMYKSDLQWMRGIGWVSIGSLDVEKCKRATEILSDKIYRQPPDRF 2940
NebV3
SDVIHARQAYDLQSDNMYKSDLQWMRGIGWVSIGSLDVEKCKRATEILSDKIYRQPPDRF 2940

************************************************************

NebV2
KFTSVTDSLEQVLAKNNAITMNKRLYTEAWDKDKTQIHIMPDTPEIMLARMNKINYSESL 3000
NebV3
KFTSVTDSLEQVLAKN---------------------------------------------- 2956
***************

NebV2
YKLANEEAKKKGYDLRSDAIPIVAAKASRDIISDYKYKDGYCKQLGHHIGARNIEDDPKM 3060
NebV3
------------------------------------------------------------


NebV2
MWSMHVAKIQSDREYKKDFEKWKTKFSSPVDMLGVVLAKKCQTLVSDVDYKNYLHEWTCL 3120
NebV3
------------------------------------------------------------


NebV2
PDQSDVIHARQAYDLQSDNIYKSDLQWLRGIGWVPIGSMDVVKCKRATEILSDNIYRQPP 3180
NebV3
------------------------------------------------------------


NebV2
DKLKFTSVTDSLEQVLAKNNALNMNKRLYTEAWDKDKTQIHIMPDTPEIMLARQNKINYS 3240
NebV3
-------------------NALNMNKRLYTEAWDKDKTQIHIMPDTPEIMLARQNKINYS 2997

                    ****************************************


NebV2
ETLYKLANEEAKKKGYDLRSDAIPIVAAKASRDVISDYKYKDGYRKQLGHHIGARNIEDD 3300
NebV3
ETLYKLANEEAKKKGYDLRSDAIPIVAAKASRDVISDYKYKDGYRKQLGHHIGARNIEDD 3057

************************************************************

NebV2
PKMMWSMHVAKIQSDREYKKDFEKWKTKFSSPVDMLGVVLAKKCQTLVSDVDYKNYLHEW 3360
NebV3
PKMMWSMHVAKIQSDREYKKDFEKWKTKFSSPVDMLGVVLAKKCQTLVSDVDYKNYLHEW 3117

************************************************************
```

```
NebV2
TCLPDQNDVIHARQAYDLQSDNIYKSDLQWLRGIGWVPIGSMDVVKCKRAAEILSDNIYR 3420
NebV3
TCLPDQNDVIHARQAYDLQSDNIYKSDLQWLRGIGWVPIGSMDVVKCKRAAEILSDNIYR 3177

************************************************************

NebV2
QPPDKLKFTSVTDSLEQVLAKNNALNMNKRLYTEAWDKDKTQVHIMPDTPEIMLARQNKI 3480
NebV3
QPPDKLKFTSVTDSLEQVLAKNNALNMNKRLYTEAWDKDKTQVHIMPDTPEIMLARQNKI 3237

************************************************************

NebV2
NYSESLYRQAMEEAKKEGYDLRSDAIPIVAAKASRDIASDYKYKEAYRKQLGHHIGARAV 3540
NebV3
NYSESLYRQAMEEAKKEGYDLRSDAIPIVAAKASRDIASDYKYKEAYRKQLGHHIGARAV 3297

************************************************************

NebV2
HDDPKIMWSLHIAKVQSDREYKKDFEKYKTRYSSPVDMLGIVLAKKCQTLVSDVDYKHPL 3600
NebV3
HDDPKIMWSLHIAKVQSDREYKKDFEKYKTRYSSPVDMLGIVLAKKCQTLVSDVDYKHPL 3357

************************************************************

NebV2
HEWICLPDQNDIIHARKAYDLQSDNLYKSDLEWMKGIGWVPIDSLEVVRAKRAGELLSDT 3660
NebV3
HEWICLPDQNDIIHARKAYDLQSDNLYKSDLEWMKGIGWVPIDSLEVVRAKRAGELLSDT 3417

************************************************************

NebV2
IYRQRPETLKFTSITDTPEQVLAKNNALNMNKRLYTEAWDNDKKTIHVMPDTPEIMLAKL 3720
NebV3
IYRQRPETLKFTSITDTPEQVLAKNNALNMNKRLYTEAWDNDKKTIHVMPDTPEIMLAKL 3477

************************************************************

NebV2
NRINYSDKLYKLALEESKKEGYDLRLDAIPIQAAKASRDIASDYKYKEGYRKQLGHHIGA 3780
NebV3
NRINYSDKLYKLALEESKKEGYDLRLDAIPIQAAKASRDIASDYKYKEGYRKQLGHHIGA 3537

************************************************************

NebV2
RNIKDDPKMMWSIHVAKIQSDREYKKEFEKWKTKFSSPVDMLGVVLAKKCQILVSDIDYK 3840
NebV3
RNIKDDPKMMWSIHVAKIQSDREYKKEFEKWKTKFSSPVDMLGVVLAKKCQILVSDIDYK 3597

************************************************************
```

```
NebV2
HPLHEWTCLPDQNDVIQARKAYDLQSDAIYKSDLEWLRGIGWVPIGSVEVEKVKRAGEIL 3900
NebV3
HPLHEWTCLPDQNDVIQARKAYDLQSDAIYKSDLEWLRGIGWVPIGSVEVEKVKRAGEIL 3657

************************************************************


NebV2
SDRKYRQPADQLKFTCITDTPEIVLAKNNALTMSKHLYTEAWDADKTSIHVMPDTPDILL 3960

NebV3
SDRKYRQPADQLKFTCITDTPEIVLAKNNALTMSKHLYTEAWDADKTSIHVMPDTPDILL 3717

************************************************************

NebV2
AKSNSANISQKLYTKGWDESKMKDYDLRADAISIKSAKASRDIASDYKYKEAYEKQKGHH 4020
NebV3
AKSNSANISQKLYTKGWDESKMKDYDLRADAISIKSAKASRDIASDYKYKEAYEKQKGHH 3777

************************************************************

NebV2
IGAQSIEDDPKIMCAIHAGKIQSEREYKKEFQKWKTKFSSPVDMLSILLAKKCQTLVTDI 4080
NebV3
IGAQSIEDDPKIMCAIHAGKIQSEREYKKEFQKWKTKFSSPVDMLSILLAKKCQTLVTDI 3837

************************************************************

NebV2
DYRNYLHEWTCMPDQNDIIQAKKAYDLQSDSVYKADLEWLRGIGWMPEGSVEMNRVKVAQ 4140
NebV3
DYRNYLHEWTCMPDQNDIIQAKKAYDLQS------------------------------ 3866
****************************

NebV2
DLVNERLYRTRPEALSFTSIVDTPEVVLAKANSLQISEKLYQEAWNKDKSNITIPSDTPE 4200
NebV3
------------------------------------------------------------


NebV2
MLQAHINALQISNKLYQKDWNDAKQKGYDIRADAIEIKHAKASREIASEYKYKEGYRKQL 4260
NebV3
------------------------------------------------------------


NebV2
GHHMGFRTLQDDPKSVWAIHAAKIQSDREYKKAYEKSKGIHNTPLDMMSIVQAKKCQVLV 4320
NebV3
------------------------------------------------------------


NebV2
SDIDYRNYLHQWTCLPDQNDVIQAKKAYDLQSDNLYKSDLEWLKGIGWLPEGSVEVMRVK 4380
NebV3
------------------------------------------------------------


NebV2
NAQNLLNERLYRIKPEALKFTSIVDTPEVIQAKINAVQISEPLYRDAWEKEKANVNVPAD 4440
```

```
NebV3
------------------------------------------------------------

NebV2
TPLMLQSKINALQISNKRYQQAWEDVKMTGYDLRADAIGIQHAKASRDIASDYLYKTAYE 4500

NebV3
------------------------------------------------------------


NebV2
KQKGHYIGCRSAKEDPKLVWAANVLKMQNDRLYKKAYNDHKAKISIPVDMVSISAAKEGQ 4560
NebV3
------------------------------------------------------------


NebV2
ALASDVDYRHYLHHWSCFPDQNDVIQARKAYDLQSDSVYKADLEWLRGIGWMPEGSVEMN 4620
NebV3
------------------------------------------------------------


NebV2
RVKVAQDLVNERLYRTRPEALSFTSIVDTPEVVLAKANSLQISEKLYQEAWNKDKSNITI 4680
NebV3
------------------------------------------------------------


NebV2
PSDTPEMLQAHINALQISNKLYQKDWNDTKQKGYDIRADAIEIKHAKASREIASEYKYKE 4740
NebV3
------------------------------------------------------------


NebV2
GYRKQLGHHMGFRTLQDDPKSVWAIHAAKIQSDREYKKAYEKSKGIHNTPLDMMSIVQAK 4800
NebV3
------------------------------------------------------------


NebV2
KCQVLVSDIDYRNYLHQWTCLPDQNDVIQAKKAYDLQSDNLYKSDLEWLKGIGWLPEGSV 4860
NebV3
------------------------------------------------------------


NebV2
EVMRVKNAQNLLNERLYRIKPEALKFTSIVDTPEVIQAKINAVQISEPLYRNAWEKEKAN 4920
NebV3
------------------------------------------------------------


NebV2
VNVPADTPLMLQSKINALQISNKRYQQAWEDVKMTGYDLRADAIGIQHAKASRDIASDYL 4980
NebV3
------------------------------------------------------------


NebV2
YKTAYEKQKGHYIGCRSAKEDPKLVWAANVLKMQNDRLYKKAYNDHKAKISIPVDMVSIS 5040
NebV3
------------------------------------------------------------
```

```
NebV2
AAKEGQALASDVDYRHYLHHWSCFPDQNDVIQARKAYDLQSDSVYKADLEWLRGIGWMPE 5100
NebV3
------------------------------------------------------------


NebV2
GSVEMNRVKVAQDLVNERLYRTRPEALSFTSIVDTPEVVLAKANSLQISEKLYQEAWNKD 5160
NebV3
------------------------------------------------------------


NebV2
KSNITIPSDTPEMLQAHINALQISNKLYQKDWNDTKQKGYDIRADAIEIKHAKASREIAS 5220
NebV3
------------------------------------------------------------


NebV2
EYKYKEGYRKQLGHHMGFRTLQDDPKSVWAIHAAKIQSDREYKKAYEKSKGIHNTPLDMM 5280
NebV3
------------------------------------------------------------


NebV2
SIVQAKKCQVLVSDIDYRNYLHQWTCLPDQNDVIQAKKAYDLQSDNLYKSDLEWLKGIGW 5340
NebV3
------------------------------------------------------------


NebV2
LPEGSVEVMRVKNAQNLLNERLYRIKPEALKFTSIVDTPEVIQAKINAVQISEPLYRDAW 5400
NebV3
------------------------------------------------------------


NebV2
EKEKANVNVPADTPLMLQSKINALQISNKRYQQAWEDVKMTGYDLRADAIGIQHAKASRD 5460
NebV3
------------------------------------------------------------


NebV2
IASDYLYKTAYEKQKGHYIGCRSAKEDPKLVWAANVLKMQNDRLYKKAYNDHKAKISIPV 5520
NebV3
------------------------------------------------------------


NebV2
DMVSISAAKEGQALASDVDYRHYLHRWSCFPDQNDVIQARKAYDLQSDALYKADLEWLRG 5580
NebV3
-----------------------------------------------DALYKADLEWLRG 3879

                                                  **************
```

```
NebV2
IGWMPQGSPEVLRVKNAQNIFCDSVYRTPVVNLKYTSIVDTPEVVLAKSNAENISIPKYR 5640
NebV3
IGWMPQGSPEVLRVKNAQNIFCDSVYRTPVVNLKYTSIVDTPEVVLAKSNAENISIPKYR 3939

************************************************************

NebV2
EVWDKDKTSIHIMPDTPEINLARANALNVSNKLYREGWDEMKAGCDVRLDAIPIQAAKAS 5700
NebV3
EVWDKDKTSIHIMPDTPEINLARANALNVSNKLYREGWDEMKAGCDVRLDAIPIQAAKAS 3999

************************************************************

NebV2
REIASDYKYKLDHEKQKGHYVGTLTARDDNKIRWALIADKLQNEREYRLDWAKWKAKIQS 5760
NebV3
REIASDYKYKLDHEKQKGHYVGTLTARDDNKIRWALIADKLQNEREYRLDWAKWKAKIQS 4059

************************************************************

NebV2
PVDMLSILHSKNSQALVSDMDYRNYLHQWTCMPDQNDVIQAKKAYELQSDNVYKADLEWL 5820
NebV3
PVDMLSILHSKNSQALVSDMDYRNYLHQWTCMPDQNDVIQAKKAYELQSDNVYKADLEWL 4119

************************************************************

NebV2
RGIGWMPNDSVSVNHAKHAADIFSEKKYRTKIETLNFTPVDDRVDYVTAKQSGEILDDIK 5880
NebV3
RGIGWMPNDSVSVNHAKHAADIFSEKKYRTKIETLNFTPVDDRVDYVTAKQSGEILDDIK 4179

************************************************************

NebV2
YRKDWNATKSKYTLTETPLLHTAQEAARILDQYLYKEGWERQKATGYILPPDAVPFVHAH 5940
NebV3
YRKDWNATKSKYTLTETPLLHTAQEAARILDQYLYKEGWERQKATGYILPPDAVPFVHAH 4239

************************************************************

NebV2
HCNDVQSELKYKAEHVKQKGHYVGVPTMRDDPKLVWFEHAGQIQNERLYKEDYHKTKAKI 6000
NebV3
HCNDVQSELKYKAEHVKQKGHYVGVPTMRDDPKLVWFEHAGQIQNERLYKEDYHKTKAKI 4299

************************************************************

NebV2
NIPADMVSVLAAKQGQTLVSDIDYRNYLHQWMCHPDQNDVIQARKAYDLQSDNVYRADLE 6060
NebV3
NIPADMVSVLAAKQGQTLVSDIDYRNYLHQWMCHPDQNDVIQARKAYDLQSDNVYRADLE 4359

************************************************************
```

```
NebV2
WLRGIGWIPLDSVDHVRVTKNQEMMSQIKYKKNALENYPNFRSVVDPPEIVLAKINSVNQ 6120
NebV3
WLRGIGWIPLDSVDHVRVTKNQEMMSQIKYKKNALENYPNFRSVVDPPEIVLAKINSVNQ 4419

************************************************************

NebV2
SDVKYKETFNKAKGKYTFSPDTPHISHSKDMGKLYSTILYKGAWEGTKAYGYTLDERYIP 6180
NebV3
SDVKYKETFNKAKGKYTFSPDTPHISHSKDMGKLYSTILYKGAWEGTKAYGYTLDERYIP 4479

************************************************************

NebV2
IVGAKHADLVNSELKYKETYEKQKGHYLAGKVIGEFPGVVHCLDFQKMRSALNYRKHYED 6240
NebV3
IVGAKHADLVNSELKYKETYEKQKGHYLAGKVIGEFPGVVHCLDFQKMRSALNYRKHYED 4539

************************************************************

NebV2
TKANVHIPNDMMNHVLAKRCQYILSDLEYRHYFHQWTSLLEEPNVIRVRNAQEILSDNVY 6300
NebV3
TKANVHIPNDMMNHVLAKRCQYILSDLEYRHYFHQWTSLLEEPNVIRVRNAQEILSDNVY 4599

************************************************************

NebV2
KDDLNWLKGIGCYVWDTPQILHAKKSYDLQSQLQYTAAGKENLQNYNLVTDTPLYVTAVQ 6360
NebV3
KDDLNWLKGIGCYVWDTPQILHAKKSYDLQSQLQYTAAGKENLQNYNLVTDTPLYVTAVQ 4659

************************************************************

NebV2
SGINASEVKYKENYHQIKDKYTTVLETVDYDRTRNLKNLYSSNLYKEAWDRVKATSYILP 6420
NebV3
SGINASEVKYKENYHQIKDKYTTVLETVDYDRTRNLKNLYSSNLYKEAWDRVKATSYILP 4719

************************************************************

NebV2
SSTLSLTHAKNQKHLASHIKYREEYEKFKALYTLPRSVDDDPNTARCLRVGKLNIDRLYR 6480
NebV3
SSTLSLTHAKNQKHLASHIKYREEYEKFKALYTLPRSVDDDPNTARCLRVGKLNIDRLYR 4779

************************************************************

NebV2
SVYEKNKMKIHIVPDMVEMVTAKDSQKKVSEIDYRLRLHEWICHPDLQVNDHVRKVTDQI 6540
NebV3
SVYEKNKMKIHIVPDMVEMVTAKDSQKKVSEIDYRLRLHEWICHPDLQVNDHVRKVTDQI 4839

************************************************************
```

```
NebV2
SDIVYKDDLNWLKGIGCYVWDTPEILHAKHAYDLRDDIKYKAHMLKTRNDYKLVTDTPVY 6600
NebV3
SDIVYKDDLNWLKGIGCYVWDTPEILHAKHAYDLRDDIKYKAHMLKTRNDYKLVTDTPVY 4899

************************************************************

NebV2
VQAVKSGKQLSDAVYHYDYVHSVRGKVAPTTKTVDLDRALHAYKLQSSNLYKTSLRTLPT 6660
NebV3
VQAVKSGKQLSDAVYHYDYVHSVRGKVAPTTKTVDLDRALHAYKLQSSNLYKTSLRTLPT 4959

************************************************************

NebV2
GYRLPGDTPHFKHIKDTRYMSSYFKYKEAYEHTKAYGYTLGPKDVPFVHVRRVNNVTSER 6720
NebV3
GYRLPGDTPHFKHIKDTRYMSSYFKYKEAYEHTKAYGYTLGPKDVPFVHVRRVNNVTSER 5019

************************************************************

NebV2
LYRELYHKLKDKIHTTPDTPEIRQVKKTQEAVSELIYKSDFFKMQGHMISLPYTPQVIHC 6780
NebV3
LYRELYHKLKDKIHTTPDTPEIRQVKKTQEAVSELIYKSDFFKMQGHMISLPYTPQVIHC 5079

************************************************************

NebV2
RYVGDITSDIKYKEDLQVLKGFGCFLYDTPDMVRSRHLRKLWSNYLYTDKARKMRDKYKV 6840
NebV3
RYVGDITSDIKYKEDLQVLKGFGCFLYDTPDMVRSRHLRKLWSNYLYTDKARKMRDKYKV 5139

************************************************************

NebV2
VLDTPEYRKVQELKTHLSELVYRAAGKKQKSIFTSVPDTPDLLRAKRGQKLQSQYLYVEL 6900
NebV3
VLDTPEYRKVQELKTHLSELVYRAAGKKQKSIFTSVPDTPDLLRAKRGQKLQSQYLYVEL 5199

************************************************************

NebV2
ATKERPHHHAGNQTTALKHAKDVKDMVSEKKYKIQYEKMKDKYTPVPDTPILIRAKRAYW 6960
NebV3
ATKERPHHHAGNQTTALKHAKDVKDMVSEKKYKIQYEKMKDKYTPVPDTPILIRAKRAYW 5259

************************************************************

NebV2
NASDLRYKETFQKTKGKYHTVKDALDIVYHRKVTDDISKIKYKENYMSQLGIWRSIPDRP 7020
NebV3
NASDLRYKETFQKTKGKYHTVKDALDIVYHRKVTDDISKIKYKENYMSQLGIWRSIPDRP 5319

************************************************************
```

```
NebV2
EHFHHRAVTDTVSDVKYKEDLTWLKGIGCYAYDTPDFTLAEKNKTLYSKYKYKEVFERTK 7080
NebV3
EHFHHRAVTDTVSDVKYKEDLTWLKGIGCYAYDTPDFTLAEKNKTLYSKYKYKEVFERTK 5379

************************************************************

NebV2
SDFKYVADSPINRHFKYATQLMNERKYKSSAKMFLQHGCNEILRPDMLTALYNSHMWSQI 7140
NebV3
SDFKYVADSPINRHFKYATQLMNEKKYRADYEQRKDKYHLVVDEPRHLLAKTAGDQISQI 5439

************************:**:::. :   ::    : .*  * *   ..  ***

NebV2
KYRKNYEKSKDKFTSIVDTPEHLRTTKVNKQISDILYKLEYNKAKPRGYTTIHDTPMLLH 7200
NebV3
KYRKNYEKSKDKFTSIVDTPEHLRTTKVNKQISDILYKLEYNKAKPRGYTTIHDTPMLLH 5499

************************************************************

NebV2
VRKVKDEVSDLKYKEVYQRNKSNCTIEPDAVHIKAAKDAYKVNTNLDYKKQYEANKAHWK 7260
NebV3
VRKVKDEVSDLKYKEVYQRNKSNCTIEPDAVHIKAAKDAYKVNTNLDYKKQYEANKAHWK 5559

************************************************************

NebV2
WTPDRPDFLQAAKSSLQQSDFEYKLDREFLKGCKLSVTDDKNTVLALRNTLIESDLKYKE 7320
NebV3
WTPDRPDFLQAAKSSLQQSDFEYKLDREFLKGCKLSVTDDKNTVLALRNTLIESDLKYKE 5619

************************************************************

NebV2
KHVKERGTCHAVPDTPQILLAKTVSNLVSENKYKDHVKKHLAQGSYTTLPETRDTVHVKE 7380
NebV3
KHVKERGTCHAVPDTPQILLAKTVSNLVSENKYKDHVKKHLAQGSYTTLPETRDTVHVKE 5679

************************************************************

NebV2
VTKHVSDTNYKKKFVKEKGKSNYSIMLEPPEVKHAMEVAKKQSDVAYRKDAKENLHYTTV 7440
NebV3
VTKHVSDTNYKKKFVKEKGKSNYSIMLEPPEVKHAMEVAKKQSDVAYRKDAKENLHYTTV 5739

************************************************************

NebV2
ADRPDIKKATQAAKQASEVEYRAKHRKEGSHGLSMLGRPDIEMAKKAAKLSSQVKYRENF 7500
NebV3
ADRPDIKKATQAAKQASEVEYRAKHRKEGSHGLSMLGRPDIEMAKKAAKLSSQVKYRENF 5799

************************************************************
```

```
NebV2
DKEKGKTPKYNPKDSQLYKVMKDANNLASEVKYKADLKKLHKPVTDMKESLIMNHVLNTS 7560
NebV3
DKEKGKTPKYNPKDSQLYKVMKDANNLASEVKYKADLKKLHKPVTDMKESLIMNHVLNTS 5859

************************************************************

NebV2
QLASSYQYKKKYEKSKGHYHTIPDNLEQLHLKEATELQSIVKYKEKYEKERGKPMLDFET 7620
NebV3
QLASSYQYKKKYEKSKGHYHTIPDNLEQLHLKEATELQSIVKYKEKYEKERGKPMLDFET 5919

************************************************************

NebV2
PTYITAKESQQMQSGKEYRKDYEESIKGRNLTGLEVTPALLHVKYATKIASEKEYRKDLE 7680
NebV3
PTYITAKESQQMQSGKEYRKDYEESIKGRNLTGLEVTPALLHVKYATKIASEKEYRKDLE 5979

************************************************************

NebV2
ESIRGKGLTEMEDTPDMLRAKNATQILNEKEYKRDLELEVKGRGLNAMANETPDFMRARN 7740
NebV3
ESIRGKGLTEMEDTPDMLRAKNATQILNEKEYKRDLELEVKGRGLNAMANETPDFMRARN 6039

************************************************************

NebV2
ATDIASQIKYKQSAEMEKANFTSVVDTPEIIHAQQVKNLSSQKKYKEDAEKSMSYYETVL 7800
NebV3
ATDIASQIKYKQSAEMEKANFTSVVDTPEIIHAQQVKNLSSQKKYKEDAEKSMSYYETVL 6099

************************************************************

NebV2
DTPEIQRVRENQKNFSLLQYQCDLKNSKGKITVVQDTPEILRVKENQKNFSSVLYKEDVS 7860
NebV3
DTPEIQRVRENQKNFSLLQYQCDLKNSKGKITVVQDTPEILRVKENQKNFSSVLYKEDVS 6159

************************************************************

NebV2
PGTAIGKTPEMMRVKQTQDHISSVKYKEAIGQGTPIPDLPEVKRVKETQKHISSVMYKEN 7920
NebV3
PGTAIGKTPEMMRVKQTQDHISSVKYKEAIGQGTPIPDLPEVKRVKETQKHISSVMYKEN 6219

************************************************************

NebV2
LGTGIPTTVTPEIERVKRNQENFSSVLYKENLGKGIPTPITPEMERVKRNQENFSSILYK 7980
NebV3
LGTGIPTTVTPEIERVKRNQENFSSVLYKENLGKGIPTPITPEMERVKRNQENFS----- 6274

*****************************************************
```

```
NebV2
ENLSKGTPLPVTPEMERVKLNQENFSSVLYKENVGKGIPIPITPEMERVKHNQENFSSVL 8040
NebV3
------------------------------------------------------------


NebV2
YKENLGTGIPIPITPEMQRVKHNQENLSSVLYKENMGKGTPLPVTPEMERVKHNQENISS 8100
NebV3
------------------------------------------------------------


NebV2
VLYKENMGKGTPLPVTPEMERVKHNQENISSVLYKENMGKGTPLAVTPEMERVKHNQENI 8160
NebV3
------------------------------SVLYKENMGKGTPLAVTPEMERVKHNQENI 6304

                                ****************************

NebV2
SSVLYKENVGKATATPVTPEMQRVKRNQENISSVLYKENLGKATPTPFTPEMERVKRNQE 8220
NebV3
SSVLYKENVGKATATPVTPEMQRVKRNQENISSVLYKENLGKATPTPFTPEMERVKRNQE 6364

************************************************************

NebV2
NFSSVLYKENMRKATPTPVTPEMERAKRNQENISSVLYSDSFRKQIQGKAAYVLDTPEMR 8280
NebV3
NFSSVLYKENMRKATPTPVTPEMERAKRNQENISSVLYSDSFRKQIQGKAAYVLDTPEMR 6424

************************************************************

NebV2
RVRETQRHISTVKYHEDFEKHKGCFTPVVTDPITERVKKNMQDFSDINYRGIQRKVVEME 8340
NebV3
RVRETQRHISTVKYHEDFEKHKGCFTPVVTDPITERVKKNMQDFSDINYRGIQRKVVEME 6484

************************************************************

NebV2
QKRNDQDQETITGLRVWRTNPGSVFDYDPAEDNIQSRSLHMINVQAQRRSREQSRSASAL 8400
NebV3
QKRNDQDQETITGLRVWRTNPGSVFDYDPAEDNIQSRSLHMINVQAQRRSREQSRSASAL 6544

************************************************************

NebV2
SISGGEEKSEHSEAPDHHLSTYSDGGVFAVSTAYKHAKTTELPQQRSSSVATQQTTVSSI 8460
NebV3
SISGGEEKSEHSEAPDHHLSTYSDGGVFAVSTAYKHAKTTELPQQRSSSVATQQTTVSSI 6604

************************************************************

NebV2
PSHPSTAGKIFRAMYDYMAADADEVSFKDGDAIINVQAIDEGWMYGTVQRTGRTGMLPAN 8520
NebV3
PSHPSTAGKIFRAMYDYMAADADEVSFKDGDAIINVQAIDEGWMYGTVQRTGRTGMLPAN 6664

************************************************************
```

```
NebV2            YVEAI 8525
NebV3            YVEAI 6669
                 *****
```

Nebulin Fragment Variation 2

D T V S D V K Y K E D L T W L K G I G C Y A Y D T P D F T L A E K N K T L Y S K Y K Y K E V F E R T K S D F K Y V A D S P I N R H F K Y A T Q L M N E R K Y K S S A K M F L Q H G C N E I L R P

Nebulin Fragment Variation 3

D A L D I V Y H R K V T D D I S K I K Y K E N Y M S Q L G I W R S I P D R P E H F H H R A V T D T V S D V K Y K E D L T W L K G I G C Y A Y D T P D F T L A E K N K T L Y S K Y K Y K E V F E R T K S D F K Y V A D S P I N R H F K Y A T Q L M N E K K Y R A D Y E Q R K D K Y H L V V D E P R H L L A K T A G D Q I S Q I K Y R K N Y E K S K D K F T S I V D T P E H L R T T K V N K Q I S D I L Y K

Nebulin exon 144 based on gene bank entry Z28496.1 (Donner and others, 2004)

K X V A D S P I N R H F K Y A T Q L M N E X K Y K S S A K M F L Q H G C N E I L R P D M L T A L Y N S H M W S Q X K Y K K X K K

Nebulin exon 144 based on gene bank entry AA099760 (Donner and others, 2004)

G G P F L I V Q S I S T T E Q S L T Q S V X V K Y K E D L T W L K G I G C Y A Y D T P D F T L A E K N K T L Y S K Y K Y K E V F E R T K S D F K Y V A D S P I N R H F K Y A T Q L M N E R K Y K S S A K M F L Q H G C N E I L R P D M L T A L L Q F R I C G A R S N T X T X K T M X N Q R T X L

A.5 Analysis of the Nebulin Isoforms II

A.5.1 Amino Acid Alignment for Nebulin Isoform 1 and Nebulin Isoform 2

The amino acid sequences for Nebulin Isoform 2 and Isoform 3 were aligned using Clustal2W software. The sequences of DNA fragments for clones from the Hybrigenics Y-2-H screen are indicated in grey (for Nebulin Isoform2)

```
CLUSTAL 2.1 multiple sequence alignment


NebV1           MADDEDYEEVVEYYTEEVVYEEVPGETITKIYETTTTRTSDYEQSETSKPALAQPALAQP
NebV2           MADDEDYEEVVEYYTEEVVYEEVPGETITKIYETTTTRTSDYEQSETSKPALAQPALAQP
                ************************************************************

NebV1           ASAKPVERRKVIRKKVDPSKFMTPYIAHSQKMQDLFSPNKYKEKFEKTKGQPYASTTDTP
NebV2           ASAKPVERRKVIRKKVDPSKFMTPYIAHSQKMQDLFSPNKYKEKFEKTKGQPYASTTDTP
                ************************************************************

NebV1           ELRRIKKVQDQLSEVKYRMDGDVAKTICHVDEKAKDIEHAKKVSQQVSKVLYKQNWEDTK
NebV2           ELRRIKKVQDQLSEVKYRMDGDVAKTICHVDEKAKDIEHAKKVSQQVSKVLYKQNWEDTK
                ************************************************************

NebV1           DKYLLPPDAPELVQAVKNTAMFSKKLYTEDWEADKSLFYPYNDSPELRRVAQAQKALSDV
NebV2           DKYLLPPDAPELVQAVKNTAMFSKKLYTEDWEADKSLFYPYNDSPELRRVAQAQKALSDV
                ************************************************************

NebV1           AYKKGLAEQQAQFTPLADPPDIEFAKKVTNQVSKQKYKEDYENKIKGKWSETPCFEVANA
NebV2           AYKKGLAEQQAQFTPLADPPDIEFAKKVTNQVSKQKYKEDYENKIKGKWSETPCFEVANA
                ************************************************************

NebV1           RMNADNISTRKYQEDFENMKDQIYFMQTETPEYKMNKKAGVAASKVKYKEDYEKNKGKAD
NebV2           RMNADNISTRKYQEDFENMKDQIYFMQTETPEYKMNKKAGVAASKVKYKEDYEKNKGKAD
                ************************************************************

NebV1           YNVLPASENPQLRQLKAAGDALSDKLYKENYEKTKAKSINYCETPKFKLDTVLQNFSSDK
NebV2           YNVLPASENPQLRQLKAAGDALSDKLYKENYEKTKAKSINYCETPKFKLDTVLQNFSSDK
                ************************************************************

NebV1           KYKDSYLKDILGHYVGSFEDPYHSHCMKVTAQNSDKNYKAEYEEDRGKGFFPQTITQEYE
NebV2           KYKDSYLKDILGHYVGSFEDPYHSHCMKVTAQNSDKNYKAEYEEDRGKGFFPQTITQEYE
                ************************************************************

NebV1           AIKKLDQCKDHTYKVHPDKTKFTQVTDSPVLLQAQVNSKQLSDLNYKAKHESEKFKCHIP
NebV2           AIKKLDQCKDHTYKVHPDKTKFTQVTDSPVLLQAQVNSKQLSDLNYKAKHESEKFKCHIP
                ************************************************************

NebV1           PDTPAFIQHKVNAYNLSDNLYKQDWEKSKAKKFDIKVDAIPLLAAKANTKNTSDVMYKKD
NebV2           PDTPAFIQHKVNAYNLSDNLYKQDWEKSKAKKFDIKVDAIPLLAAKANTKNTSDVMYKKD
                ************************************************************

NebV1           YEKNKGKMIGVLSINDDPKMLHSLKVAKNQSDRLYKENYEKTKAKSMNYCETPKYQLDTQ
NebV2           YEKNKGKMIGVLSINDDPKMLHSLKVAKNQSDRLYKENYEKTKAKSMNYCETPKYQLDTQ
                ************************************************************

NebV1           LKNFSEARYKDLYVKDVLGHYVGSMEDPYHTHCMKVAAQNSDKSYKAEYEEDKGKCYFPQ
NebV2           LKNFSEARYKDLYVKDVLGHYVGSMEDPYHTHCMKVAAQNSDKSYKAEYEEDKGKCYFPQ
                ************************************************************
```

```
NebV1           TITQEYEAIKKLDQCKDHTYKVHPDKTKFTAVTDSPVLLQAQLNTKQLSDLNYKAKHEGE
NebV2           TITQEYEAIKKLDQCKDHTYKVHPDKTKFTAVTDSPVLLQAQLNTKQLSDLNYKAKHEGE
                ************************************************************

NebV1           KFKCHIPADAPQFIQHRVNAYNLSDNVYKQDWEKSKAKKFDIKVDAIPLLAAKANTKNTS
NebV2           KFKCHIPADAPQFIQHRVNAYNLSDNVYKQDWEKSKAKKFDIKVDAIPLLAAKANTKNTS
                ************************************************************

NebV1           DVMYKKDYEKSKGKMIGALSINDDPKMLHSLKTAKNQSDREYRKDYEKSKTIYTAPLDML
NebV2           DVMYKKDYEKSKGKMIGALSINDDPKMLHSLKTAKNQSDREYRKDYEKSKTIYTAPLDML
                ************************************************************

NebV1           QVTQAKKSQAIASDVDYKHILHSYSYPPDSINVDLAKKAYALQSDVEYKADYNSWMKGCG
NebV2           QVTQAKKSQAIASDVDYKHILHSYSYPPDSINVDLAKKAYALQSDVEYKADYNSWMKGCG
                ************************************************************

NebV1           WVPFGSLEMEKAKRASDILNEKKYRQHPDTLKFTSIEDAPITVQSKINQAQRSDIAYKAK
NebV2           WVPFGSLEMEKAKRASDILNEKKYRQHPDTLKFTSIEDAPITVQSKINQAQRSDIAYKAK
                ************************************************************

NebV1           GEEIIHKYNLPPDLPQFIQAKVNAYNISENMYKADLKDLSKKGYDLRTDAIPIRAAKAAR
NebV2           GEEIIHKYNLPPDLPQFIQAKVNAYNISENMYKADLKDLSKKGYDLRTDAIPIRAAKAAR
                ************************************************************

NebV1           QAASDVQYKKDYEKAKGKMVGFQSLQDDPKLVHYMNVAKIQSDREYKKDYEKTKSKYNTP
NebV2           QAASDVQYKKDYEKAKGKMVGFQSLQDDPKLVHYMNVAKIQSDREYKKDYEKTKSKYNTP
                ************************************************************

NebV1           HDMFNVVAAKKAQDVVSNVNYKHSLHHYTYLPDAMDLELSKNMMQIQSDNVYKEDYNNWM
NebV2           HDMFNVVAAKKAQDVVSNVNYKHSLHHYTYLPDAMDLELSKNMMQIQSDNVYKEDYNNWM
                ************************************************************

NebV1           KGIGWIPIGSLDVEKVKKAGDALNEKKYRQHPDTLKFTSIVDSPVMVQAKQNTKQVSDIL
NebV2           KGIGWIPIGSLDVEKVKKAGDALNEKKYRQHPDTLKFTSIVDSPVMVQAKQNTKQVSDIL
                ************************************************************

NebV1           YKAKGEDVKHKYTMSPDLPQFLQAKCNAYNISDVCYKRDWYDLIAKGNNVLGDAIPITAA
NebV2           YKAKGEDVKHKYTMSPDLPQFLQAKCNAYNISDVCYKRDWYDLIAKGNNVLGDAIPITAA
                ************************************************************

NebV1           KASRNIASDYKYKEAYEKSKGKHVGFRSLQDDPKLVHYMNVAKLQSDREYKKNYENTKTS
NebV2           KASRNIASDYKYKEAYEKSKGKHVGFRSLQDDPKLVHYMNVAKLQSDREYKKNYENTKTS
                ************************************************************

NebV1           YHTPGDMVSITAAKMAQDVATNVNYKQPLHHYTYLPDAMSLEHTRNVNQIQSDNVYKDEY
NebV2           YHTPGDMVSITAAKMAQDVATNVNYKQPLHHYTYLPDAMSLEHTRNVNQIQSDNVYKDEY
                ************************************************************

NebV1           NSFLKGIGWIPIGSLEVEKVKKAGDALNERKYRQHPDTVKFTSVPDSMGMVLAQHNTKQL
NebV2           NSFLKGIGWIPIGSLEVEKVKKAGDALNERKYRQHPDTVKFTSVPDSMGMVLAQHNTKQL
                ************************************************************

NebV1           SDLNYKVEGEKLKHKYTIDPELPQFIQAKVNALNMSDAHYKADWKKTIAKGYDLRPDAIP
NebV2           SDLNYKVEGEKLKHKYTIDPELPQFIQAKVNALNMSDAHYKADWKKTIAKGYDLRPDAIP
                ************************************************************

NebV1           IVAAKSSRNIASDCKYKEAYEKAKGKQVGFLSLQDDPKLVHYMNVAKIQSDREYKKGYEA
NebV2           IVAAKSSRNIASDCKYKEAYEKAKGKQVGFLSLQDDPKLVHYMNVAKIQSDREYKKGYEA
                ************************************************************

NebV1           SKTKYHTPLDMVSVTAAKKSQEVATNANYRQSYHHYTLLPDALNVEHSRNAMQIQSDNLY
NebV2           SKTKYHTPLDMVSVTAAKKSQEVATNANYRQSYHHYTLLPDALNVEHSRNAMQIQSDNLY
                ************************************************************

NebV1           KSDFTNWMKGIGWVPIESLEVEKAKKAGEILSEKKYRQHPEKLKFTYAMDTMEQALNKSN
NebV2           KSDFTNWMKGIGWVPIESLEVEKAKKAGEILSEKKYRQHPEKLKFTYAMDTMEQALNKSN
                ************************************************************
```

```
NebV1           KLNMDKRLYTEKWNKDKTTIHVMPDTPDILLSRVNQITMSDKLYKAGWEEEKKKGYDLRP
NebV2           KLNMDKRLYTEKWNKDKTTIHVMPDTPDILLSRVNQITMSDKLYKAGWEEEKKKGYDLRP
                ************************************************************

NebV1           DAIAIKAARASRDIASDYKYKKAYEQAKGKHIGFRSLEDDPKLVHFMQVAKMQSDREYKK
NebV2           DAIAIKAARASRDIASDYKYKKAYEQAKGKHIGFRSLEDDPKLVHFMQVAKMQSDREYKK
                ************************************************************

NebV1           GYEKSKTSFHTPVDMLSVVAAKKSQEVATNANYRNVIHTYNMLPDAMSFELAKNMMQIQS
NebV2           GYEKSKTSFHTPVDMLSVVAAKKSQEVATNANYRNVIHTYNMLPDAMSFELAKNMMQIQS
                ************************************************************

NebV1           DNQYKADYADFMKGIGWLPLGSLEAEKNKKAMEIISEKKYRQHPDTLKYSTLMDSMNMVL
NebV2           DNQYKADYADFMKGIGWLPLGSLEAEKNKKAMEIISEKKYRQHPDTLKYSTLMDSMNMVL
                ************************************************************

NebV1           AQNNAKIMNEHLYKQAWEADKTKVHIMPDIPQIILAKANAINMSDKLYKLSLEESKKKGY
NebV2           AQNNAKIMNEHLYKQAWEADKTKVHIMPDIPQIILAKANAINMSDKLYKLSLEESKKKGY
                ************************************************************

NebV1           DLRPDAIPIKAAKASRDIASDYKYKYNYEKGKGKMVGFRSLEDDPKLVHSMQVAKMQSDR
NebV2           DLRPDAIPIKAAKASRDIASDYKYKYNYEKGKGKMVGFRSLEDDPKLVHSMQVAKMQSDR
                ************************************************************

NebV1           EYKKNYENTKTSYHTPADMLSVTAAKDAQANITNTNYKHLIHKYILLPDAMNIELTRNMN
NebV2           EYKKNYENTKTSYHTPADMLSVTAAKDAQANITNTNYKHLIHKYILLPDAMNIELTRNMN
                ************************************************************

NebV1           RIQSDNEYKQDYNEWYKGLGWSPAGSLEVEKAKKATEYASDQKYRQHPSNFQFKKLTDSM
NebV2           RIQSDNEYKQDYNEWYKGLGWSPAGSLEVEKAKKATEYASDQKYRQHPSNFQFKKLTDSM
                ************************************************************

NebV1           DMVLAKQNAHTMNKHLYTIDWNKDKTKIHVMPDTPDILQAKQNQTLYSQKLYKLGWEEAL
NebV2           DMVLAKQNAHTMNKHLYTIDWNKDKTKIHVMPDTPDILQAKQNQTLYSQKLYKLGWEEAL
                ************************************************************

NebV1           KKGYDLPVDAISVQLAKASRDIASDYKYKQGYRKQLGHHVGFRSLQDDPKLVLSMNVAKM
NebV2           KKGYDLPVDAISVQLAKASRDIASDYKYKQGYRKQLGHHVGFRSLQDDPKLVLSMNVAKM
                ************************************************************

NebV1           QSEREYKKDFEKWKTKFSSPVDMLGVVLAKKCQELVSDVDYKNYLHQWTCLPDQNDVVQA
NebV2           QSEREYKKDFEKWKTKFSSPVDMLGVVLAKKCQELVSDVDYKNYLHQWTCLPDQNDVVQA
                ************************************************************

NebV1           KKVYELQSENLYKSDLEWLRGIGWSPLGSLEAEKNKRASEIISEKKYRQPPDRNKFTSIP
NebV2           KKVYELQSENLYKSDLEWLRGIGWSPLGSLEAEKNKRASEIISEKKYRQPPDRNKFTSIP
                ************************************************************

NebV1           DAMDIVLAKTNAKNRSDRLYREAWDKDKTQIHIMPDTPDIVLAKANLINTSDKLYRMGYE
NebV2           DAMDIVLAKTNAKNRSDRLYREAWDKDKTQIHIMPDTPDIVLAKANLINTSDKLYRMGYE
                ************************************************************

NebV1           ELKRKGYDLPVDAIPIKAAKASREIASEYKYKEGFRKQLGHHIGARNIEDDPKMMWSMHV
NebV2           ELKRKGYDLPVDAIPIKAAKASREIASEYKYKEGFRKQLGHHIGARNIEDDPKMMWSMHV
                ************************************************************

NebV1           AKIQSDREYKKDFEKWKTKFSSPVDMLGVVLAKKCQTLVSDVDYKNYLHQWTCLPDQSDV
NebV2           AKIQSDREYKKDFEKWKTKFSSPVDMLGVVLAKKCQTLVSDVDYKNYLHQWTCLPDQSDV
                ************************************************************

NebV1           IHARQAYDLQSDNLYKSDLQWLKGIGWMTSGSLEDEKNKRATQILSDHVYRQHPDQFKFS
NebV2           IHARQAYDLQSDNLYKSDLQWLKGIGWMTSGSLEDEKNKRATQILSDHVYRQHPDQFKFS
                ************************************************************

NebV1           SLMDSIPMVLAKNNAITMNHRLYTEAWDKDKTTVHIMPDTPEVLLAKQNKVNYSEKLYKL
NebV2           SLMDSIPMVLAKNNAITMNHRLYTEAWDKDKTTVHIMPDTPEVLLAKQNKVNYSEKLYKL
                ************************************************************
```

```
NebV1           GLEEAKRKGYDMRVDAIPIKAAKASRDIASEFKYKEGYRKQLGHHIGARAIRDDPKMMWS
NebV2           GLEEAKRKGYDMRVDAIPIKAAKASRDIASEFKYKEGYRKQLGHHIGARAIRDDPKMMWS
                ************************************************************

NebV1           MHVAKIQSDREYKKDFEKWKTKFSSPVDMLGVVLAKKCQTLVSDVDYKNYLHQWTCLPDQ
NebV2           MHVAKIQSDREYKKDFEKWKTKFSSPVDMLGVVLAKKCQTLVSDVDYKNYLHQWTCLPDQ
                ************************************************************

NebV1           SDVIHARQAYDLQSDNMYKSDLQWMRGIGWVSIGSLDVEKCKRATEILSDKIYRQPPDRF
NebV2           SDVIHARQAYDLQSDNMYKSDLQWMRGIGWVSIGSLDVEKCKRATEILSDKIYRQPPDRF
                ************************************************************

NebV1           KFTSVTDSLEQVLAKNNAITMNKRLYTEAWDKDKTQIHIMPDTPEIMLARMNKINYSESL
NebV2           KFTSVTDSLEQVLAKNNAITMNKRLYTEAWDKDKTQIHIMPDTPEIMLARMNKINYSESL
                ************************************************************

NebV1           YKLANEEAKKKGYDLRSDAIPIVAAKASRDIISDYKYKDGYCKQLGHHIGARNIEDDPKM
NebV2           YKLANEEAKKKGYDLRSDAIPIVAAKASRDIISDYKYKDGYCKQLGHHIGARNIEDDPKM
                ************************************************************

NebV1           MWSMHVAKIQSDREYKKDFEKWKTKFSSPVDMLGVVLAKKCQTLVSDVDYKNYLHEWTCL
NebV2           MWSMHVAKIQSDREYKKDFEKWKTKFSSPVDMLGVVLAKKCQTLVSDVDYKNYLHEWTCL
                ************************************************************

NebV1           PDQSDVIHARQAYDLQSDNIYKSDLQWLRGIGWVPIGSMDVVKCKRATEILSDNIYRQPP
NebV2           PDQSDVIHARQAYDLQSDNIYKSDLQWLRGIGWVPIGSMDVVKCKRATEILSDNIYRQPP
                ************************************************************

NebV1           DKLKFTSVTDSLEQVLAKNNALNMNKRLYTEAWDKDKTQIHIMPDTPEIMLARQNKINYS
NebV2           DKLKFTSVTDSLEQVLAKNNALNMNKRLYTEAWDKDKTQIHIMPDTPEIMLARQNKINYS
                ************************************************************

NebV1           ETLYKLANEEAKKKGYDLRSDAIPIVAAKASRDVISDYKYKDGYRKQLGHHIGARNIEDD
NebV2           ETLYKLANEEAKKKGYDLRSDAIPIVAAKASRDVISDYKYKDGYRKQLGHHIGARNIEDD
                ************************************************************

NebV1           PKMMWSMHVAKIQSDREYKKDFEKWKTKFSSPVDMLGVVLAKKCQTLVSDVDYKNYLHEW
NebV2           PKMMWSMHVAKIQSDREYKKDFEKWKTKFSSPVDMLGVVLAKKCQTLVSDVDYKNYLHEW
                ************************************************************

NebV1           TCLPDQNDVIHARQAYDLQSDNIYKSDLQWLRGIGWVPIGSMDVVKCKRAAEILSDNIYR
NebV2           TCLPDQNDVIHARQAYDLQSDNIYKSDLQWLRGIGWVPIGSMDVVKCKRAAEILSDNIYR
                ************************************************************

NebV1           QPPDKLKFTSVTDSLEQVLAKNNALNMNKRLYTEAWDKDKTQVHIMPDTPEIMLARQNKI
NebV2           QPPDKLKFTSVTDSLEQVLAKNNALNMNKRLYTEAWDKDKTQVHIMPDTPEIMLARQNKI
                ************************************************************

NebV1           NYSESLYRQAMEEAKKEGYDLRSDAIPIVAAKASRDIASDYKYKEAYRKQLGHHIGARAV
NebV2           NYSESLYRQAMEEAKKEGYDLRSDAIPIVAAKASRDIASDYKYKEAYRKQLGHHIGARAV
                ************************************************************

NebV1           HDDPKIMWSLHIAKVQSDREYKKDFEKYKTRYSSPVDMLGIVLAKKCQTLVSDVDYKHPL
NebV2           HDDPKIMWSLHIAKVQSDREYKKDFEKYKTRYSSPVDMLGIVLAKKCQTLVSDVDYKHPL
                ************************************************************

NebV1           HEWICLPDQNDIIHARKAYDLQSDNLYKSDLEWMKGIGWVPIDSLEVVRAKRAGELLSDT
NebV2           HEWICLPDQNDIIHARKAYDLQSDNLYKSDLEWMKGIGWVPIDSLEVVRAKRAGELLSDT
                ************************************************************

NebV1           IYRQRPETLKFTSITDTPEQVLAKNNALNMNKRLYTEAWDNDKKTIHVMPDTPEIMLAKL
NebV2           IYRQRPETLKFTSITDTPEQVLAKNNALNMNKRLYTEAWDNDKKTIHVMPDTPEIMLAKL
                ************************************************************

NebV1           NRINYSDKLYKLALEESKKEGYDLRLDAIPIQAAKASRDIASDYKYKEGYRKQLGHHIGA
NebV2           NRINYSDKLYKLALEESKKEGYDLRLDAIPIQAAKASRDIASDYKYKEGYRKQLGHHIGA
                ************************************************************
```

```
NebV1           RNIKDDPKMMWSIHVAKIQSDREYKKEFEKWKTKFSSPVDMLGVVLAKKCQILVSDIDYK
NebV2           RNIKDDPKMMWSIHVAKIQSDREYKKEFEKWKTKFSSPVDMLGVVLAKKCQILVSDIDYK
                ************************************************************

NebV1           HPLHEWTCLPDQNDVIQARKAYDLQSDAIYKSDLEWLRGIGWVPIGSVEVEKVKRAGEIL
NebV2           HPLHEWTCLPDQNDVIQARKAYDLQSDAIYKSDLEWLRGIGWVPIGSVEVEKVKRAGEIL
                ************************************************************

NebV1           SDRKYRQPADQLKFTCITDTPEIVLAKNNALTMSKHLYTEAWDADKTSIHVMPDTPDILL
NebV2           SDRKYRQPADQLKFTCITDTPEIVLAKNNALTMSKHLYTEAWDADKTSIHVMPDTPDILL
                ************************************************************

NebV1           AKSNSANISQKLYTKGWDESKMKDYDLRADAISIKSAKASRDIASDYKYKEAYEKQKGHH
NebV2           AKSNSANISQKLYTKGWDESKMKDYDLRADAISIKSAKASRDIASDYKYKEAYEKQKGHH
                ************************************************************

NebV1           IGAQSIEDDPKIMCAIHAGKIQSEREYKKEFQKWKTKFSSPVDMLSILLAKKCQTLVTDI
NebV2           IGAQSIEDDPKIMCAIHAGKIQSEREYKKEFQKWKTKFSSPVDMLSILLAKKCQTLVTDI
                ************************************************************

NebV1           DYRNYLHEWTCMPDQNDIIQAKKAYDLQSDSVYKADLEWLRGIGWMPEGSVEMNRVKVAQ
NebV2           DYRNYLHEWTCMPDQNDIIQAKKAYDLQSDSVYKADLEWLRGIGWMPEGSVEMNRVKVAQ
                ************************************************************

NebV1           DLVNERLYRTRPEALSFTSIVDTPEVVLAKANSLQISEKLYQEAWNKDKSNITIPSDTPE
NebV2           DLVNERLYRTRPEALSFTSIVDTPEVVLAKANSLQISEKLYQEAWNKDKSNITIPSDTPE
                ************************************************************

NebV1           MLQAHINALQISNKLYQKDWNDAKQKGYDIRADAIEIKHAKASREIASEYKYKEGYRKQL
NebV2           MLQAHINALQISNKLYQKDWNDAKQKGYDIRADAIEIKHAKASREIASEYKYKEGYRKQL
                ************************************************************

NebV1           GHHMGFRTLQDDPKSVWAIHAAKIQSDREYKKAYEKSKGIHNTPLDMMSIVQAKKCQVLV
NebV2           GHHMGFRTLQDDPKSVWAIHAAKIQSDREYKKAYEKSKGIHNTPLDMMSIVQAKKCQVLV
                ************************************************************

NebV1           SDIDYRNYLHQWTCLPDQNDVIQAKKAYDLQSDNLYKSDLEWLKGIGWLPEGSVEVMRVK
NebV2           SDIDYRNYLHQWTCLPDQNDVIQAKKAYDLQSDNLYKSDLEWLKGIGWLPEGSVEVMRVK
                ************************************************************

NebV1           NAQNLLNERLYRIKPEALKFTSIVDTPEVIQAKINAVQISEPLYRDAWEKEKANVNVPAD
NebV2           NAQNLLNERLYRIKPEALKFTSIVDTPEVIQAKINAVQISEPLYRDAWEKEKANVNVPAD
                ************************************************************

NebV1           TPLMLQSKINALQISNKRYQQAWEDVKMTGYDLRADAIGIQHAKASRDIASDYLYKTAYE
NebV2           TPLMLQSKINALQISNKRYQQAWEDVKMTGYDLRADAIGIQHAKASRDIASDYLYKTAYE
                ************************************************************

NebV1           KQKGHYIGCRSAKEDPKLVWAANVLKMQNDRLYKKAYNDHKAKISIPVDMVSISAAKEGQ
NebV2           KQKGHYIGCRSAKEDPKLVWAANVLKMQNDRLYKKAYNDHKAKISIPVDMVSISAAKEGQ
                ************************************************************

NebV1           ALASDVDYRHYLHHWSCFPDQNDVIQARKAYDLQSDSVYKADLEWLRGIGWMPEGSVEMN
NebV2           ALASDVDYRHYLHHWSCFPDQNDVIQARKAYDLQSDSVYKADLEWLRGIGWMPEGSVEMN
                ************************************************************

NebV1           RVKVAQDLVNERLYRTRPEALSFTSIVDTPEVVLAKANSLQISEKLYQEAWNKDKSNITI
NebV2           RVKVAQDLVNERLYRTRPEALSFTSIVDTPEVVLAKANSLQISEKLYQEAWNKDKSNITI
                ************************************************************

NebV1           PSDTPEMLQAHINALQISNKLYQKDWNDTKQKGYDIRADAIEIKHAKASREIASEYKYKE
NebV2           PSDTPEMLQAHINALQISNKLYQKDWNDTKQKGYDIRADAIEIKHAKASREIASEYKYKE
                ************************************************************

NebV1           GYRKQLGHHMGFRTLQDDPKSVWAIHAAKIQSDREYKKAYEKSKGIHNTPLDMMSIVQAK
NebV2           GYRKQLGHHMGFRTLQDDPKSVWAIHAAKIQSDREYKKAYEKSKGIHNTPLDMMSIVQAK
                ************************************************************
```

```
NebV1           KCQVLVSDIDYRNYLHQWTCLPDQNDVIQAKKAYDLQSDNLYKSDLEWLKGIGWLPEGSV
NebV2           KCQVLVSDIDYRNYLHQWTCLPDQNDVIQAKKAYDLQSDNLYKSDLEWLKGIGWLPEGSV
                ************************************************************

NebV1           EVMRVKNAQNLLNERLYRIKPEALKFTSIVDTPEVIQAKINAVQISEPLYRNAWEKEKAN
NebV2           EVMRVKNAQNLLNERLYRIKPEALKFTSIVDTPEVIQAKINAVQISEPLYRNAWEKEKAN
                ************************************************************

NebV1           VNVPADTPLMLQSKINALQISNKRYQQAWEDVKMTGYDLRADAIGIQHAKASRDIASDYL
NebV2           VNVPADTPLMLQSKINALQISNKRYQQAWEDVKMTGYDLRADAIGIQHAKASRDIASDYL
                ************************************************************

NebV1           YKTAYEKQKGHYIGCRSAKEDPKLVWAANVLKMQNDRLYKKAYNDHKAKISIPVDMVSIS
NebV2           YKTAYEKQKGHYIGCRSAKEDPKLVWAANVLKMQNDRLYKKAYNDHKAKISIPVDMVSIS
                ************************************************************

NebV1           AAKEGQALASDVDYRHYLHHWSCFPDQNDVIQARKAYDLQSDSVYKADLEWLRGIGWMPE
NebV2           AAKEGQALASDVDYRHYLHHWSCFPDQNDVIQARKAYDLQSDSVYKADLEWLRGIGWMPE
                ************************************************************

NebV1           GSVEMNRVKVAQDLVNERLYRTRPEALSFTSIVDTPEVVLAKANSLQISEKLYQEAWNKD
NebV2           GSVEMNRVKVAQDLVNERLYRTRPEALSFTSIVDTPEVVLAKANSLQISEKLYQEAWNKD
                ************************************************************

NebV1           KSNITIPSDTPEMLQAHINALQISNKLYQKDWNDTKQKGYDIRADAIEIKHAKASREIAS
NebV2           KSNITIPSDTPEMLQAHINALQISNKLYQKDWNDTKQKGYDIRADAIEIKHAKASREIAS
                ************************************************************

NebV1           EYKYKEGYRKQLGHHMGFRTLQDDPKSVWAIHAAKIQSDREYKKAYEKSKGIHNTPLDMM
NebV2           EYKYKEGYRKQLGHHMGFRTLQDDPKSVWAIHAAKIQSDREYKKAYEKSKGIHNTPLDMM
                ************************************************************

NebV1           SIVQAKKCQVLVSDIDYRNYLHQWTCLPDQNDVIQAKKAYDLQSDNLYKSDLEWLKGIGW
NebV2           SIVQAKKCQVLVSDIDYRNYLHQWTCLPDQNDVIQAKKAYDLQSDNLYKSDLEWLKGIGW
                ************************************************************

NebV1           LPEGSVEVMRVKNAQNLLNERLYRIKPEALKFTSIVDTPEVIQAKINAVQISEPLYRDAW
NebV2           LPEGSVEVMRVKNAQNLLNERLYRIKPEALKFTSIVDTPEVIQAKINAVQISEPLYRDAW
                ************************************************************

NebV1           EKEKANVNVPADTPLMLQSKINALQISNKRYQQAWEDVKMTGYDLRADAIGIQHAKASRD
NebV2           EKEKANVNVPADTPLMLQSKINALQISNKRYQQAWEDVKMTGYDLRADAIGIQHAKASRD
                ************************************************************

NebV1           IASDYLYKTAYEKQKGHYIGCRSAKEDPKLVWAANVLKMQNDRLYKKAYNDHKAKISIPV
NebV2           IASDYLYKTAYEKQKGHYIGCRSAKEDPKLVWAANVLKMQNDRLYKKAYNDHKAKISIPV
                ************************************************************

NebV1           DMVSISAAKEGQALASDVDYRHYLHRWSCFPDQNDVIQARKAYDLQSDALYKADLEWLRG
NebV2           DMVSISAAKEGQALASDVDYRHYLHRWSCFPDQNDVIQARKAYDLQSDALYKADLEWLRG
                ************************************************************

NebV1           IGWMPQGSPEVLRVKNAQNIFCDSVYRTPVVNLKYTSIVDTPEVVLAKSNAENISIPKYR
NebV2           IGWMPQGSPEVLRVKNAQNIFCDSVYRTPVVNLKYTSIVDTPEVVLAKSNAENISIPKYR
                ************************************************************

NebV1           EVWDKDKTSIHIMPDTPEINLARANALNVSNKLYREGWDEMKAGCDVRLDAIPIQAAKAS
NebV2           EVWDKDKTSIHIMPDTPEINLARANALNVSNKLYREGWDEMKAGCDVRLDAIPIQAAKAS
                ************************************************************

NebV1           REIASDYKYKLDHEKQKGHYVGTLTARDDNKIRWALIADKLQNEREYRLDWAKWKAKIQS
NebV2           REIASDYKYKLDHEKQKGHYVGTLTARDDNKIRWALIADKLQNEREYRLDWAKWKAKIQS
                ************************************************************

NebV1           PVDMLSILHSKNSQALVSDMDYRNYLHQWTCMPDQNDVIQAKKAYELQSDNVYKADLEWL
NebV2           PVDMLSILHSKNSQALVSDMDYRNYLHQWTCMPDQNDVIQAKKAYELQSDNVYKADLEWL
                ************************************************************
```

```
NebV1           RGIGWMPNDSVSVNHAKHAADIFSEKKYRTKIETLNFTPVDDRVDYVTAKQSGEILDDIK
NebV2           RGIGWMPNDSVSVNHAKHAADIFSEKKYRTKIETLNFTPVDDRVDYVTAKQSGEILDDIK
                ************************************************************

NebV1           YRKDWNATKSKYTLTETPLLHTAQEAARILDQYLYKEGWERQKATGYILPPDAVPFVHAH
NebV2           YRKDWNATKSKYTLTETPLLHTAQEAARILDQYLYKEGWERQKATGYILPPDAVPFVHAH
                ************************************************************

NebV1           HCNDVQSELKYKAEHVKQKGHYVGVPTMRDDPKLVWFEHAGQIQNERLYKEDYHKTKAKI
NebV2           HCNDVQSELKYKAEHVKQKGHYVGVPTMRDDPKLVWFEHAGQIQNERLYKEDYHKTKAKI
                ************************************************************

NebV1           NIPADMVSVLAAKQGQTLVSDIDYRNYLHQWMCHPDQNDVIQARKAYDLQSDNVYRADLE
NebV2           NIPADMVSVLAAKQGQTLVSDIDYRNYLHQWMCHPDQNDVIQARKAYDLQSDNVYRADLE
                ************************************************************

NebV1           WLRGIGWIPLDSVDHVRVTKNQEMMSQIKYKKNALENYPNFRSVVDPPEIVLAKINSVNQ
NebV2           WLRGIGWIPLDSVDHVRVTKNQEMMSQIKYKKNALENYPNFRSVVDPPEIVLAKINSVNQ
                ************************************************************

NebV1           SDVKYKETFNKAKGKYTFSPDTPHISHSKDMGKLYSTILYKGAWEGTKAYGYTLDERYIP
NebV2           SDVKYKETFNKAKGKYTFSPDTPHISHSKDMGKLYSTILYKGAWEGTKAYGYTLDERYIP
                ************************************************************

NebV1           IVGAKHADLVNSELKYKETYEKQKGHYLAGKVIGEFPGVVHCLDFQKMRSALNYRKHYED
NebV2           IVGAKHADLVNSELKYKETYEKQKGHYLAGKVIGEFPGVVHCLDFQKMRSALNYRKHYED
                ************************************************************

NebV1           TKANVHIPNDMMNHVLAKRCQYILSDLEYRHYFHQWTSLLEEPNVIRVRNAQEILSDNVY
NebV2           TKANVHIPNDMMNHVLAKRCQYILSDLEYRHYFHQWTSLLEEPNVIRVRNAQEILSDNVY
                ************************************************************

NebV1           KDDLNWLKGIGCYVWDTPQILHAKKSYDLQSQLQYTAAGKENLQNYNLVTDTPLYVTAVQ
NebV2           KDDLNWLKGIGCYVWDTPQILHAKKSYDLQSQLQYTAAGKENLQNYNLVTDTPLYVTAVQ
                ************************************************************

NebV1           SGINASEVKYKENYHQIKDKYTTVLETVDYDRTRNLKNLYSSNLYKEAWDRVKATSYILP
NebV2           SGINASEVKYKENYHQIKDKYTTVLETVDYDRTRNLKNLYSSNLYKEAWDRVKATSYILP
                ************************************************************

NebV1           SSTLSLTHAKNQKHLASHIKYREEYEKFKALYTLPRSVDDDPNTARCLRVGKLNIDRLYR
NebV2           SSTLSLTHAKNQKHLASHIKYREEYEKFKALYTLPRSVDDDPNTARCLRVGKLNIDRLYR
                ************************************************************

NebV1           SVYEKNKMKIHIVPDMVEMVTAKDSQKKVSEIDYRLRLHEWICHPDLQVNDHVRKVTDQI
NebV2           SVYEKNKMKIHIVPDMVEMVTAKDSQKKVSEIDYRLRLHEWICHPDLQVNDHVRKVTDQI
                ************************************************************

NebV1           SDIVYKDDLNWLKGIGCYVWDTPEILHAKHAYDLRDDIKYKAHMLKTRNDYKLVTDTPVY
NebV2           SDIVYKDDLNWLKGIGCYVWDTPEILHAKHAYDLRDDIKYKAHMLKTRNDYKLVTDTPVY
                ************************************************************

NebV1           VQAVKSGKQLSDAVYHYDYVHSVRGKVAPTTKTVDLDRALHAYKLQSSNLYKTSLRTLPT
NebV2           VQAVKSGKQLSDAVYHYDYVHSVRGKVAPTTKTVDLDRALHAYKLQSSNLYKTSLRTLPT
                ************************************************************

NebV1           GYRLPGDTPHFKHIKDTRYMSSYFKYKEAYEHTKAYGYTLGPKDVPFVHVRRVNNVTSER
NebV2           GYRLPGDTPHFKHIKDTRYMSSYFKYKEAYEHTKAYGYTLGPKDVPFVHVRRVNNVTSER
                ************************************************************

NebV1           LYRELYHKLKDKIHTTPDTPEIRQVKKTQEAVSELIYKSDFFKMQGHMISLPYTPQVIHC
NebV2           LYRELYHKLKDKIHTTPDTPEIRQVKKTQEAVSELIYKSDFFKMQGHMISLPYTPQVIHC
                ************************************************************

NebV1           RYVGDITSDIKYKEDLQVLKGFGCFLYDTPDMVRSRHLRKLWSNYLYTDKARKMRDKYKV
NebV2           RYVGDITSDIKYKEDLQVLKGFGCFLYDTPDMVRSRHLRKLWSNYLYTDKARKMRDKYKV
                ************************************************************
```

```
NebV1           VLDTPEYRKVQELKTHLSELVYRAAGKKQKSIFTSVPDTPDLLRAKRGQKLQSQYLYVEL
NebV2           VLDTPEYRKVQELKTHLSELVYRAAGKKQKSIFTSVPDTPDLLRAKRGQKLQSQYLYVEL
                ************************************************************

NebV1           ATKERPHHHAGNQTTALKHAKDVKDMVSEKKYKIQYEKMKDKYTPVPDTPILIRAKRAYW
NebV2           ATKERPHHHAGNQTTALKHAKDVKDMVSEKKYKIQYEKMKDKYTPVPDTPILIRAKRAYW
                ************************************************************

NebV1           NASDLRYKETFQKTKGKYHTVKDALDIVYHRKVTDDISKIKYKENYMSQLGIWRSIPDRP
NebV2           NASDLRYKETFQKTKGKYHTVKDALDIVYHRKVTDDISKIKYKENYMSQLGIWRSIPDRP
                ************************************************************

NebV1           EHFHHRAVTDTVSDVKYKEDLTWLKGIGCYAYDTPDFTLAEKNKTLYSKYKYKEVFERTK
NebV2           EHFHHRAVTDTVSDVKYKEDLTWLKGIGCYAYDTPDFTLAEKNKTLYSKYKYKEVFERTK
                ************************************************************

NebV1           SDFKYVADSPINRHFKYATQLMNEKKYRADYEQRKDKYHLVVDEPRHLLAKTAGDQISQI
NebV2           SDFKYVADSPINRHFKYATQLMNERKYKSSAKMFLQHGCNEILRPDMLTALYNSHMWSQI
                ************************:**::. :   ::    : .*  * *   ..  ***

NebV1           KYRKNYEKSKDKFTSIVDTPEHLRTTKVNKQISDILYKLEYNKAKPRGYTTIHDTPMLLH
NebV2           KYRKNYEKSKDKFTSIVDTPEHLRTTKVNKQISDILYKLEYNKAKPRGYTTIHDTPMLLH
                ************************************************************

NebV1           VRKVKDEVSDLKYKEVYQRNKSNCTIEPDAVHIKAAKDAYKVNTNLDYKKQYEANKAHWK
NebV2           VRKVKDEVSDLKYKEVYQRNKSNCTIEPDAVHIKAAKDAYKVNTNLDYKKQYEANKAHWK
                ************************************************************

NebV1           WTPDRPDFLQAAKSSLQQSDFEYKLDREFLKGCKLSVTDDKNTVLALRNTLIESDLKYKE
NebV2           WTPDRPDFLQAAKSSLQQSDFEYKLDREFLKGCKLSVTDDKNTVLALRNTLIESDLKYKE
                ************************************************************

NebV1           KHVKERGTCHAVPDTPQILLAKTVSNLVSENKYKDHVKKHLAQGSYTTLPETRDTVHVKE
NebV2           KHVKERGTCHAVPDTPQILLAKTVSNLVSENKYKDHVKKHLAQGSYTTLPETRDTVHVKE
                ************************************************************

NebV1           VTKHVSDTNYKKKFVKEKGKSNYSIMLEPPEVKHAMEVAKKQSDVAYRKDAKENLHYTTV
NebV2           VTKHVSDTNYKKKFVKEKGKSNYSIMLEPPEVKHAMEVAKKQSDVAYRKDAKENLHYTTV
                ************************************************************

NebV1           ADRPDIKKATQAAKQASEVEYRAKHRKEGSHGLSMLGRPDIEMAKKAAKLSSQVKYRENF
NebV2           ADRPDIKKATQAAKQASEVEYRAKHRKEGSHGLSMLGRPDIEMAKKAAKLSSQVKYRENF
                ************************************************************

NebV1           DKEKGKTPKYNPKDSQLYKVMKDANNLASEVKYKADLKKLHKPVTDMKESLIMNHVLNTS
NebV2           DKEKGKTPKYNPKDSQLYKVMKDANNLASEVKYKADLKKLHKPVTDMKESLIMNHVLNTS
                ************************************************************

NebV1           QLASSYQYKKKYEKSKGHYHTIPDNLEQLHLKEATELQSIVKYKEKYEKERGKPMLDFET
NebV2           QLASSYQYKKKYEKSKGHYHTIPDNLEQLHLKEATELQSIVKYKEKYEKERGKPMLDFET
                ************************************************************

NebV1           PTYITAKESQQMQSGKEYRKDYEESIKGRNLTGLEVTPALLHVKYATKIASEKEYRKDLE
NebV2           PTYITAKESQQMQSGKEYRKDYEESIKGRNLTGLEVTPALLHVKYATKIASEKEYRKDLE
                ************************************************************

NebV1           ESIRGKGLTEMEDTPDMLRAKNATQILNEKEYKRDLELEVKGRGLNAMANETPDFMRARN
NebV2           ESIRGKGLTEMEDTPDMLRAKNATQILNEKEYKRDLELEVKGRGLNAMANETPDFMRARN
                ************************************************************

NebV1           ATDIASQIKYKQSAEMEKANFTSVVDTPEIIHAQQVKNLSSQKKYKEDAEKSMSYYETVL
NebV2           ATDIASQIKYKQSAEMEKANFTSVVDTPEIIHAQQVKNLSSQKKYKEDAEKSMSYYETVL
                ************************************************************

NebV1           DTPEIQRVRENQKNFSLLQYQCDLKNSKGKITVVQDTPEILRVKENQKNFSSVLYKEDVS
NebV2           DTPEIQRVRENQKNFSLLQYQCDLKNSKGKITVVQDTPEILRVKENQKNFSSVLYKEDVS
                ************************************************************
```

```
NebV1           PGTAIGKTPEMMRVKQTQDHISSVKYKEAIGQGTPIPDLPEVKRVKETQKHISSVMYKEN
NebV2           PGTAIGKTPEMMRVKQTQDHISSVKYKEAIGQGTPIPDLPEVKRVKETQKHISSVMYKEN
                ************************************************************

NebV1           LGTGIPTTVTPEIERVKRNQENFSSVLYKENLGKGIPTPITPEMERVKRNQENFSSILYK
NebV2           LGTGIPTTVTPEIERVKRNQENFSSVLYKENLGKGIPTPITPEMERVKRNQENFSSILYK
                ************************************************************

NebV1           ENLSKGTPLPVTPEMERVKLNQENFSSVLYKENVGKGIPIPITPEMERVKHNQENFSSVL
NebV2           ENLSKGTPLPVTPEMERVKLNQENFSSVLYKENVGKGIPIPITPEMERVKHNQENFSSVL
                ************************************************************

NebV1           YKENLGTGIPIPITPEMQRVKHNQENLSSVLYKENMGKGTPLPVTPEMERVKHNQENISS
NebV2           YKENLGTGIPIPITPEMQRVKHNQENLSSVLYKENMGKGTPLPVTPEMERVKHNQENISS
                ************************************************************

NebV1           VLYKENMGKGTPLPVTPEMERVKHNQENISSVLYKENMGKGTPLAVTPEMERVKHNQENI
NebV2           VLYKENMGKGTPLPVTPEMERVKHNQENISSVLYKENMGKGTPLAVTPEMERVKHNQENI
                ************************************************************

NebV1           SSVLYKENVGKATATPVTPEMQRVKRNQENISSVLYKENLGKATPTPFTPEMERVKRNQE
NebV2           SSVLYKENVGKATATPVTPEMQRVKRNQENISSVLYKENLGKATPTPFTPEMERVKRNQE
                ************************************************************

NebV1           NFSSVLYKENMRKATPTPVTPEMERAKRNQENISSVLYSDSFRKQIQGKAAYVLDTPEMR
NebV2           NFSSVLYKENMRKATPTPVTPEMERAKRNQENISSVLYSDSFRKQIQGKAAYVLDTPEMR
                ************************************************************

NebV1           RVRETQRHISTVKYHEDFEKHKGCFTPVVTDPITERVKKNMQDFSDINYRGIQRKVVEME
NebV2           RVRETQRHISTVKYHEDFEKHKGCFTPVVTDPITERVKKNMQDFSDINYRGIQRKVVEME
                ************************************************************

NebV1           QKRNDQDQETITGLRVWRTNPGSVFDYDPAEDNIQSRSLHMINVQAQRRSREQSRSASAL
NebV2           QKRNDQDQETITGLRVWRTNPGSVFDYDPAEDNIQSRSLHMINVQAQRRSREQSRSASAL
                ************************************************************

NebV1           SISGGEEKSEHSEAPDHHLSTYSDGGVFAVSTAYKHAKTTELPQQRSSSVATQQTTVSSI
NebV2           SISGGEEKSEHSEAPDHHLSTYSDGGVFAVSTAYKHAKTTELPQQRSSSVATQQTTVSSI
                ************************************************************

NebV1           PSHPSTAGKIFRAMYDYMAADADEVSFKDGDAIINVQAIDEGWMYGTVQRTGRTGMLPAN
NebV2           PSHPSTAGKIFRAMYDYMAADADEVSFKDGDAIINVQAIDEGWMYGTVQRTGRTGMLPAN
                ************************************************************

NebV1           YVEAI
NebV2           YVEAI
                *****
```

Nebulin Fragment Variation 2 (from the Y-2-H)

D T V S D V K Y K E D L T W L K G I G C Y A Y D T P D F T L A E K N K T L Y S K Y K Y K E V F E R T K S D F K Y V A D S P I N R H F K Y A T Q L M N E R K Y K S S A K M F L Q H G C N E I L R P

A.6 Analysis of KBTBD13

A.6.1 Amino Acid Alignment for KBTBD13 and Klhl31

The amino acid sequences for KBTBD13 (Gene ID: 390594) and Klhl31 (Gene ID: 401265) were aligned using Clustal2W software.

```
CLUSTAL 2.1 multiple sequence alignment


kbtbd13         ------------------------------------------------------MARGP---
Klhl31          MAPKKKIVKKNKGDINEMTIIVEDSPLNKLNALNGLLEGGNGLSCISSELTDASYGPNLL
                                                                       : **

kbtbd13         -----------QTLVQVWVGGQLFQADRALLVEHCGFFRGLFRSGMRETRAAEVRLGVLS
Klhl31          EGLSKMRQENFLCDLVIGTKTKSFDVHKSVMASCSEYFYNILKKDPSIQRVDLNDISPLG
                             : : .  : *:..::::.. . :* .:::..    *.    :. *.

kbtbd13         AGGFRATLQVLRGDRPALAAEDELLQAVECAAFLQAPALARFLEHNLTSDNCALLCDAAA
Klhl31          LATVIAYAYTGKLTLSLYTIGSIISAAVYLQIHTLVKMCSDFLIREMSVENCMYVVNIAE
                 . . *   . :   .  :  . :  **    .  .   : ** :::: :**  : : *

kbtbd13         AFGLRDVFHSAALFICD-------------------GERELAAELALP------------
Klhl31          TYSLKNAKAAAQKFIRDNFLEFAESDQFMKLTFEQINELLIDDDLQLPSEIVAFQIAMKW
                ::.*::.  :*  ** *                  .*  :  :* **

kbtbd13         ----EARAYVAALRPS-------------------------------------SYAAVSTH
Klhl31          LEFDQKRVKYAADLLSNIRFGTISAQDLVNYVQSVPRMMQDADCHRLLVDAMNYHLLPYH
                    : *.  **   *                                    .*  :. *

kbtbd13         T---------------------PAPGFLEDASRTLCYLDEEEDAWRTLAALPLEASTLLA
Klhl31          QNTLQSRRTRIRGGCRVLVTVGGRPGLTEKSLSRDILYRDPENGWSKLTEMPAKS--FNQ
                                **: *.:        : *:.* .*: :* ::  :

kbtbd13         GVATLGNKLYIVGG-----VRGASKEVVELGFCYDPDGGTWHEFPSPHQPRYDTALAGFD
Klhl31          CVAVMDGFLYVAGGEDQNDARNQAKHAVSNFCRYDPRFNTWIHLASMNQKRTHFSLSVFN
                 **.:.. **:.**     .*. :*..*.    ***  .** .:.* :* * . :*: *:

kbtbd13         GRLYAIGGEFQRTPISSVERYDPAAGCWSFVADLPQPAAGVPCAQACGRLFVCLWRPADT
Klhl31          GLVYAAGGRNAEGSLASLECYVPSTNQWQPKTPLEVARCCHASAVADGRVLVTGGYIANA
                * :** **.  . .::*:* * *::. *.  : *  . .  ..* * **::*     *::

kbtbd13         T--AVVEYAVRTDAWLPVAELRRPQSYGHCMVAHRDSLYVVRN---GP-SDDFLHCAIDC
Klhl31          YSRSVCAYDPASDSWQELPNLSTPR-GWHCAVTLSDRVYVMGGSQLGPRGERVDVLTVEC
                   :*  *   :*:*  :.:*  *:   ** *:  * :**: .   ** .: .   :::*

kbtbd13         LNLATGQWT-ALPGQFVNSKGALFTAVVRGDTVYTVN------RMFTLLYAIEGGTWRLL
Klhl31          YSPATGQWSYAAPLQVGVSTAGVSALHGRAYLVGGWNEGEKKYKKCIQCFSPELNEWTED
                 . *****: * * *.  *...: :   *.  *   *      :     :: * . *

kbtbd13         REKAGFPRPGSLQTFLLR---LPPGAPGPVTSTTAEL
Klhl31          DELPEATVGVSCCTLSMPNNVTRESRASSVSSVPVSI
                 * .  .   *  *: :       . ...*:*....:
```